NASA CR-134859
REPORT MDC J4519

DC-9 FLIGHT DEMONSTRATION PROGRAM WITH REFANNED JT8D ENGINES

FINAL REPORT

VOLUME III
PERFORMANCE AND ANALYSIS

by

Douglas Aircraft Company
McDonnell Douglas Corporation
Long Beach, California 90846

Prepared for
National Aeronautics and Space Administration
NASA Lewis Research Center
Contract NAS 3-17841
Robert W. Schroeder, Project Manager

1 Report No.	2 Government Accession No.	3 Recipient's Catalog No
NASA CR-134859		

4. Title and Subtitle	5. Report Date
DC-9 FLIGHT DEMONSTRATION PROGRAM WITH REFANNED JT8D ENGINES, FINAL REPORT, VOLUME III, PERFORMANCE AND ANALYSIS	July 1975
	6. Performing Organization Code
7. Author(s)	8. Performing Organization Report No. MDC J4519
	10. Work Unit No.
9. Performing Organization Name and Address: Douglas Aircraft Company, McDonnell Douglas Corporation, Long Beach, California 90801	11. Contract or Grant No. NAS 3-17841
	13. Type of Report and Period Covered: Contractor Report
12. Sponsoring Agency Name and Address: National Aeronautics and Space Administration, Washington, D.C. 20546	14. Sponsoring Agency Code

15. Supplementary Notes

Project Manager, Robert W. Schroeder
NASA Lewis Research Center
Cleveland, Ohio

16 Abstract

During the period of June 1973 to July 1975, analytical data were produced to support the design, fabrication, and ground and flight testing of DC-9 Refan airframe/nacelle hardware with prototype JT8D-109 engines.

The production JT8D-109 engine has a sea level static, standard day bare engine takeoff thrust of 73 840 N (16,600 lb). Installation of the JT8D-109 results in an operational weight increase of 1 041 kg (2,294 lb) and an aft operational empty weight c.g. shift of 6 to 7 percent M.A.C.. At sea level standard day conditions the additional thrust of the JT8D-109 results in 2 040 kg (4500 lb) additional takeoff gross weight capability for a given field length. Range loss of the DC-9 Refan airplane for long range cruise at 10 668 m (35,000 ft) and payloads illustrating takeoff-gross-weight and fuel capacity limited cases are 352 km (190 n.mi.) and 54 km (29 n.mi.) respectively. Range loss for 0.78 Mach number cruise at 9 144 m (30,000 ft) and payloads same as above are 326 km (176 n.mi.) and 50 km (27 n.mi.) respectively.

The Refan airplane demonstrated stall, static longitudinal stability, longitudinal control, longitudinal trim, air and ground minimum control speeds. and directional control characteristics that were similar to the DC-9-30 production airplane and did comply with production airplane airworthiness requirements. Cruise performance, with prototype JT8D-109 engines, showed the range factor 5 to 7 percent lower than an equivalent JT8D-9 powered production DC-9-30. Climb performance shows an 8 percent improvement in second segment and approach limiting weights and a 5 percent improvement in enroute limiting weight. Thrust reverser performance was demonstrated at speeds below the operational cutback speed 30.87 m/s (60 knots) with acceptable engine operation.

Structural and dynamic ground test, flight test and analytical results substantiate Refan Program requirements that the nacelle, thrust reverser hardware, and the airplane structural modifications are flightworthy and certifiable and that the airplane meet flutter speed margins.

Estimated unit cost of a DC-9 Refan retrofit program is 1.338 million in mid-1975 dollars with about an equal split in cost between airframe and engine.

17 Key Words (Suggested by Author(s))	18 Distribution Statement
Stability and Control, Retrofit and Economics, Structural and Aerodynamic damping, DC-9 Refan Flight Test, JT8D-109 Prototype Engines	Unclassified-Unlimited

19. Security Classif (of this report)	20 Security Classif (of this page)	21 No of Pages	22 Price*
Unclassified	Unclassified	238	

* For sale by the National Technical Information Service Springfield Virginia 22151

TABLE OF CONTENTS

	Page
SUMMARY	1
INTRODUCTION	3
AIRPLANE DESCRIPTION	5
ENGINE PERFORMANCE	9
AIRPLANE PERFORMANCE	21
AIRPLANE STABILITY AND CONTROL	37
Stall Characteristics	39
Static Longitudinal Stability	43
Longitudinal Control	47
Longitudinal Trim	51
Minimum Control Speed	57
AIRPLANE/ENGINE PERFORMANCE	61
Two Engine Takeoff Acceleration	63
Climb Performance	65
Cruise Performance	67
Drag Polars All Engine	71
Fuel Supply	73
Engine Starting	77
Flight Test Prototype Engine Performance	81
Installed engine calibration	81
Thrust lapse rate	100
Engine operation during MCL climb	100
Engine performance during transients	104
Engine characteristics during airplane maneuvers	112

Page

Engine Component Cooling..... 113

Constant Speed Drive Oil and Generator Cooling..... 121

Engine Fire Detector System..... 127

Engine Vibration Measurement..... 131

Thrust Reverser..... 155

Ice Protection..... 163

Auxiliary Power Plant..... 169

AIRPLANE STRUCTURAL INTEGRITY AND DYNAMICS..... 179

Structural Analyses..... 181

Pylon/Fuselage..... 182

Nacelle..... 192

Thrust reverser..... 196

Flutter Analyses..... 207

Ground Vibration Test Modes and Frequencies..... 209

Structural and Aerodynamic Damping..... 213

RETROFIT AND ECONOMICS ANALYSIS..... 215

SUMMARY OF RESULTS AND CONCLUSIONS..... 223

REFERENCES..... 227

SYMBOLS..... 229

SUMMARY

The purpose of the DC-9 Refan Program was to establish the technical and economic feasibility of reducing the noise of existing JT8D powered DC-9 aircraft. The Refan Program was divided into two phases.

Phase I provided engine and nacelle/airplane integration definition documents for installation of the JT8D-109 engine on the DC-9 series airplane, prepared preliminary design of nacelle and airplane modifications, conducted model tests for design information, and prepared analyses for economic and retrofit considerations. Phase II included detail analyses, hardware design and fabrication, and flight testing to substantiate the design and obtain flyover noise data.

The JT8D-109 engine, a derivative of the basic Pratt and Whitney JT8D-9 turbofan engine with the minimum treatment acoustic nacelle was selected in Phase I for the design, analysis, construction, and flight testing during Phase II.

The work described in this report documents the performance and analysis effort carried out under Phase II, Contract NAS 3-17841.

The sea level static, standard day bare engine takeoff thrust for the production JT8D-109 is 73 840 N (16,600 lb); relative to the JT8D-9 engine the takeoff thrust is 14.5 percent higher, the cruise TSFC at 9 144 m (30,000 ft), M = 0.80 and 19 571 N (4,400 lb) thrust is 1.5 percent lower, and the maximum cruise thrust available at the same Mach number and altitude is 4 percent higher.

The installation of the JT8D-109 engine results in an operational weight increase of 1 041 kg (2,294 lb) and an aft operational empty weight center of gravity shift of 6 to 7 percent M.A.C. At sea level standard day conditions the additional thrust of the JT8D-109 results in 2 040 kg (4,500 lb) additional takeoff gross weight capability for a given field length.

The range change of the DC-9 Refan relative to the production DC-9 airplane for long range cruise at 10 668 m (35,000 ft) and payloads illustrating takeoff-gross-weight and fuel capacity limited cases are -352 km (-190 n.mi.) and -54 km (-29 n.mi.) respectively. Also, the range changes for 0.78 Mach number cruise at 9 144 m (30,000 ft) and payloads same as above are -326 km (-176 n.mi.) and -50 km (-27 n.mi.) respectively.

Although the JT8D-109 engine has slightly better specific fuel consumption characteristics, this gain is offset by the increased weight of the engine, nacelle, and airframe modification hardware, and for typical stage lengths the actual fuel costs are about the same. At longer stage lengths the Refan airplane would burn slightly more fuel.

The Refan airplane demonstrated stall, static longitudinal stability, longitudinal control, longitudinal trim, air and ground minimum control speeds, and directional control characteristics similar to the production DC-9-30 and did comply with production airplane airworthiness requirements.

The climb performance of the DC-9 Refan airplane relative to the production DC-9-30 shows an 8 percent improvement in second segment and approach limiting weights and a 5 percent improvement in enroute limiting weight. The cruise performance data from the DC-9 airplane powered with JT8D-109 prototype engines showed the range factor from 5 to 7 percent lower than an equivalent JT8D-9 powered DC-9-30 production airplane. The engine nacelle compartment ventilation, subsystem component, generator, and constant speed drive cooling systems were demonstrated satisfactorily for ground and inflight conditions.

Thrust reverser performance was demonstrated at speeds below the operational cutback speed of 30.87 m/s (60 knots) with acceptable engine operation. The cowl ice protection system flight evaluation shows that the system provides ice protection performance which is equal to or in excess of predictions; and the auxiliary power plant test data indicated no unusual starting or operating characteristics.

The DC-9 Refan airplane structural and dynamic analytical results compared to ground and flight test data substantiate program requirements that the nacelle, thrust reverser hardware, and the airplane structural modifications are flightworthy and certifiable and that the Refan airplane meet flutter speed margins.

The retrofit and economic analysis based on the retrofit of 550 airplanes, indicate that the estimated unit cost of the retrofit program is 1.338 million in mid-1975 dollars with about an equal split in cost between airframe and engine.

INTRODUCTION

The continuing growth of the air transportation industry with resulting increased numbers of operations from established or emerging airports coupled with increased population density near airports, has resulted in an effort to control human exposure to airplane noise. The government and industrial organizations have therefore agressively supported programs directed at producing airplane and engine designs offering meaningful reductions in airport community noise.

During the late 1960's research related to the noise within the engine itself and research related to absorptive materials were sufficiently refined to have been applied to the development of the quieter high bypass ratio turbofan power plants for the new generation of wide-body commercial airplanes.

However, a large portion of the existing and expanding fleet of standard bodied transports are powered by the JT3D or JT8D low bypass ratio engines. Since early retirement of these airplanes or re-engining with a totally new high-bypass ratio engine are not competitive in terms of timeliness or economics, two approaches to solve the noise problem of these low bypass ratio engines appear to be feasible.

One approach would be to apply the technology of sound absorbing materials (SAM) to nacelle treatment with possibly a jet noise suppressor. A number of government and industry studies have considered this approach (SAM) and standard body transports being delivered in the mid-1970's include this technology.

A second approach would be to incorporate the technology of the high-bypass ratio engines into the JT3D and JT8D family. This would require replacement of the present low bypass ratio engine fans with larger fans while maintaining the hardware and general operating characteristics of the core engine. This would result in a substantial reduction in jet exhaust noise, of particular interest for the JT8D engine, with the possibility of improved engine fuel consumption and a substantial improvement in thrust.

In August 1972, the NASA Lewis Research Center authorized the Douglas Aircraft Company, The Boeing Company, and Pratt and Whitney Aircraft to develop and establish the economic and technical feasibility of reducing noise by developing engine and airframe/nacelle modifications. The program covered the JT3D engine and the DC-8 and B-707 it powers and the JT8D engine and the DC-9, B-727 and B-737 it powers. At the end of approximately four and one-half months all effort on the JT3D was terminated. All subsequent studies were performed on a derivative of the Pratt and Whitney JT8D-9 engine designated the JT8D-109. The Douglas Aircraft Company Phase I effort is summarized in reference 1.

On the basis of the results of the Phase I effort the Douglas Aircraft Company was authorized on 30 June 1973 to proceed with a Phase II study that would include the nacelle/airplane design and construction, kit costs, ground compatibility tests, flight worthiness, flight engine/airplane performance and flyover noise tests.

This volume (Volume III) of the NASA Refan program Phase II final report contains the following:

1) A comparison of the performance and physical characteristics of the production JT8D-109 and JT8D-9 engines.

2) A comparison of the performance of the production DC-9-30 and the DC-9 Refan airplane with production JT8D-9 and JT8D-109 engines installed, respectively.

3) An evaluation of the stability and control characteristics of the DC-9 Refan airplane.

4) An evaluation of the DC-9 Refan airplane/engine performance with the two prototype JT8D-109 flight test engines installed.

5) A summary of the structural and dynamic analysis.

6) An evaluation of the results from ground tests that were conducted prior to flight testing and an evaluation and comparison of flight test data with analytical results.

7) An evaluation of the results from the structural and aerodynamic damping flight tests.

8) A summary of the retrofit and economic analysis.

A summary of the design and construction, performance and analysis, and flyover noise test results for the DC-9 Refan flight demonstration airplane is presented in Volume I, reference 2.

The design effort that established the DC-9 Refan airplane flight demonstration configuration for the nacelle, pylon, thrust reverser, sub-systems, and fuselage including hardware construction is reported in Volume II, reference 3.

FAR Part 36 noise levels, EPNL and dB(A) - distance maps, noise contours, spectral studies on extra ground attenuation, turbulence, ground reflection, noise source levels, static-to-flight predictions, and the engine/nacelle acoustical characteristics of the DC-9 Refan airplane are reported in Volume IV, reference 4.

This report contains both U.S. Customary and International System (SI) Units; however, all calculations and measurements were made using the U.S. Customary Units.

AIRPLANE DESCRIPTION

The DC-9 airplane is a low wing, two-engine, T-tail, short-to-medium range, commercial transport produced in five basic Series (10, 20, 30, 40 and 50 plus derivatives of those series). The engines are located at the rear of the airplane and mounted on pylons attached to the left and right side of the fuselage. Production models of the DC-9 are the -14/15, -15F, -20, -31, 32, -32F, 40, -50, the Air Force C-9A and the Navy C-9B. These models vary widely in takeoff gross weights, fuel tank arrangement, fuselage length, wing area and JT8D engine model (figure 1).

Figure 1 shows a simplified genealogy of the DC-9 family starting from the first model (Series 10) and showing the important changes made from model to model through the latest "stretched" versions. The most significant change in the DC-9 model was introduced with the initiation of the DC-9-30 Series. At that time, the fuselage was lengthened approximately 4.57 m (179 in), the wing span was increased 1.22 m (48 in) and full span leading edge slats were incorporated.

A production model DC-9-31 with a structurally modified fuselage, a new shorter span pylon, a new larger long duct nacelle and thrust reverser with the JT8D-109 engine installed was used for the DC-9 Refan flight demonstration (figure 2). The Refan airplane was operated at takeoff gross weights up to 49 032 kg (108,000 lb), and landing gross weights of 44 946 kg (99,000 lb).

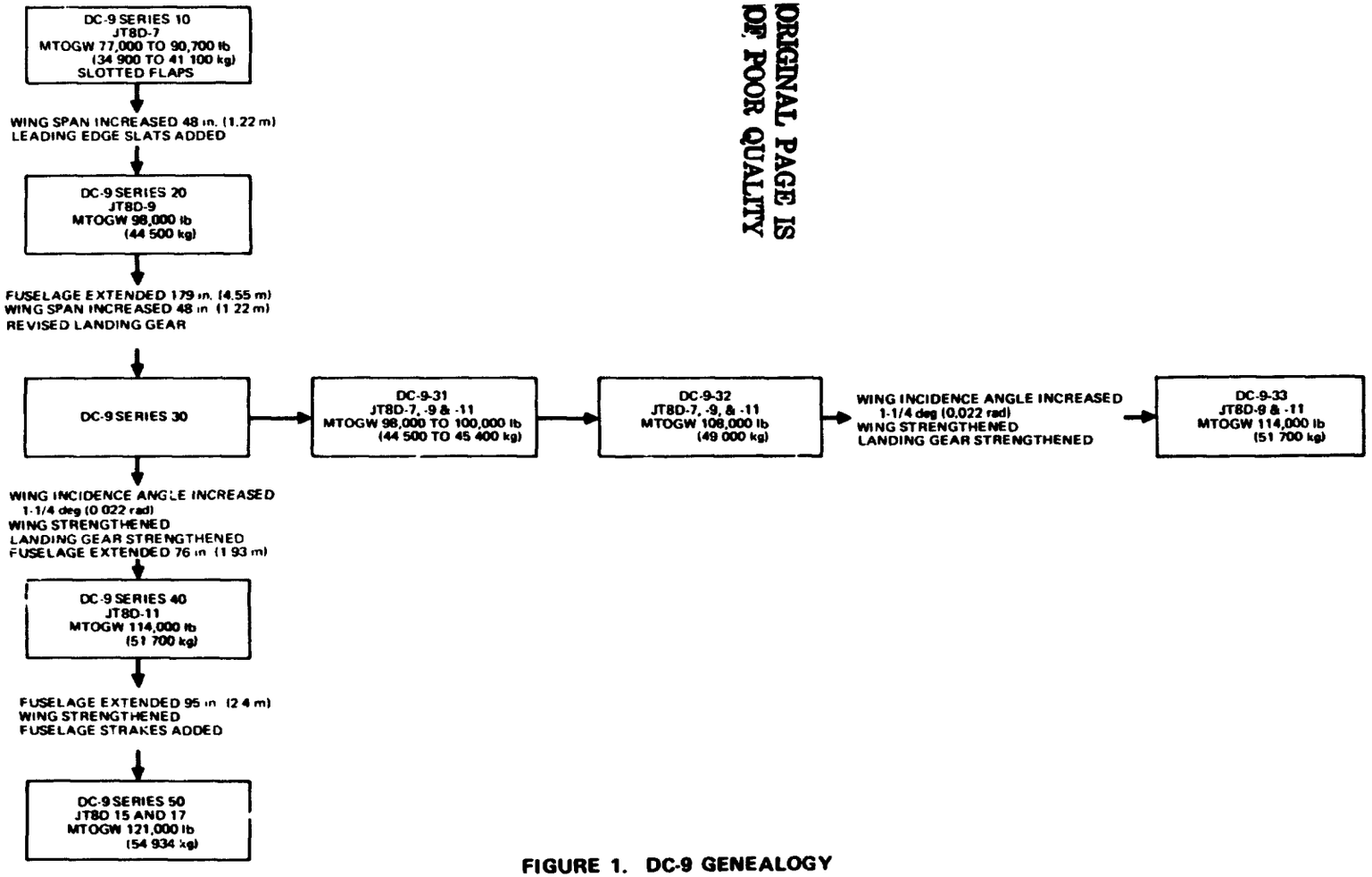

FIGURE 1. DC-9 GENEALOGY

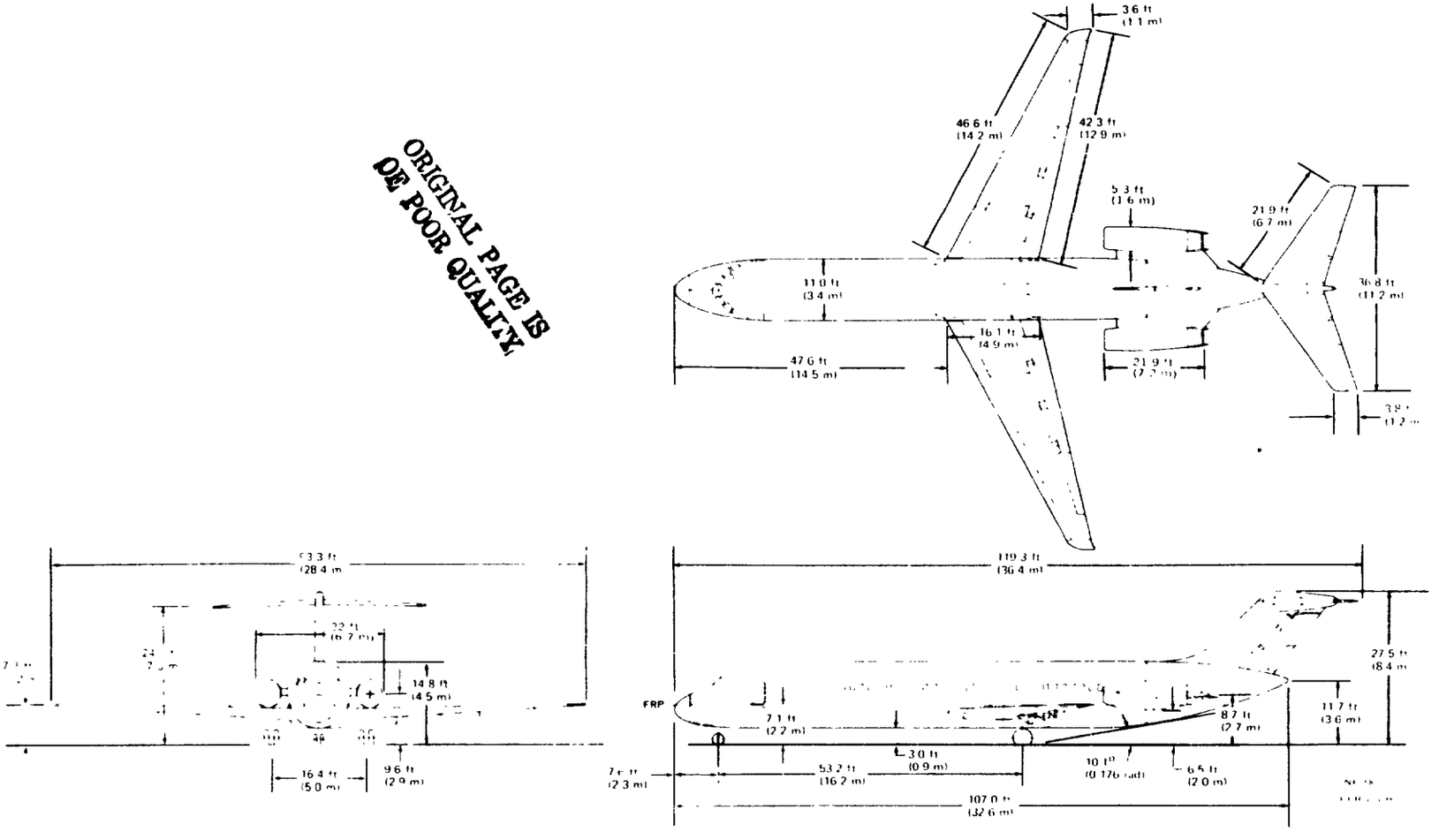

FIGURE 2. DC-9 REFAN THREE VIEW

ENGINE PERFORMANCE

The JT8D-109 engine is a derivative of the basic Pratt and Whitney Aircraft JT8D-9 turbofan engine. It is an axial flow two spool ducted turbofan engine with a mechanically coupled single stage fan and six low pressure compressor stages driven by a three stage turbine. The seven stage high pressure compressor is driven by a single stage turbine through concentric shafting. The burner section consists of nine separate chambers in an annular array. The turbine in temperature on a 15°C (59°F) day is 975°C (1789°F).

The annular fan duct delivers the fan air rearward where it is combined with the main engine air and discharged through a common jet nozzle. The compressor system generates a takeoff compression ratio of 15.5 and a bypass ratio of 2.12. A cross section comparison of the JT8D-109 and JT8D-9 engine and nacelle is depicted in figure 3.

The performance and physical characteristics of a production JT8D-109 and JT8D-9 are compared in table 1. The direct comparison of bare engine performance is based on conditions at the Pratt and Whitney Aircraft reference nozzle using a fuel lower heating value of 10 224 kg cal/kg (18,400 Btu/lb) (figure 4 and 5).

Figures 6 and 7 show the Douglas Aircraft Company nozzle performance coefficients which were estimated by adjusting the Pratt and Whitney Aircraft nozzle performance in engine deck CCD 0287-01.0 with actual test data obtained during the JT8D-109 engine/nacelle hardware compatibility test conducted by Pratt and Whitney Aircraft in Hartford.

The Douglas Aircraft Company nozzle velocity coefficient for the takeoff condition is 0.978 and for the max cruise condition is 0.98[illegible] at 9 144 m (30,000 ft) and 0.80 M (figure 6). The discharge coefficient for the takeoff condition is 0.974 and for the max cruise condition is 0.989 at 9 144 m (30,000 ft) and 0.80 M (figure 7).

The installed engine performance of the production JT8D-109 and JT8D-9 engine is compared in figures 8 and 9. Performance comparisons between the JT8D-9 and JT8D-109 engines are shown for takeoff and cruise conditions. A direct comparison can be made between the two engine installations because of the identical reference nozzles and charging stations used by Pratt and Whitney Aircraft. The data presented include all installation effects for normal operation. The installation losses applied to the JT8D-9 and JT8D-109 engines include the following: Douglas inlet, fan and compressor bleeds, power extraction, Douglas nozzle loss and nacelle drag.

The inlet total-pressure loss was based in part on available experimental data at static conditions (inlet reciprocal mass-flow ratio, $A_i/A_0 = 0$). The experimental data are shown in figure 10 for both the Douglas inlet and the Pratt and Whitney Aircraft bellmouth and were obtained from inlet pressure measurements during the Pratt and Whitney ground tests.

Figure 11 shows the inlet loss coefficient as a function of reciprocal mass-flow ratio, A_i/A_0. The loss coefficent curve passes through the

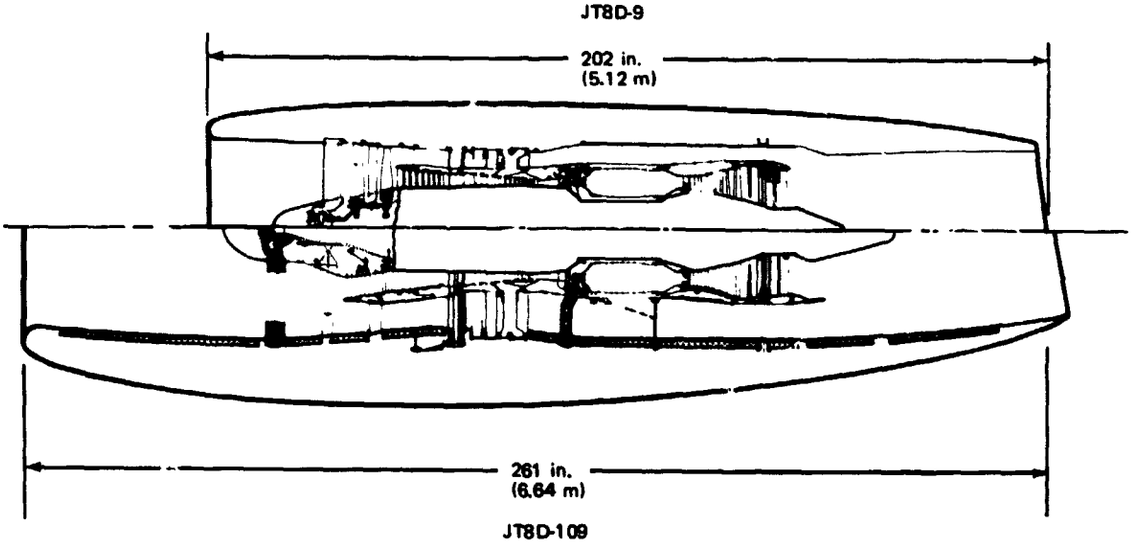

FIGURE 3. JT8D ENGINE/NACELLE COMPARISON

TABLE 1

BARE ENGINE CHARACTERISTICS COMPARISON

		JT8D-9*	JT8D-109**
TAKEOFF THRUST (SEA LEVEL STATIC, STANDAR DAY)	lb (N)	14,500 (64 500)	16,600 (73 840)
FAN TIP SPEED, SEA LEVEL STATIC TAKEOFF	ft/s (m/s)	1,420 (432.8)	1,567 (477.6)
BYPASS RATIO		1.05	2.12
MAXIMUM AIRFLOW	lb/s (kg/s)	340 (154)	510 (231)
FAN PRESSURE RATIO		1.97	1.66
MAXIMUM CRUISE THRUST –30,000 ft (9 144 m), 0.80 M	lb (N)	4,540 (20 195)	4,720 (20 996)
CRUISE TSFC – 30,000 ft (9 144 m), 0.80 M, 4,400 lb (19 571 N) THRUST	lb/hr/lb (kg/hr/N)	0.793 (0.0809)	0.781 (0.0796)
FAN TIP DIAMETER	in. (m)	40.5 (1.03)	49.2 (1.25)
OVERALL BARE ENGINE LENGTH (LESS SPINNER)	in. (m)	119.97 (3.047)	127.19 (3.231)
BARE ENGINE WEIGHT	lb (kg)	3,217 (1 460)	3,822 (1 734)

*BASED ON CCD 0219-01.1 WITH P&WA NOZZLE

**BASED ON CCD 0287-01.0 WITH P&WA NOZZLE

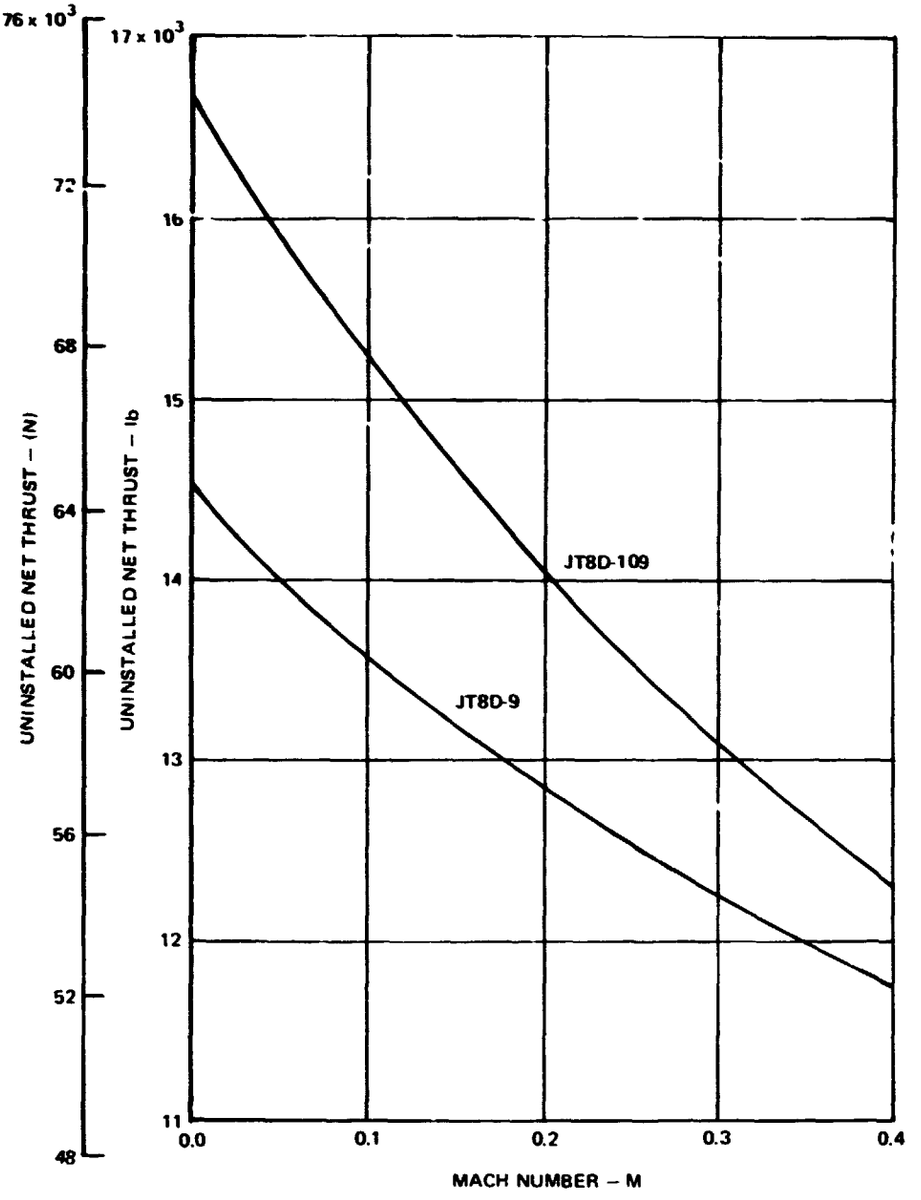

FIGURE 4. DC-9 REFAN BARE ENGINE PERFORMANCE, PRATT AND WHITNEY NOZZLE, TAKEOFF, SEA LEVEL STANDARD DAY

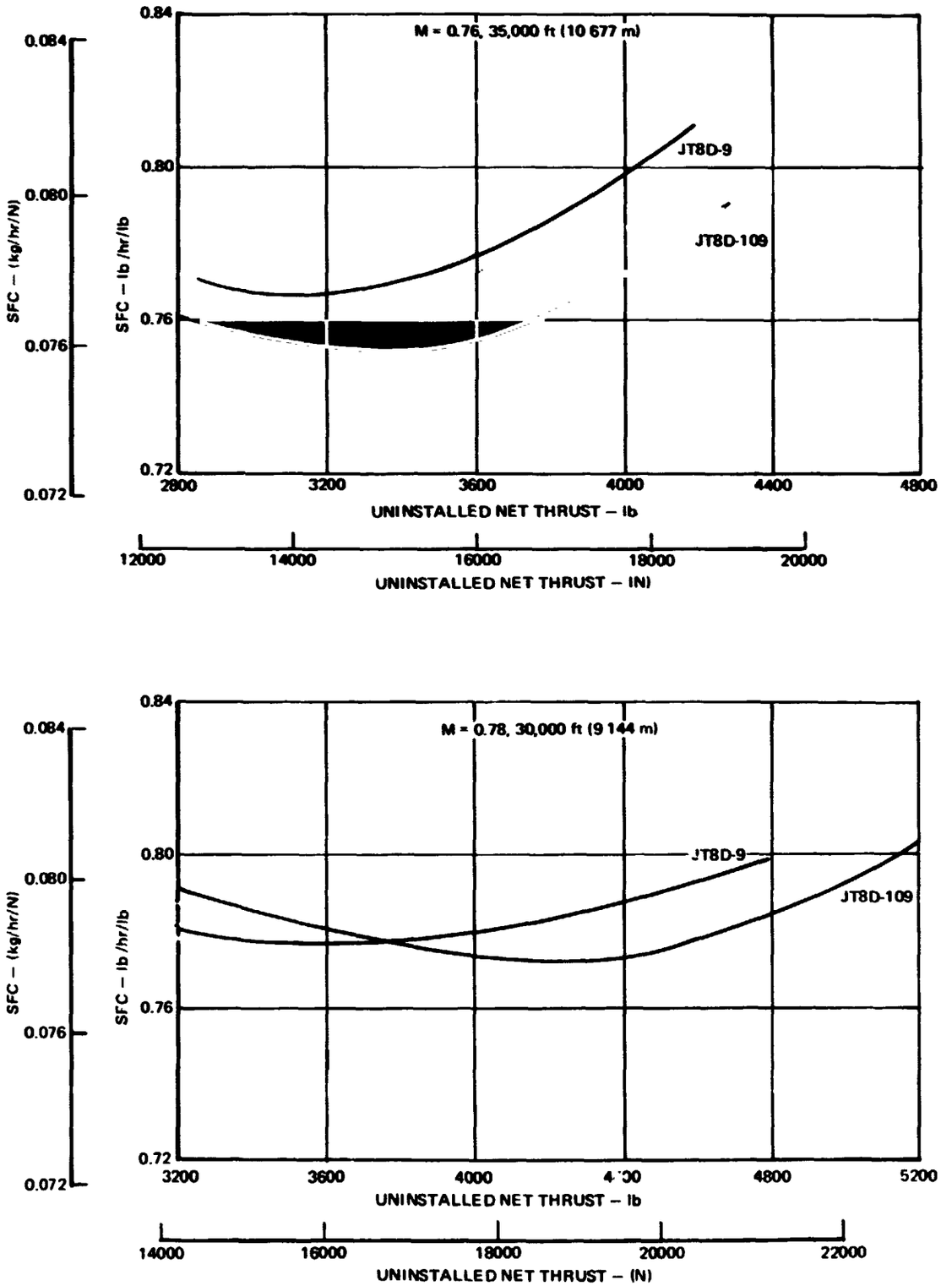

FIGURE 5. DC-9 REFAN BARE ENGINE PERFORMANCE, PRATT AND WHITNEY NOZZLE, STANDARD DAY, CRUISE

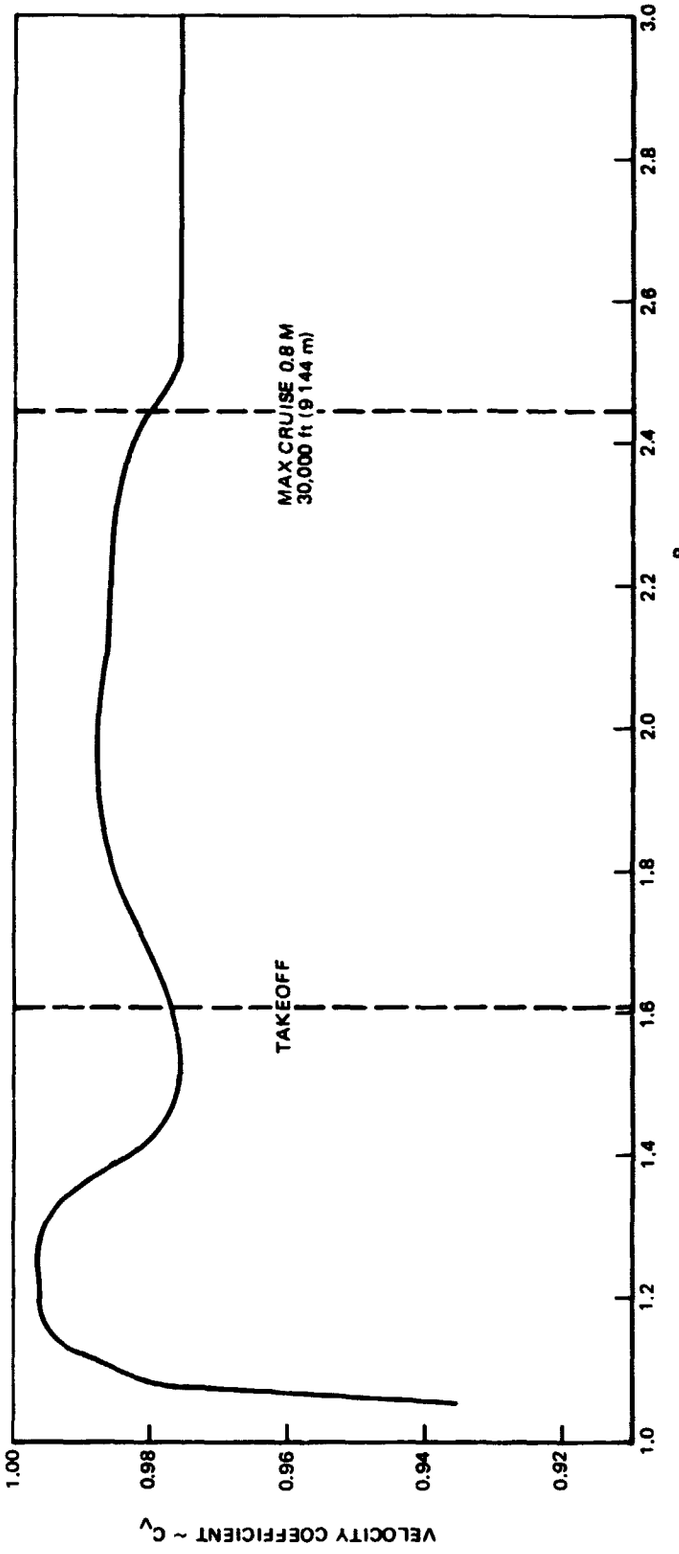

FIGURE 6. JT8D-109 ESTIMATED NOZZLE VELOCITY COEFFICIENT

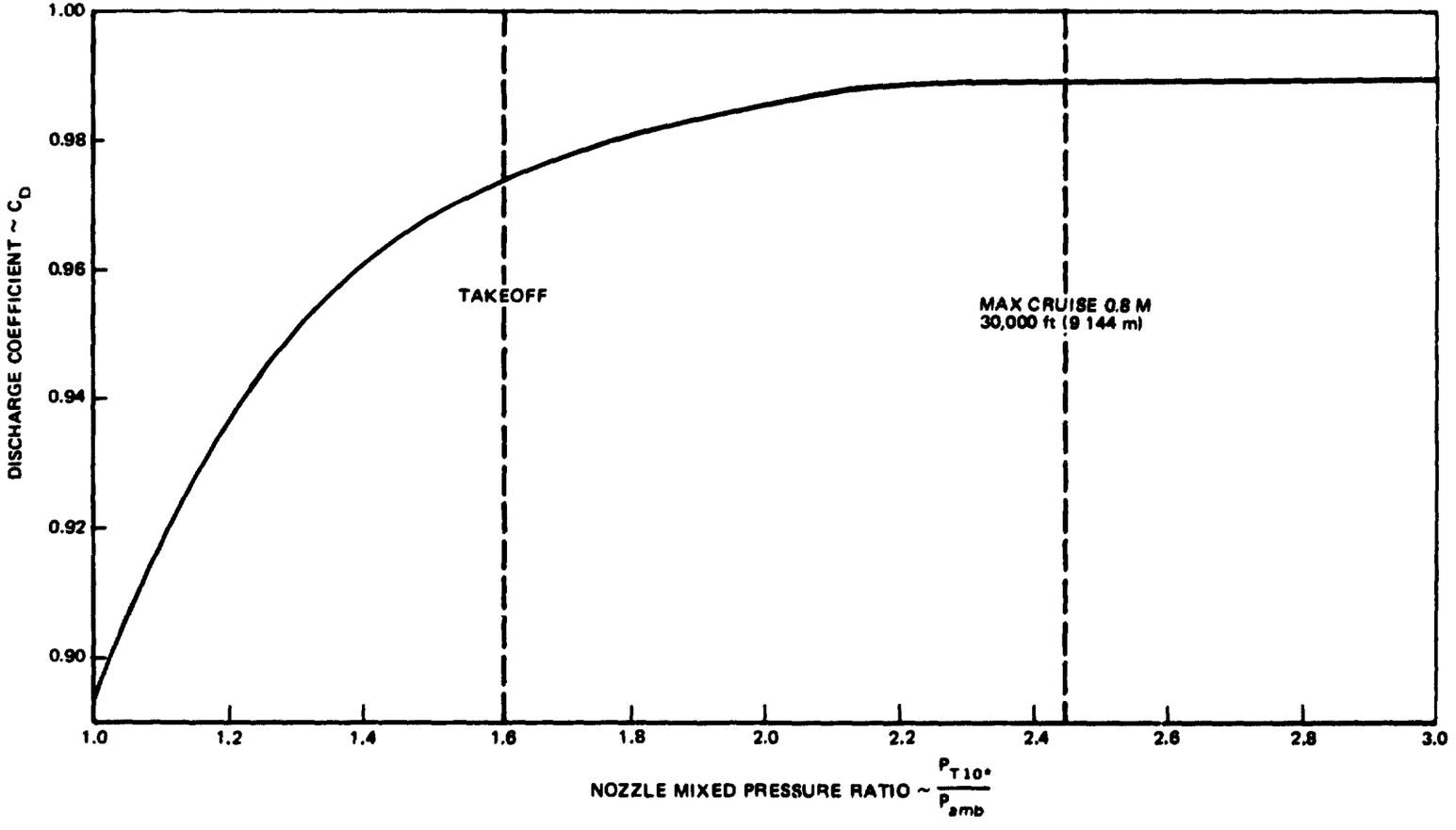

FIGURE 7. JT8D-109 ESTIMATED NOZZLE DISCHARGE COEFFICIENT

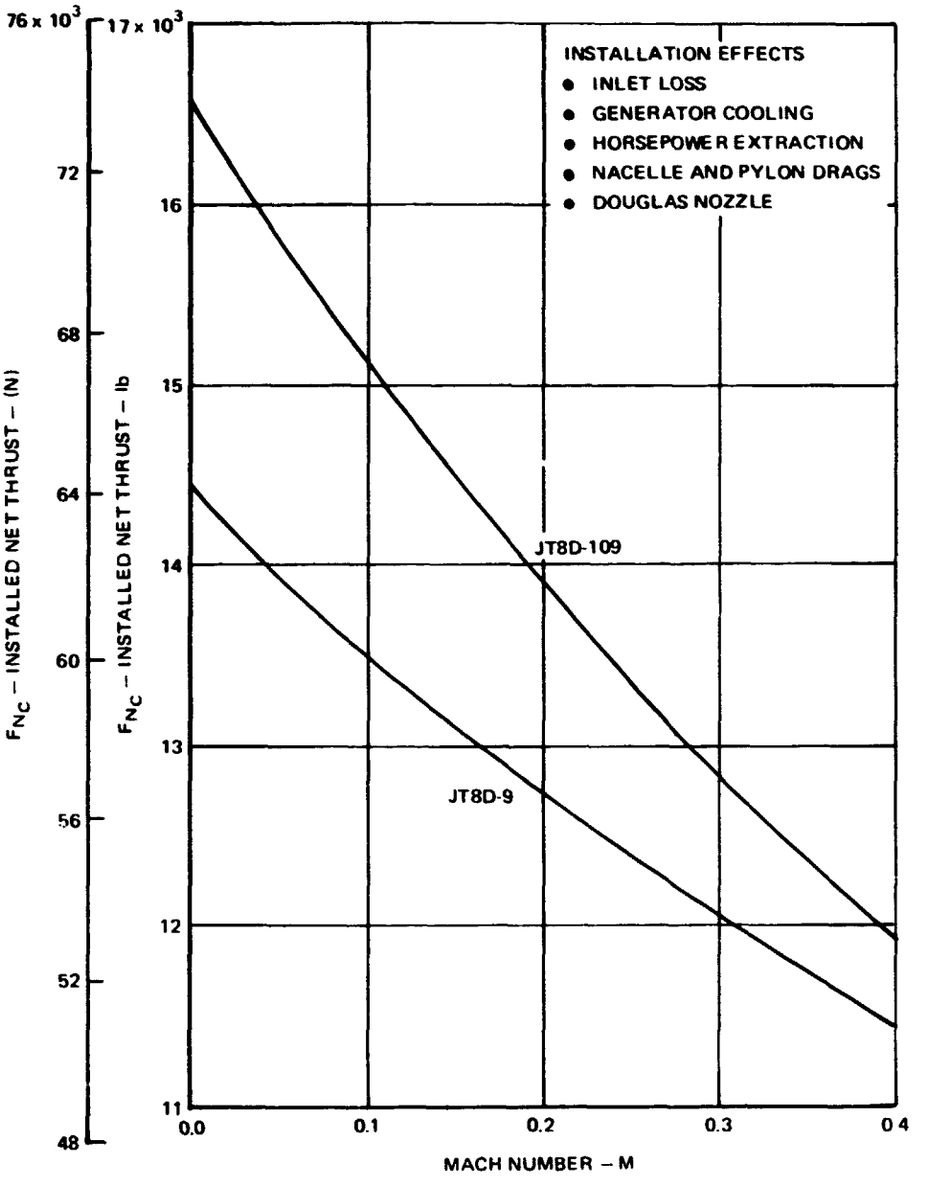

FIGURE 8. DC-9 REFAN INSTALLED ENGINE PERFORMANCE, TAKEOFF, SEA LEVEL, STANDARD DAY

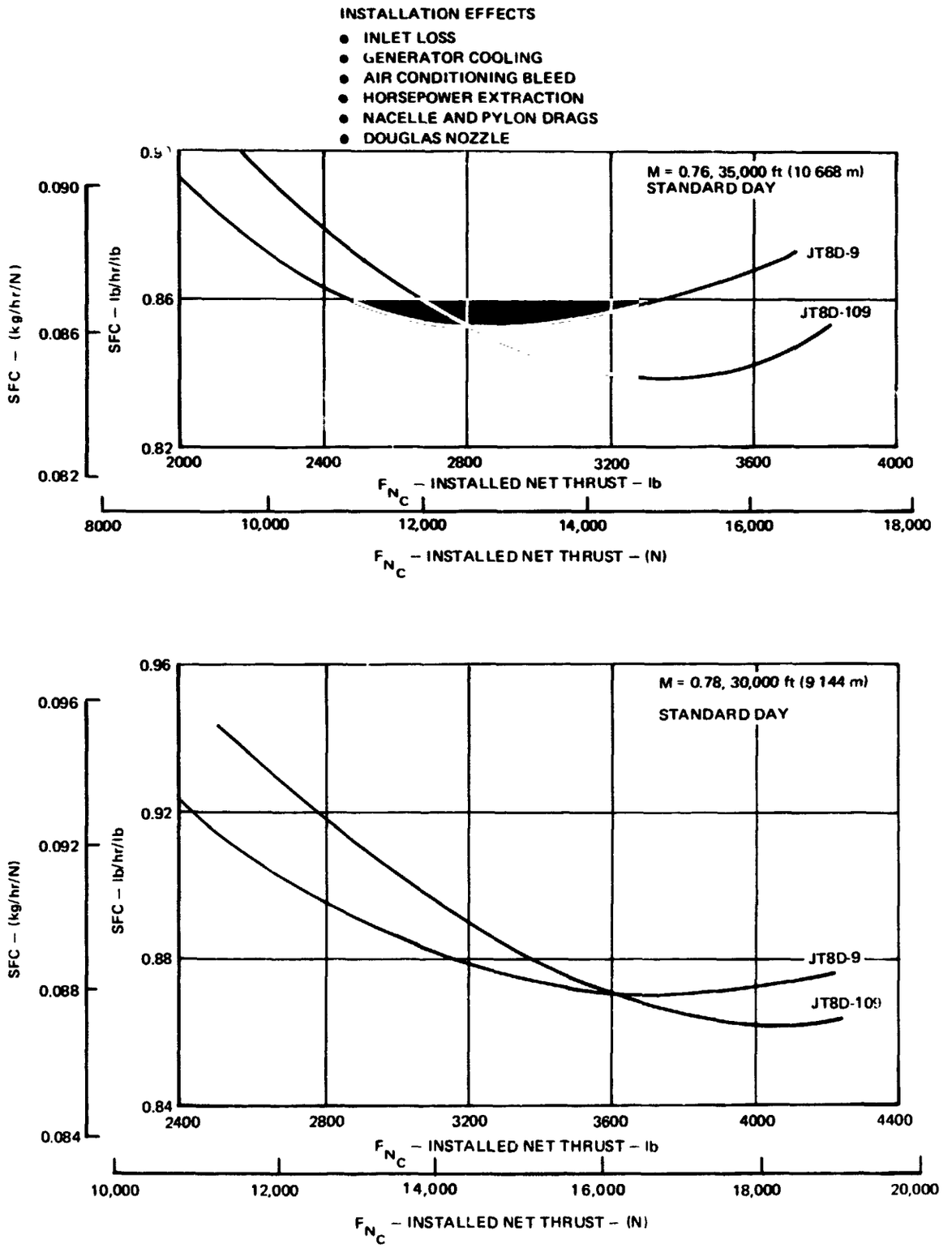

FIGURE 9. DC-9 REFAN INSTALLED CRUISE PERFROMANCE

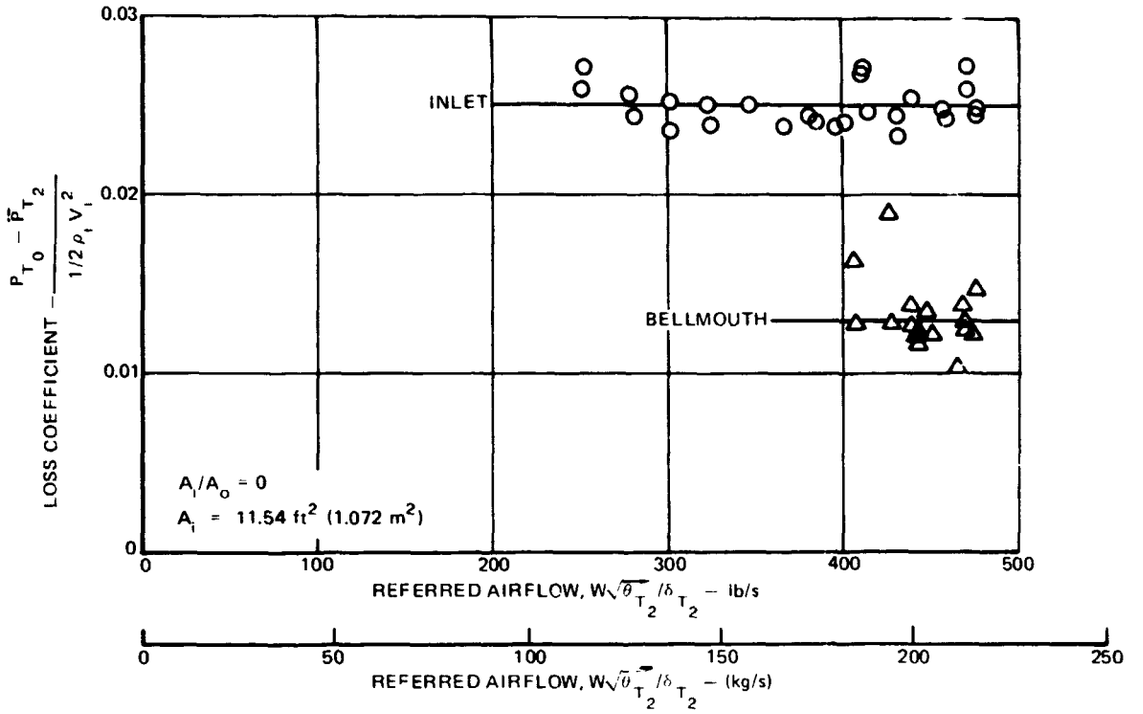

FIGURE 10. DC-9 REFAN INLET LOSS COEFFICIENT FROM GROUND TEST DATA

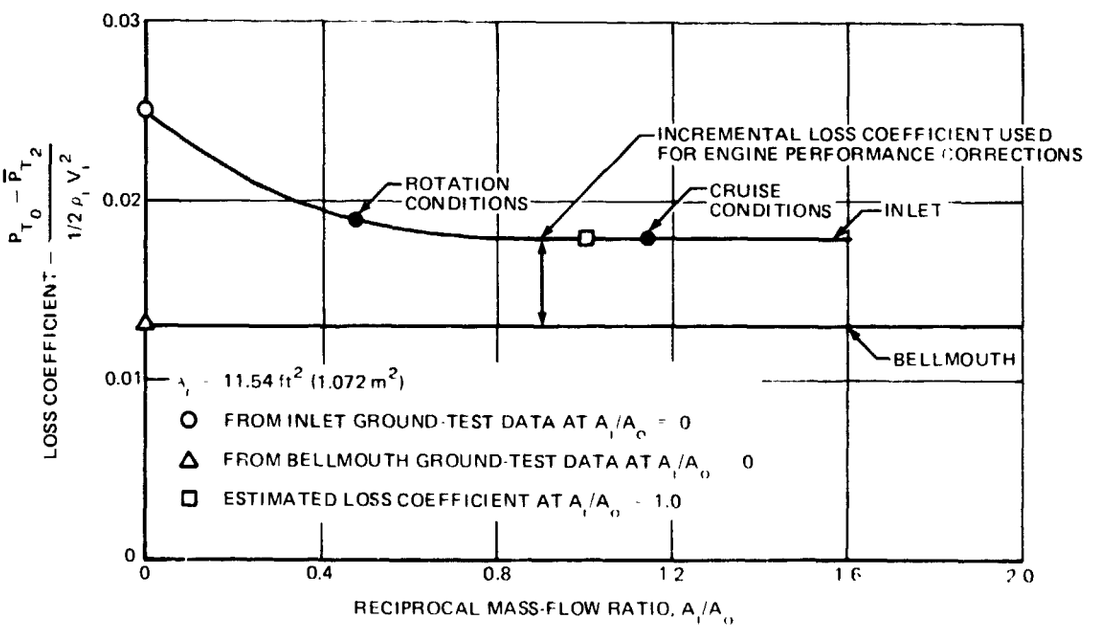

FIGURE 11. DC-9 REFAN INLET LOSS COEFFICIENT vs RECIPROCAL MASS-FLOW RATIO

experimental level at A_i/A_0 = 0 and through an analytical estimate level at A_i/A_0 = 1.0. The analytical estimate was made by calculation of the internal drag coefficient of the inlet and then conversion of the drag coefficient into an equivalent total-pressure loss coefficient. The decreasing level of loss-coefficient with increasing A_i/A_0 is due to the diminishing lip loss as the size of the engine airflow streamtube at free stream conditions, A_0, approaches the size of the inlet, A_i. The effect of variables other than reciprocal mass-flow ratio (inlet angle of attack and engine airflow) on inlet loss coefficient is not significant for the DC-9 operating envelope.

Bare engine performance demonstrations are made with a bellmouth installed and no correction is made by the engine manufacturer for bellmouth loss. Therefore, only the difference between the inlet and bellmouth loss levels shown in figure 11 is applied for the calculation of installed engine performance.

Table 2 compares (at the same conditions) the production DC-9-30 engine installation losses for a typical takeoff condition of Mach number 0.27, sea level standard day with the DC-9 Refan engine installation losses. The installation loss comparison for a typical high speed cruise is shown in table 3. The cruise conditions are as follows: Mach number 0.78, altitude of 9 144 m (30,000 ft) and an installed thrust of 16 014 N (3,600 lb) per engine.

TABLE 2

PRODUCTION ENGINE INSTALLATION LOSS COMPARISON

TAKEOFF

M = 0.27, Sea Level, Standard Day

ENGINE			JT8D-9	JT8D-109
	F_N (PWA RERERENCE NOZZLE)	lb (N)	12,400 (55,154)	13,375 (59 490)
$\frac{\Delta FN}{FN}$: THRUST CHANGE DUE TO	Cg (DOUGLAS NOZZLE COEFFICIENT)		-.0043	-.0024
	INLET LOSS		0.0	-.0040
	GENERATOR COOLING AND POWER EXTRACTION		-.0003	-.0024
	NACELLE AND PYLON DRAG		-.0094	-.0098
	TOTAL		-.0140	-.0186
	FNC (INSTALLED NET THRUST)	lb (N)	12,225 (54 375)	13,125 (58 378)

$$FNC = FN \times \left(1 + \frac{\Delta FN}{FN}_{Total}\right)$$

TABLE 3

PRODUCTION ENGINE INSTALLATION LOSS COMPARISON

TYPICAL HIGH SPEED CRUISE

FNC = 3,600 lb (16 014 N), M = 0.78, ALT = 30,000 ft. (9 144 m), Standard Day

		$\frac{\Delta FN}{FN}$ - THRUST CHANGE DUE TO INSTALLATION		$\frac{\Delta SFC}{SFC}$ - SFC CHANGE DUE TO INSTALLATION	
ENGINE		JT8D-9	JT8D-109	JT8D-9	JT8D-109
FN (PWA REFERENCE NOZZLE)	lb (N)	4,035 (17 947)	4,180 (18 592)		
SFC (PRATT AND WHITNEY REFERENCE NOZZLE)	lb/hr/lb (kg/hr/N)			.780 (.080)	.773 (.079)
Cg (DOUGLAS NOZZLE COEFFICIENT)		-.0056	-.0008	+.0056	-.0004
INLET LOSS		0.0	-.0041	0.0	+.0015
BLEED AND POWER EXTRACTION		-.0292	-.0462	+.0267	+.0295
NACELLE AND PYLON DRAGS		-.0735	-.0872	+.0795	+.0956
TOTAL		-.1083	-.1383	+.1118	+.1262
FNC (INSTALLED NET THRUST)	lb (N)	3,600 (16 014)	3,600 (16 014)		
SFCC (INSTALLED SFC)	lb/hr/lb (kg/hr/N)			0.870 (0.089)	0.870 (0.089)

$$FNC = FN \times \left(1 + \frac{FN}{FN\ Total}\right); \quad SFCC = SFC \times \left(1 + \frac{SFC}{SFC\ Total}\right)$$

AIRPLANE PERFORMANCE

The installation of the JT8D-109 engine results in an operational weight increase of 1 041 kg (2,294 lb) and an aft Operational Empty Weight (OEW) center of gravity shift of 6 to 7 percent M.A.C. A weight breakdown is presented in table 4 for the production DC-9-32 and the DC-9 Refan airplane. The weight increase is split about equally between the airframe and the engine. Retrofit weights are approximately 91 kg (200 lb) less than the flight test weights because of the incorporation of weight reduction items that were identified during the hardware design and through analyses of the flight test results.

A review of the production DC-9 Series 30 "inservice fleet" was made to survey the loadability changes associated with the DC-9 Refan engine installation. Figure 12 indicates a wide range in OEW and center of gravity among basic customer configurations. These configurations include: single and mixed class passenger, convertible freighter, rapid change and all freighter. The ballast weight range and number of airplanes in each group is also shown. Most operators will avoid the use of ballast by choosing other methods, which are technically feasible, to correct any adverse balance effect on their operations.

During ground maintenance, some configurations may be subjected to a tip-over condition by ground gusts, snow loads and towing. For these airplane configurations several alternative corrections are readily available. One simple method, which is used at the Douglas Aircraft Company, is to install water ballast drums at hard points which exist on the fuselage nose section.

A comparison of the DC-9-32 FAA takeoff field length as a function of takeoff gross weight is shown in figure 13 for the JT8D-109 and JT8D-9 engine installations. At sea level standard day conditions the additional thrust of the JT8D-109 engine results in about 2 040 kg (4,500 lb) additional takeoff gross weight capability for a given field length of which about one half is the increased OEW and one half is increased payload. Also, the airplane is not second segment climb limited (i.e., no reduction in flap setting, with its resulting greater field length, required to meet the engine-out climb gradient requirement). The minimum field length, as limited by airplane minimum control speed, is indicated in figure 13. The Refan configuration has an increase in ground minimum control speed of 1.5 m/s (2.9 knots).

Comparisons of the DC-9-32 payload range characteristics for the JT8D-9 and JT8D-109 engine installations are presented in figures 14 through 17. High speed cruise is flown at 0.78 Mach number. Long range cruise is flown at the speed at which the specific range is 99 percent of the maximum nautical miles per pound attainable at the cruise weight. Payload range characteristics for high speed cruise and long range cruise at 10 668 m (35,000 ft) altitude are presented in figures 14 and 15 respectively. The payload range characteristics for high speed and long range cruise at 9 144 m (30,000 ft) are shown in figures 16 and 17. High speed climb and descent schedules are used with 0.78 Mach number cruise and long range climb and descent schedules are used with long range cruise. Domestic reserves are used with all cases. Maximum fuel capacity assumes the use of the 2 195 liter (580 gal) centerline fuel tank.

TABLE 4 - DC-9 PRODUCTION WEIGHT BREAKDOWN COMPARISON

	PRODUCTION CONFIGURATION			
	JT8D-9		JT8D-109	
	lb	(kg)	lb	(kg)
NOSE COWLS	212	(96)	624	(283)
ACCESS DOORS	436	(198)	550	(249)
THRUST REVERSERS	490	(222)	884	(401)
ENGINE MOUNTS	100	(45)	114	(52)
EXHAUST SYSTEMS	282	(128)	522	(237)
APRON STRUCTURES	120	(54)	146	(66)
PYLONS	450	(204)	514	(233)
FUSELAGE	84	(38)	110	(50)
ACCESSORIES	480	(218)	480	(218)
SYSTEMS	650	(295)	514	(233)
TOTAL WEIGHT PER AIRCRAFT	3,304	(1 498)	4,458	(2 022)
ENGINES 2 PER P&WA WEIGHT	6,504	(2 950)	7,644	(3 467)
MANUFACTURER'S EMPTY WEIGHT	55,216	(25 046)	57,510	(26 086)
OPERATIONAL EMPTY WEIGHT	59,076	(26 796)	61,370	(27 837)
MAXIMUM ZERO FUEL WEIGHT	87,000	(39 463)	87,000	(39 463)
MAXIMUM LANDING WEIGHT	99,000	(44 906)	99,000	(44 906)
MAXIMUM TAKEOFF WEIGHT	108,000	(48 988)	108,000	(48 988)
MAXIMUM TAXI WEIGHT	109,000	(49 442)	109,000	(49 442)

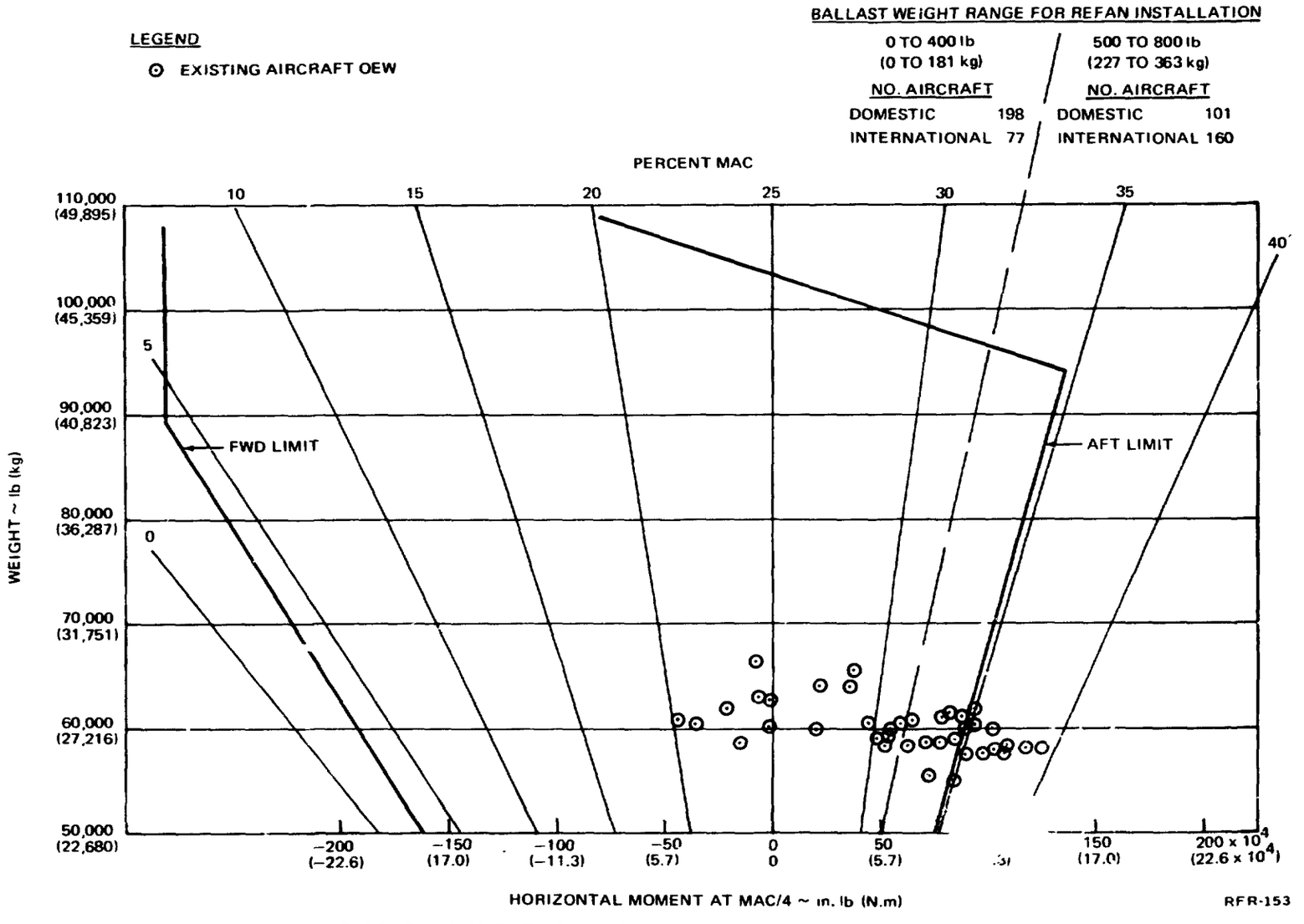

FIGURE 12. HORIZONTAL MOMENT AT MAC/4 VERSUS BASIC AIRCRAFT OEW FOR DC-9-30 SERIES

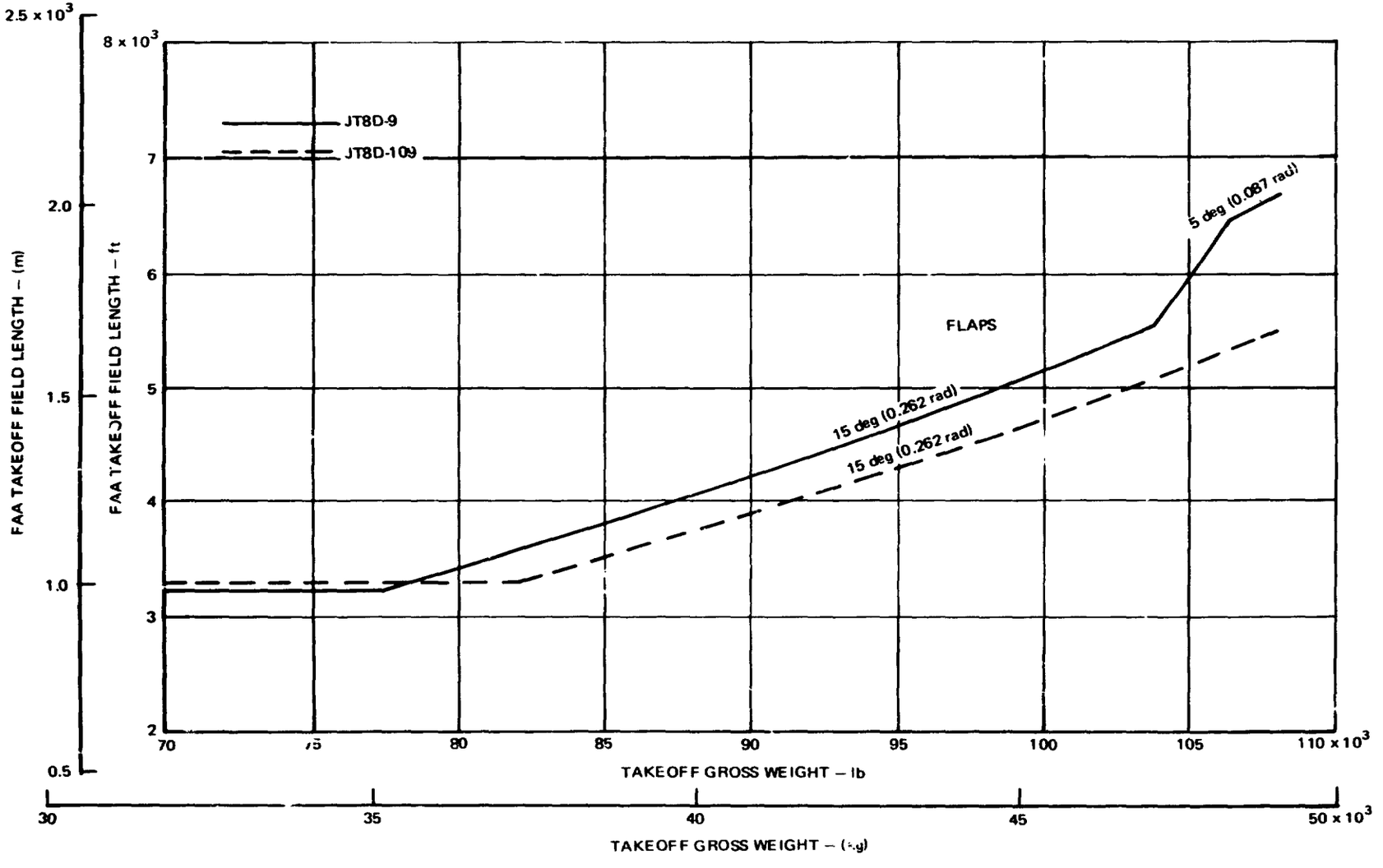

FIGURE 13. DC-9 REFAN TAKEOFF PERFORMANCE, SEA LEVEL, STANDARD DAY, BLEEDS OFF

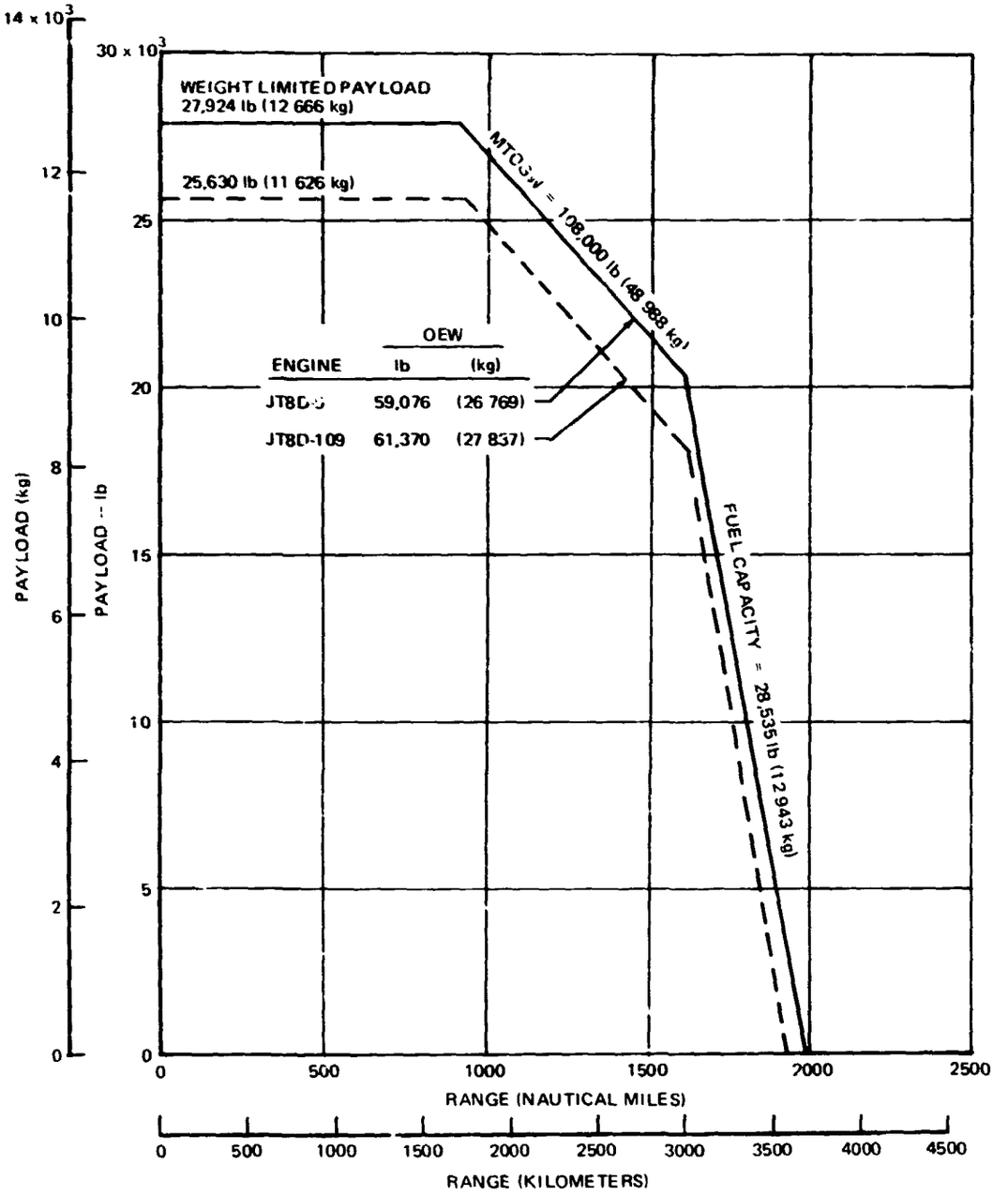

FIGURE 14. DC-9 REFAN PAYLOAD-RANGE CAPABILITY, CRUISE AT M = 0.78 AND hp = 35,000 ft (10 668 m)

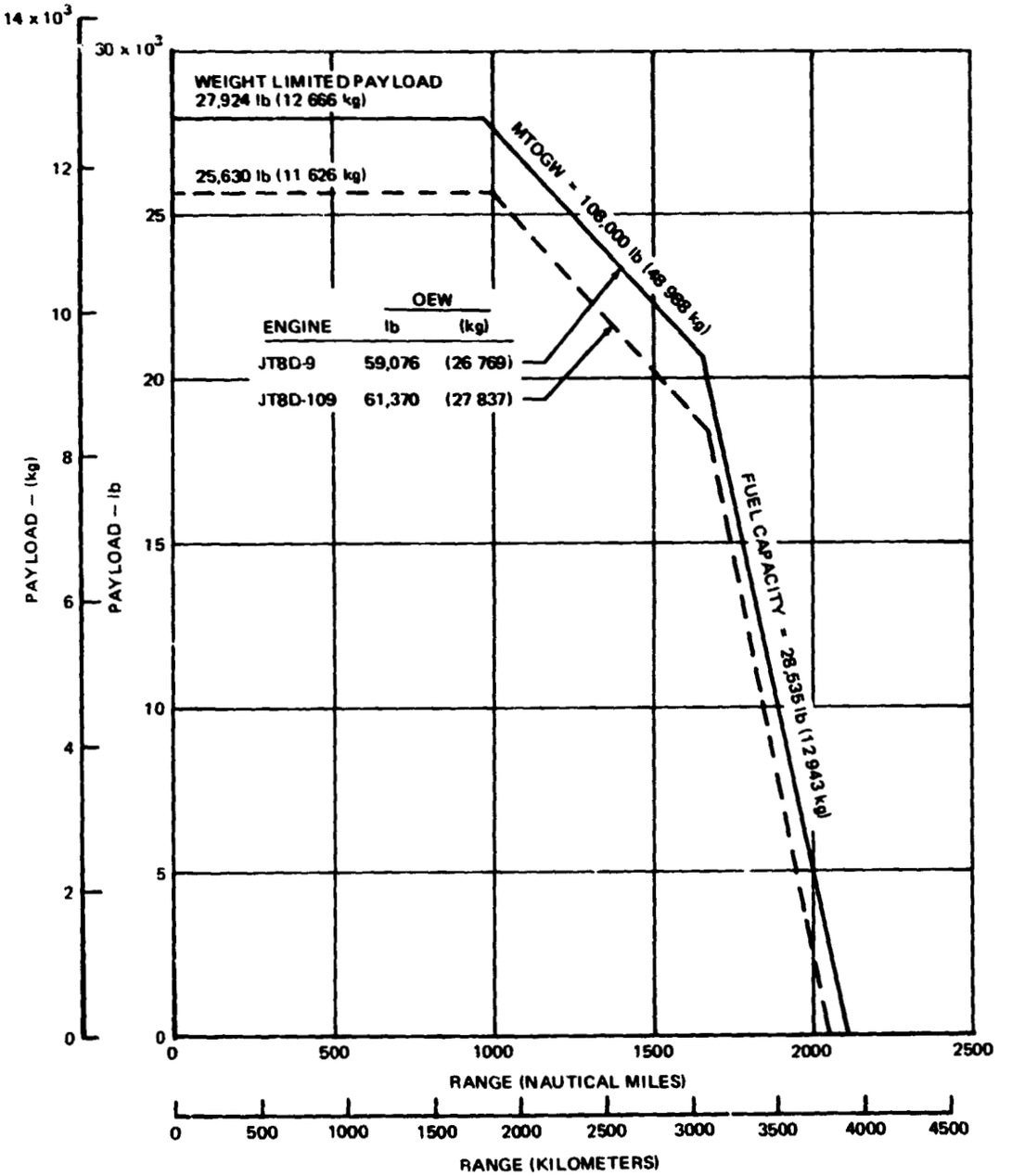

FIGURE 15. DC-9 REFAN PAYLOAD-RANGE CAPABILITY, LONG-RANGE CRUISE AT 35,000 ft (10 668 m)

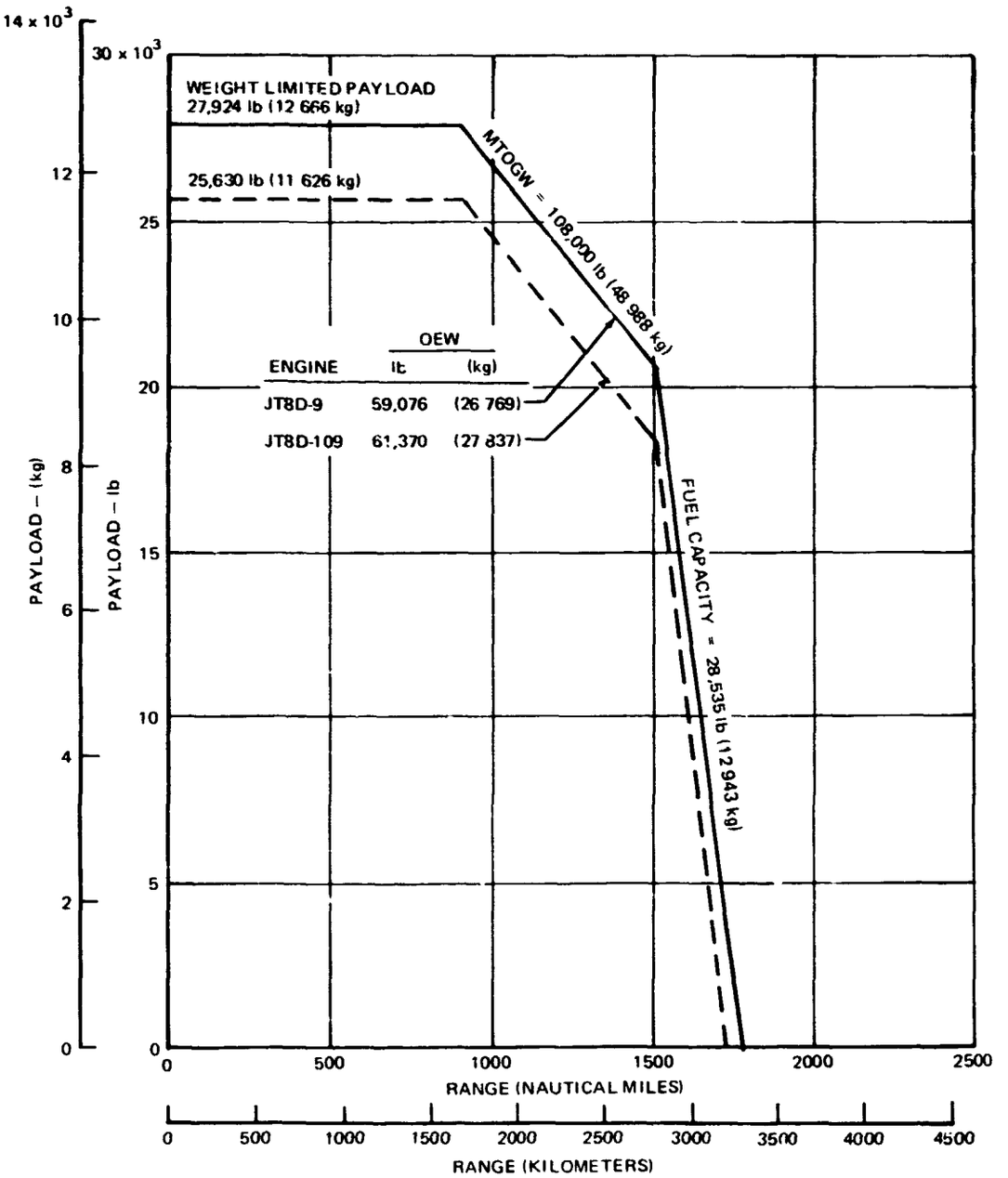

FIGURE 16. DC-9 REFAN PAYLOAD-RANGE CAPABILITY, CRUISE AT M = 0.78 AND hp = 30,000 ft (9 144 m)

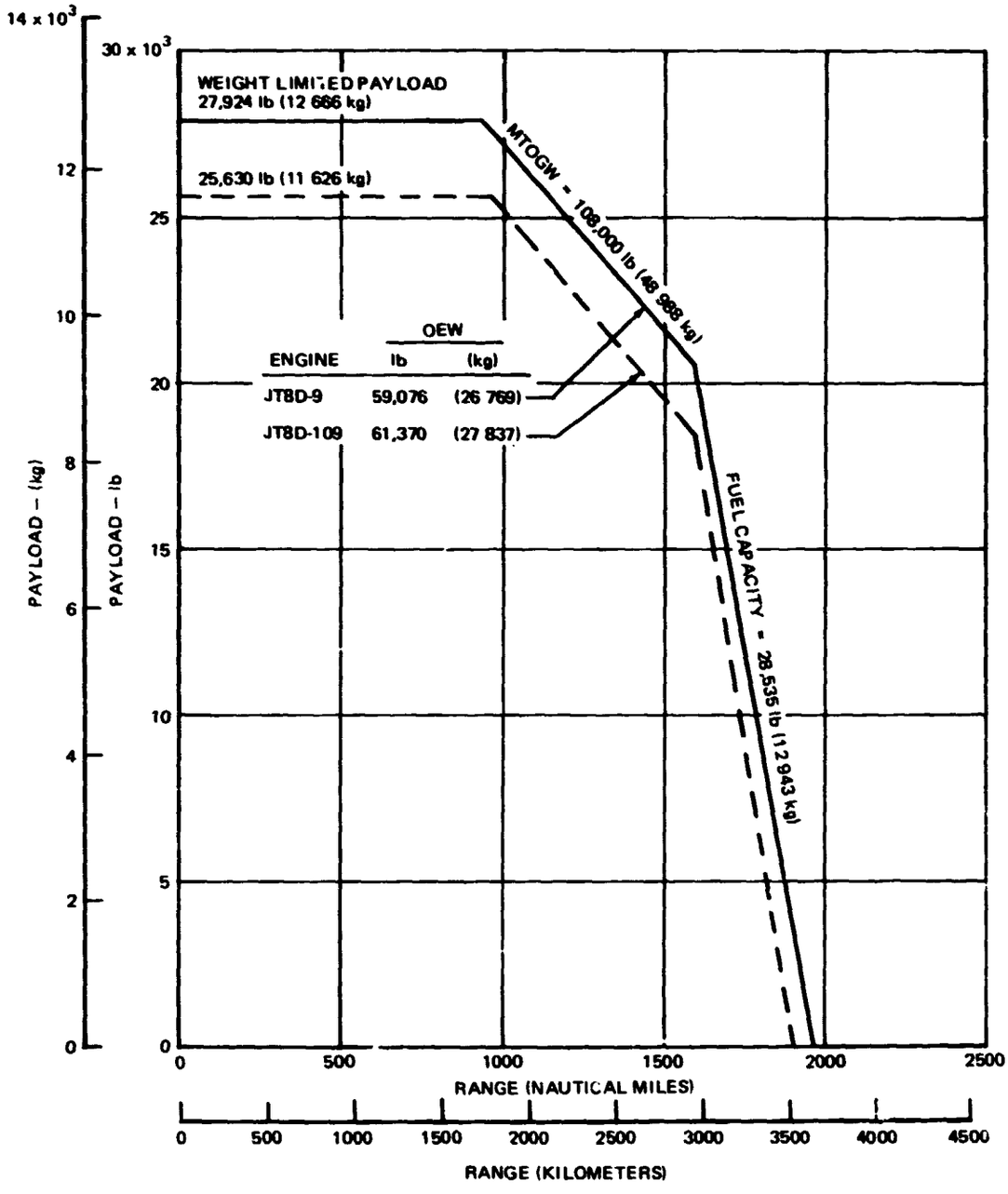

FIGURE 17. DC-9 REFAN PAYLOAD-RANGE CAPABILITY, LONG-RANGE CRUISE AT 30,000 ft (9 144 m)

Breakdowns of the maximum range increments due to weight and SFC differences between the JT8D-9 and JT8D-109 powered versions of the DC-9-32 are shown in tables 5 and 6 for long range cruise at 10 668 m (35,000 ft) and 0.78 Mach number cruise at 9 144 m (30,000 ft). The breakdowns are shown for two payloads, 10 433 kg (23,000 lb) and 6 804 kg (15,000 lb), to illustrate both takeoff-gross-weight limited and fuel-capacity limited cases. As shown, the SFC and drag changes between the engine installations result in a small range gain for the DC-9 Refan; but the additional OEW results in a moderate range loss when the airplane is fuel-capacity limited and a substantial range loss when the airplane is takeoff-gross-weight limited.

While payload-range shows the maximum capability of the airplane, another useful way of presenting airplane capability is by field length-range which shows how much range can be attained out of a given field length. This approach treats the field-length-limited cases. FAA takeoff field length as a function of range for the DC-9-32 with JT8D-109 and JT8D-9 engine installations is compared in figure 18. The range was determined using high speed cruise at 9 144 m (30,000 ft) and domestic reserves. The takeoff field lengths are for sea level, standard day conditions. Data are shown for two payloads, 6 804 kg (15,000 lb) and 10 433 kg (23,000 lb). At a given field length the additional takeoff thrust of the JT8D-109 engine installation results in about a 222 km (120 n.mi.) increase in range for a 6 804 kg (15,000 lb) payload and a 260 km (140 n.mi.) increase for a 10 433 kg (23,000 lb) payload.

The changes in significant performance parameters between the two configurations are presented in tables 7 through 10. These performance parameters include fuel burned, takeoff gross weight, block speed, and takeoff field length. Each table shows the performance increments between the JT8D-9 and JT8D-109 configurations for the typical mission 694 km (375 n.mi.), an intermediate mission 1 556 km (840 n.mi.), and the maximum range for the JT8D-109 configuration. The tables are for long range cruise at 10 668 m (35,000 ft) and 0.78 Mach number cruise at 9 144 m (30,000 ft) for a 6 804 kg (15,000 lb) typical mission payload and a 10 433 kg (23,000 lb) space limited payload.

Tables 7 through 10 show a slight increase in block fuel for the JT8D-109 powered DC-9 airplane. For the space limited payload of 10 433 kg (23,000 lb), the typical 694 km (375 n.mi.), intermediate 1556 km (840 n.mi.), and maximum range missions, tables 7 and 8 show an increase in block fuel of less than 1 percent for both long range cruise at 10 668 m (35,000 ft) and 0.78 Mach number cruise at 9 144 m (30,000 ft). For the typical mission payload 6 804 kg (15,000 lb) and range 694 km (375 n.mi.), tables 9 and 10 show less than 1 percent increase in block fuel for both the long range cruise and 0.78 Mach number cruise cases.

TABLE 5

RANGE CHANGE FOR THE JT8D-109 RELATIVE TO THE JT8D-9
LONG RANGE CRUISE AT 35,000 ft (10 668 m)

COMPONENTS AFFECTING MAXIMUM RANGE	PAYLOAD = 15,000 lb (6 804 kg) (limited by max fuel capacity)	PAYLOAD = 23,000 lb (10 433 kg) (limited by max takeoff gross weight)
SFC (Including effect of Nacelle and Pylon Drag Changes)	+16 n. mi. (+29 km)	+24 n. mi. (+44 km)
WEIGHT INCREASE	-45 n. mi. (-83 km)	-214 n. mi. (-396 km)
TOTAL CHANGE	-29 n. mi. (-54 km)	-190 n. mi. (-352 km)

TABLE 6

RANGE CHANGE FOR THE JT8D-109 RELATIVE TO THE JT8D-9
CRUISE AT M = 0.78 AT 30,000 ft (9 144 m)

COMPONENTS AFFECTING MAXIMUM RANGE	PAYLOAD = 15,000 lb (6 804 kg) (limited by max fuel capacity)	PAYLOAD = 23,000 lb (10 433 kg) (limited by max takeoff gross weight)
SFC (Including effect of Nacelle and Pylon Drag Changes)	+2 n. mi. (+4 km)	+14 n. mi. (+26 km)
WEIGHT INCREASE	-29 n. mi. (-54 km)	-190 n. mi. (-352 km)
TOTAL CHANGE	-27 n. mi. (-50 km)	-176 n. mi. (-326 km)

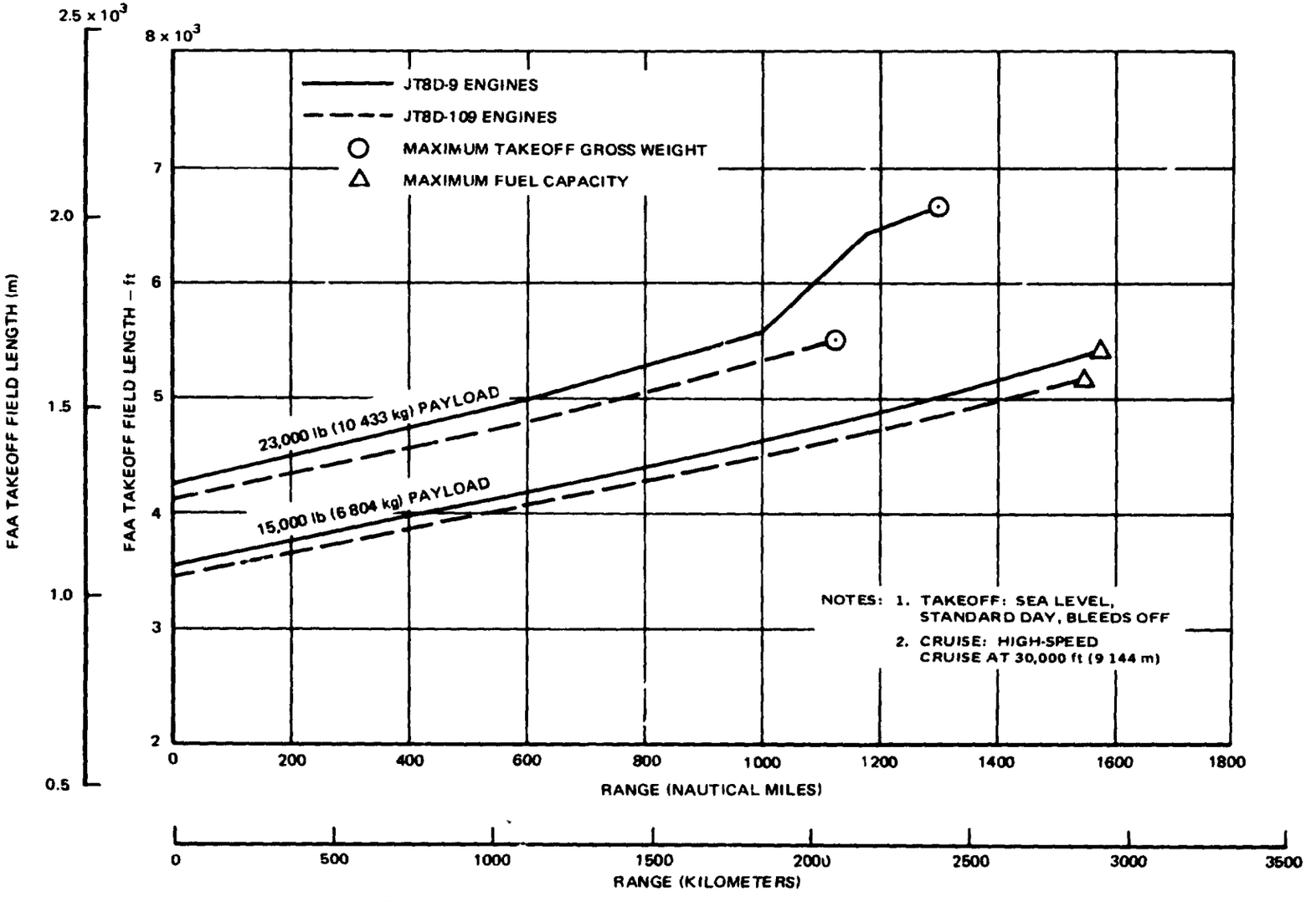

FIGURE 18. DC-9 REFAN FIELD LENGTH – RANGE PERFORMANCE

TABLE 7

PERFORMANCE CHANGE FOR THE JT8D-109 RELATIVE TO THE JT8D-9
LONG RANGE CRUISE AT 35,000 ft (10 668 m)
PAYLOAD = 23,000 lb (10 433 kg)

RANGE	375 n. mi. (694 km)	840 n. mi. (1 556 km)	1,238 n. mi.* (2 293 km)
FUEL BURNED INCREMENT	-7 lb (-3 kg)	+77 lb (+35 kg)	+147 lb (+67 kg)
TAKEOFF GROSS WEIGHT INCREMENT	+2,290 lb (+1 039 kg)	+2,373 lb (+1 076 kg)	+2,459 lb (+1 115 kg)
BLOCK SPEED INCREMENT	+1.4 knots (+2.6 km/hr)	+0.8 knots (+1.5 km/hr)	+0.7 knots (+1.3 km/hr)
TAKEOFF FIELD LENGTH INCREMENT (SEA LEVEL, STANDARD DAY)	-155 ft (-47 m)	-205 ft (-62 m)	-635 ft (-194 m)
TOTAL FUEL BURNED (JT8D-109)	6,248 lb (2 834 kg)	11,893 lb (5 395 kg)	16,933 lb (7 681 kg)

* Maximum range with JT8D-109 Engine

TABLE 8

PERFORMANCE CHANGE FOR THE JT8D-109 RELATIVE TO THE JT8D-9
CRUISE AT M = 0.78 AT 30,000 ft (9 144 m)
PAYLOAD = 23,000 lb (10 433 kg)

RANGE	375 n. mi. (694 km)	840 n. mi. (1 156 km)	1,125 n. mi.* (2 084 km)
FUEL BURNED INCREMENT	+16 lb (+7 kg)	+97 lb (+44 kg)	+145 lb (+66 kg)
TAKEOFF GROSS WEIGHT INCREMENT	+2,321 lb (+1 053 kg)	+2,403 lb (+1 090 kg)	+2,463 lb (+1 117 kg)
BLOCK SPEED INCREMENT	+2.5 knots (+4.6 km/hr)	+1.5 knots (+2.8 km/hr)	+1.3 knots (+2.4 km/hr)
TAKEOFF FIELD LENGTH INCREMENT (SEA LEVEL, STANDARD DAY)	-165 ft (-50 m)	-210 ft (-64 m)	-635 ft (-194 m)
TOTAL FUEL BURNED (JT8D-109)	6,707 lb (3 042 kg)	12,987 lb (5 891 kg)	16,933 lb (7 681 kg)

* Maximum range with JT8D-109 Engine

TABLE 9

PERFORMANCE CHANGE FOR THE JT8D-109 RELATIVE TO THE JT8D-9
LONG RANGE CRUISE AT 35,000 ft (10 668 m)
PAYLOAD = 15,000 lb (6 804 kg)

RANGE	375 n. mi. (694 km)	840 n. mi. (1 556 km)	1,746 n. mi.* (3 234 km)
FUEL BURNED INCREMENT	+16 lb (+7 kg)	+95 lb (+43 kg)	+300 lb (+136 kg)
BLOCK SPEED INCREMENT	-0.3 knots (-0.6 km/hr)	-2.1 knots (-3.9 km/hr)	-1.2 knots (-2.2 km/hr)
TAKEOFF FIELD LENGTH INCREMENT (SEA LEVEL, STANDARD DAY)	-115 ft (-35 m)	-130 ft (-40 m)	-200 ft (-61 m)
TOTAL FUEL BURNED (JT8D-109)	5,926 (2 552 kg)	11,175 lb (5 068 kg)	22,109 lb (10 028 kg)

* Maximum range with JT8D-109 Engine

TABLE 10

PERFORMANCE CHANGE FOR THE JT8D-109 RELATIVE TO THE JT8D-9
CRUISE AT M = 0.78 AT 30,000 ft (9 144 m)
PAYLOAD = 15,000 lb (6 804 kg)

RANGE	375 n. mi. (694 km)	840 n. mi. (1 556 km)	1,553 n. mi.* (2 876 km)
FUEL BURNED INCREMENT	+52 lb (+24 kg)	+172 lb (+78 kg)	+309 lb (+140 kg)
TAKEOFF GROSS WEIGHT INCREMENT	+2,412 lb (+1 094 kg)	+2,510 lb (+1 139 kg)	+2,659 lb (+1 206 kg)
BLOCK SPEED INCREMENT	+1.9 knots (+3.5 km/hr)	+1.1 knots (+2.0 km/hr)	+0.9 knots (+1.7 km/hr)
TAKEOFF FIELD LENGTH INCREMENT	-105 ft (-32 m)	-125 ft (-38 m)	-200 ft (-61 m)
TOTAL FUEL BURNED (JT8D-109)	6,477 lb (2 938 kg)	12,523 lb (5 680 kg)	22,110 lb (10 029 kg)

* Maximum range with JT8D-109 Engine

AIRPLANE STABILITY AND CONTROL

The stability and control characteristics of the DC-9 Refan airplane were evaluated to determine the affect of the installation of the larger diameter JT8D-109 engine and nacelle, the reduced span pylon and weight increases.

The Refan airplane demonstrated stall characteristics similar to the DC-9-30 production airplane with no change in characteristics due to the installation of the JT8D-109 engine.

The static longitudinal stability appears to be slightly less than that of the production DC-9-30. However, the stability of the Refan configuration is considered sufficient to meet the requirements of previous production airplane certification tests and complies with airplane airworthiness requirements.

The longitudinal control characteristics of the Refan airplane are not significantly changed from that of the production DC-9-30 and comply with airplane airworthiness requirements.

The Refan airplane longitudinal trim characteristics are unchanged from that of the production DC-9-30 in the landing configuration and slightly more airplane nose-up in the cruise configuration. The Refan trimmability does comply with airworthiness requirements.

The Refan airplane air and ground minimum control speeds indicate little or no significant change from those of the production DC-9-30; and the controllability with both symmetrical and asymmetrical reverse thrust under all conditions tested was acceptable.

Stall Characteristics

The stall characteristics of the Refan airplane were evaluated to obtain a quantitative appreciation of the stall speeds, particularly at the forward center of gravity.

"Idle power" stall tests were conducted with the airplane at both the forward and aft center of gravity and "power on" stall tests were conducted with the airplane at the forward center of gravity in the following configurations:

- Stall Characteristics - Idle Power

Flaps/Slats	Landing Gear
Up/Retract	Up
0°/Extend	Up
0.436 rad (25 deg)/Extend	Down
0.873 rad (50 deg)/Extend	Down

- Stall Characteristics - Power On

Flaps/Slats	Landing Ge
Up/Retract	Up
0.87[illegible] rad (50 deg)/Extend	Down

The normal stall speed test procedure, which is to apply a pull force to the elevator column to obtain the required airplane stall entry rate and maintain this column pull force through three beeps on the Supplementary Stall Recognition System (SSRS) horn, was modified for the Refan airplane. The Refan procedure was continued until the first beep of the SSRS horn occurred, at which time the elevator column was released and the engines were slowly accelerated.

For the "idle power" stall tests the airplane was trimmed at the specified power setting at an airspeed of 1.4 V_S. Thrust values set for the "power on" stall tests were determined by trimming the airplane to the thrust required for level flight in the approach configuration at an airspeed of 1.6 V_S and maximum landing weight.

During the "power on" stall tests the EPR values varied from 1.34 at higher speeds, to 1.41 at the lowest speed. The airplane stall characteristics were acceptable.

Although the normal stall speed test procedures (maintaining column pull force through three beeps on the SSRS horn) were not followed, stall speeds have been evaluated and are shown in figure 19. Stick shaker actuation speeds are shown in figure 20 with nominal lines and tolerances based on the Production Flight Procedures Manual. All data fall within the tolerances.

Stall characteristics are similar to those of the production DC-9-30 aircraft with no change in characteristics due to the installation of the JT8D-109 engine. The forward center of gravity airplane stall speeds are within production DC-9 tolerances, although the test procedure used was not designed to determine minimum stall speeds. On the basis of these data FAA certified stall speeds can be demonstrated using normal minimum stall speed procedures.

SYM	GROSS WEIGHT lb	GROSS WEIGHT (kg)	cg (% MAC)	FLAPS/SLATS	GEAR	TYPE STALL
○	100,000	(45 360)	8.8	UP/RETRACT	UP	IDLE
△	99,000	(44 906)	8.6	0 deg/EXTEND	UP	IDLE
□	102,000	(46 267)	9.4	25 deg (0.436 rad)/EXTEND	DOWN	IDLE
▽	101,000	(45 814)	9.1	50 deg (0.873 rad)/EXTEND	DOWN	IDLE
●	98,000	(44 453)	8.3	UP/RETRACT	UP	POWER ON
▼	98,000	(44 453)	8.3	50 deg (0.873 rad)/EXTEND	DOWN	POWER ON

DC-9 SERIES 30 CERTIFICATION DATA

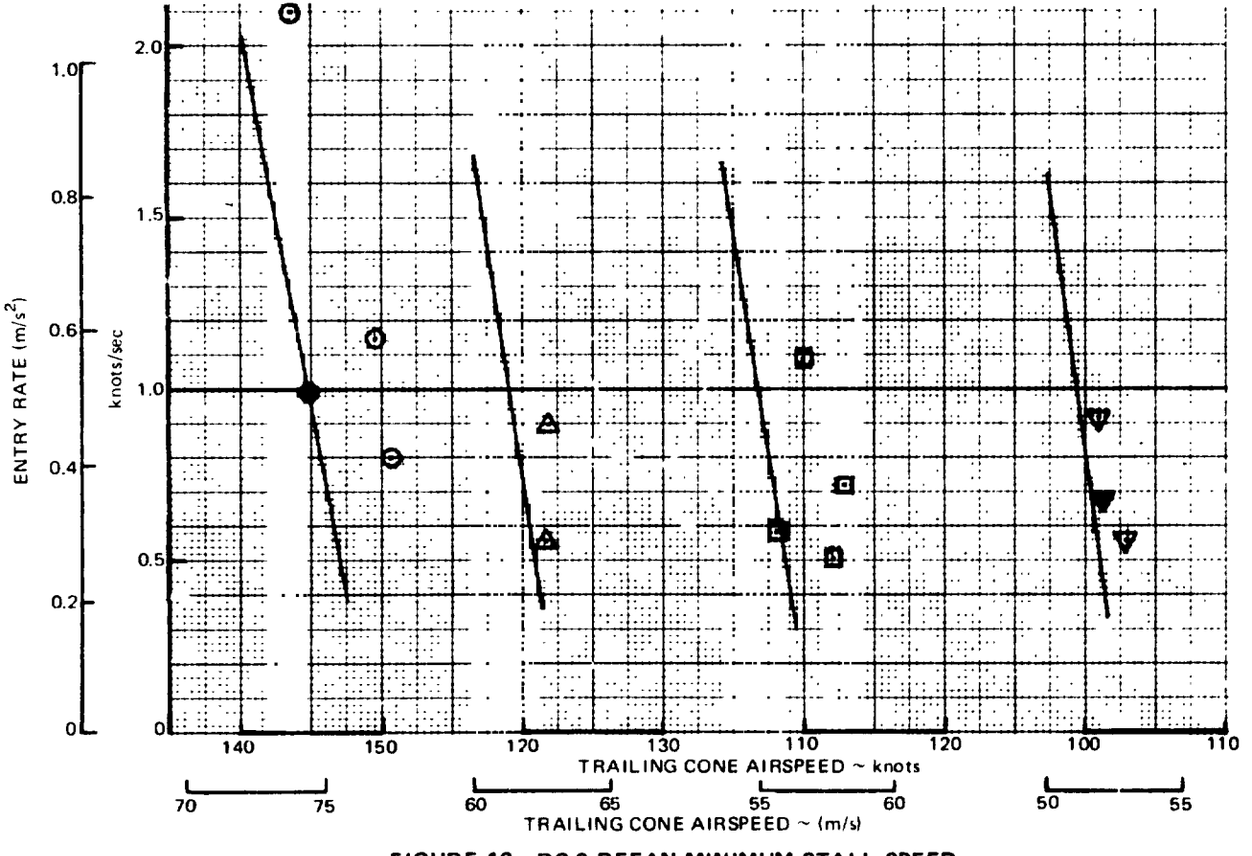

FIGURE 19. DC-9 REFAN MINIMUM STALL SPEED

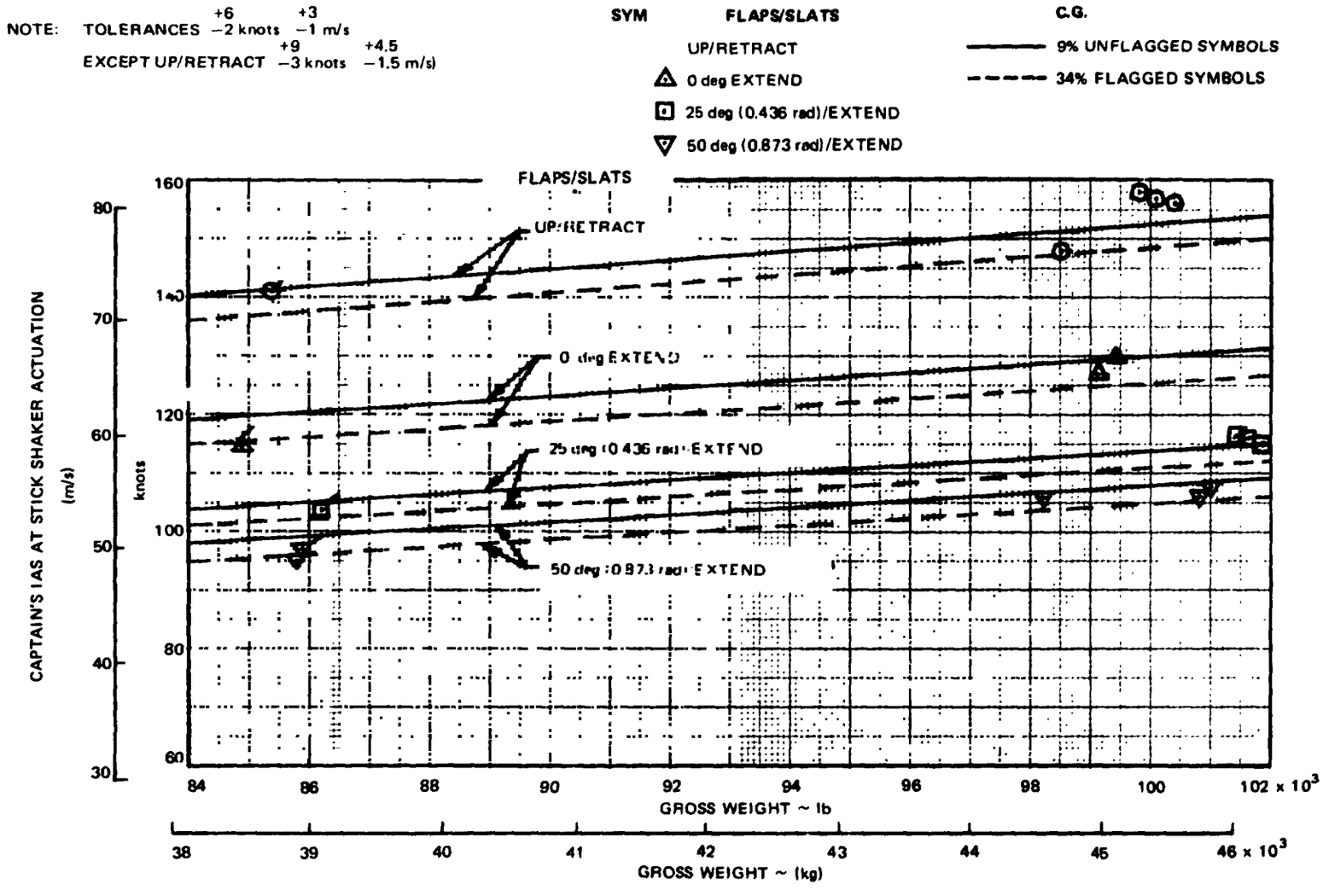

FIGURE 20. DC-9 REFAN STICK SHAKER ACTUATION SPEEDS

Static Longitudinal Stability

The static longitudinal stability characteristics of the Refan airplane were evaluated for high speed climb and during cruise. Flight tests were accomplished for the following configurations and conditions:

Flight Condition	Engine Thrust	Center of Gravity	Airplane Speed Knots(m/s)	Altitude ft (m)	Flaps/ Slats
High Speed Climb	MCT	Aft	320 (165)	5000-10,000 (1524-3048)	Up/Retract
Cruise	TFLF	Aft	0.8 M	23,000 (7010)	Up/Retract

The demonstrated stick-free and stick-fixed static longitudinal stability characteristics of the DC-9-30 Refan and production DC-9-30 are presented in figures 21 and 22 for the climb and cruise configurations, respectively. These data show comparative DC-9-30 Refan and production DC-9-30 stick forces and elevator deflections required to stabilize the airplanes at airspeeds above and below the designated trim speed. In addition, free-return characteristics are shown for both airplanes. These show the stabilized airspeeds, stick forces, and elevator deflections resulting when the control column is released at speeds well above and below the trim speeds. The DC-9-30 production airplane data were obtained from airplane certification tests.

The stick-free stability data show the production DC-9-30 and Refan elevator column force variations required with airspeed. The Refan column forces were obtained with an Ames hand-held force gauge during the flight test, while the production DC-9-30 column forces were obtained from an instrumented elevator column. This would explain some of the scatter shown in the Refan force data. These data indicate comparable levels of stability for the two airplanes but, under the circumstances, they do not provide the most reliable comparison. A better comparison can be made using the stick-fixed stability plots.

The stick-fixed stability data shows -30 production airplane and Refan elevator deflections required with variations in airspeed. These data indicate a very modest reduction in static longitudinal stability for the Refan. In the climb condition shown in figure 21, the stability ($\partial\delta e/\partial v$) is essentially unaltered. At the high-speed cruise condition shown in figure 22, the stability of the Refan is shown to be slightly diminished (approximately 1/2 degree over a M = 0.15 speed range). However, it is not felt this minor reduction in stability is representative of the Refan, since there is no reason to believe that the comparison should be different than that for the climb configuration.

In either condition, the comparison is considered good, and the differences in stability shown between the two airplanes are no worse than might be seen for the same airplane on separate tests.

MODEL	SYM	ALTITUDE ft	ALTITUDE (m)	cg (% MAC)	GROSS WEIGHT lb	GROSS WEIGHT (kg)	THRUST	i_H deg	i_H (rad)
DC-9-30	○	5230	(1594)	34.3	84,700	(38 419	MCT	0.1	(0.0017) ANU
DC-9-30 REFAN	□	6700 ~ 12,400	(2042 ~ 3780)	33.0	84,600	(38 374)	MCT	0.2	(0.0035) ANU

NOTES: 1. CONTROL FORCES MEASURED WITH HAND-HELD AMES GAUGE
2. SHADED SYMBOLS ARE FREE RETURN DATA

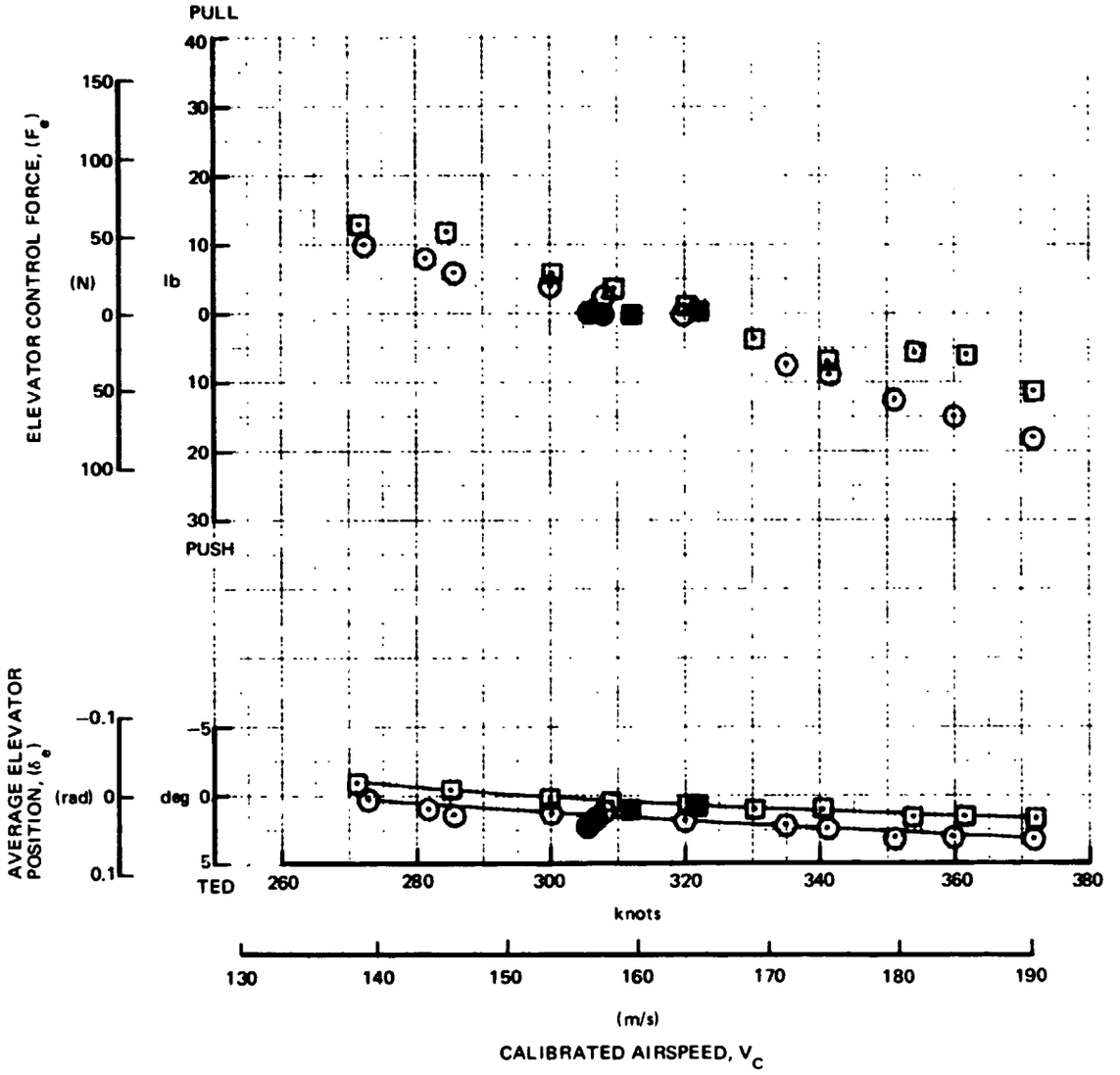

FIGURE 21. DC-9 REFAN STATIC LONGITUDINAL STABILITY – DURING CLIMB – FLAPS/SLATS; UP/RETRACT, GEAR UP

MODEL	SYM	ALTITUDE ft	(m)	cg (% MAC)	GROSS WEIGHT lb	(kg)	i_H deg	(rad)
DC-9-30	⊕	23,800	(7254)	34.1	86,300	(39 145)	0.4	(0.007) AND
DC-9-30 REFAN	⊡	22,000	(6706)	34.2	87,600	(39 735)	0.4	(0.007) AND

NOTES: 1. CONTROL FORCES MEASURED WITH HAND-HELD AMES GAUGE
2. SHADED SYMBOLS ARE FREE RETURN DATA

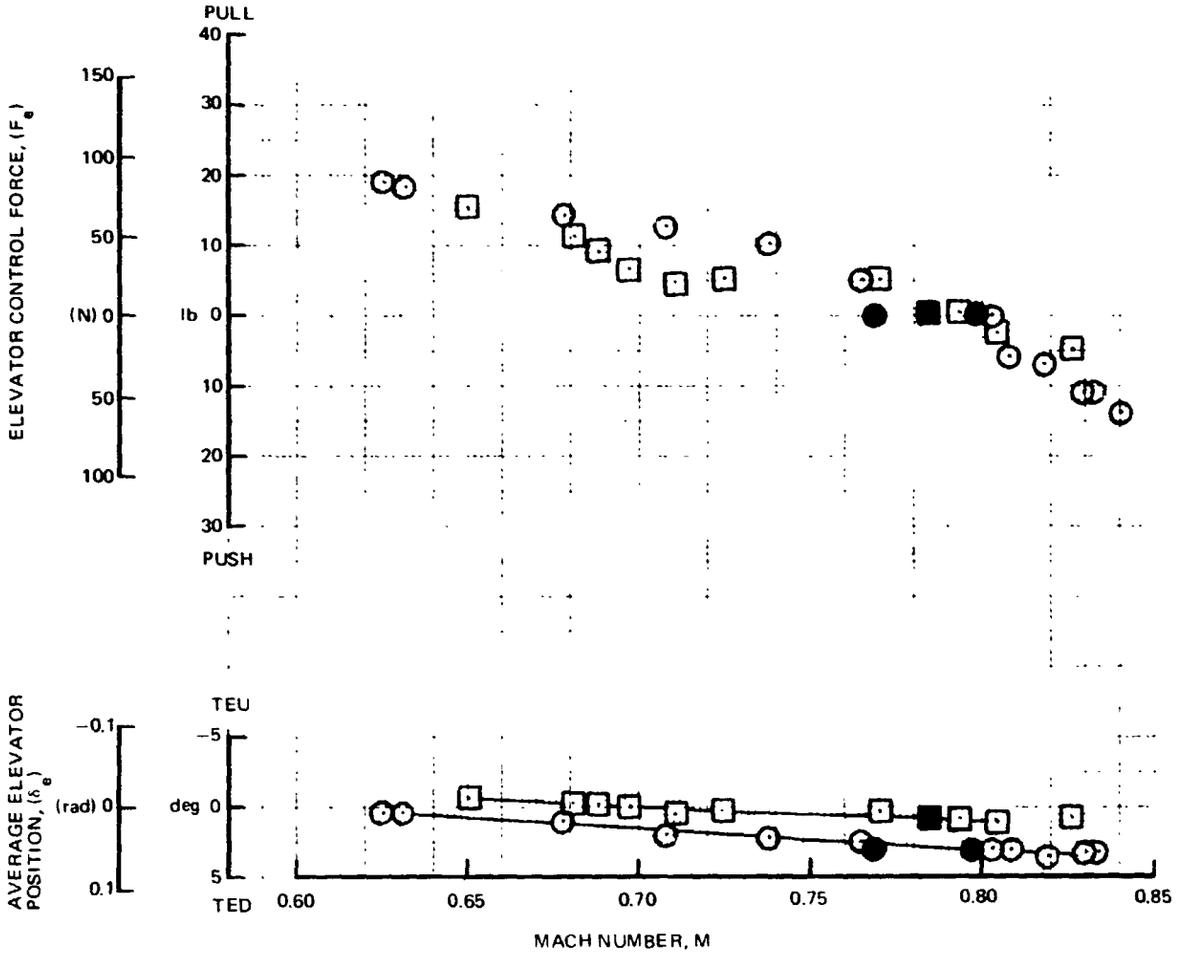

FIGURE 22. DC-9 REFAN STATIC LONGITUDINAL STABILITY – HIGH-SPEED CRUISE – FLAPS/SLATS; UP/RETRACT, GEAR UP, TFLF

The free-return characteristics of the two airplanes are comparable within normal flight test data accuracy.

The static longitudinal stability of the DC-9-30 Refan appears to be slightly less than that of the production DC-9-30. However, the stability of the Refan configuration is sufficient to meet the requirements of previous production airplane certification tests and is considered certifiable at the existing aft c.g. limit.

Longitudinal Control

The DC-9 Refan airplane longitudinal control system capability to control the airplane was evaluated during flight condition changes such as (1) airspeed variation, (2) power application and (3) flap/slat retraction with simultaneous power application. This evaluation was conducted to demonstrate the one-hand longitudinal controllability of the Refan airplane under critical trim-change conditions. One-hand controllability, for the purposes of FAA certification requirements, is interpreted as no more than 222.41 N (50 lb) of column force.

The test results are shown in tabular form in table II. All DC-9-30 production airplane data were obtained from certification tests. These data cover three different controllability tests: (1) airspeed variation (1.1 V_S to 1.7 Vs @ forward c.g. and full down flaps), (2) power application at both forward and aft c.g., flaps/slats; up/retract and landing gear down, and (3) power application with simultaneous flap and slat retraction at forward and aft c.g. The table shows detailed test conditions and results in terms of required incremental elevator deflection, column force, and altitude changes where applicable.

Although controllability in these tests is normally measured by required control forces, these forces were not available on the DC-9-30 Refan, because the elevator column was not instrumented and all column force readings required the use of a hand-held Ames gauge. The use of the hand-held gauge was found to be unsuitable for determining the transient-like column forces that occur during these tests. Controllability was evaluated, however, by comparison of the required elevator control deflections of the Refan with that of the DC-9-30 production airplane.

- Airspeed Variation

The airplane was trimmed with idle power at 1.4 V_S in the landing configuration at forward c.g. with flaps/slats 0.873 rad (50 deg)/extend and landing gear down. One hand control was evaluated without changing trim, while airspeed was varied from 1.1 to 1.7 V_S. The Refan configuration showed a 0.314 rad (18 deg) elevator deflection change between 1.1 V_S and 1.7 V_S compared to 0.262 rad (15 deg) for the production DC-9-30. The 0.262 rad (15 deg) elevator deflection on the DC-9-30 production airplane required 129 N (29 lb) of column force. The 0.314 rad (18 deg) elevator deflection on the Refan was 20 percent higher and would yield a column force on the order of 155.69 N (35 lb), well under the allowable 222.41 N (50 lb).

- Power Application

The airplane was trimmed with idle power at 1.4 V_S in the landing configuration. One hand control was evaluated while quickly applying inflight takeoff thrust and maintaining airspeed. Controllability was evaluated at both forward and aft c.g., flaps/slats; up/retract and landing gear down. These tests were conducted at a constant speed (while the thrust is advanced from idle to inflight takeoff) to avoid the influence of static longitudinal stability and confine the source of the trim change to thrust effects only.

TABLE 11
DC-9-30 REFAN LONGITUDINAL CONTROL SUMMARY
(GEAR DOWN)

CONDITION*	TARGET SPEED V_s	cg	FLAPS/SLATS deg (rad)	DC-9 SERIES	GROSS WEIGHT lb	GROSS WEIGHT (kg)	THRUST SETTING	AIRSPEED knots	AIRSPEED (m/s)	ALTITUDE ft	ALTITUDE (m)	cg (% MAC)	STICK FORCE CHANGE ΔFe (PUSH) lb	STICK FORCE CHANGE ΔFe (PUSH) (kg)	ALTITUDE CHANGE ft	ALTITUDE CHANGE (m)	ELEVATOR CHANGE Δδe (A.N.D.) deg	ELEVATOR CHANGE Δδe (A.N.D.) (rad)
1	1.1-1.7	FWD	50 (.873)/ EXTEND	−30 REFAN	80,250 102,100	(36 400) (46 312)	IDLE	99-153 116-176	(51-79) (60-91)	10,500 5,820	(3200) (1774)	5.7 8.8	29 –	(13.2) –	– –	– –	15 18	(.262) (.314)
3	1.2	FWD	50 (.873)/ EXTEND	−30 REFAN	100,000 100,100	(45 359) (45 405)	TFLF TO T.O.	120-173 126-173	(62-89) (65-89)	3,765 4,530	(1148) (1381)	7.7 8.2	18 –	(8.2) –	0 0	(0) (0)	4 5	(.070) (.087)
3	1.2	AFT	50 (.873)/ EXTEND	−30 REFAN	95,500 92,800	(43 318) (42 093)	TFLF TO T.O.	118-164 118-162	(61-84) (61-83)	3,965 8,510	(1209) (2594)	33.9 33.8	2 –	(.9) –	– −35	– (−10.7)	3 2	(.052) (.035)
2	1.4	FWD	0/ RETRACT	−30 REFAN	93,750 99,100	(42 524) (44 951)	IDLE TO T.O.	201 206	(103) (106)	2,820 2,780	(860) (847)	5.9 8.0	8 –	(3.6) –	– –	– –	2 2	(.035) (.035)
2	1.4	AFT	0/ RETRACT	−30 REFAN	87,100 92,600	(39 508) (42 003)	IDLE TO T.O.	186 195	(96) (100)	8,530 8,530	(2600) (2600)	34.7 33.9	5 –	(2.3) –	– –	– –	2 2	(.035) (.035)
2	1.4	FWD	50 (.873)/ EXTEND	−30 REFAN	90,000 100,900	(40 823) (45 767)	IDLE TO T.O.	131 145	(67) (75)	1,550 4,600	(472) (1402)	6.0 8.5	14 –	(6.4) –	– –	– –	3 3	(.052) (.052)
2	1.4	AFT	50 (.873)/ EXTEND	−30 REFAN	87,850 93,300	(39 848) (42 320)	IDLE TO T.O.	130 130	(67) (67)	5,080 8,850	(1548) (2697)	34.5 33.5	10 –	(4.5) –	– –	– –	2.5 2.5	(.044) (.044)

*1) AIRSPEED VARIATION
2) POWER APPLICATION
3) FLAPS/SLATS RETRACT WITH SIMULTANEOUS POWER APPLICATION

Control deflections were noted at approximately 1.4 V_S before and after power application. The control data shown in table 11 indicated that the trim change is easily controllable for all conditions tested and that the Refan controllability is essentially the same as that of the production DC-9-30. No elevator deflections greater than 0.052 rad (3 deg) are required, and no column forces greater than 62.28 N (14 lb) are required.

- Power Application with Flap/Slat Retraction

The airplane was trimmed at 1.2 V_S with thrust for level flight in the landing configuration. The flaps and slats were retracted with simultaneous application of MCT power while maintaining the speed schedule and holding altitude loss to a minimum. Controllability under "go around" conditions was evaluated at both forward and aft c.g. flaps/slats; 0.873 rad (50 deg)/extend and landing gear down.

The altitude lost after initiation of this maneuver is of equal interest with that of the control requirements. In the forward c.g. configuration, neither the DC-9-30 production airplane nor the Refan lost any significant altitude during the maneuver. The production DC-9-30 showed an elevator deflection of 0.070 rad (4 deg) required, yielding a column force of approximately 75.62 N (17 lb) push. The Refan configuration showed 0.087 rad (5 deg), which would yield aproximately 93.40 N (21 lb).

In the aft c.g. configuration the DC-9-30 production airplane again showed no altitude loss while the Refan showed an initial altitude loss of approximately 10.67 m (35 ft). This altitude loss can probably be attributed to a descending flight path at the initiation of the test. The control required at aft c.g. was only 0.035 rad (2 deg) for the Refan as compared to 0.052 rad (3 deg) for the production DC-9-30. The DC-9-30 production airplane required only 8.90 N (2 lb) of column force, so that the Refan would require slightly less force.

The longitudinal control characteristics of the DC-9 Refan airplane are not significantly changed from that of the production DC-9-30. All conditions are considered easily controllable.

Control deflections required for airspeed variation (1.1 V_S to 1.7 V_S) are approximately 0.052 rad (3 deg) more for the Refan airplane, control of power application (idle thrust to inflight takeoff thrust) is essentially the same for both airplanes and the Refan control deflections required during "go-around" (flap/slat retraction + power application) were within 0.018 rad (1 deg) of those for the DC-9-30 production airplane.

The DC-9 Refan airplane longitudinal control characteristics comply with airplane airworthiness requirements.

Longitudinal Trim

The longitudinal trim capabilities of the DC-9 Refan airplane were evaluated during stabilized flight at various airspeeds and airplane configurations.

The DC-9 Refan airplane was trimmed hands-off during glide with both engines at idle, flaps/slats, 0.873 rad (50 deg)/Extend, gear down, forward c.g., at speeds varying from 1.2 V_S to 1.8 V_S and during level flight at aft c.g. and two altitudes: 1) 3048 m (10,000 ft) from 128.6 m/s (250 knots) to 180 m/s (350 knots), V_{MO}, with the landing gear retracted and from 92.6 m/s (180 knots) to 154.3 m/s (300 knots) with the gear extended; 2) 7925 m (26,000 ft) altitude from Mach number 0.70 to M_{MO} (0.84) with the gear retracted.

The longitudinal trim characteristics of the DC-9-30 Refan and the DC-9-30 production airplanes are summarized in figures 23 through 26. These data show comparative Refan and production DC-9-30 trim characteristics in the landing and cruise configuration.

Longitudinal trim characteristics in the landing configuration (flaps/slats) 0.873 rad (50 deg)/Extended, gear down and idle thrust) are shown in figure 23 for the Refan and the production DC-9-30. These data show the same characteristics for both airplanes, indicating a capability to trim at speeds down to 1.3 V_S with minus 0.210 rad (12 deg) of horizontal stabilizer incidence. The specifications of CAM 4b require trimmability at speeds down to 1.4 V_S, thus the Refan, like the DC-9-30 production airplane will comply with this requirement at the existing forward c.g. limit.

Longitudinal trim characteristics in the cruise configuration (flaps/slats: up/retract, gear up, thrust for level flight) are shown in figure 24 for the Refan and the production DC-9-30. These data show the Refan requiring 0.004 rad (0.2 deg) to 0.010 rad (0.6 deg) more airplane-nose-up trim. The differences shown in trim characteristics are small, and like those of the stability and controllability tests, fall within what is considered normal flight test data scatter.

An additional test was conducted in the cruise configuration with the landing gear extended. The Refan data from this test, presented in figure 25 showed inconsistencies in landing gear effects. When these data are compared to the gear-up data they indicate an airplane-nose-down trim change resulting from gear extension, whereas all previous Series 30 DC-9 airplanes show a characteristics airplane-nose-up trim change. The gear-down trim data are believed to be in error since they are not consistent with the Refan characteristics in the landing configuration or with any previous production DC-9-30 data.

At the higher cruise altitude and speeds (figure 26), the trim characteristics with landing gear retracted are relatively the same as at the low altitude. The required stabilizer is indicated slightly higher for the Refan.

MODEL	SYM	ALTITUDE ft	ALTITUDE (m)	cg (% MAC)	GROSS WEIGHT lb	GROSS WEIGHT (kg)
DC-9-30	△	8328	(2538)	5.7	89,600	(40 642)
DC-9-30	◇	6510	(1984)	5.7	89,500	(40 597)
DC-9-30	○	4700	(1430)	9.0	97,500	(44 250)
DC-9-30	△	7445	(2270)	6.4	91,700	(41 600)
DC-9-30 REFAN	□	6300	(1920)	7.8	98,400	(44 650)

NOTE: THE DC-9-30 POINTS HAVE BEEN ADJUSTED TO REFLECT A CENTER OF GRAVITY POSITION OF 7.8% MAC

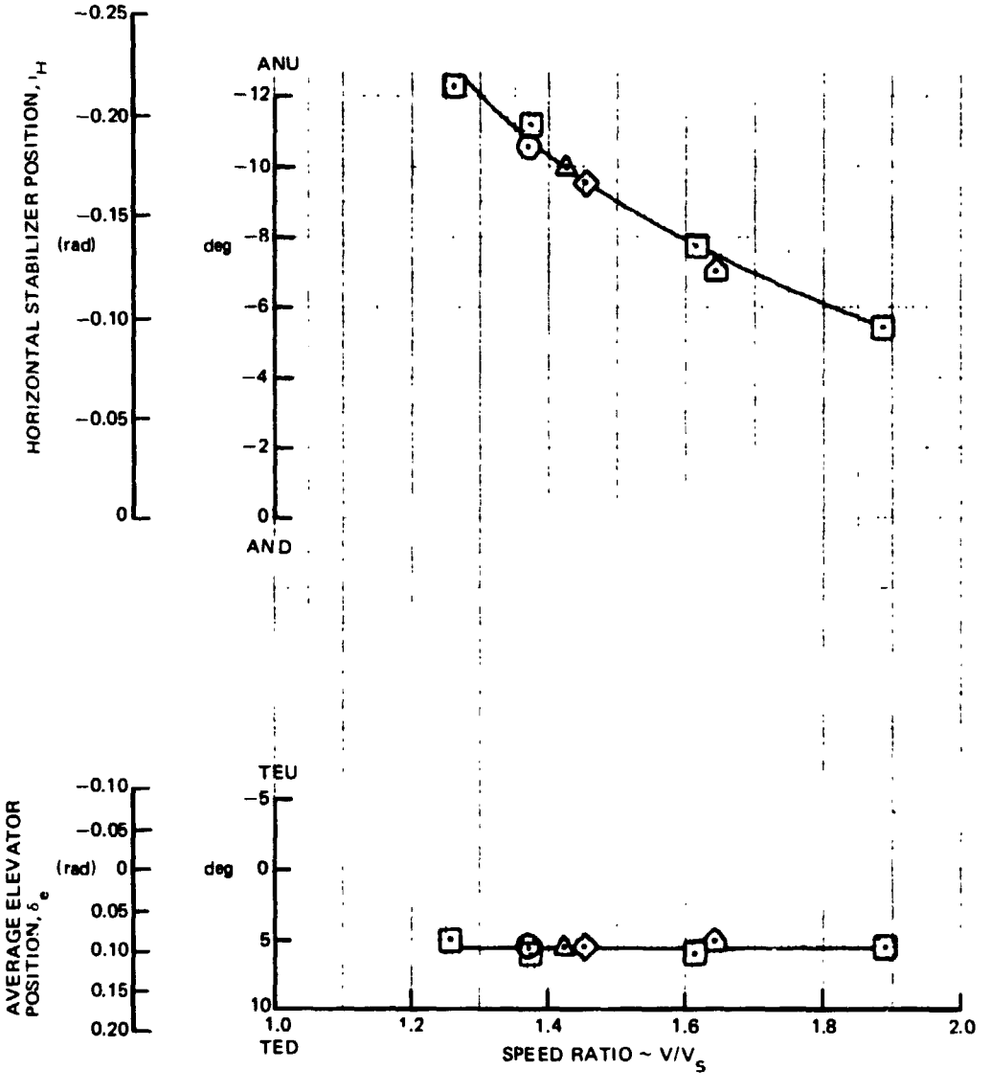

FIGURE 23. DC-9 REFAN LONGITUDINAL TRIM – LANDING CONFIGURATION – FLAPS/SLATS: 50 (0.873)/EXT, GEAR DOWN, IDLE THRUST

MODEL	SYM	ALTITUDE ft	(m)	cg (% MAC)	GROSS WEIGHT lb	(kg)
DC-9-30	○	10,000	(3050)	34.0	94,250	(42 750)
DC-9-30 REFAN	□	10,000	(3050)	34.1	84,300	(38 250)

NOTE: THE DC-9-30 REFAN DATA POINTS HAVE BEEN ADJUSTED TO REFLECT A GROSS WEIGHT OF 94,250 lb (42 751 kg)

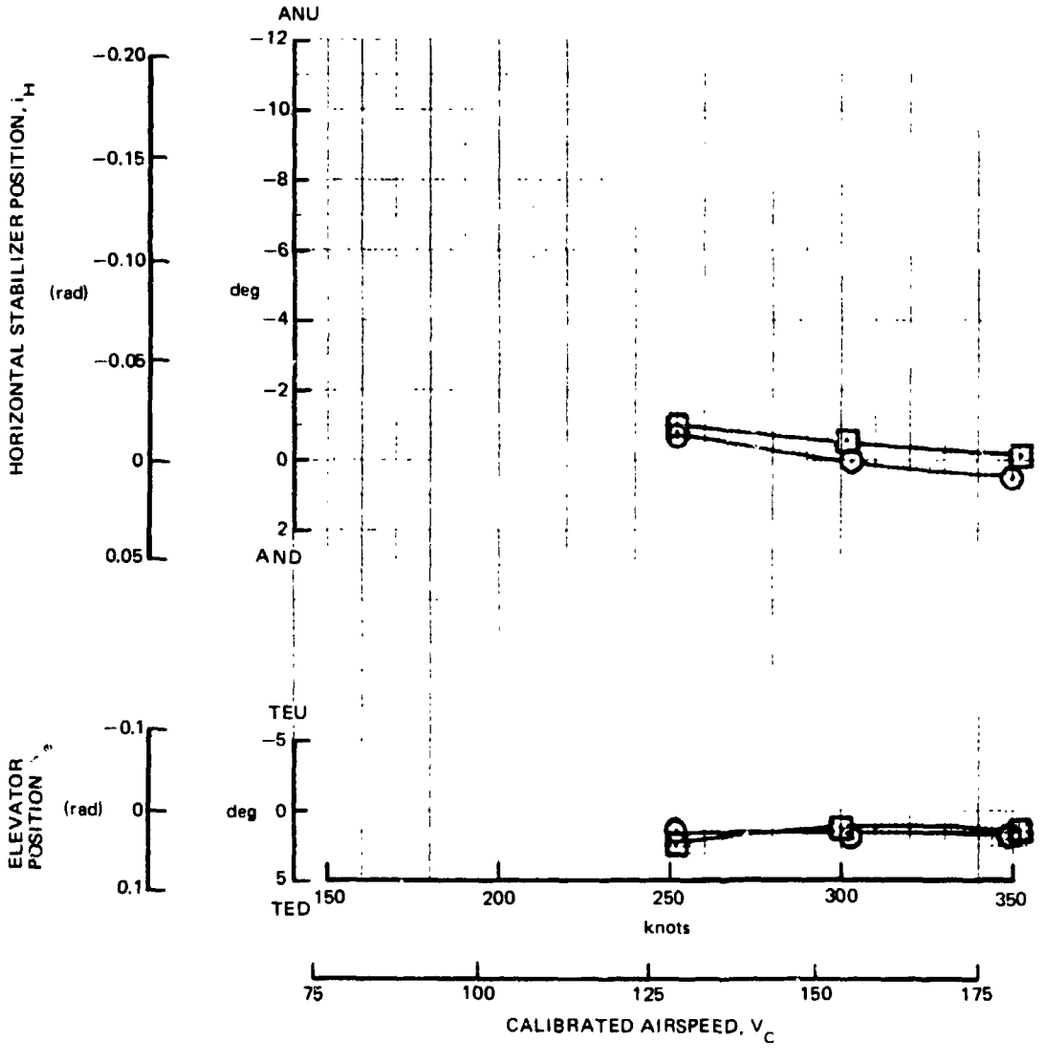

FIGURE 24. DC-9 REFAN LONGITUDINAL TRIM – CRUISE CONFIGURATION – FLAPS/SLATS: UP/RET, GEAR UP, TFLF

MODEL	SYM	ALTITUDE ft	ALTITUDE (m)	cg (% MAC)	GROSS WEIGHT lb	GROSS WEIGHT (kg)
DC-9-30	⊙	10,000	(3050)	34.6	92,900	(42 150)
DC-9-30REFAN	⊡	10,000	(3050)	34.2	74,500	(33 800)

NOTE: THE DC-9-30R DATA POINTS HAVE BEEN ADJUSTED TO REFLECT A GROSS WEIGHT OF 92,900 lb (42 139 kg)

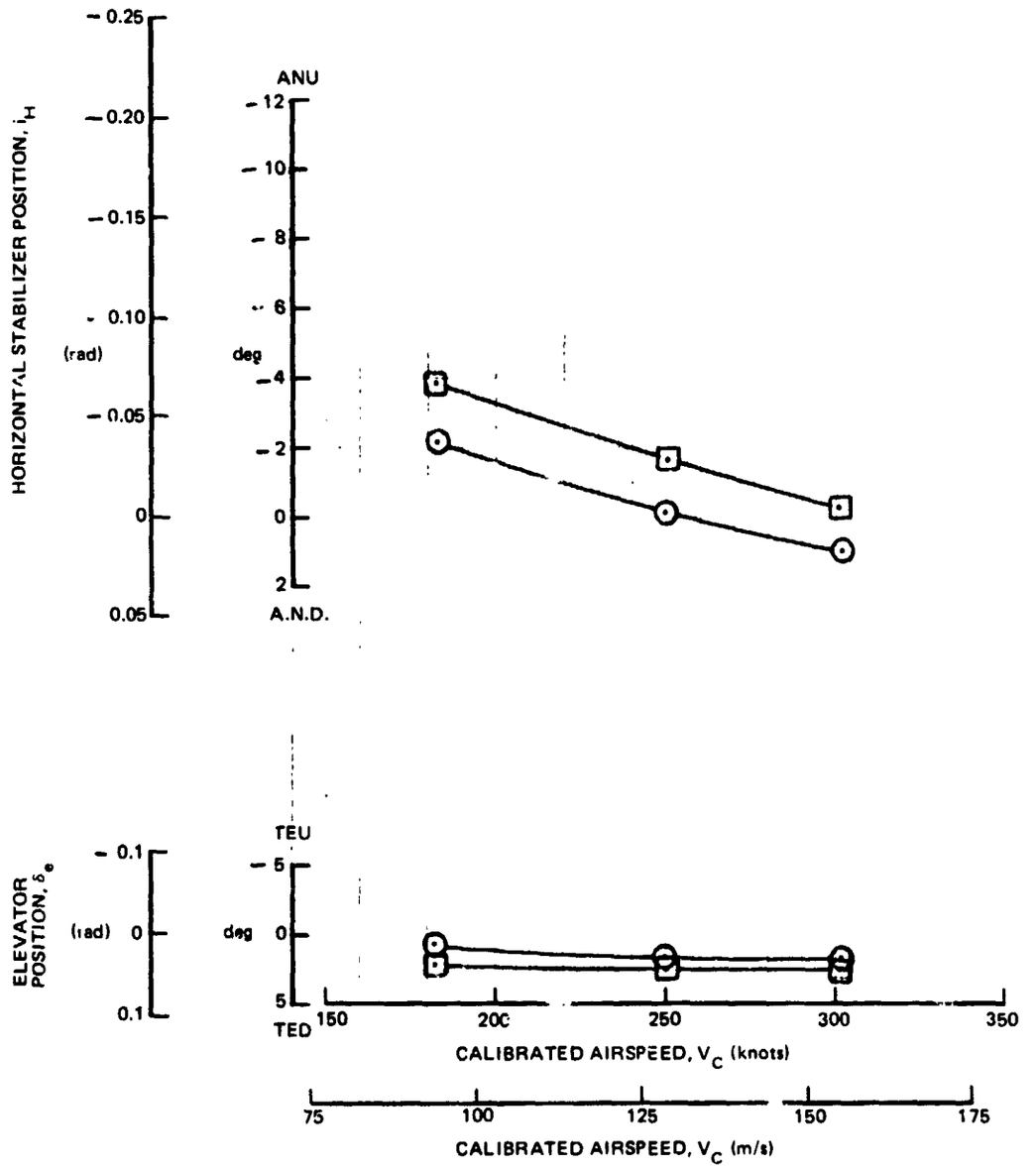

FIGURE 25. DC-9 REFAN LONGITUDINAL TRIM – CRUISE CONFIGURATION FLAPS/SLATS: UP/RET, GEAR DOWN, TFLF

MODEL	SYM	ALTITUDE ft	(m)	cg (% MAC)	GROSS WEIGHT lb	(kg)
DC-9-30	⊙	26,000	(7900)	34.5	84,000	(38 100)
DC-9-30 REFAN	⊡	26,000	(7900)	34.2	89,100	(40 400)

NOTE: THE DC-9-30 RFFAN DATA POINTS HAVE BEEN ADJUSTED TO REFLECT A GROSS WEIGHT OF 84,000 lb (38 102 kg) AND A cg OF 34.5% MAC

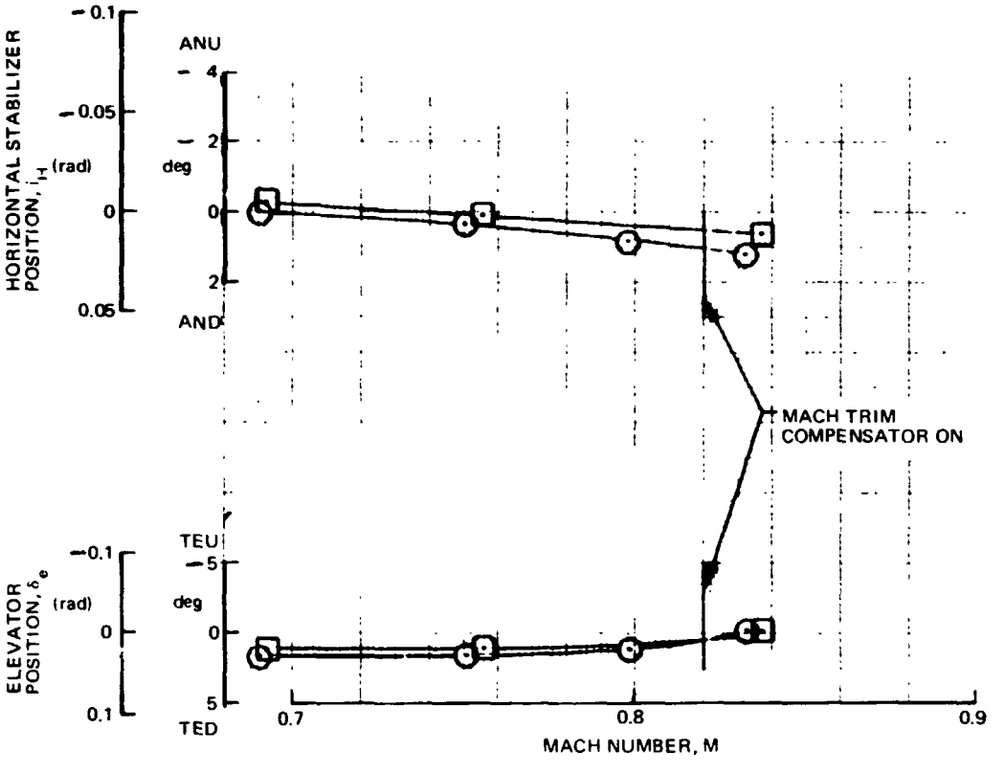

FIGURE 26. DC-9 REFAN LONGITUDINAL TRIM – CRUISE CONFIGURATION – FLAPS/SLATS: 0/RET, GEAR UP, TFLF

The DC-9 Refan airplane longitudinal trim characteristics are shown to be unchanged from that of the DC-9-30 production airplane in the landing configuration and slightly more airplane nose-up in the cruise configuration. All flight test data comparisons are considered good and fall within the normal range of test data scatter. The Refan trimmability complies with airplane airworthiness requirements.

Minimum Control Speed

The minimum speed at which the DC-9 Refan has sufficient control to offset the asymmetric thrust condition of single engine operation was evaluated for flight, takeoffs, and normal reverser landings and asymmetric reverse thrust landings.

- V_{mca} - Air

The minimum control speed in the air was evaluated with one engine shut down and the other set at inflight takeoff thrust. The test configuration was: aft c.g. with flaps/slats set at 0.087 rad (5 deg)/Extend and at 0.262 rad (15 deg)/Extend with rudder power on.

The air minimum control speeds for the DC-9-30 Refan and DC-9-30 production airplane with 0.087 rad (5 deg) and 0.262 rad (15 deg) flaps are shown in figure 27. The flight data indicate that no significant change has resulted from the Refan installation. With 0.087 rad (5 deg) flaps, these data show that the Refan V_{mca} is 1.03 m/s (2 knots) below the approved production DC-9-30 V_{mca} at equal thrust. At 0.262 rad (15 deg) flaps these data show that the Refan V_{mca} is approximately 0.257 m/s (1/2 knot) higher. It should be noted that considerable data scatter is normally encountered from the V_{mca} test. The Refan points fall within this scatter band.

- V_{mcg} - Ground Takeoff

An operational check of the minimum control speed on the ground during takeoff was evaluated by reducing one of the engines to idle during the takeoff roll. The speed at which the engine cut occurred was reduced in 2.57 m/s (5 knot) increments until a lateral deviation of 4.57 m (15 ft) occurred. This test was accomplished with the rudder pedal nose wheel steering disconnected to simulate an icy runway.

The ground minimum control speeds for the production DC-9-30 and the DC-9-30 Refan are shown in figure 28. These data indicate that the Refan V_{mcg} is 1.29 m/s (2-1/2 knots) higher than the approved production DC-9-30 speed at equal thrust. An additional flight point, obtained with an alternate DC-9-30 production airplane, is included on this plot, showing considerable data scatter. Again the Refan data are considered within the normal scatter band for this test, indicating little or no significant effect of the Refan installation on V_{mcg}.

- V_{mcg} - Ground Landing with Reverse Thrust

An operational check of airplane directional control was accomplished during normal reverser landings and during reverser landings where one engine was suddenly reduced to idle from high reverser power.

The directional control test was accomplished with rudder pedal nose wheel steering connected and disconnected and with manual rudder and with rudder power on.

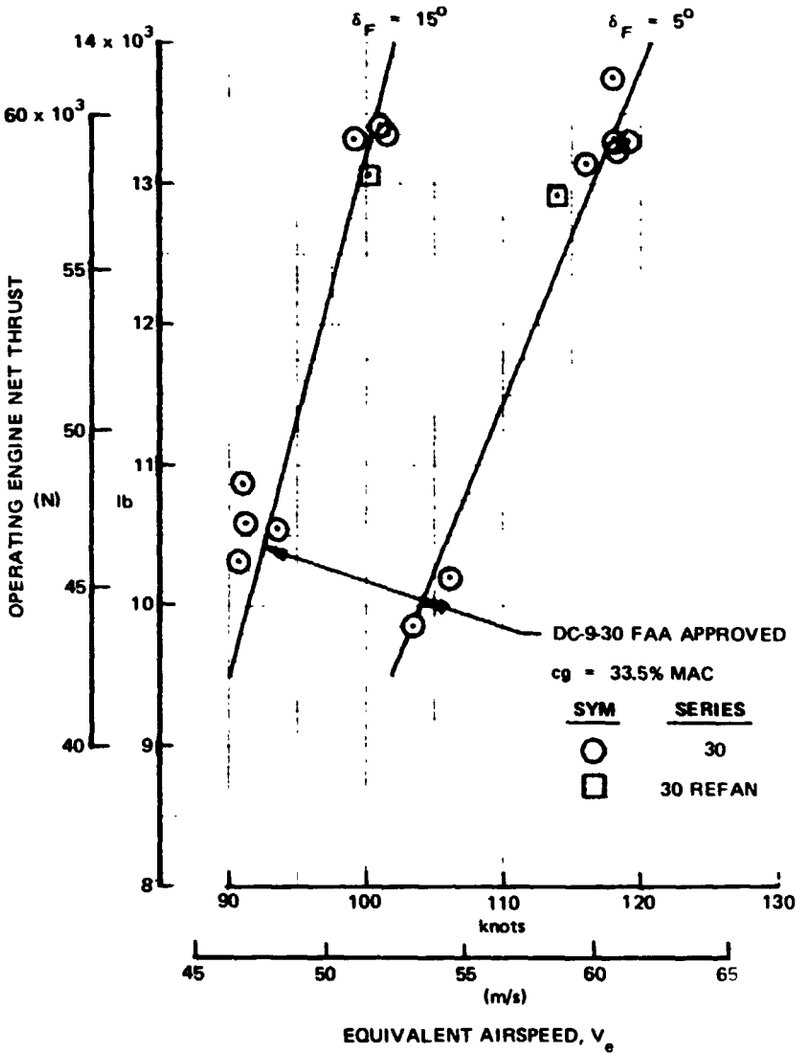

FIGURE 27. DC-9 REFAN MINIMUM CONTROL SPEED – AIR – SLATS EXTENDED, RUDDER POWER ON

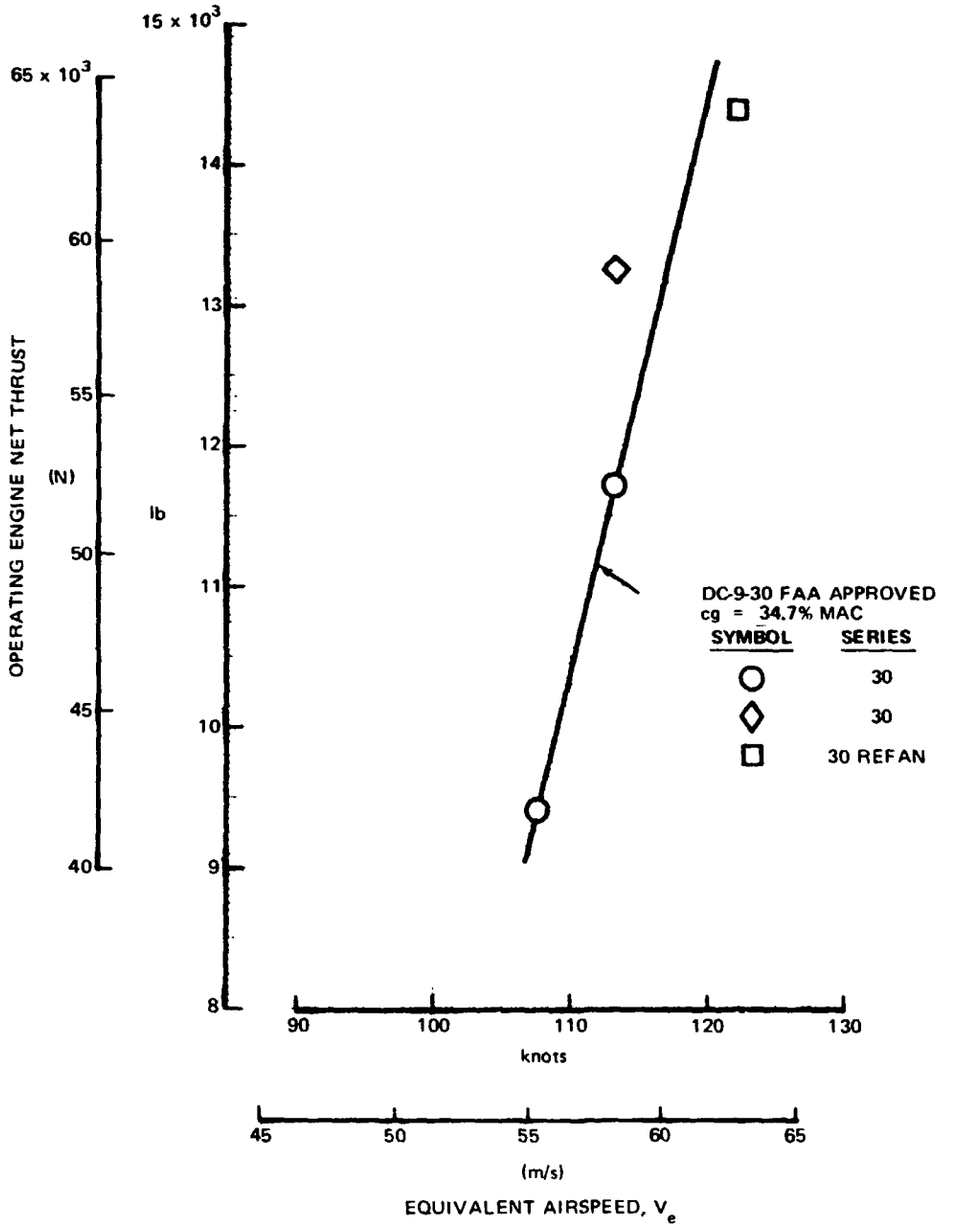

FIGURE 28. DC-9 REFAN MINIMUM CONTROL SPEED – GROUND – FLAPS/SLATS; 5(0.087)/EXT, RUDDER POWER ON

Controllability with both symmetrical and asymmetrical reverse thrust was also demonstrated. Although insufficient data are available for quantitative analysis of results, pilots have indicated that full controllability was available under all conditions tested, and that the airplane response characteristics are essentially the same as that of the DC-9-30 production airplane.

The Refan airplane minimum control speeds are essentially the same as those of the production DC-9-30; and the airplane controllability with both symmetrical and asymmetrical reverse thrust under all conditions tested was acceptable.

AIRPLANE/ENGINE PERFORMANCE

The DC-9 Refan airplane and installed JT8D-109 engine performance was evaluated with respect to the production (DC-9-30/JT8D-9) airplane to determine the extent of the changes resulting from the airplane, engine and nacelle modifications.

Test flights were conducted to establish the performance levels of the airplane and engine during takeoff, climb, cruise and landing. Engine performance was evaluated during suction fuel feeding, windmill and ground engine starts, snap throttle retards, jam accelerations, airplane stall, high sideslip angles and abused takeoffs. Airplane/engine subsystem performance and the auxiliary power plant (APU) performance and starting characteristics (ground and flight) were also evaluated.

Refan takeoff acceleration performance when compared with DC-9 Series 30 production airplane data corrected for the difference in thrust showed good agreement.

The climb performance of the DC-9 Refan airplane relative to the JT8D-9 powered DC-9-30 production airplane shows an 8 percent improvement in second segment and approach limiting weights and a 5 percent improvement in enroute limiting weight.

The cruise performance testing of the DC-9 Refan airplane, with the two prototype JT8D-109 engines installed, showed the range factor from 5 to 7 percent lower than an equivalent JT8D-9 powered DC-9-30 production airplane. While approximately 2 percent of this increment was due to the drag increase of the larger nacelle, the balance was due to the higher engine SFC of the prototype JT8D-109 engines.

During the JT8D-109 engine performance tests no signs of engine instability were noted by the pilots while the maximum climb thrust maneuver utilizing fuel suction feed was being conducted. Engine ground starting characteristics were satisfactory with little or no change from other JT8D versions. The low speed inflight starting envelope was also verified to be satisfactory. Overall, the engine operations were excellent with no major problems encountered and engine performance very close to predicted levels.

The airplane/engine subsystem performance tests showed that the JT8D-109 engine nacelle compartment ventilation and component cooling requirements were satisfied for ground and inflight conditions. The JT8D-109 engine generator and CSD cooling systems were demonstrated satisfactorily for the critical (100% load) ground idle condition and for all inflight conditions.

During the thrust reverser performance evaluation normal reverse thrust operation was demonstrated at speeds below the operational cutback speed of 30.87 m/s (60 knots) with acceptable engine operation; and the peak empennage temperatures remained below the maximum allowable 121°C (250°F) for the aluminum skin.

The auxiliary power plant (APU) tests showed no unusual starting or operating characteristics during ground starts; and electric and windmill airstarts with the modified exhaust were accomplished at the extremes of the production APU certified airstart envelope.

Two Engine Takeoff Acceleration

The DC-9 Refan two-engine takeoff acceleration performance was evaluated to obtain installed JT8D-109 engine operating characteristics and aircraft acceleration data during normal takeoffs, which is required to establish all-engine takeoff profiles for the flyover noise testing.

Takeoff accelerations were obtained for two takeoff configurations flaps/slats,0/Extend and 0.262 rad (15 deg)/Extend.

The DC-9 Refan airplane measured acceleration was compared with FAA approved DC-9 Series 30 production data corrected for the difference in thrust between the JT8D-109 and JT8D-9 engines. These data show good agreement for both takeoff flap configurations.

Because these data showed good agreement, the production DC-9-30 FAA approved data corrected for thrust differences were used to establish all-engine takeoff acceleration performance required to calculate the takeoff profiles for the flyover FAR Part 36 noise data.

Climb Performance

The climb performance of the DC-9 Refan airplane was evaluated to determine the incremental effect of the JT8D-109 engines relative to the JT8D-9 powered production DC-9-30.

The climb increments were obtained for the conditions listed below, since the aircraft can be limited by any one of these.

1) Second segment climb (engine-out, takeoff configuration)

2) Enroute climb (engine-out, clean wing configuration)

3) Approach climb (engine-out, go-around flaps)

Several pairs of reciprocal heading climbs were accomplished for each of the conditions listed above. Reciprocal heading climbs were conducted, at constant heading and airspeed, to eliminate wind shear effects. Specified power was set well below the target altitude so that approximately 3 minutes of stabilized climb data were obtained climbing through the target altitude, while maintaining airspeed and power levels constant. Sufficient rudder was input to maintain constant heading.

The flight measured Refan climb data have been compared to existing production DC-9 Series 30 climb results and the incremental differences in terms of thrust-to-weight ratio are presented as a function of climb gradient in figure 29 for the various conditions tested.

The estimated incremental difference shown accounts for the increased nacelle skin friction drag, increased windmilling engine drag, and decreased lateral trim drag resulting from a smaller thrust moment arm for the JT8D-109 engine installation. The flight-measured data shows good agreement with the estimated incremental difference for each of the climb conditions.

The penalty associated with the Refan installation in terms of increased thrust-to-weight ratio (poorer L/D) is from 1 to 1-1/2 percent at the second segment and approach climb limiting gradients and about 4 percent at the enroute condition.

The JT8D-109 engine has more thrust available at the takeoff setting than the JT8D-9 engine; thus, at a given thrust-to-weight ratio, the DC-9 Refan airplane will have a higher limiting weight than the production DC-9-30.

The net result of climb performance associated with the Refan installation, including the improvement due to the increased thrust available and the penalty due to the increased thrust-to-weight ratio required is an 8 percent improvement in second segment and approach limiting weights and a 5 percent improvement in enroute limiting weight.

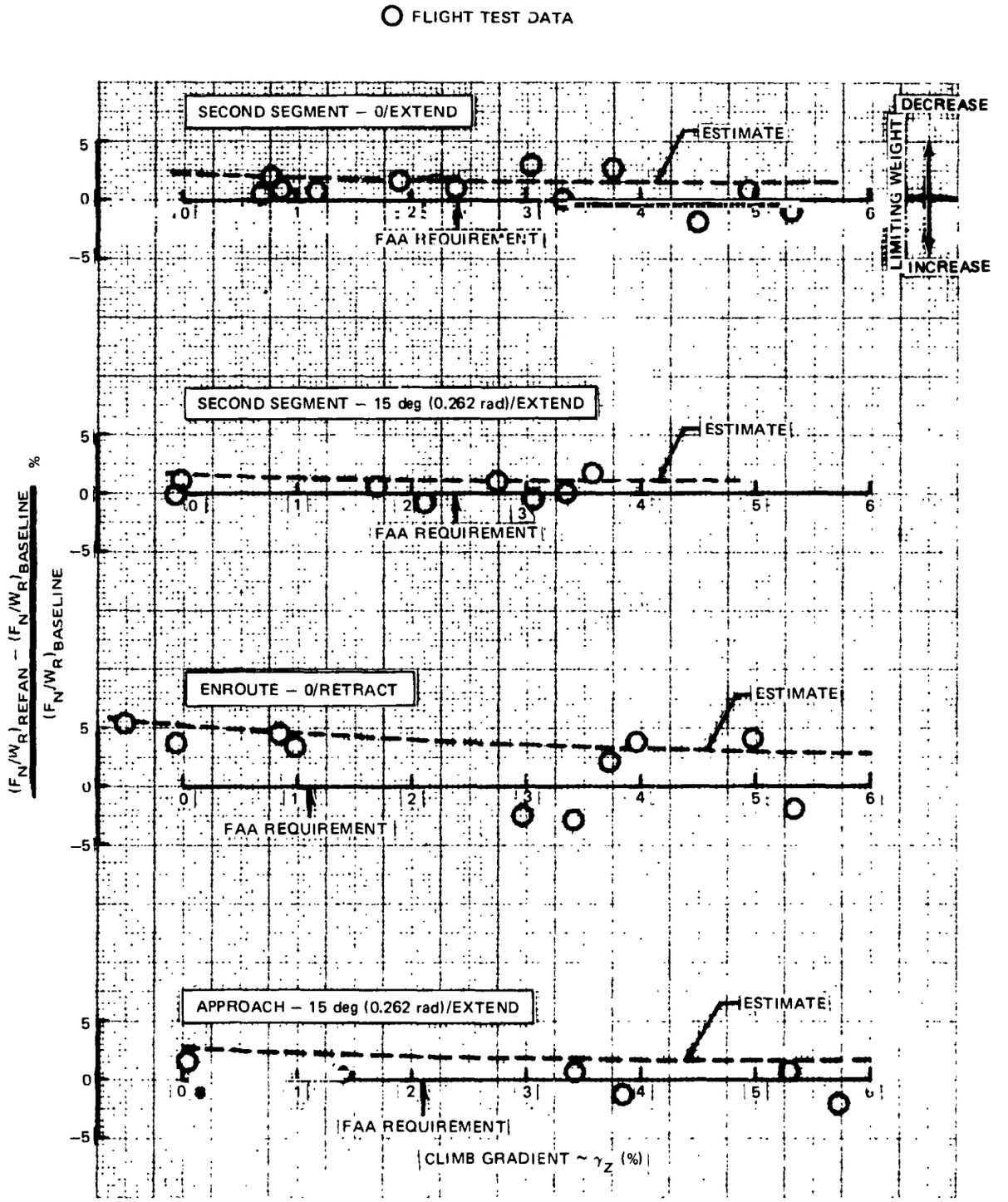

FIGURE 29. DC-9 REFAN CLIMB PERFORMANCE

Cruise Performance

Cruise performance tests were conducted to obtain airplane drag information and overall airplane performance in the form of range factor, which was used to determine the incremental effect on specific range due to the DC-9 Refan airplane with JT8D-109 engines relative to the JT8D-9 powered production DC-9-30.

The airplane was stabilized for level, unaccelerated flight at the specified airspeed. Altitude and gross weight conditions were chosen to obtain W/δ values of 181 400 kg (400,000 lb), 158 800 kg (350,000 lb), 136 100 kg (300,000 lb), and 90 700 kg (200,000 lb). The incremental airplane performance data were determined in the cruise (clean wing) configuration.

The cruise performance increment for installing JT8D-109 Refan engines was evaluated based on drag and range factor increments. The JT8D-9 powered DC-9-30 production airplane drag is based on the composite drag of three separate airplanes. The range factor is also based on the average of three separate airplanes, all powered by JT8D-9 engines.

Figure 30 shows the measured drag increase at four W/δ's due to installing the JT8D-109 engine. The four W/δ's tested are representative of cruise operation at altitudes of 6 096 m (20,000 ft), 8 839 m (29,000 ft), 9 449 m (31,000 ft) and 10 668 m (35,000 ft)(higher W/δ for higher altitude). The data points indicate that the drag penalty is about as estimated (skin friction and form drag only), about a 2 percent increase in airplane drag. This is not Mach number dependent for W/δ = 90 700 kg (200,000 lb), 136 100 kg (300,000 lb), or 158 800 kg (350,000 lb); only at W/δ = 181 400 kg (400,000 lb) is there any indication of the favorable interference (effect of engine stream tube reducing wing compressibility drag) that was measured in the wind tunnel.

Figure 31 shows the measured range factor reduction at four W/δ's for installing JT8D-109 engines. For the important operating conditions (M_0 = 0.75 - 0.78) the range factor is reduced by about 5 to 7 percent.

About 2 percent is due to the increased drag of the larger nacelle. The balance (3-5 percent) is due to the poorer SFC of the prototype JT8D-109 engines. The SFC difference is in agreement with the JT8D-109 SFC measured during the engine calibration tests and the test data generated from the engine deck (CCD0281-00.0) built from the ground static and NASA Lewis altitude tests conducted on a Pratt and Whitney test engine (S/N P-667091). For comparison the deck data are used to represent the average of the two prototype flight test engines. The range factor decrement is about one percent or so worse at W/δ = 90 700 kg (200,000 lb) due to the poorer SFC of the JT8D-109 prototype engine at the lower thrust settings.

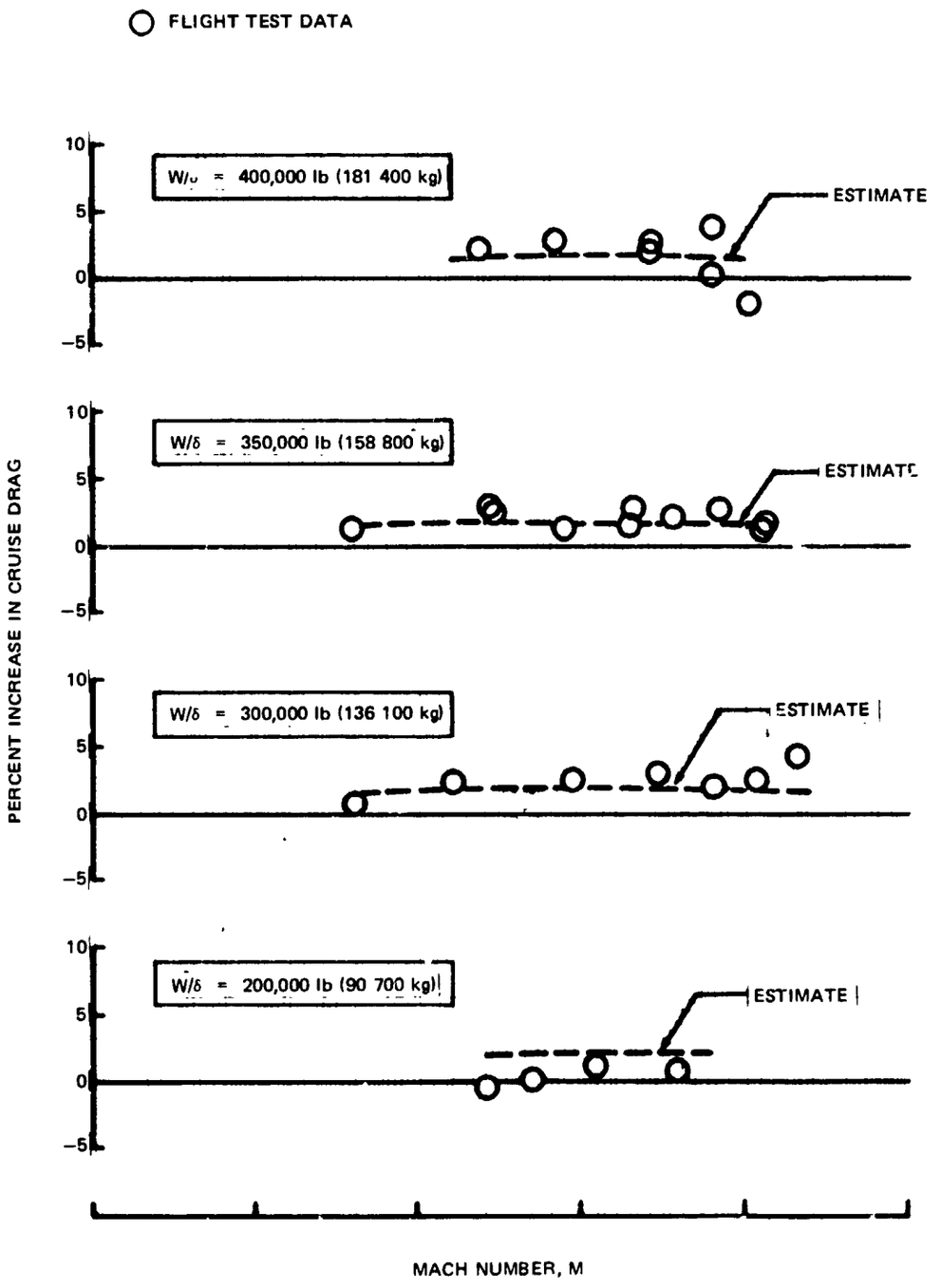

FIGURE 30. DC-9 REFAN CRUISE DRAG CHARACTERISTICS

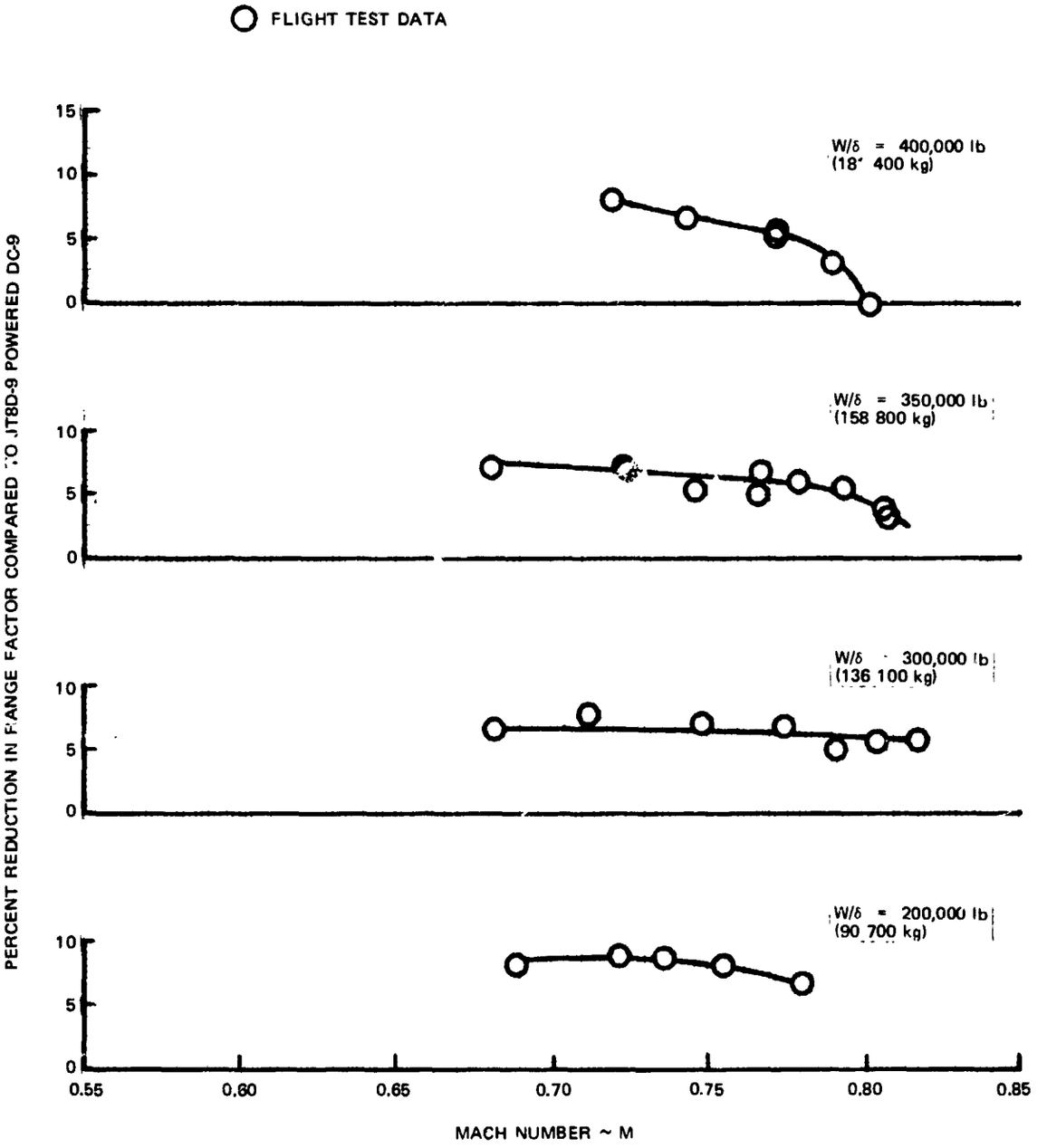

FIGURE 31. DC-9 REFAN RANGE FACTOR CHARACTERISTICS

Drag Polars - All-Engine

In order to accurately define the flight profiles and thrust requirement for FAR Part 36 flyover noise level measurements, test flights were made to determine the trimmed drag of the DC-9 Refan airplane.

DC-9 Refan drag polars were evaluated at an operational c.g. of about 19 percent M.A. C. for two configurations: flaps/slats 0°/Extend for the takeoff noise profile and 0.873 rad (50 deg)/Extend for the approach noise profile. Three minutes of continuous data were recorded during stabilized level unaccelerated flight at various airspeeds in the takeoff and landing configurations.

The flight measured results are in good agreement with an estimate based on the production DC-9 Series 30 drag polars. The estimate accounts for the increased nacelle skin friction drag of the JT8D-109 engine installation.

The drag polars obtained for these two configurations were used to define the takeoff flight paths and approach thrust requirements for the FAR Part 36 noise data.

Fuel Supply

The suction fuel feed capability of the JT8D-109 engine was evaluated during a climb to altitude.

At approximately 488 m (1,600 ft), MCL thrust was set and the climb conducted to the following schedule.

129 m/s (250 KIAS) to 3 048 m (10,000 ft)

165 m/s (320 KIAS) to 0.74 M_N

0.74 M_N to 9 144 m (30,000 ft) cruise altitude

The LH tank boost pumps were turned OFF at about 1 524 m (5,000 ft) and the LH engine operated on suction fuel feed for the remainder of the climb to 9 144 m (30,000 ft). The boost pumps were returned to normal configuration after the climb was completed.

The systems configuration for the test was normal for climb except the LH fuel tank boost pump was OFF and fuel crossfeed CLOSED.

No signs of engine instability were noted by the pilots during the MCL climb utilizing fuel suction feed. Prior to turning off the boost pumps (figure 32 and 33), the fuel pump inlet pressure was 172-207 kPa (25-30 psig) and interstage pressure was 538-607 kPa (78-88 psig). With the engine operating on suction feed, the inlet pressure was -7 to 0 kPa (-1 to 0 psig) and interstage pressure was about 483 kPa-552 kPa (60-70 psig). Cockpit indicated fuel flows were normal for the engine power settings.

The Refan engine suction fuel capability during the climb to altitude was demonstrated satisfactorily with no indication of engine instability and no unusual certification requirements anticipated.

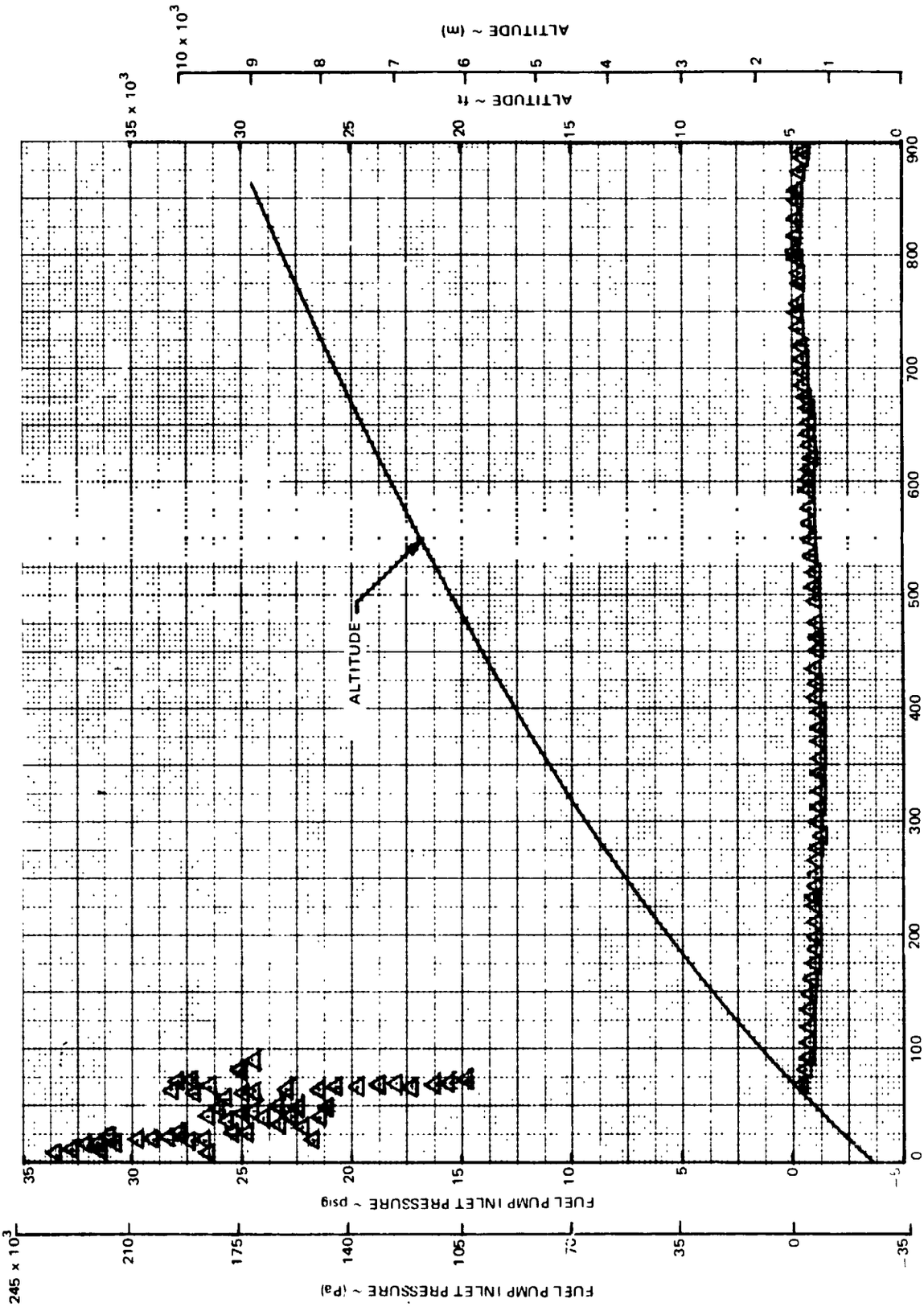

FIGURE 32. DC-: REFAN FUEL PUMP INLET PRESSURE

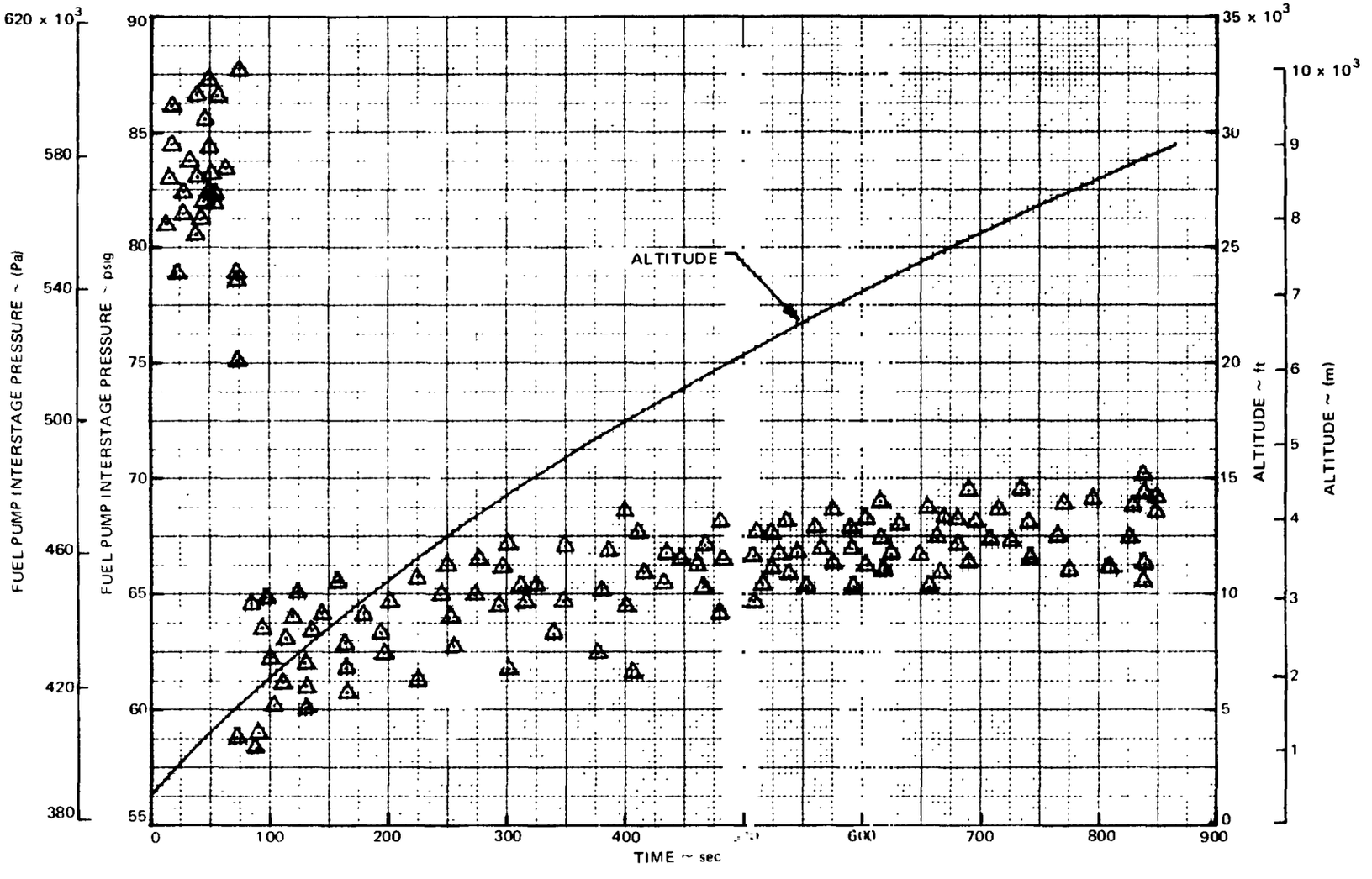

FIGURE 33. DC-9 REFAN FUEL PUMP INTERSTAGE PRESSURE

Engine Starting

The JT8D-109 engine starting characteristics were determined to verify ground starting and the low speed portion of the windmill start envelope in flight.

- Engine Starting - Ground

  The ground start tests were conducted for a range of ambient conditions and are considered satisfactory with little change from other JT8D versions for the conditions monitored.

- Engine Starting - Inflight

  Inflight starts were conducted using normal inflight engine start procedure for windmill starting. The test engine was restarted after a normal cool down and shutdown of the test engine with N_1 and N_2 stabilized.

Stabilized windmill data (N_1 and N_2) prior to initiation of the start is presented in figure 34. A comparison to readily available JT8D-15 engine N_2 data is also shown. The airstarts conducted are shown on a summary envelope similar to current JT8D engines in figure 35. A slow speed start outside the published envelope (figure 35) resulted in a peak EGT of 523°C (973°F), limit is 520°C (968°F).

The low speed inflight starting envelope was verified to be satisfactory.

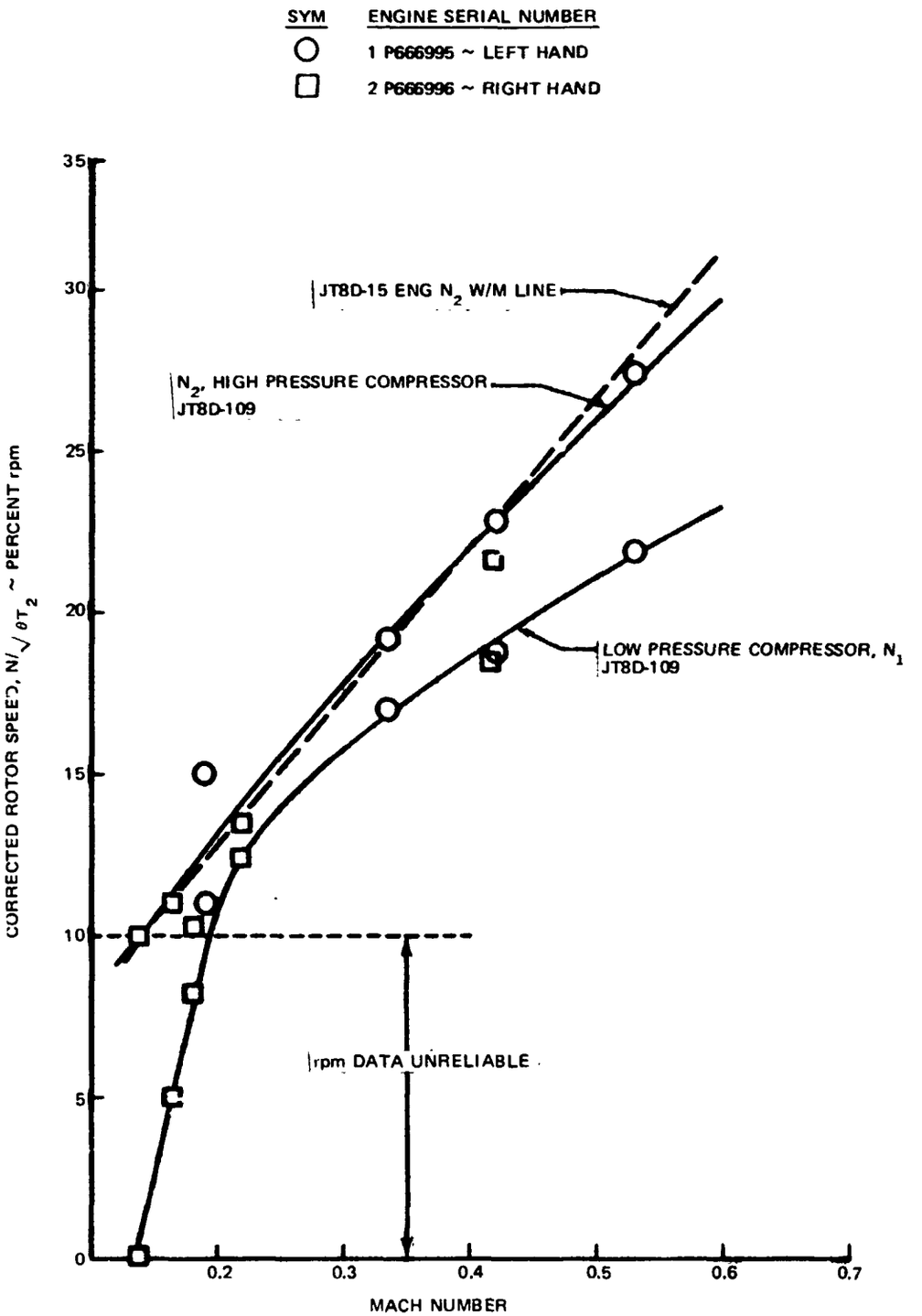

FIGURE 34. DC-9 REFAN WINDMILL SPEED vs MACH NUMBER

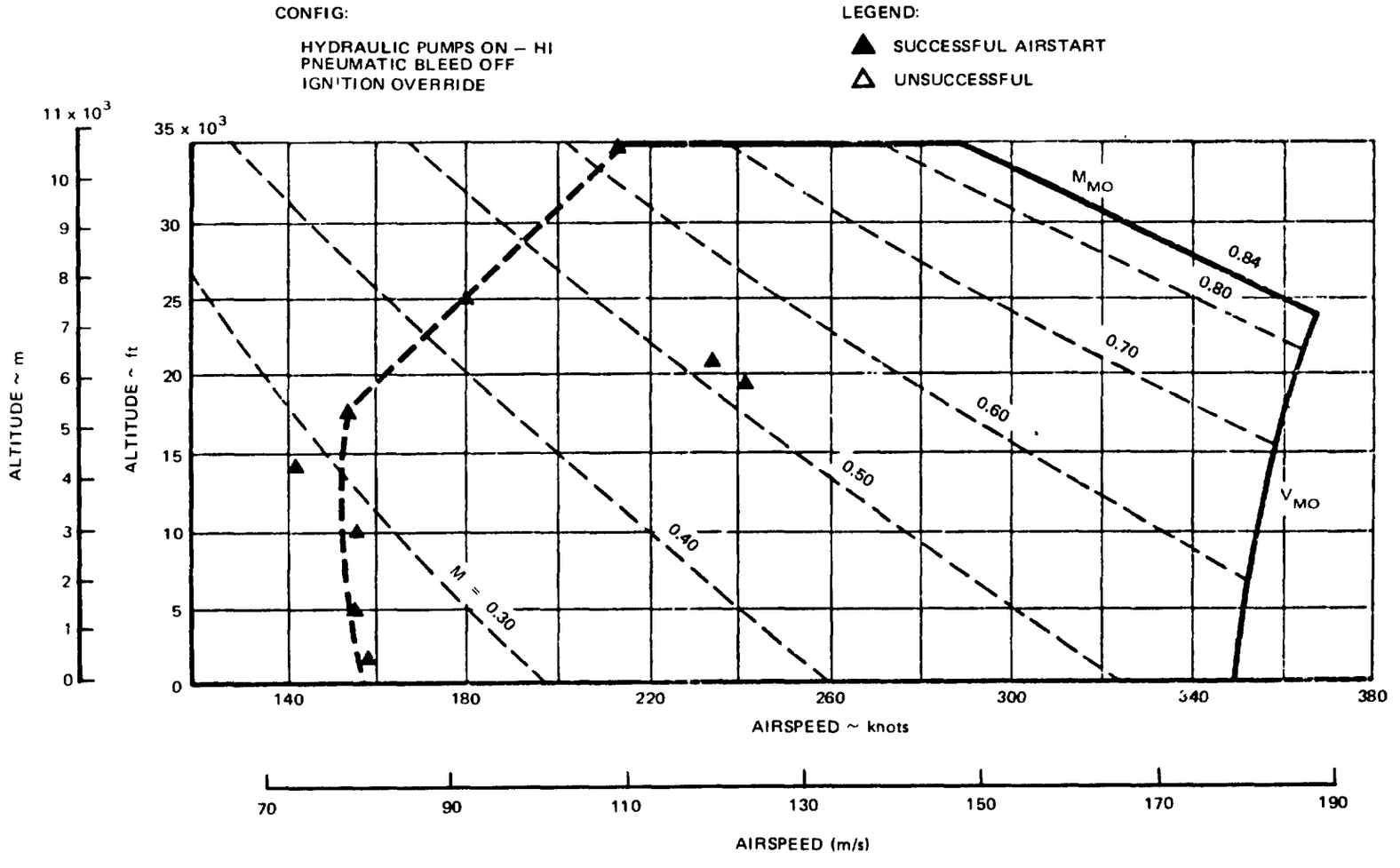

FIGURE 35. DC-9 REFAN ENGINE AIR START ENVELOPE

Flight Test Prototype Engine Performance

Engine performance was evaluated to assess the compatibility of the JT8D-109 engine with the airframe and subsystems on the ground and inflight.

Installed engine calibration data, thrust lapse rate data, maximum climb thrust data, engine transient data and effects of airplane stall on engine operations were evaluated during the test program.

Overall, the engine operations were excellent with no major problems encountered. Engine performance was very close to the predicted levels.

Installed engine calibration. - The performance parameters of the JT8D-109 engine installed in the DC-9 Refan airplane were measured to obtain stabilized gas generator data at various combinations of power settings, flight conditions, bleed, and power extractions. These data were needed to establish the effects of normal and maximum (ground only) engine system configurations on engine performance.

The engine system configurations for the inflight and ground tests, are shown in table 12.

TABLE 12

ENGINE SYSTEM CONFIGURATION SUMMARY

SYSTEM DESIGNATION	GENERATOR	HYDRAULICS	PNEUMATICS
Minimum	Off	Off	Off
Normal	On	High	One A/C Pack
Maximum	On	High	Two A/C Pack X-Feed Open

The installed engine performance and the effects of power extraction and bleed air on engine performance was evaluated. Calculated net thrust and measured engine parameters are presented compared against Pratt and Whitney test data which has been adjusted to include the installed effects of the Douglas Aircraft Company inlet, nozzle, subsystems and bleeds.

The Pratt and Whitney Aircraft test data used was generated from an engine deck (CCD 0281-00.0) that was built by Pratt from the experimental JT8D-109 Engine #3 (S/N P-667091) Ground Static and NASA Lewis Altitude Test data. Data from this source used herein is referred to by the engine deck number CCD 0281.

- Installed Engine Calibration - Ground

Stabilized data was obtained at sea level, static conditions from test runs on left and right hand engines for power settings from idle to takeoff with engine system configurations of minimum, normal and maximum.

Corrected measured and calculated engine performance parameters obtained from the sea level static tests for minimum, normal and maximum engine system configurations were plotted versus engine pressure ratio (EPR) for the left and right hand engines, and are shown in figures 36 through 39. Data from the CCD 0281 deck was generated for the normal system configuration and is plotted on the same figures.

The effects of bleed and power extraction are shown (figure 39) as percent delta change of the maximum and normal system configurations compared against the minimum condition and plotted versus EPR. The effects of bleed and power extraction on thrust, fan pressure ratio and low pressure rotor speed were small enough to be considered insignificant and were not plotted.

- Installed Engine Calibration - Inflight

Stabilized data from both engines were obtained with minimum and normal engine system configurations at the following conditions:

a) 762 m (2,500 ft) altitude, 0.23 M, inflight takeoff to minimum approach power, normal system configuration only.

b) 7 620 m (25,000 ft) altitude, 0.72 M, MCT to minimum power required for level flight.

c) 10 668 m (35,000 ft) altitude, 0.80 M, MCT to minimum power required for level flight, test conducted on left hand engine only.

Engine calibration data were obtained (figures 40, 41, and 42) at 762 m (2,500 ft) to satisfy the thrust determination portion of the flyover noise tests. No bleed and power extraction effects were evaluated.

Figures 43, 44, and 45 present engine calibration data at 7 620 m (25,000 ft) for the minimum and normal engine system configurations. The effects of system configuration changes on engine performance are shown in figure 46. The effects on thrust, fan pressure ratio and low pressure rotor were small (very similar to what was seen in the sea level static data) and were not plotted.

Figure 47 presents corrected specific fuel consumption versus corrected net thrust at 7 620 m (25,000 ft), 0.72 M for the normal engine system configuration. Pratt and Whitney Aircraft test data generated from the CCD 0281 engine deck for the same conditions are plotted on the same figure.

Engine calibration data was obtained at 10 668 m (35,000 ft), 0.80 M for the minimum and normal system configurations on the left hand engine only. These data are shown in figures 48 through 51. Corrected specific fuel consumption versus corrected net thrust is shown in figure 52.

Installation and testing of two prototype flight test engines (P-666995 and P-666996) on Ship No. 741 was accomplished within the scope of normal and predictable procedures with no unusual problems.

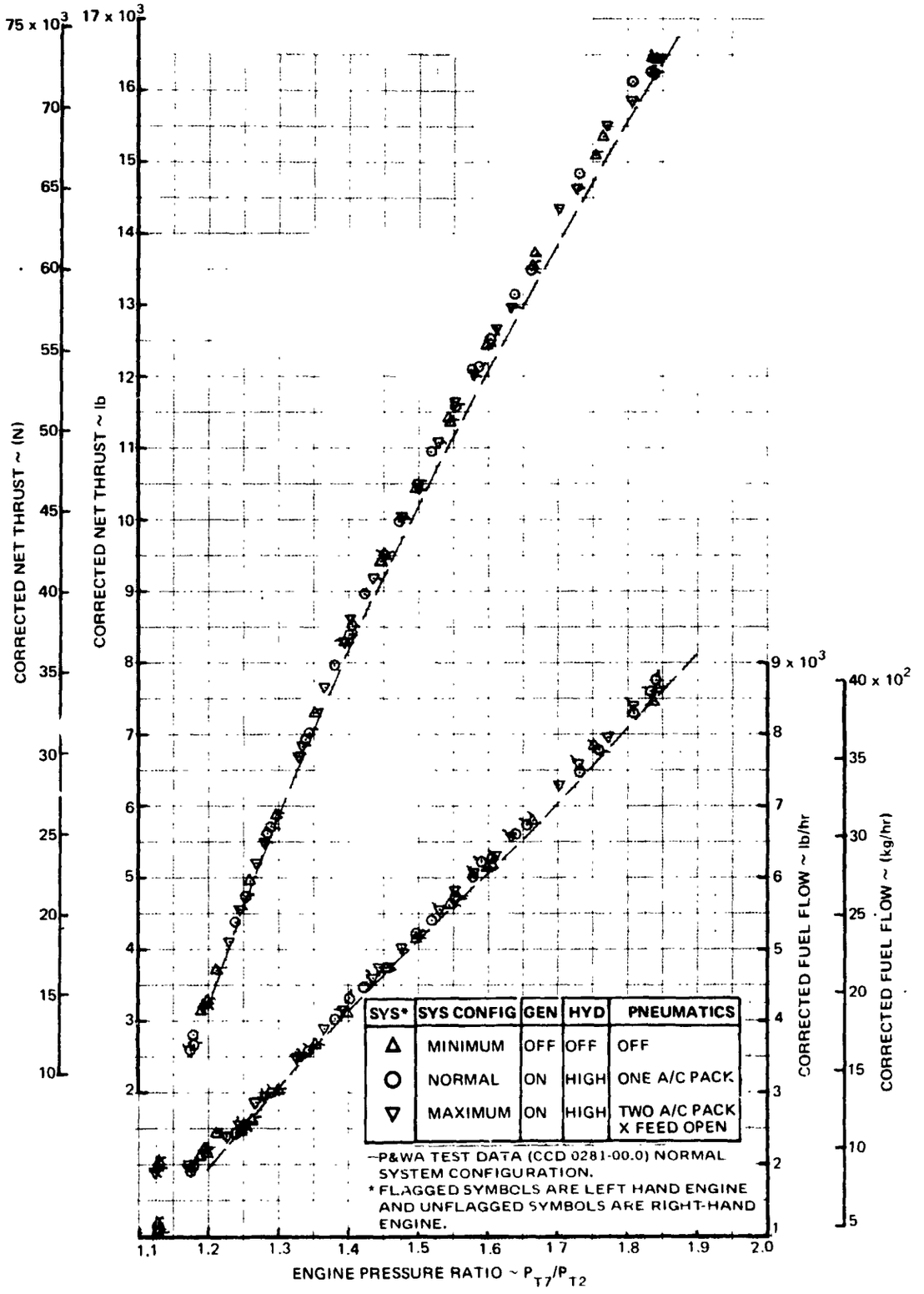

FIGURE 36. DC-9 REFAN – JT8D-109 INSTALLED ENGINE CALIBRATION SEA LEVEL, STATIC, THRUST AND FUEL FLOW

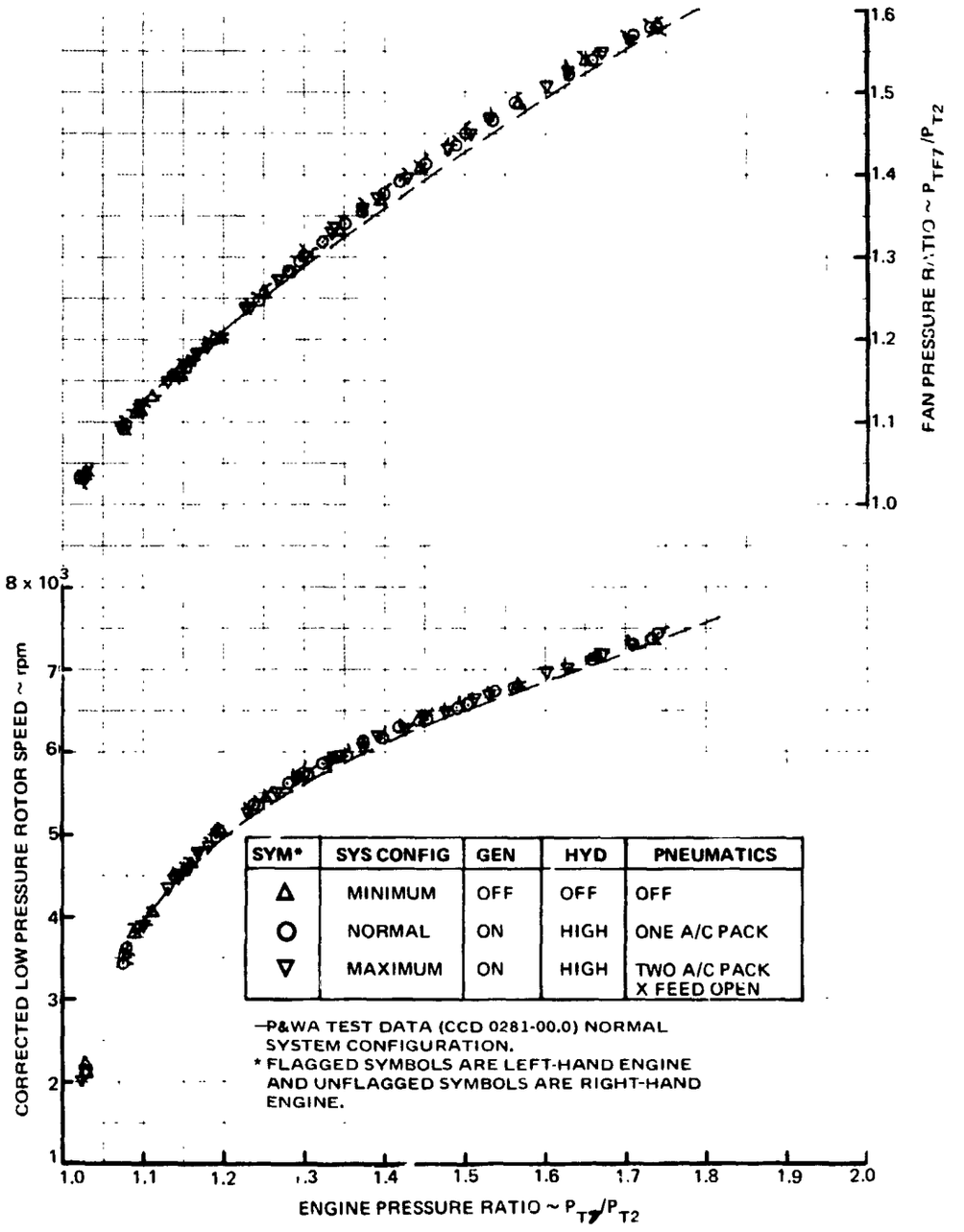

FIGURE 37. DC-9 REFAN – JT8D-109 INSTALLED ENGINE CALIBRATION SEA LEVEL, STATIC, L.P. ROTOR SPEED AND FAN PRESSURE RATIO

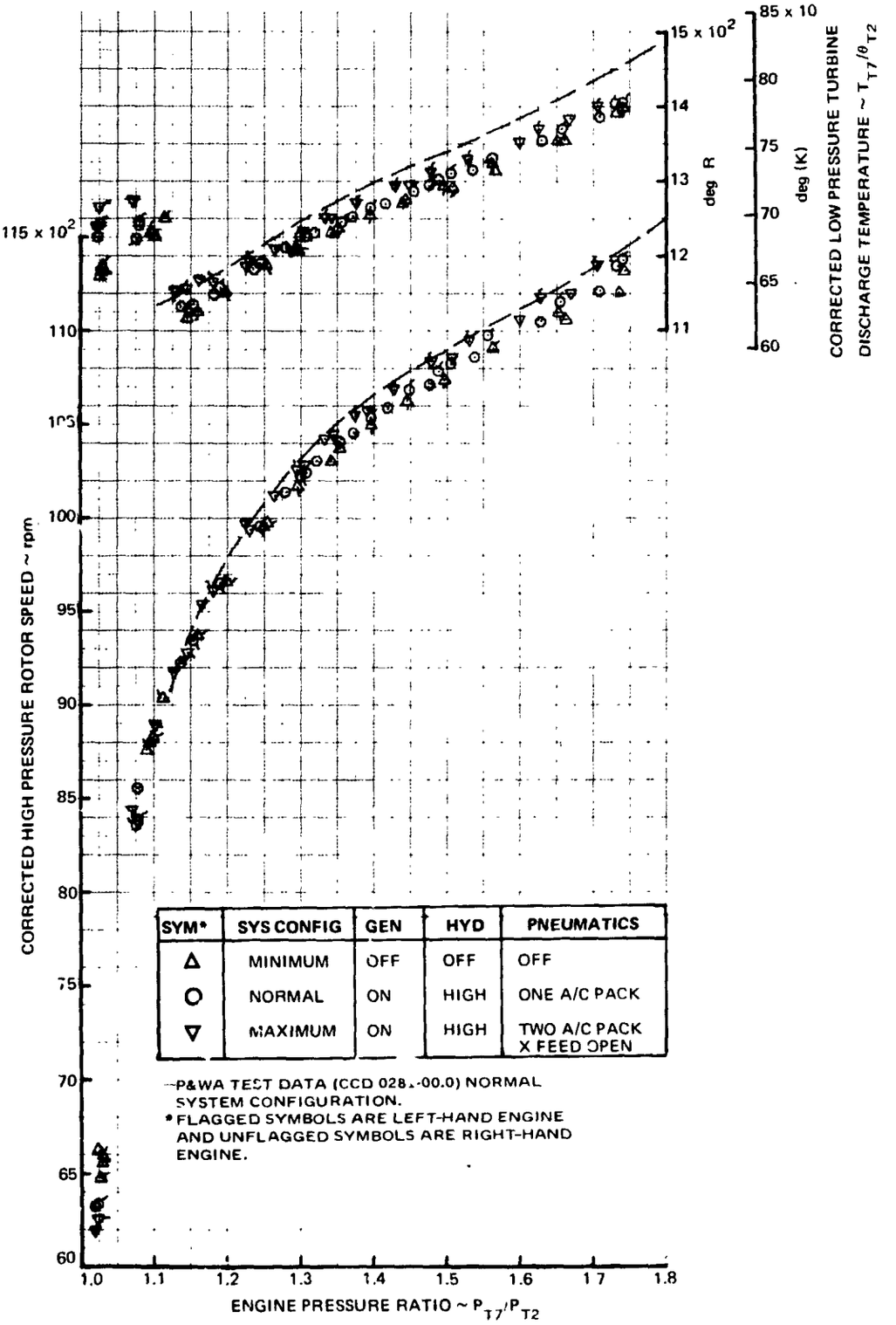

FIGURE 38. DC-9 REFAN – JT8D-109 INSTALLED ENGINE CALIBRATION SEA LEVEL, STATIC, H.P. ROTOR SPEED AND L.P. DISCHARGE TEMP.

SYM	SYS CONFIG	GEN	HYD	PNEUMATICS
O	NORMAL	ON	HIGH	ONE A/C PACK
▽	MAXIMUM	ON	HIGH	TWO A/C PACK X FEED OPEN

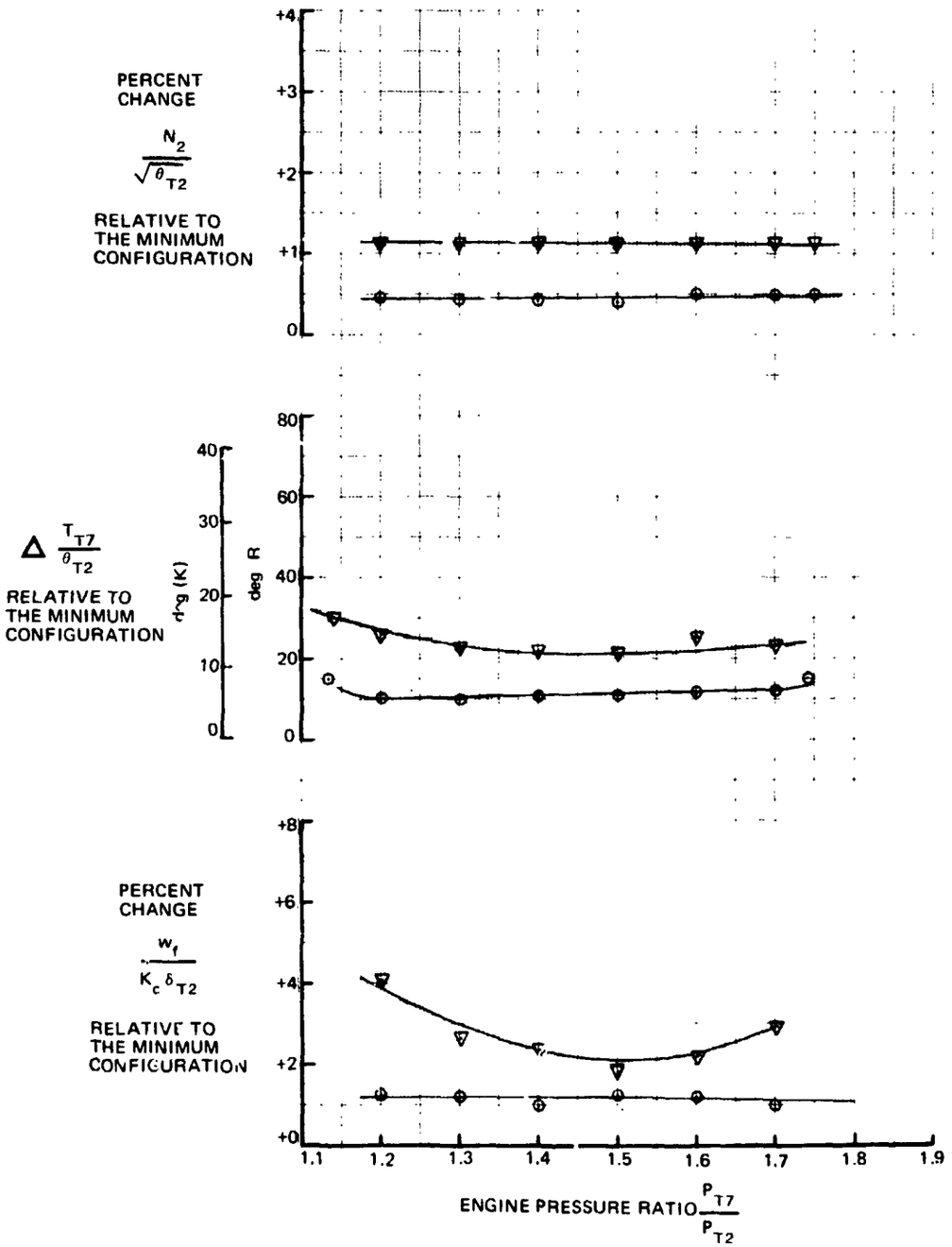

FIGURE 39. DC-9 REFAN – JT8D-109 INSTALLED ENGINE CALIBRATION SEA LEVEL, STATIC, EFFECTS OF BLEED AND POWER EXTRACTION

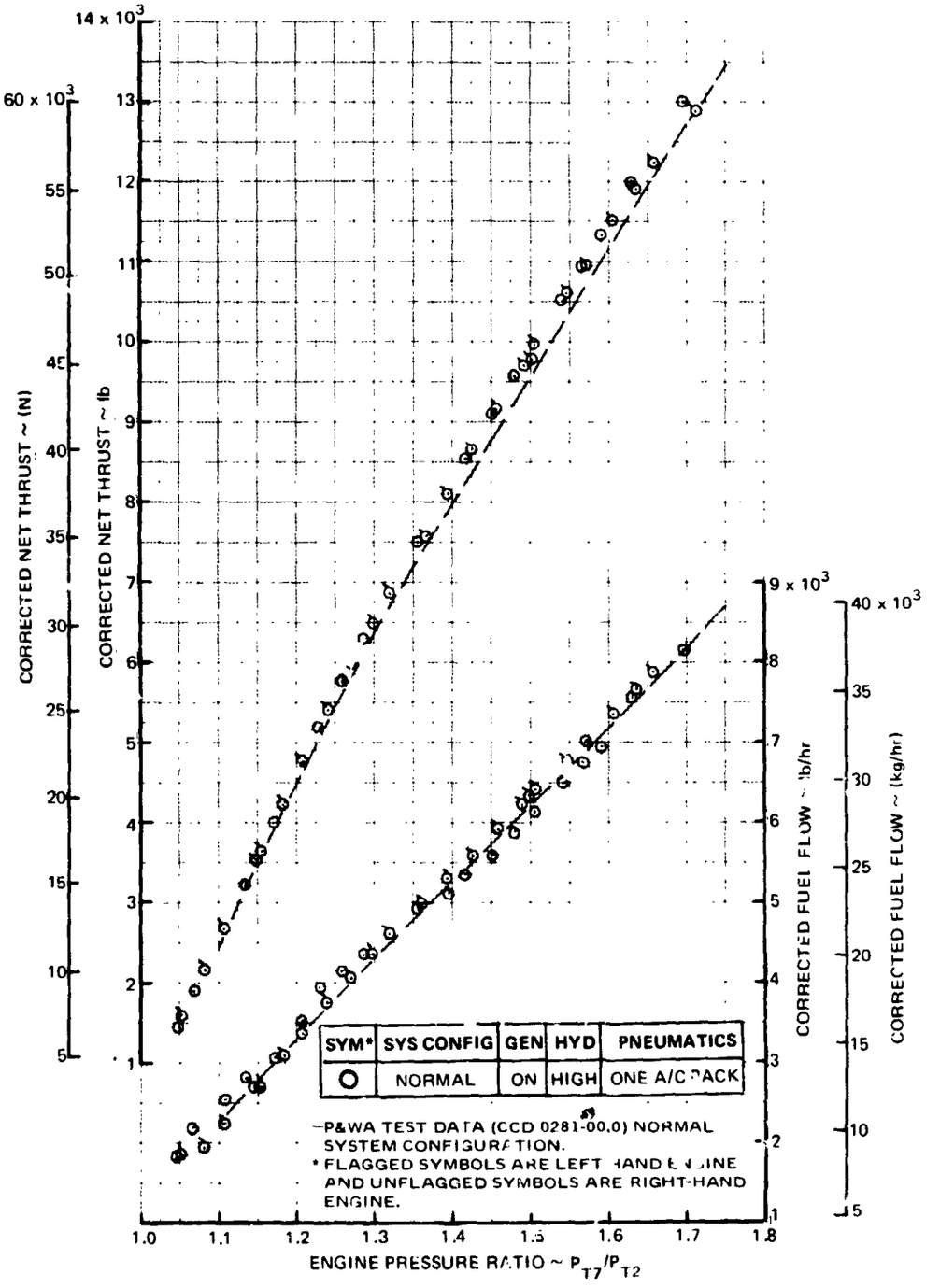

FIGURE 40. DC-9 REFAN – JT8D-109 INSTALLED ENGINE CALIBRATION
2,500 ft (762 m), 140 KNOTS (72 m/s), THRUST AND FUEL FLOW

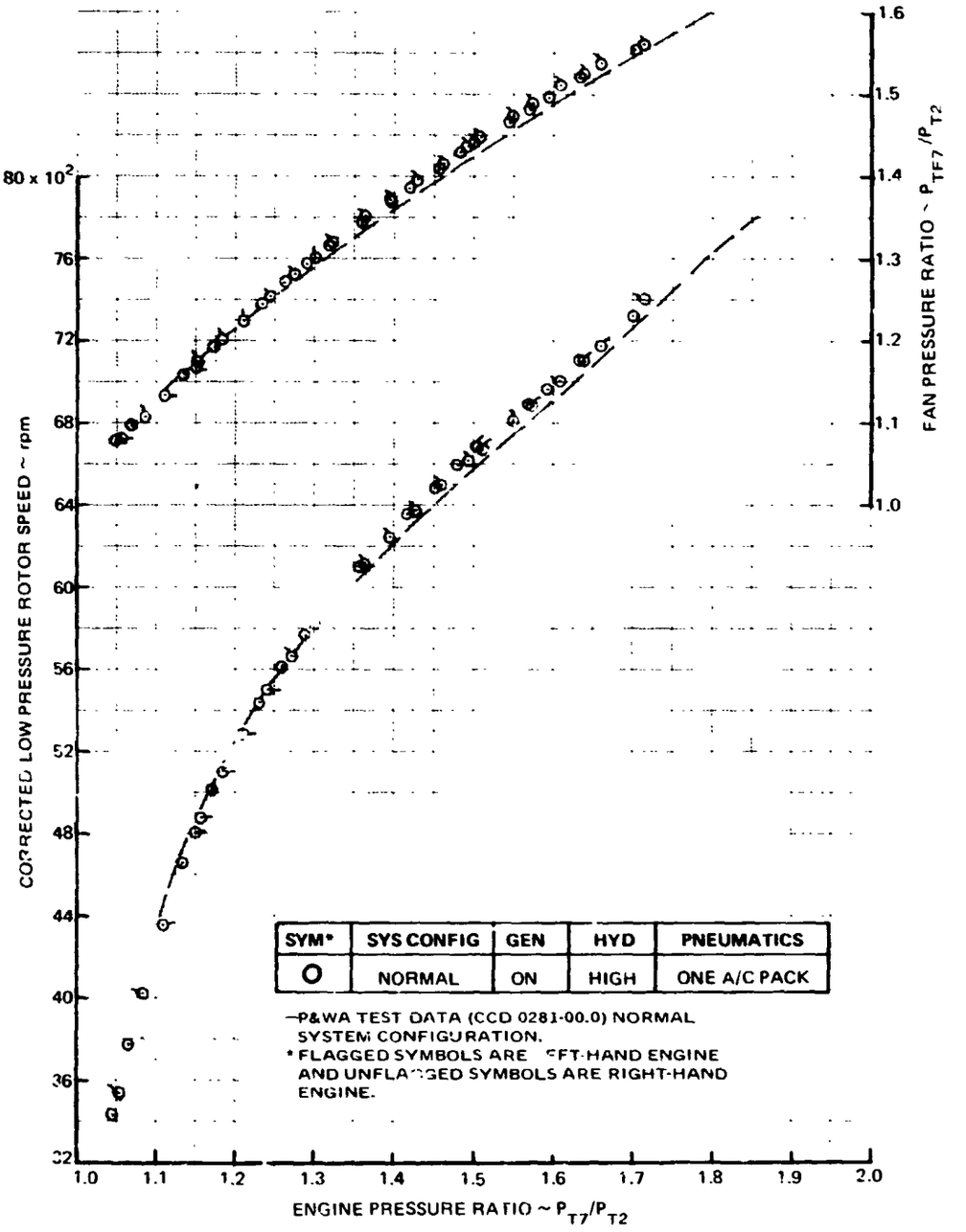

FIGURE 41. DC-9 REFAN – JT8D-109 INSTALLED ENGINE CALIBRATION 2 500 ft (762 m), 140 KNOTS (72 m/s) L.P. ROTOR SPEED AND FAN PRESSURE RATIO

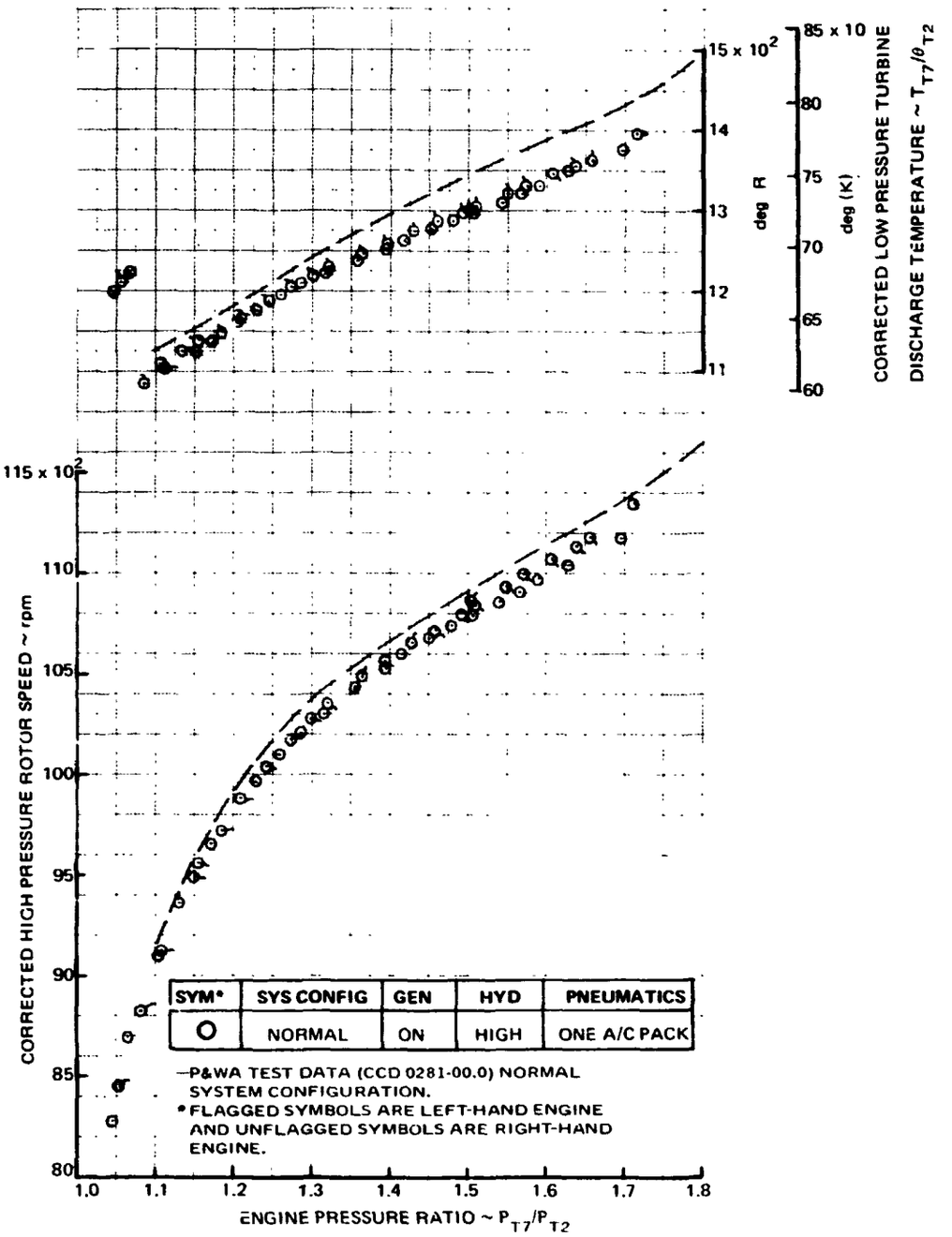

FIGURE 42 DC-9 REFAN – JT8D-109 INSTALLED ENGINE CALIBRATION 2,500 ft (762 m), 140 KNOTS (72 m/s) H.P. ROTOR SPEED AND L.P. TURBINE DISCHARGE TEMP.

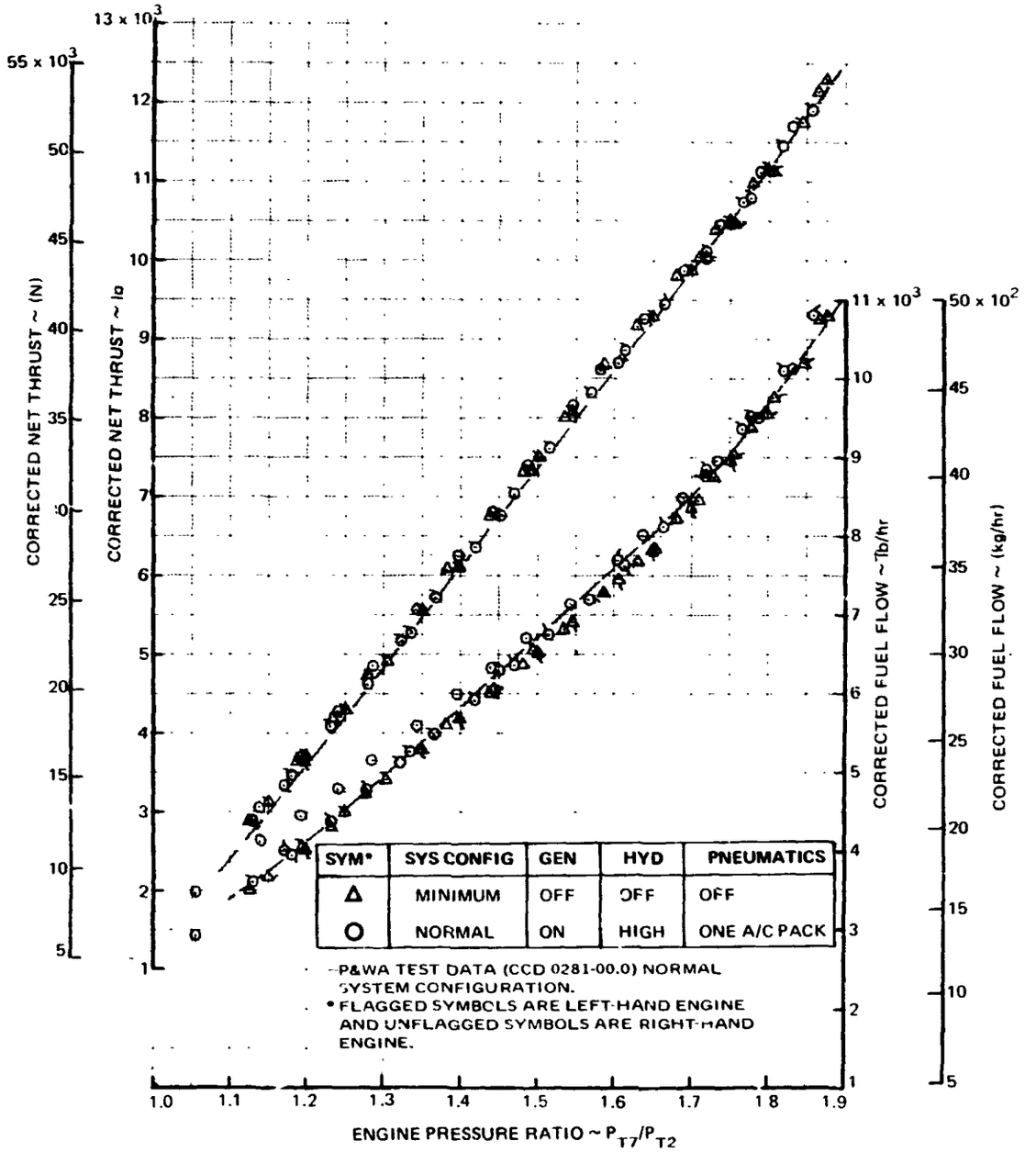

FIGURE 43. DC-9 REFAN – JT8D-109 INSTALLED ENGINE CALIBRATION 25,000 ft (7 620 m), 0.72 MACH NUMBER, THRUST AND FUEL FLOW

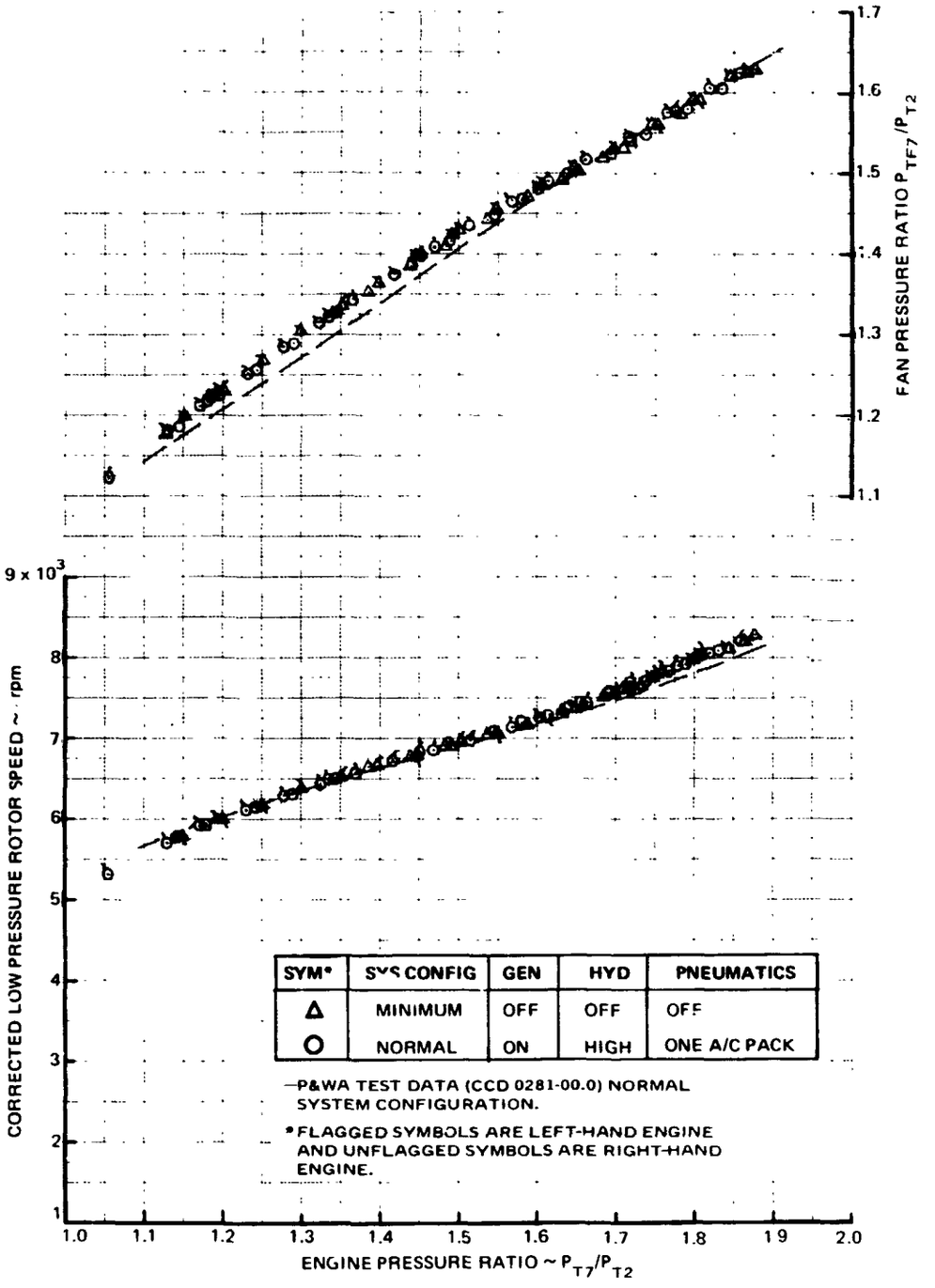

FIGURE 44. DC-9 REFAN – JT8D-109 INSTALLED ENGINE CALIBRATION 25,000 ft (7 620 m), 0.72 MACH NUMBER, L.P. ROTOR SPEED AND FAN PRESSURE RATIO

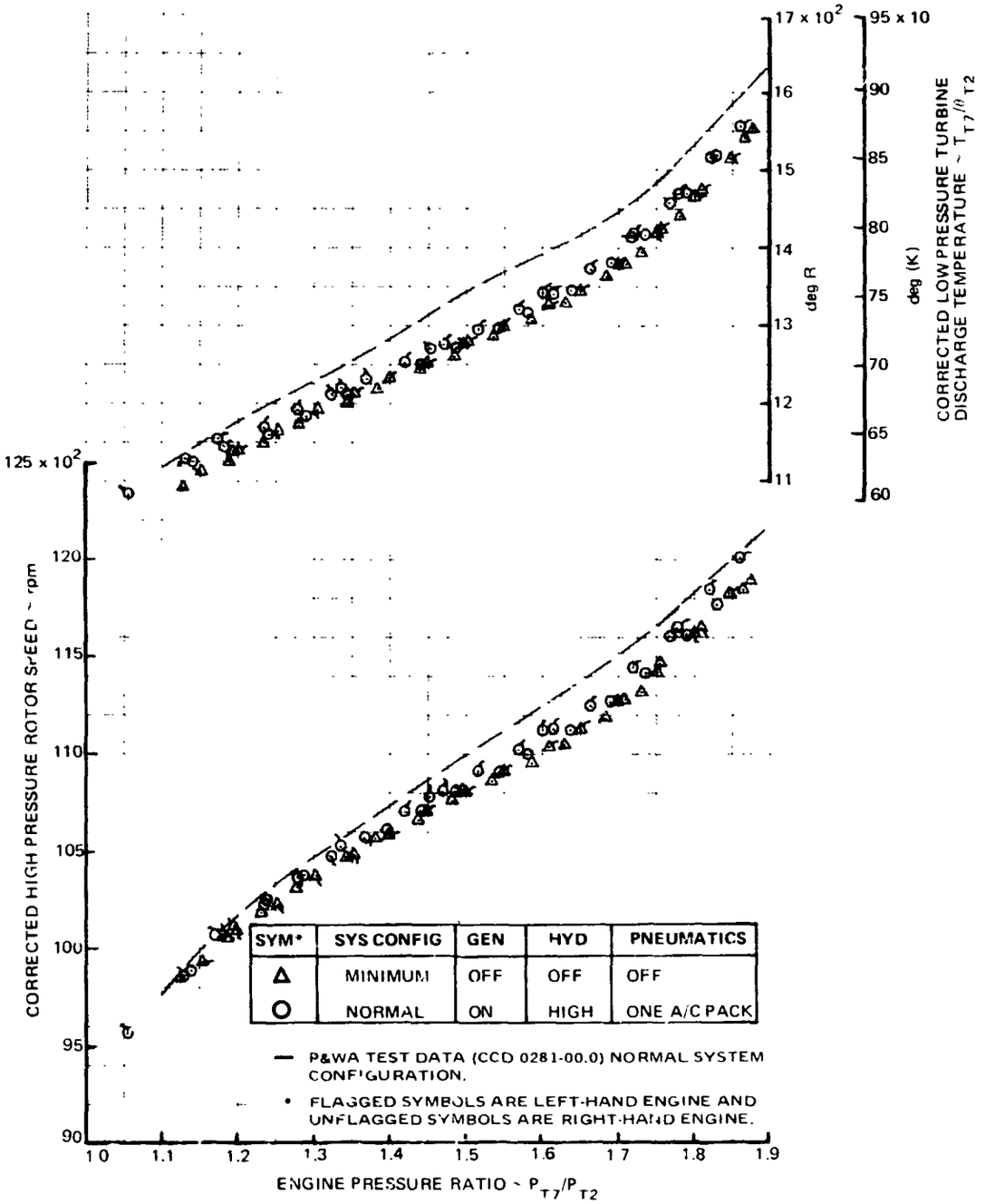

FIGURE 45. DC-9 REFAN – JT8D-109 INSTALLED ENGINE CALIBRATION 25,000 ft (7620 m), 0.72 MACH NUMBER, H.P. ROTOR SPEED AND L.P. TURBINE DISCHARGE TEMP

SYM	SYS CONFIG	GEN	HYD	PNEUMATICS
O	NORMAL	ON	HIGH	ONE A/C PACK

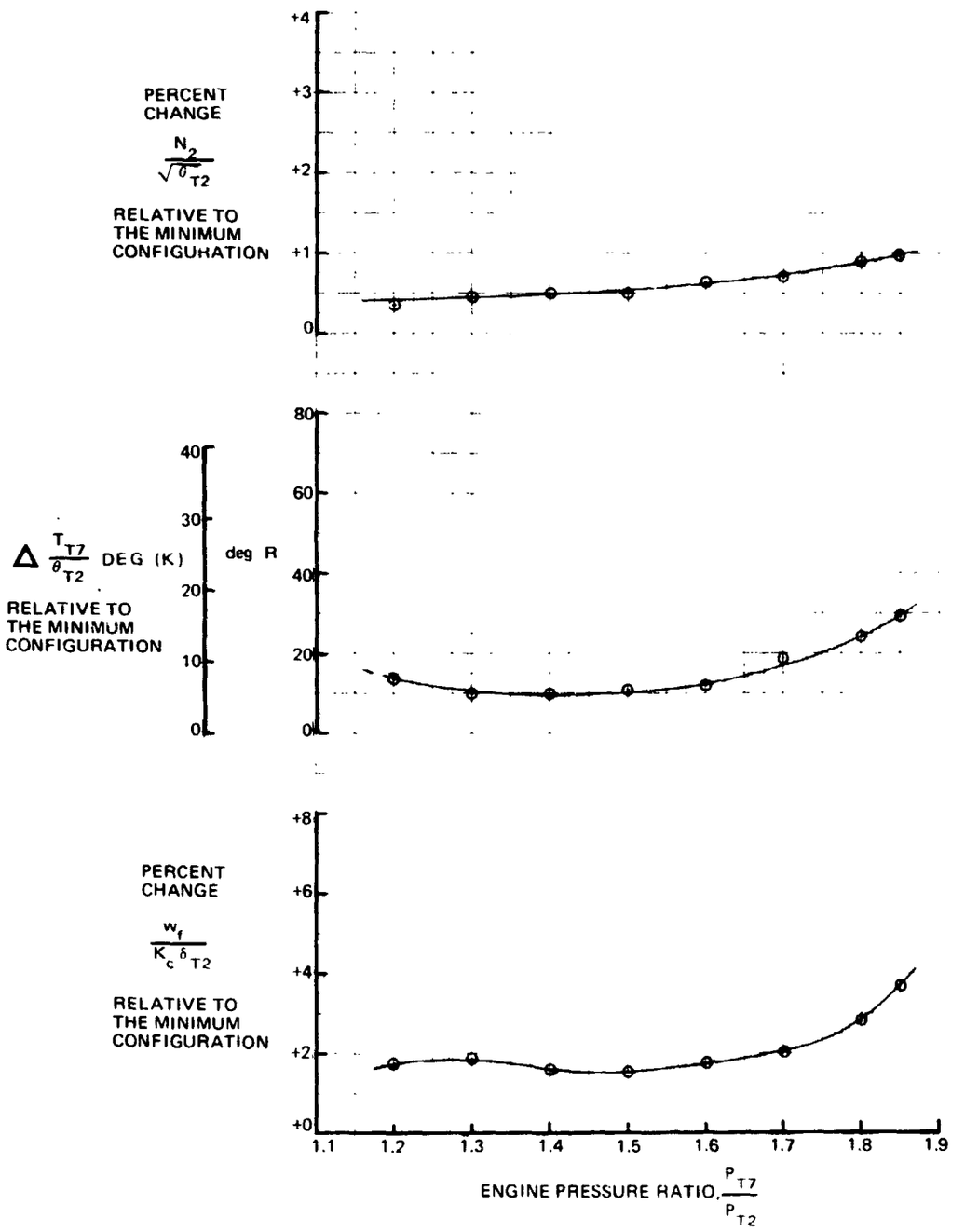

FIGURE 46. DC-9 REFAN – JT8D-109 INSTALLED ENGINE CALIBRATION 25,000 ft (7 620 m), 0.72 MACH – EFFECTS OF BLEED AND POWER EXTRACTION

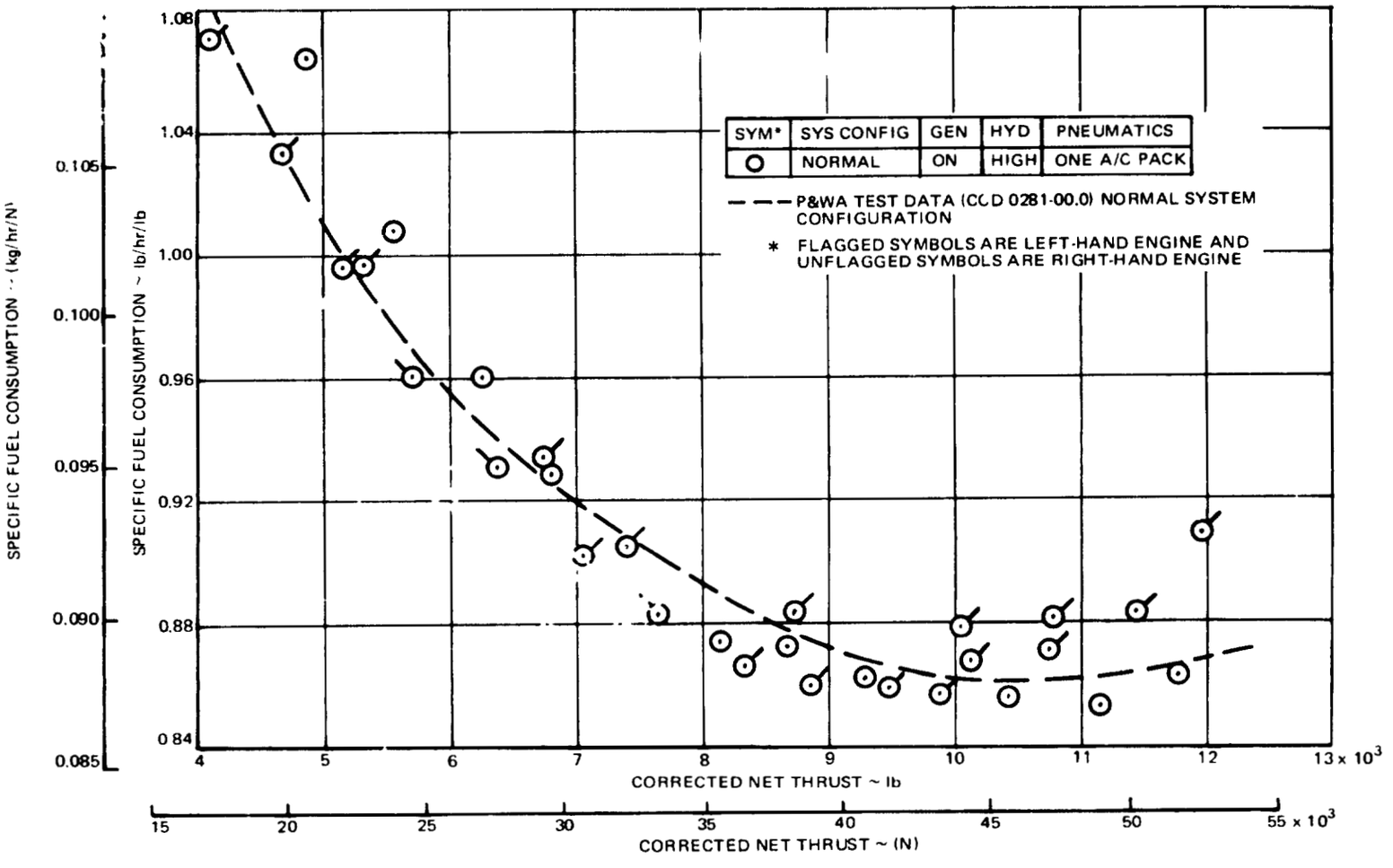

FIGURE 47. DC-9 REFAN – JT8D-109 INSTALLED ENGINE CALIBRATION
25,000 ft (7620 m), 0.72 MACH NUMBER, THRUST vs SPECIFIC FUEL CONSUMPTION

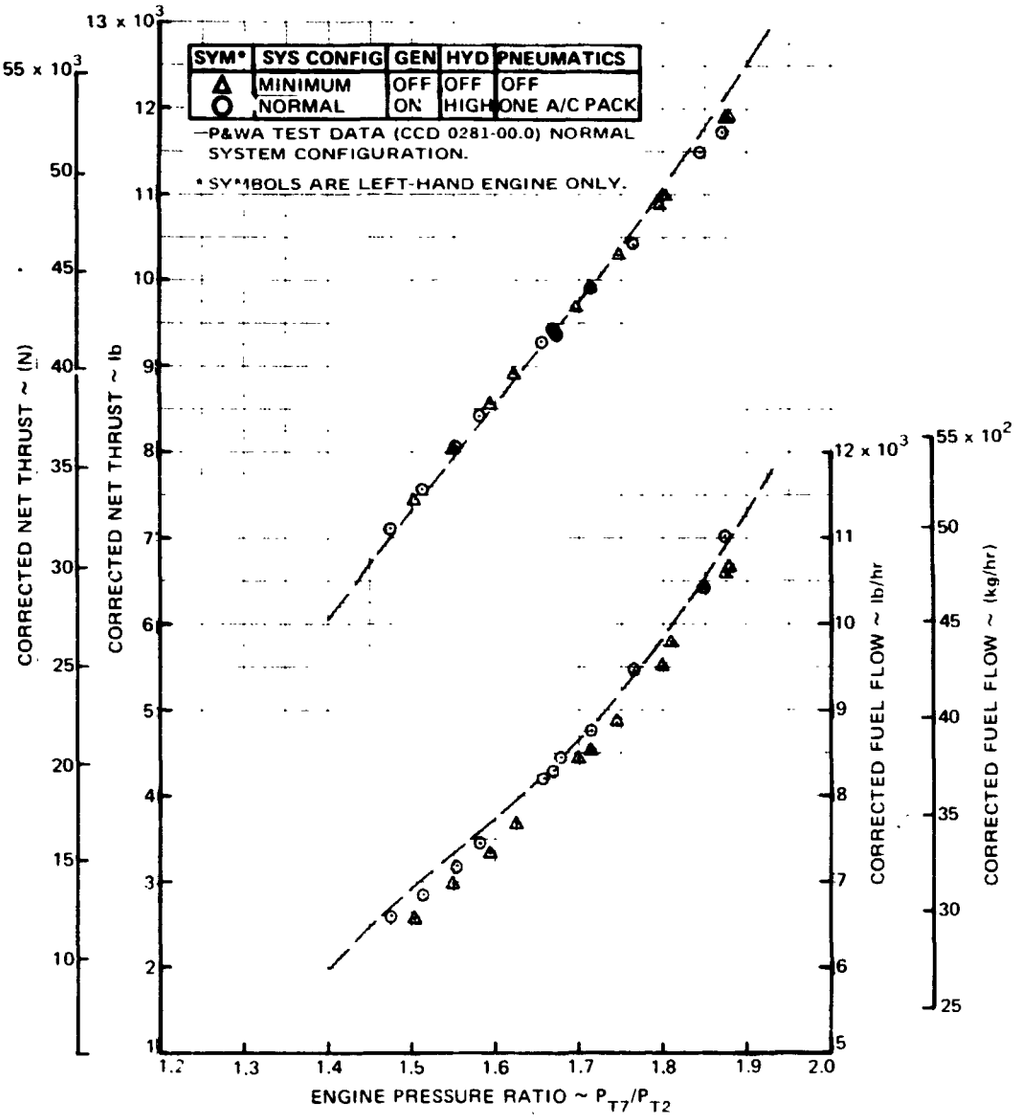

FIGURE 48. DC-9 REFAN – JT8D-109 INSTALLED ENGINE CALIBRATION 35,000 ft (10,668 m), 0.8 MACH NUMBER THRUST AND FUEL FLOW

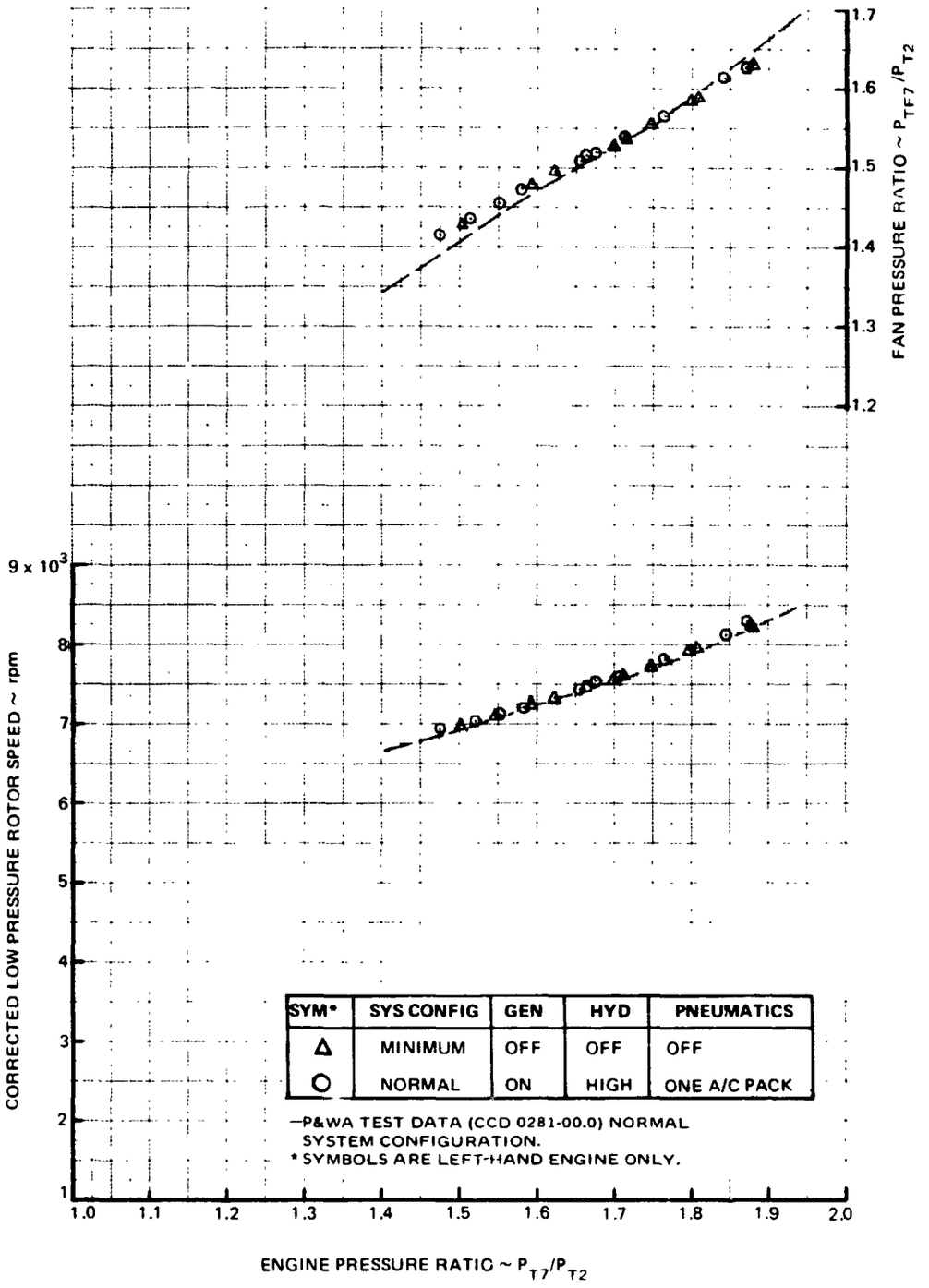

FIGURE 49. **DC-9 REFAN – JT8D-109 INSTALLED ENGINE CALIBRATION 35,000 ft (10,668 m), 0.8 MACH NUMBER, L.P. ROTOR SPEED AND FAN PRESSURE RATIO**

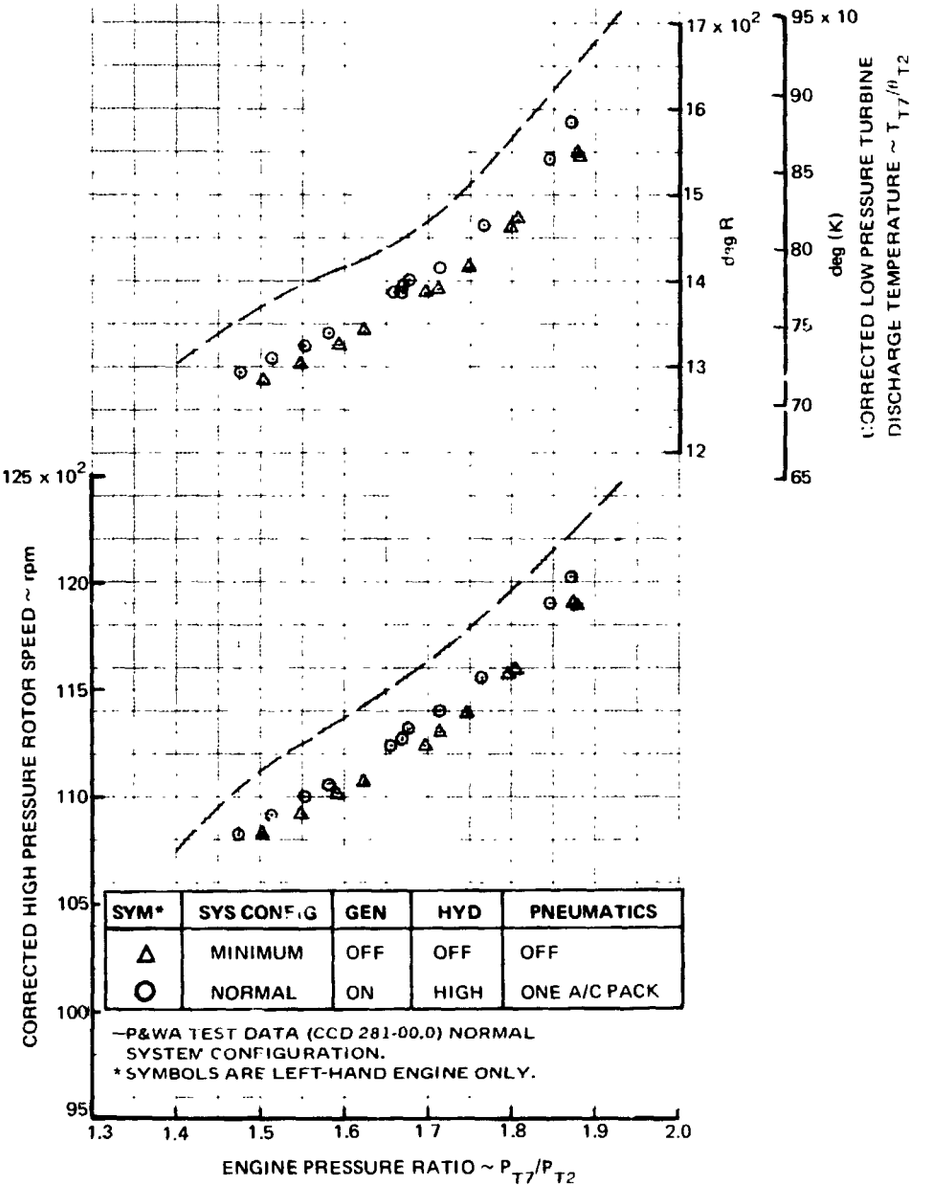

FIGURE 50. DC-9 REFAN – JT8D 109 INSTALLED ENGINE CALIBRATION 35,000 ft (10,668 m) 0.8 MACH NUMBER, H.P. ROTOR SPEED AND L.P. TURBINE DISCHARGE TEMP.

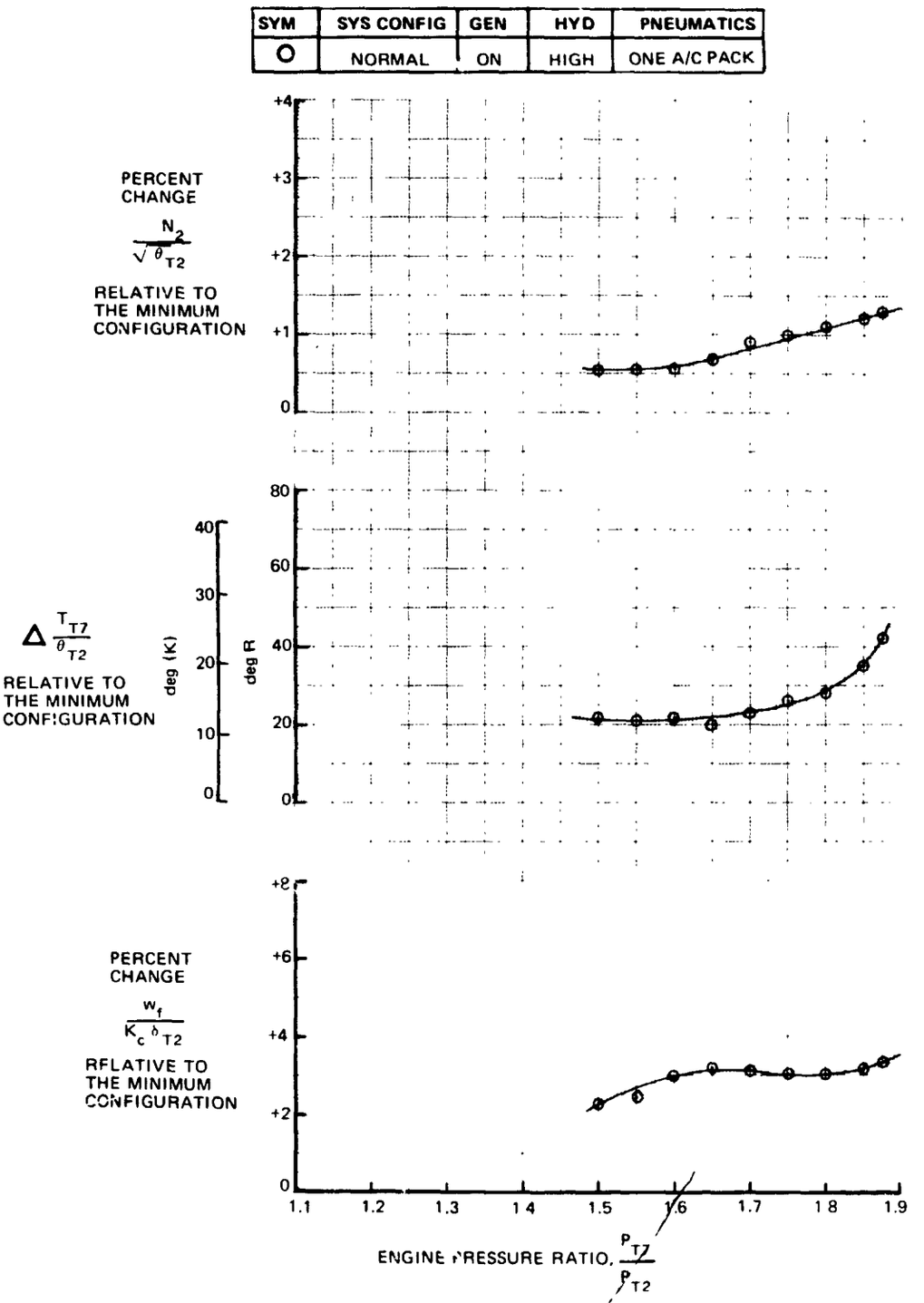

FIGURE 51. DC-9 REFAN – JT8D 109 INSTALLED ENGINE CALIBRATION 35,000 ft (10,668 m), 0.8 MACH NUMBER, EFFECTS OF BLEED AND POWER EXTRACTION

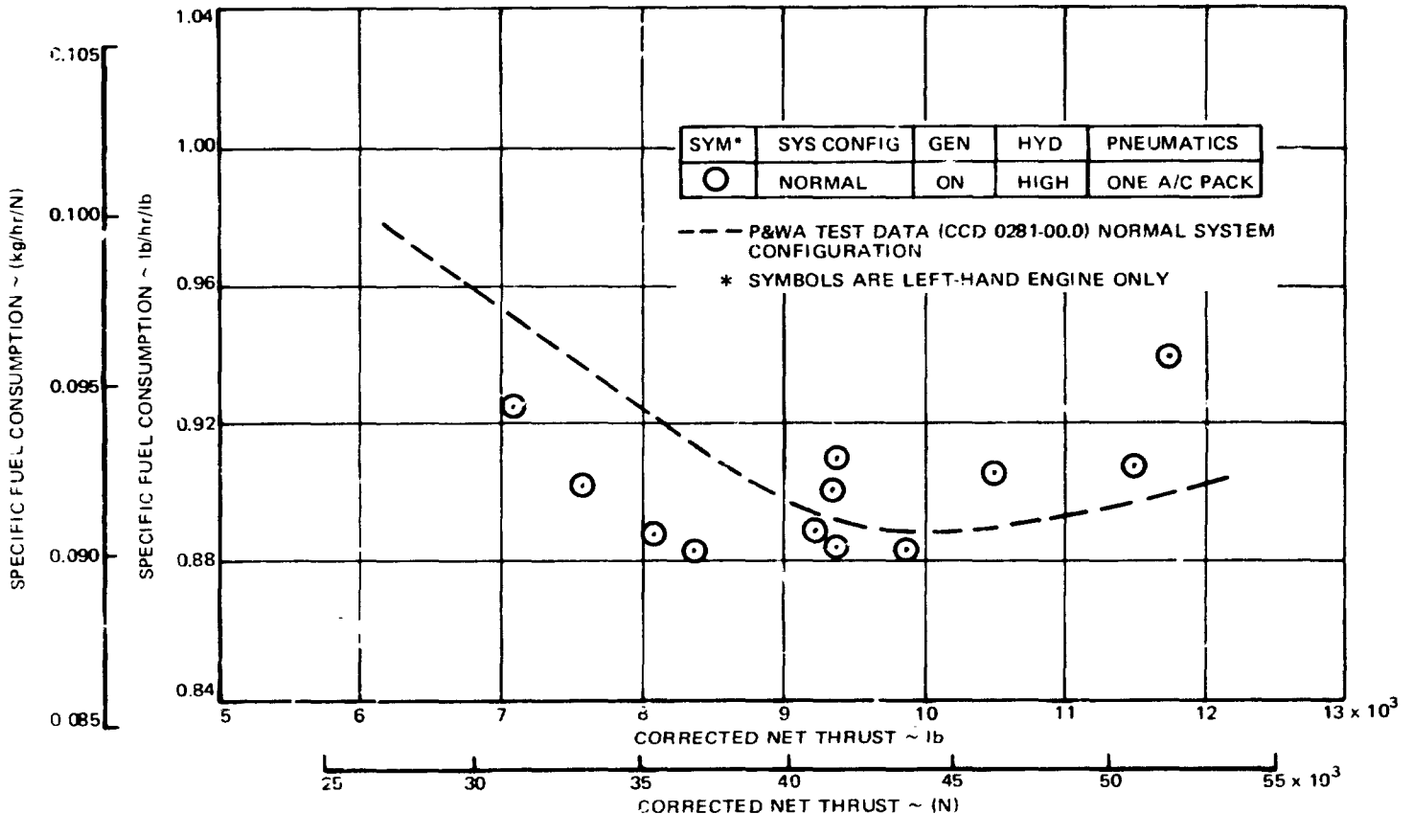

FIGURE 52. DC-9 REFAN – JT8D-109 INSTALLED ENGINE CALIBRATION
35,000 ft (10,668 m), 0.8 MACH NUMBER, THRUST vs SPECIFIC FUEL CONSUMPTION

Comparison of the flight test data with the test data generated from the CCD 0281 engine deck, indicates that the performance and effects of bleed and power extraction loads are reasonably predictable.

Generally, the flight engine performance was not modeled exactly by the engine deck; however, parameter deviations appear to be consistent, e.g., corrected net thrust, fan pressure ratio and corrected Low Pressure Rotor Speed at the same EPR and other conditions were higher than the CCD 0281 data. The corrected High Pressure Rotor Speed and the corrected Low Pressure Turbine Discharge Temperature at the same EPR and other conditions were lower than the CCD 0281 data. The corrected fuel flow parameter was the most inconsistent, at various altitudes and Mach numbers the deck data would be higher than flight results and at other conditions lower.

Thrust lapse rate. - Thrust lapse rates for the JT8D-109 engine installed in the DC-9 Refan airplane were established from data obtained during static and rolling takeoffs. The thrust lapse rate was defined with bleeds off by recording data from takeoff to altitudes of 457 m (1,500 ft) above the field.

Figure 53 shows the EPR (P_{t7}/P_{t2}) lapse rate that was demonstrated by the prototype JT8D-109 flight test engines. From the EPR lapse rate, the inflight thrust determination procedure was used to calculate the thrust values along the flight path for both takeoff procedures described above.

The thrust lapse rate with speed demonstrated by the flight test engines is shown in figure 54. Also shown is the lapse rate curve that was generated from CCD 267-3.1 engine deck and used for Refan performance estimates.

At the typical production DC-9-30 second segment speeds, the thrust lapse rate as demonstrated by the flight test engines, is approximately 2-1/2 percent better than the predicted lapse rate.

Engine operation during MCL climb. - The operation of the JT8D-109 engine during MCL climbs was evaluated to determine the pilot workload and to evaluate the ability of the JT8D-109 engine to follow the maximum climb thrust power setting schedule during climb to altitude.

Maximum climb thrust was set and the climb started at approximately 129 m/s (250 KIAS) and 488 m (1,600 ft), continued to 6 096 m (20,000 ft) and 165 m/s (320 KIAS) and terminated at 9 144 m (30,000 ft) and M = 0.74 (figure 55).

During the climb several ambient temperature inversions made the MCL EPR difficult to maintain and throttle resets were required (figure 55 and 56). The workload, in each case, was satisfactory to the pilots.

Although pilot workload was acceptable, the reset criteria of 0.01 EPR used for the DC-9 Refan airplane tests are considered too restrictive and should be 0.02 EPR units as on other current JT8D engines. During the climb tests the throttles were reset when the indicated EPR differed from the target value by 0.01 EPR.

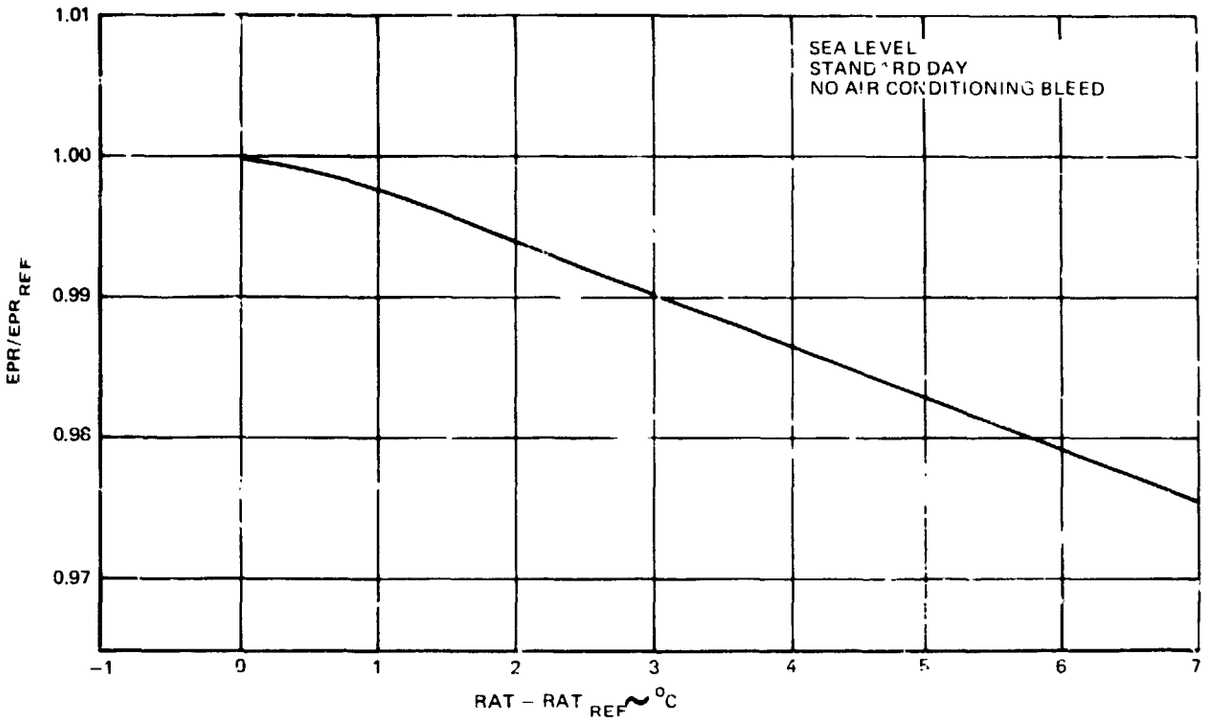

FIGURE 53. DC-9 REFAN EPR LAPSE RATE

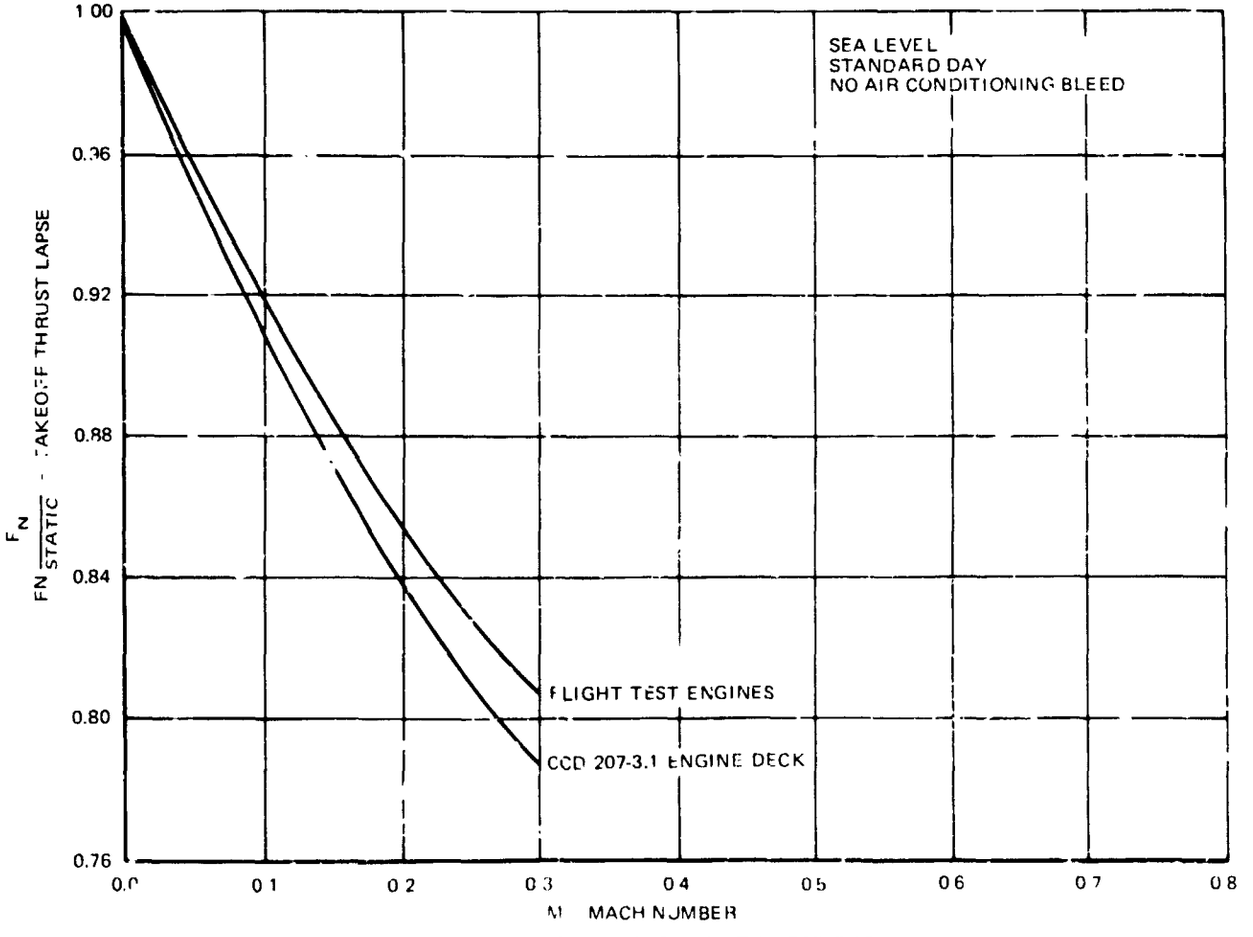

FIGURE 54. DC-9 REFAN THRUST LAPSE RATE

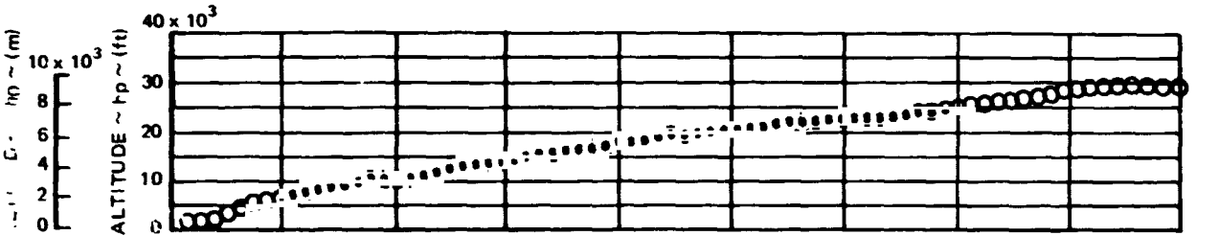

(a) AIRPLANE ALTITUDE (hp)

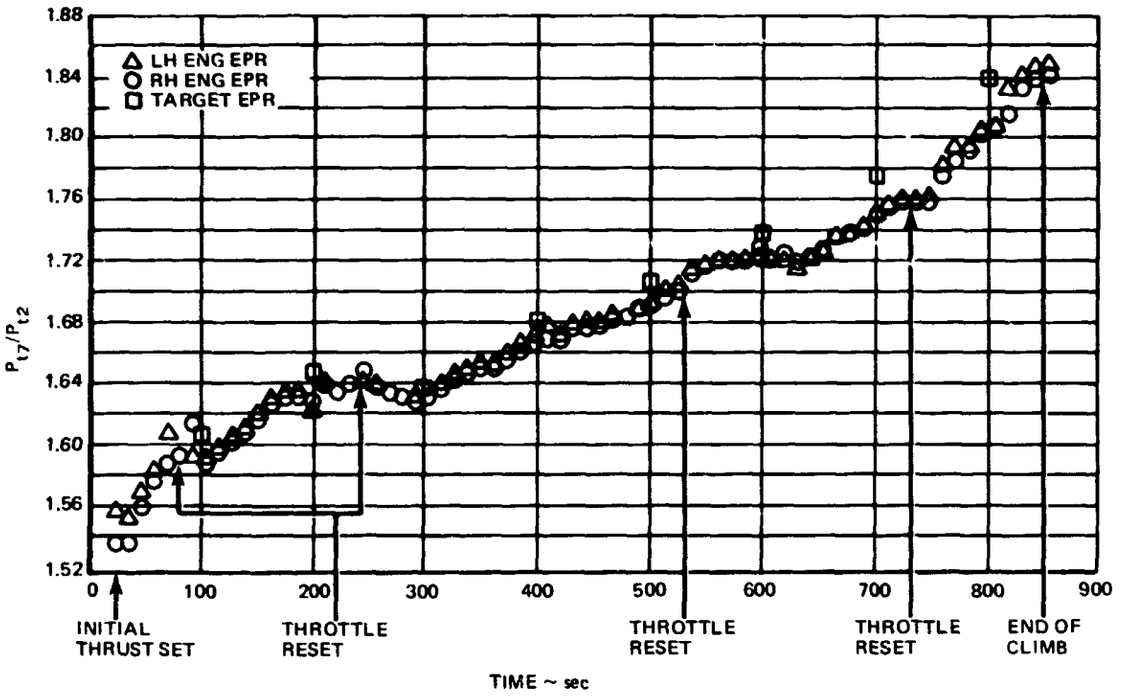

(b) ENGINE PRESSURE RATIO (EPR)

FIGURE 55. DC-9 REFAN THROTTLE RESET DURING MCL CLIMB

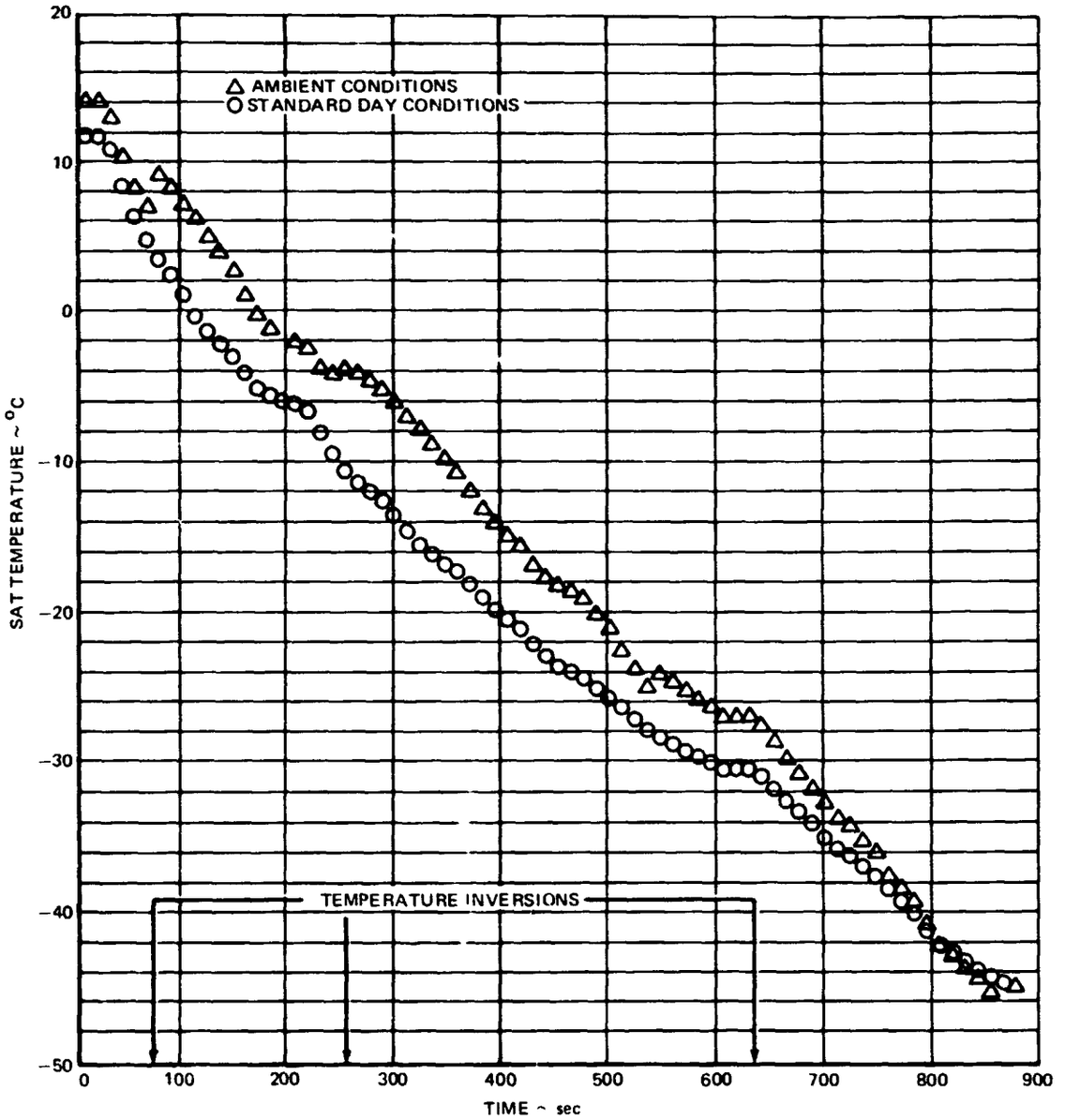

FIGURE 56. DC-9 REFAN STATIC AIR TEMPERATURE DURING MCL CLIMB

Engine performance during transients. - Engine transient tests were conducted to determine the JT8D-109 engine response characteristics to snap throttle retards and jam accelerations with normal and full service bleed configurations for ground, inflight and landing-climb operations.

Test data was obtained on both the left hand engine S/N 666995 and the right hand engine S/N 666996. The bleed configuration was normal for ground transients and for inflight accelerations and decelerations. Bleed system configuration for the landing climb accelerations are noted below. The aircraft configuration during the landing climb acceleration test was maximum landing weight, gear down and flaps/slats, 0.873 rad (50 deg)/Extend.

- Engine Transients - Ground and Inflight

A series of accelerations and decelerations were conducted on each engine. Initially, the test engine was stabilized at idle. Then a slow acceleration to takeoff power (1.74 EPR) was performed and the engine allowed to stabilize. A slow deceleration followed. The test was repeated for a moderate and rapid acceleration and deceleration. Then a series of bodie accelerations and decelerations were conducted (jam accelerations from idle to takeoff and snap decelerations from takeoff power) in rapid succession without allowing the engine to stabilize.

Inflight transients were conducted for each engine where initially the airplane was stabilized at test altitude and airspeed (airspeed decreased during the tests). From stabilized idle, the test engine was accelerated to MCT (1.88-1.77 EPR) at a moderate rate. After allowing the engine to stabilize at MCT (about 10 seconds), a moderate deceleration to idle was conducted. The tests were repeated with a rapid acceleration and deceleration.

Engine response to throttle inputs was acceptable for the ground and inflight acceleration-deceleration tests with normal bleeds. Typical response characteristics of the left and right hand flight test engines for the ground static and inflight tests are presented in figures 57, 58, 59 and 60 respectively.

- Landing Climb Accelerations

Landing climb accelerations were conducted with full service bleeds and the configuration normal for icing.

An airline type approach descent of about 4 m/s (13 ft/sec) was established with both engines at the power required to maintain the rate of descent for the airplane in the landing configuration at maximum gross weight. At 2 865 m (9,400 ft), both engines were retarded to 65 percent N_2, simulating flight idle. Airspeed was targeted at 66 m/s (128 knots). At 2 621 m (8,600 ft), jam accelerations were conducted simultaneously on both engines attempting to reach the target inflight takeoff EPR. The test was repeated for an idle power of approximately 60% N_2, and for ground idle power.

Additional tests were conducted for idle N_2's of 63%, 62%, 52.5% with the configuration and procedure the same.

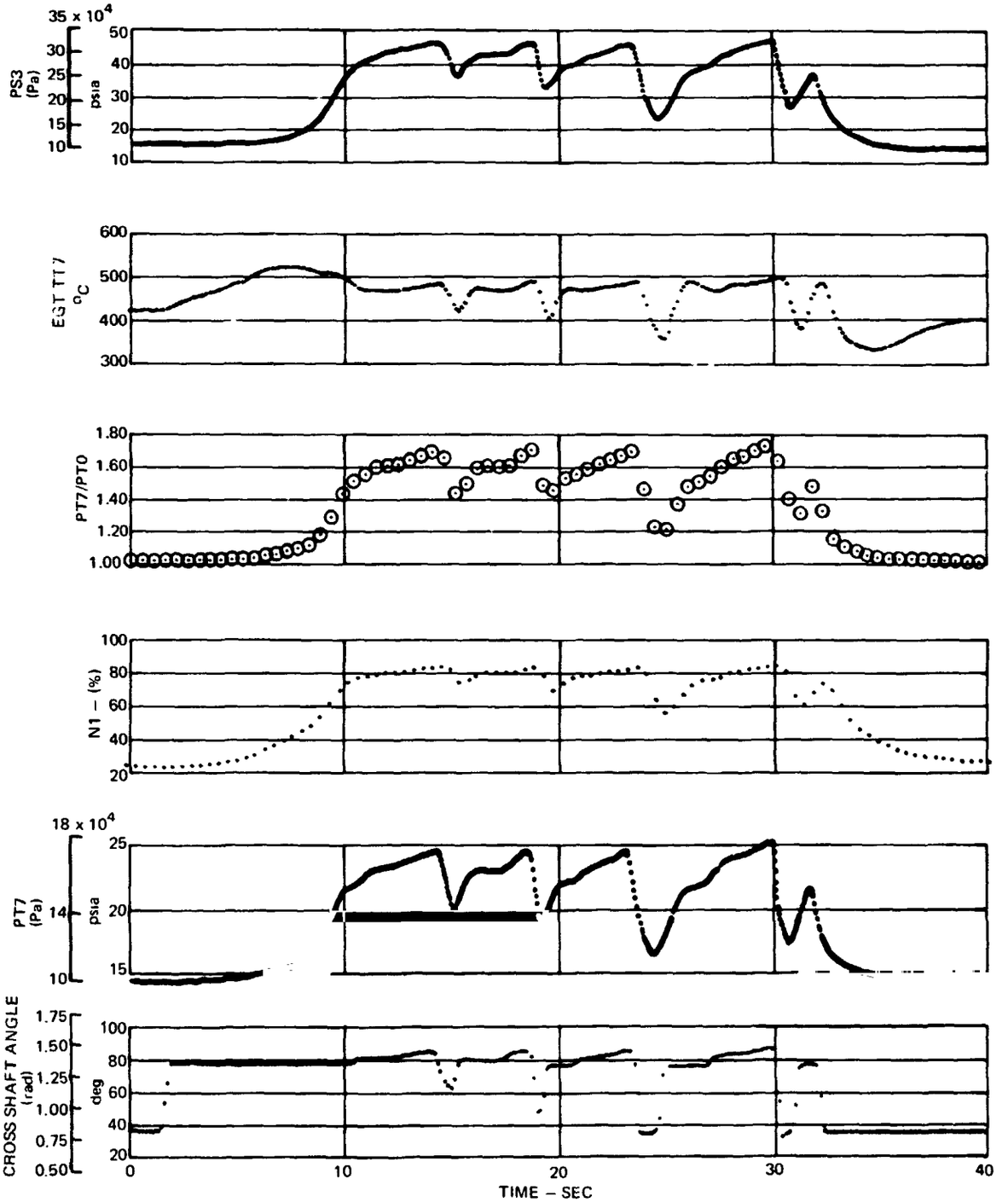

FIGURE 57. DC-9 REFAN LH ENGINE PERFORMANCE DURING ACCELERATION AND DECELERATION – GROUND – AMBIENT AIR TEMPERATURE 19°C

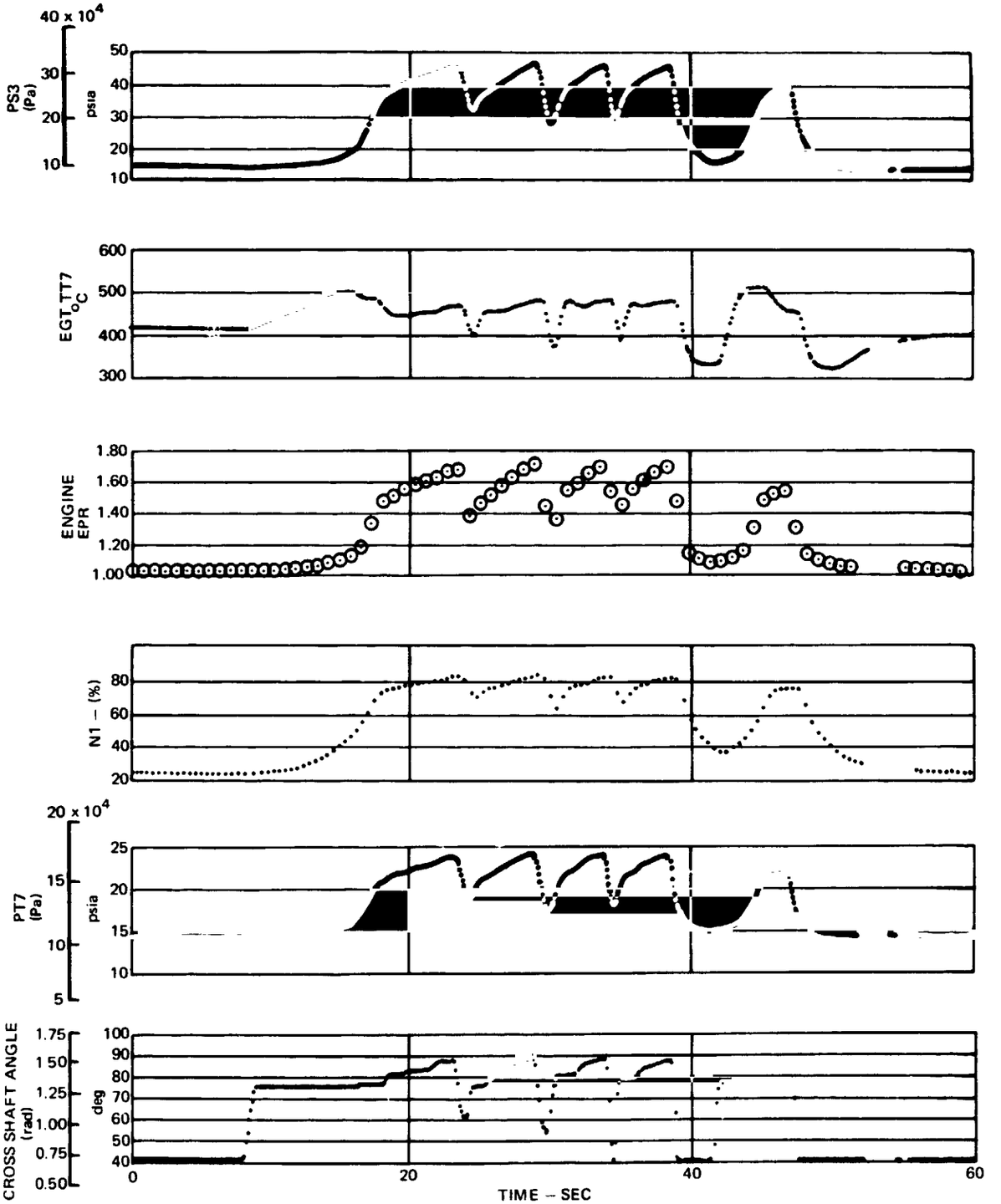

FIGURE 58. DC-9 REFAN RH ENGINE PERFORMANCE DURING ACCELERATION AND DECELERATION – GROUND – AMBIENT AIR TEMPERATURE 19°C

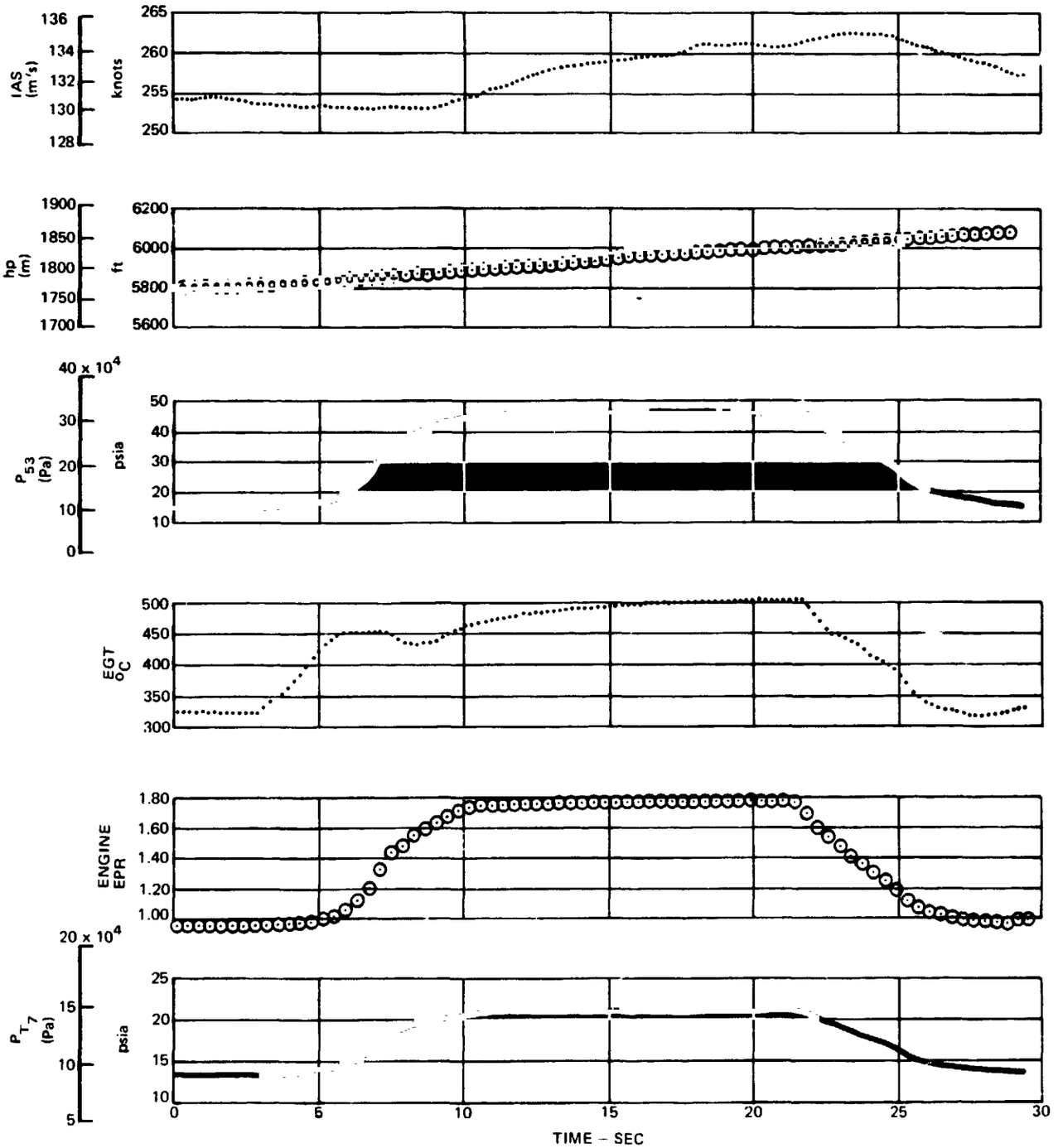

FIGURE 59. DC-9 REFAN LH ENGINE PERFORMANCE DURING ACCELERATION AND DECELERATION – IN FLIGHT – RAM AIR TEMPERATURE 8°C

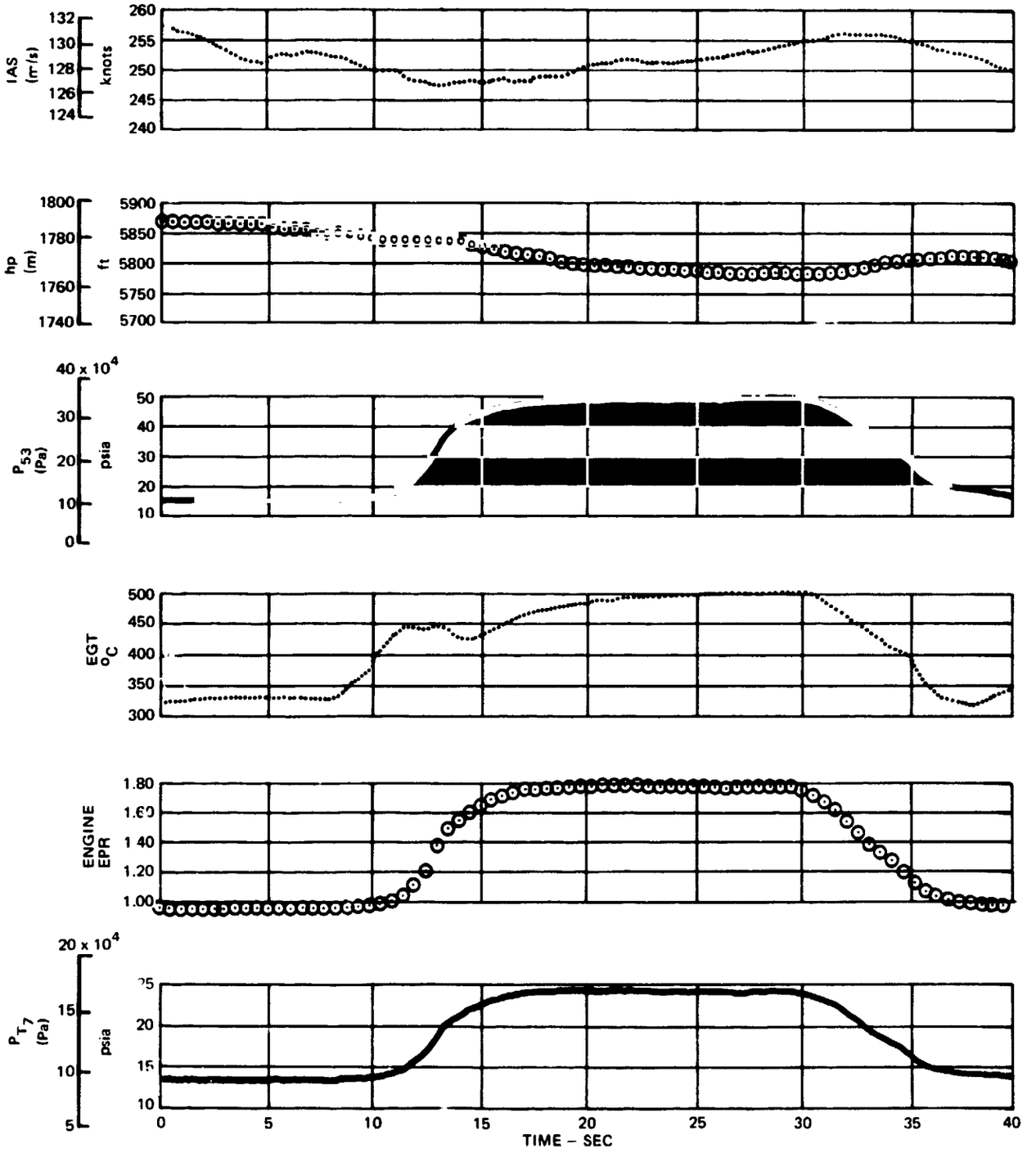

FIGURE 60. DC-9 REFAN RH ENGINE PERFORMANCE DURING ACCELERATION AND DECELERATION – IN FLIGHT – RAM AIR TEMPERATURE 7°C

Jam acceleration tests were also conducted on the left and right hand engines separately, with the initial bleed configuration normal for landing. The aircraft was stabilized at 2 621 m (8,600 ft) and 66 m/s (128 knots). The ground idle thrust was set on the test engine. Power on the remaining engine was as required to maintain altitude and airspeed. Maximum bleeds were then set on the test engine with:

a) Engine and Airfoil Anti-Ice: ON (Test Engine Supplies Both Wings)

b) Test Pneumatic Cross Feed: OPEN

c) Non-Test Pneumatic Cross Feed: CLOSED

A jam acceleration, attempting inflight takeoff power, was then performed on the test engine. The tests were repeated for the other engine. With maximum bleeds from each engine, a jam acceleration was then conducted simultaneously on both engines from ground idle to an attempted target of inflight takeoff thrust, (pneumatic crossfeed open).

A summary of pertinent engine powers and times for the landing-climb accelerations is attached table 13. N_2 measuring capabilities at the time of the tests were not sufficient to permit evaluation of the time required for engine stabilization at idle after retard from approach powers.

All landing-climb engine accelerations from ground idle with maximum pneumatic bleeds failed to reach inflight takeoff power within the 8 second time target.

A flight idle N_2 caution light was installed to illuminate when N_2 RPM dropped below 64.5%. This light setting results in an estimated thrust of 6 717 N (1,510 lb) per engine at sea level, 72 m/s (140 knots) and was intended to ensure the 8 second capability from idle to inflight takeoff EPR at 2 621 m (8,600 ft) with normal engine bleeds and power extraction.

A summary of idle N_2's at throttle advance and EPR's at 8 seconds are presented on figure 61. A trend was established for the idle N_2 and 8 second EPR except for the LH engine response data, which displayed noteably higher EPR than data from other acceleration attempts. The RH engine failed to attain the target inflight takeoff EPR during all of the acceleration attempts.

Landing-climb accelerations from ground idle to inflight takeoff power with anti-icing bleeds did not satisfy the 8 second requirement. LH engine characteristics from higher idle N_2's approximated the 8 second criterion of other JT8D engines but because of the significant difference between this and the other JT8D-109 landing close up climb data, the LH engine bleed configuration has been questioned.

To ensure reaching inflight takeoff power with maximum bleed configuration at 2 621 m (8,600 ft) the idle N_2 must be above 66% N_2.

TABLE 13

DC-9 REFAN LANDING CLIMB ACCELERATIONS
FULL SERVICE BLEED CONFIGURATION
LANDING CONFIGURATION

LH ENGINE S/N 666995
RH ENGINE S/N 666996

TIME AT IDLE ~ sec		FLT IDLE % N_2		GND IDLE % N_2		TARGET INFLT T.O. POWER P_{t7}/P_{to} (3)	MAXIMUM P_{t7}/P_{to}		TIME TO REACH T.O. POWER – sec		P_{t7}/P_{to} 8 sec AFTER ADVANCE	
LH	RH	LH	RH	LH	RH		LH	RH	LH	RH	LH	RH
60	58	65.7	64.6	54.2	54.2	1.795	1.804	1.748	6.5	9.2 (1)	(2)	1.748
30	30	59.0	59.1	54.2	54.2	1.795	1.801	1.748	7.9	13.1 (1)	(2)	1.41
19	19	58.0	54.0	54.2	54.2	1.795	1.778	1.765	8.6	14.2 (1)	1.769	1.17
18	19	58.0	54.0	54.2	54.2	1.795	1.795	1.757	9.0	13.4 (1)	1.760	1.18
473	–	52.3	–	54.2	—	1.75	1.762	–	13.7	–	1.09	–
–	163	—	52.8	—	54.2	1.75	—	1.743	–	15.2 (1)	–	1.08
47	47	52.8	52.4	54.2	54.2	1.75	1.763	1.728	12.0	13.1 (1)	1.11	1.08
45	45	63.0	63.0	54.2	54.2	1.75	1.800	1.743	8.0	8.2 (1)	1.750	1.733
50	50	62.0	62.5	54.2	54.2	1.75	1.791	1.730	8 5	9.4 (1)	1.662	1.429
40	40	52.5	52.5	54.2	54.2	1.75	1.786	1.725	11.7	12.6 (1)	1.13	1.09

(1) TIME OF THROTTLE RETARD THE ENGINE DID NOT ATTAIN INFLIGHT TAKEOFF POWER BUT STABILIZED AT A LOWER POWER.

(2) THE ENGINE REACHED THE TARGET INFLIGHT TAKEOFF POWER LESS THAN 8 SECONDS AFTER THROTTLE ADVANCE.

(3) TARGET EPR WAS CALCULATED FROM COCKPIT RAT (PRODUCTION PROBE).

(4) ACCELERATION WAS CONDUCTED ON SINGLE ENGINE WHICH SUPPLIED BLEEDS FOR BOTH WINGS. DATA ARE NOT CONSIDERED VALID FOR LANDING CLIMB TESTS.

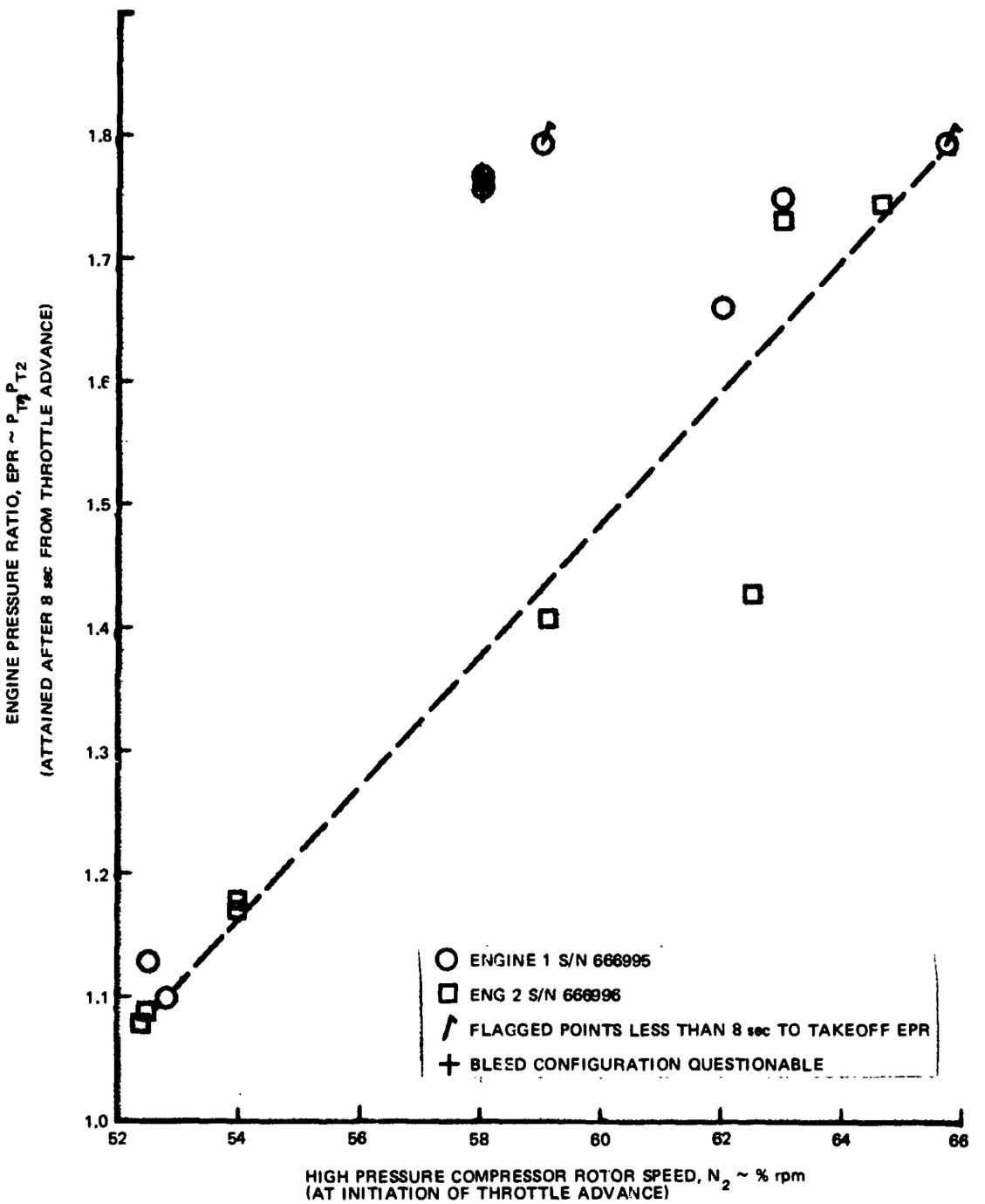

FIGURE 61. DC-9 REFAN LANDING CLIMB ACCELERATION -- JT8D-109 ENGINE INFLIGHT IDLE N_2 DETERMINATION

Engine characteristics during airplane maneuvers. - A number of flight tests were made to evaluate the operation of the JT8D-109 engine during aircraft stall with different power settings, during stabilized flight at high angles of attack and high sideslip angles and to verify that engine operation was satisfactory during an abused takeoff.

- Engine Operating Characteristics - Approach to Stalls

The engines were at idle or low powers with continuous ignition, the engine hydraulic pumps at high flow with auxiliary hydraulic pumps, alternate hydraulic pumps, yaw dampers and APU on.

During the approach to stalls testing three compressor stalls occurred on the R.H. engine during a moderate retard from about 1.77 EPR to idle. A 50°C (122°F) rise in EGT resulted. No other unusual events were reported. The pilots felt that in all cases acceleration was good above 1.1 EPR.

The R.H. engine (S/N 666996) appeared to have less stall margin than the left (S/N 666995) by the occurrence of occasional compressor stalls during the approach to or recovery from airplane stalls.

- Engine Operating Characteristics - Stalls

Stall tests were performed with symmetrical power and with the system configuration the same as for the approach to stalls tests, except the yaw dampers were off.

During the power "on" stall tests one compressor stall was reported on the right hand engine during engine acceleration after recovery from an airplane stall with flaps/slats, up/ret. Otherwise the engine operating characteristics were regarded as good.

During the slowdown with MCT stalls the engine demonstrated no unusual operating characteristics.

During the high angle of attack evaluation test, the engine operation was normal at local angles of attack up to .576 rad (33 deg) ANU.

- Engine Operating Characteristics - High Sideslip Angles

Engine operation was also evaluated at various angles of sideslip with the L.H. engine set at MCT. The system configuration was normal for takeoff with the pneumatic supply off on the left engine for some flights and on normal for other flights.

No abnormal engine operating characteristics occurred during the high angles of sideslip evaluation.

- Engine Operating Characteristics - Abused Takeoff

The system configuration for the abused takeoff was normal (bleeds on) for takeoff with flaps/slats, .262 rad (15 deg)/Extend.

The JT8D-109 Refan engine operating characteristics and stability during the abused takeoff maneuver were satisfactory.

Engine Component Cooling

This test was performed to establish that the Refanned engine nacelle compartment ventilation and component cooling configuration was within allowable limits both on the ground and in flight.

The system configuration for the ground and the flight test was engine hydraulic pumps on high, one air conditioning pack per engine was on and all ice protection was off; the generator load is noted for each test.

Engine component cooling instrumentation locations are shown in figures 62 thru 66. For all testing a one to one correction was added to ambient temperatures to adjust for a hot day. A hot day is defined as an ambient temperature of 50°C up to 2 591 m (8,500 ft) and standard +35°C above 2 591 m (8,500 ft).

During ground testing, with normal takeoff power, all corrected temperatures remained within allowable limits.

During flight testing all uncorrected engine component temperatures were satisfactory. However, when corrected to a hot day the PRBC valve body was 8°C (15°F) over the limit. Normal takeoff power was set for test ambient conditions, and a one to one correction added to all temperatures to adjust to a hot day. This correction resulted in cycle and component temperatures higher than would exist on an actual hot day. A more realistic correction method was applied to the PRBC valve body in lieu of the one to one correction.

A mathematical thermal model was tailored for computer use to match test day values of engine case, bleed flow, ambient, nacelle wall, and PRBC valve temperatures. Hot day values for engine case, bleed flow, ambient and nacelle wall temperatures were then input and PRBC valve body temperatures calculated. This correction procedure resulted in PRBC valve temperatures below limit.

Maximum uncorrected and corrected values for engine component temperatures during the ground and flight test are presented in table 14. The JT8D-109 engine nacelle compartment ventilation and component cooling requirements were satisfied for ground and inflight conditions and could be expected to meet FAA certification requirements.

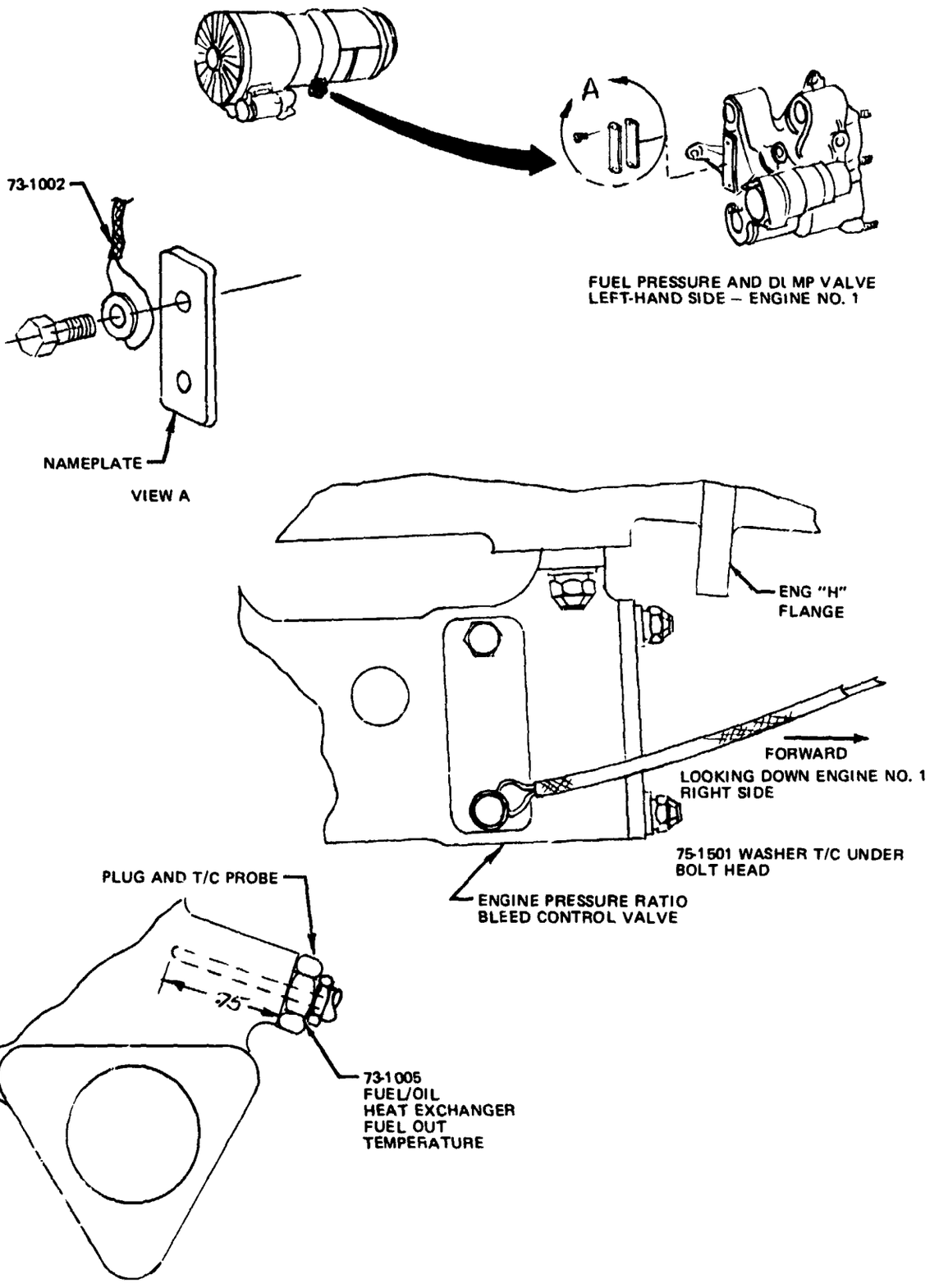

FIGURE 62. DC-9 REFAN TEMPERATURE INSTRUMENTATION LOCATIONS OF ENGINE COMPONENTS

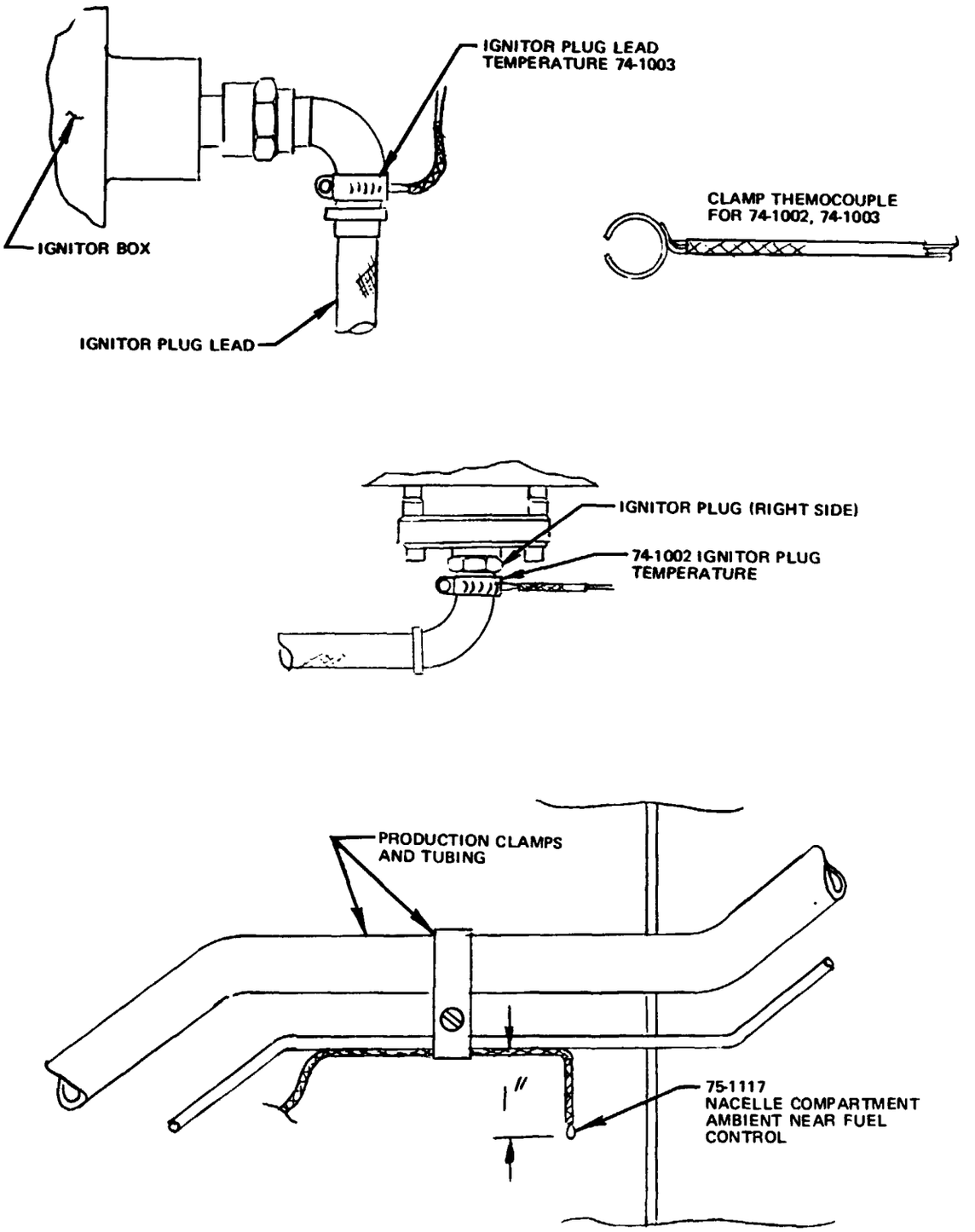

FIGURE 63. DC-9 REFAN TEMPERATURE INSTRUMENTATION LOCATIONS OF IGNITOR AND NACELLE COMPARTMENT AMBIENT

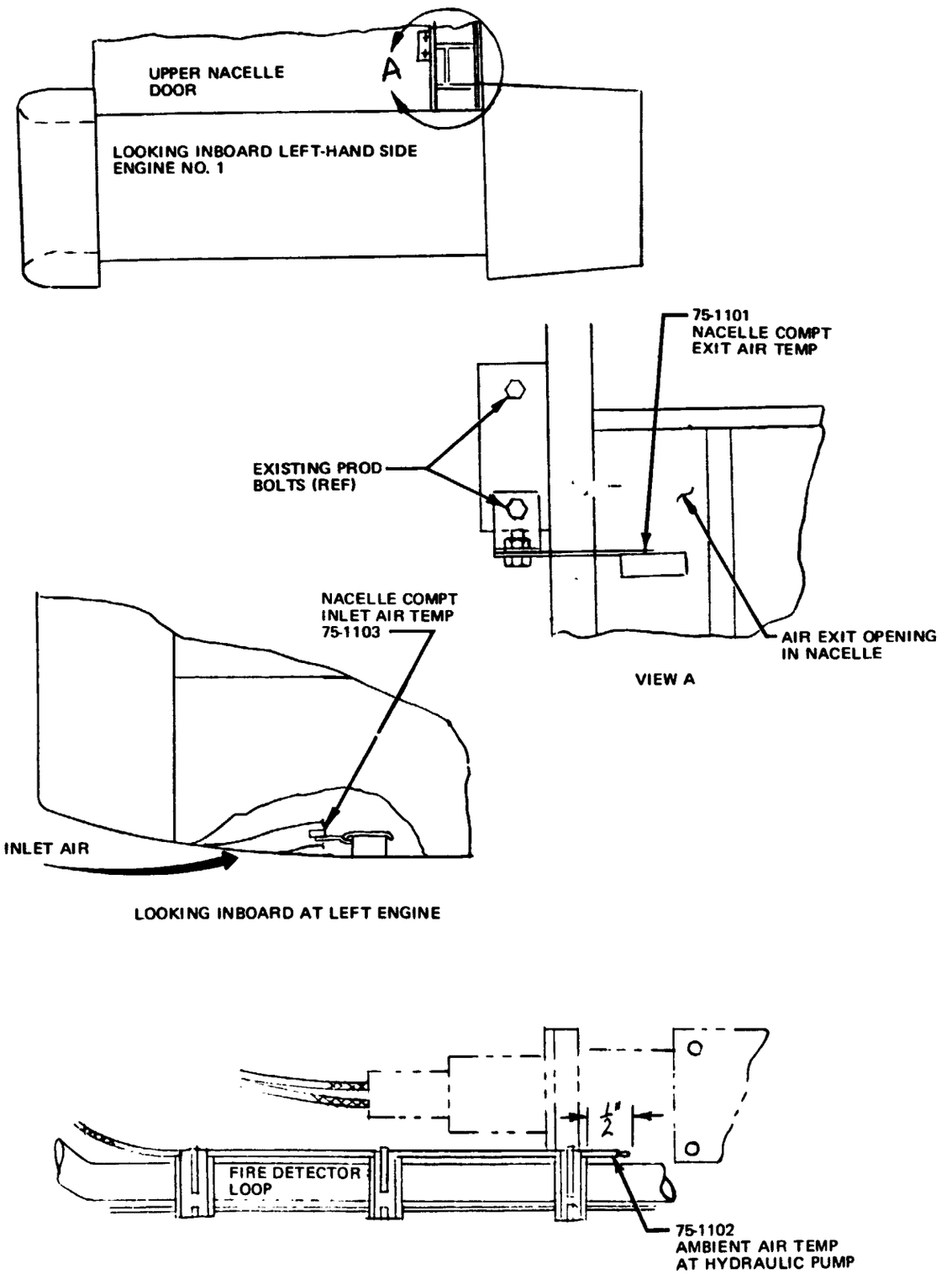

FIGURE 64. DC-9 REFAN TEMPERATURE INSTRUMENTATION LOCATIONS OF NACELLE COMPARTMENT

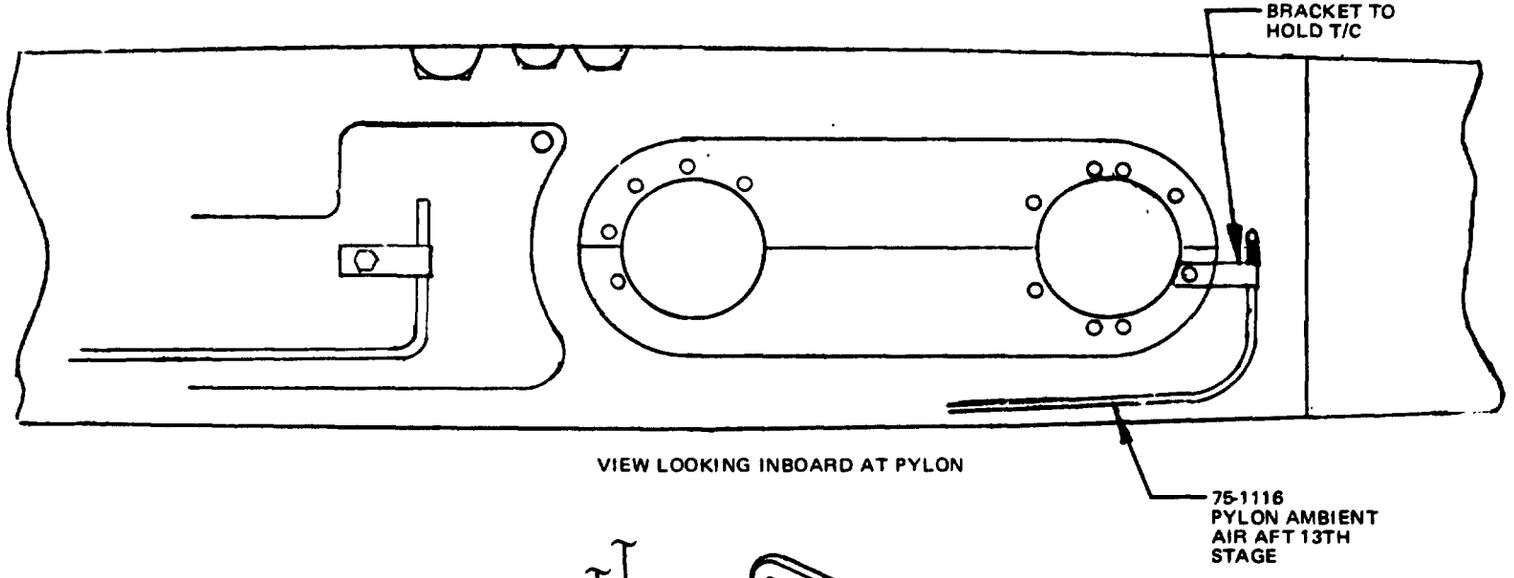

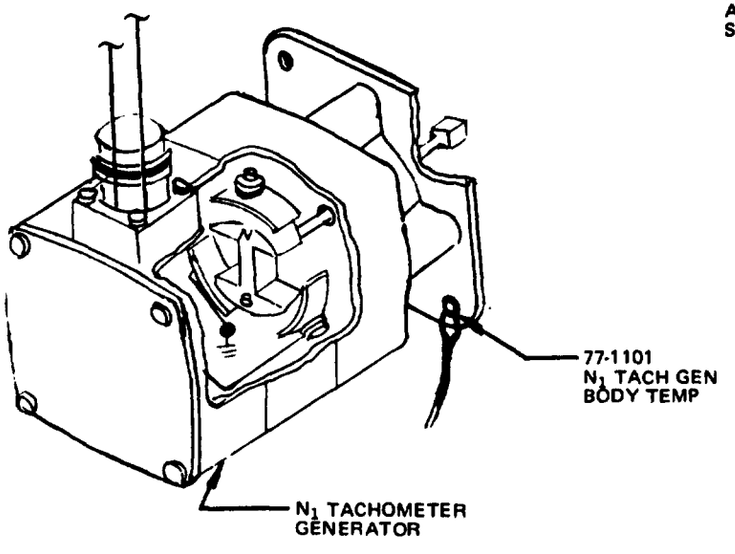

FIGURE 65. DC-9 REFAN TEMPERATURE INSTRUMENTATION LOCATIONS OF N_1 TACH AND PYLON AMBIENT AIR

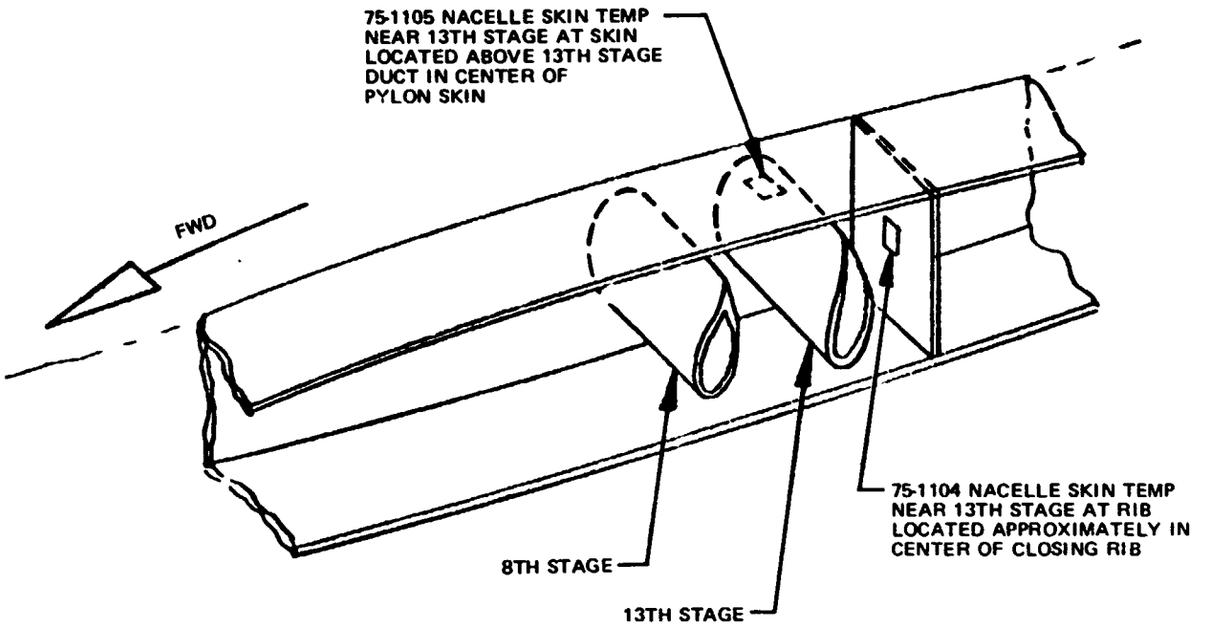

FIGURE 66. DC-9 REFAN INSTRUMENTATION LOCATION OF NACELLE SKIN TEMPERATURE

TABLE 14

JT8D-109 ENGINE NACELLE COMPARTMENT COOLING

PARAM NO.	MAX TEMP GROUND °F (°C)	MAX TEMP INFLIGHT °F (°C)	*CORR MAX TEMP GRD °F (°C)	*CORR MAX TEMP FLT °F (°C)	MAX ALLOW. TEMP °F (°C)	PARAMETER
75-1101	166 (74)	135 (57)	212 (100)	230 (110)		NAC COMPT EXIT AIR TEMP
75-1103	107 (42)	60 (16)	152 (67)	140 (60)		NAC COMPT INLET AIR TEMP
75-1102	118 (48)	90 (32)	168 (76)	188 (87)	225 (107)	AMB AIR AT HYDR PUMP TEMP
74-1002	142 (61)	130 (54)	188 (87)	228 (109)	450 (232)	IGNITOR PLUG TEMP
74-1003	108 (42)	105 (41)	161 (72)	202 (93)	450 (232)	IGNITOR PLUG LEAD TEMP
73-1002	190 (88)	139 (59)	238 (114)	228	275 (135)	FUEL P&D VLV BODY TEMP
73-1005	204 (96)	135 (57)	***			FUEL/OIL H/X FUEL OUT TEMP
75-1501	235 (113)	218 (103)	281 (138)	299**(149)	300 (149)	PRBC BODY TEMP
77-1101	157 (69)	138 (59)	212 (100)	230 (110)	275 (135) (Cont)	
					300 (149) (15 min)	N_1 TACH GEN BODY TEMP
75-1104	135 (57)	114 (46)	181 (109)	215 (102)	250 (121)	NAC SKIN TEMP NR 13TH STG AT RIB
75-1105	97 (36)	78 (26)	147 (64)	143 (62)	250 (121)	NAC SKIN TEMP NR 13TH STG AT SKIN
75-1116	160 (71)	155 (68)	205 (96)	240 (116)		PYLON AMB AFT OF 13TH STG TEMP
75-1117	104 (40)	79 (26)	149 (65)	177 (81)		NAC COMPT AMB NR FUEL CONTR

*THE FOLLOWING "ONE-TO-ONE" CORRECTION FOR HOT DAY WAS APPLIED TO ENGINE COMPONENT TEMPERATURES.

$T_3 = T_1 + (HDT - T_2)$ WHERE

T_3 = CORRECTED TEMPERATURE OF COMPONENT, °F (°C)

T_1 = TEMPERATURE OF COMPONENT DURING TEST, °F (°C)

T_2 = AMBIENT TEMPERATURE (SAT CALCULATED FROM TAT), °F (°C)

HDT = 122°F (50°C) SL — 8500 ft (2591 m)

HDT = STD • 95°F (35°C) > 8500 ft (2591 m)

**TEMPERATURE CORRECTED USING THERMAL MODEL.

***AMBIENT TEMPERATURE CORRECTION NOT APPLICABLE TO FLUID TEMPERATURE.

NOTE: CORRECTED TEMPERATURES USING ONE-TO-ONE CORRECTION ARE ESTIMATED TO BE HIGHER THAN WOULD EXIST FOR ACTUAL HOT DAY CONDITIONS.

Constant Speed Drive Oil and Generator Cooling

This test was performed (a) to determine if the constant speed drive (CSD) generator is load limited whenever 100% load is applied; (b) to determine if the Refan engine idle power rpm is compatible with the production CSD and generator; and (c) to evaluate the effectiveness of the CSD and generator cooling systems on the ground and during flight.

A CSD instrumented to measure oil-in and oil-out temperatures and an instrumented Westinghouse generator was installed on the LH engine. The engine and airfoil anti-ice was off, the engine hydraulic pumps were on high, air-conditioning packs and auxiliary hydraulic pumps were on, the alternate hydraulic pumps off, and the pneumatic cross feed closed.

- Constant Speed Drive

The CSD oil-in temperatures and CSD oil-out temperatures were measured for the cooling tests. The rise in oil temperature across the CSD was calculated.

A set of points over the takeoff and climb range was selected from the flight test data. Cases at those test conditions, altitude, airspeed, true air temperature, and engine pressure ratio (Set 1) were input into the Pratt and Whitney Aircraft JT8D-109 engine cycle deck. The same test altitudes and airspeeds were also run in the deck with hot day ambient temperatures and hot day power required (Set 2), table 15.

TABLE 15

REFAN ENGINE CYCLE DECK INPUT

CONFIGURATION	ALTITUDE ft (m)	IAS knots (m/s)	TAT °C	EPR	N_2 %
SET 1 ACTUAL TEST CONDITIONS	SL	0	21	1 73	51
	SL	0	21	1 73	51
	SL	0	14	1 73	51
	2,500 (762)	210 (108)	10	1 73	51
	5,000 (1524)	210 (108)	5	1 77	51
	7,500 (2286)	205 (105)	2	1 80	51
	8,500 (2591)	205 (105)	1	1 80	51
	10,000 (3048)	205 (105)	-2	1 81	51
	12,500 (3810)	205 (105)	3	1 80	51
	15,000 (4572)	205 (105)	-3	1 8<	51
	17,500 (5334)	205 (105)	-8	1 87	51
	20,000 (6096)	205 (105)	-12	1 88	51
SET 2 HOT DAY CONDITIONS	SL	0	50	1 55	53 7
	SL	0	50	1 55	53 7
	2,500 (762)	210 (108)	57 2	1 49	53 7
	5,000 (1524)	210 (108)	57 9	1 48	53 7
	7,500 (2286)	205 (105)	58 2	1 38	53 7
	8,500 (2591)	205 (105)	58 5	1 375	53 7
	8,500 (2591)	205 (105)	41 2	1 51	53 7
	10,000 (3048)	205 (105)	38 6	1 535	53 7
	12,500 (3810)	205 (105)	34 4	1 570	53 7
	15,000 (4572)	205 (105)	30 1	1 607	53 7
	17,500 (5334)	205 (105)	25 7	1 64	53 7
	20,000 (6096)	205 (105)	21 5	1 68	53 7

CSD heat rejection at 100% generator load was determined from the cycle deck N_2 output and a Sunstrand CSD performance curve. CSD oil cooler heat rejection was determined from the cycle deck fan performance data and a Janitrol heat exchanger performance curve. The oil temperature out of the CSD was calculated for test conditions and hot day conditions. The different between the hot and test day oil out temperatures is the hot day correction factor. This factor was added to the measured oil out temperature obtained from the flight test data. Aircraft altitude, airspeed, true air temperature, engine pressure ratio and CSD oil out temp are shown on figure 67.

Since no flight test information was available on CSD cooling at cruise, an analytical solution was required. To reach an analytical solution the Pratt and Whitney Aircraft CCD 281.0 cycle deck was run for three hot day cruise points. The CSD oil out temperature was determined by the same procedure used for T.O. and climb.

The highest CSD oil out temperature was found at 35,000 feet Std day +35°C. That temperature was 128°C (262°F) which is 5°C (9°F) below the continuous limit temperature (table 16).

TABLE 16

ALT. ft (m)	Mn	TAT °C	EPR	CSD Oil Out Temp °C Analytical	CSD Oil Out Temp °C Corrected To Hot Day
25,000 (7 620)	0.8	23.7	1.442	111	114
30,000 (9 144)	0.8	24.4	1.44	119	122
35,000 (10 668)	0.8	13.3	1.64	126	128

The measured CSD oil out temperature, when corrected to hot day ambient conditions and with 100% generator load results in temperatures below the transient limit of 146°C (295°F) during takeoff and climb up to 3 048 m (10,000 ft) and below the maximum continuous limit of 133°C (271°F) for climb above 3 048 m (10,000 ft). The cruise condition temperatures, based on analytical data related to test data, are also below the maximum continuous limit.

The CSD cooling system provides adequate cooling for the JT8D-109 engine installation on the DC-9 Refan airplane. The system performance is such that CSD cooling could be expected to meet FAA certification criteria if flown to FAA flight test procedures.

- Generator

The generator cooling system effectiveness was evaluated by using pressure and temperature data obtained during ground and flight tests along with generator airflow calibration data obtained during laboratory tests.

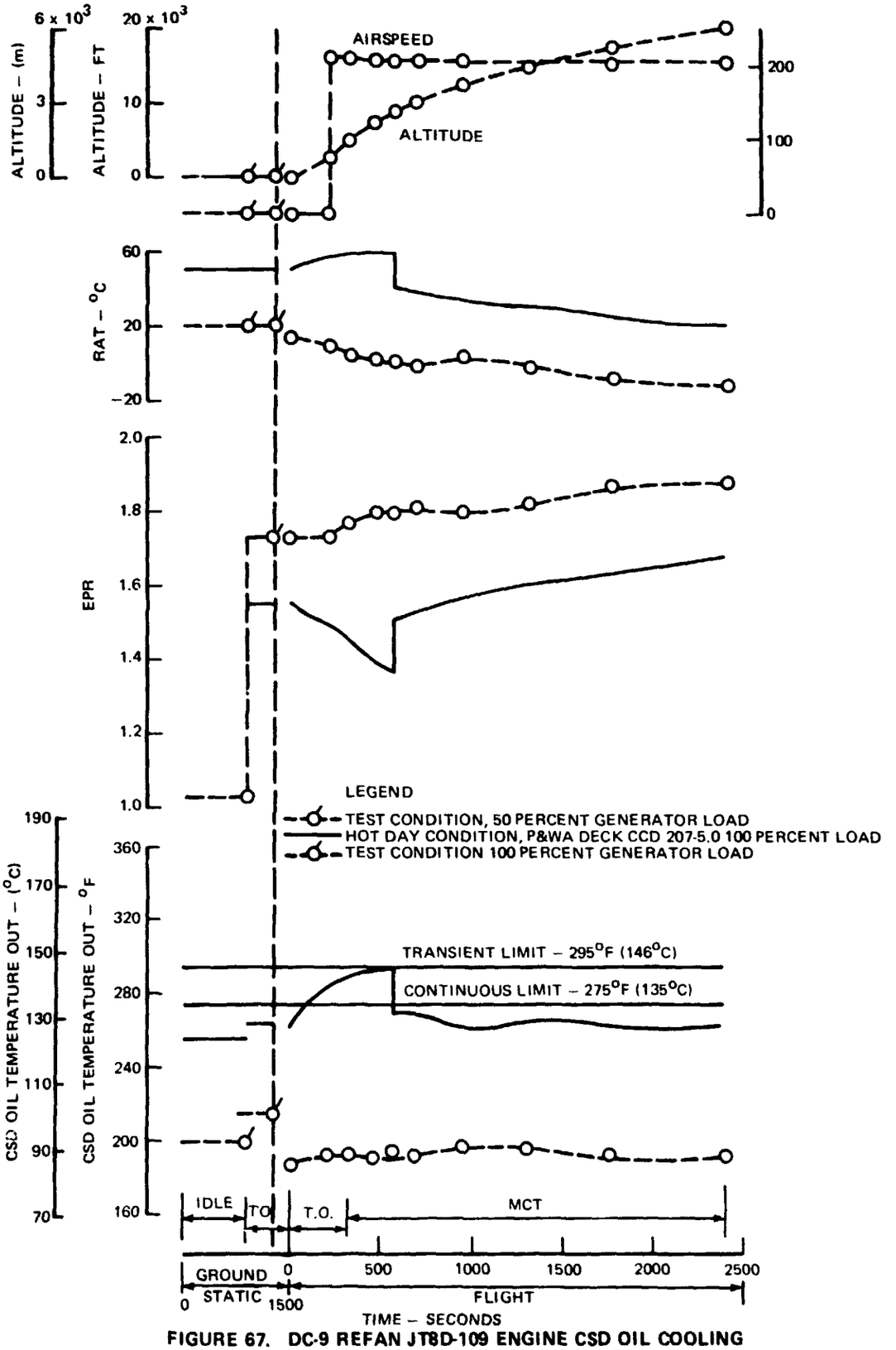

FIGURE 67. DC-9 REFAN JT8D-109 ENGINE CSD OIL COOLING

The instrumented production generator, cooling inlet and exit ducts were set up and operated in the laboratory to obtain measured airflow versus generator pressure drop at a constant generator rpm. The results were plotted and used with generator cooling flight test data to determine the available airflow. A curve of corrected generator airflow versus engine fan pressure ratio was constructed using the flight test P_{TF7}/P_{am} and the available airflow (figure 68).

The maximum available airflow was determined by running the JT8D-109 engine cycle deck at the EPR, bleed airflow, power extraction, altitude and airspeed at the production DC-9-30 certified operating limits. These limits are 50°C for idle and takeoff operation, sea level to 2 591 m (8,500 ft) and standard temperature plus 35°C for all enroute cases. The fan pressure ratio and temperature data obtained from the cycle deck output was used in conjunction with figure 68 to obtain the generator cooling airflow. Figure 69 presents the available generator airflow and the required generator airflow versus the generator inlet temperature.

The test data shows that the available generator cooling airflow exceeds the hot day 100% load airflow requirements for idle, takeoff, climb and cruise. Therefore, the DC-9 Refan generator cooling system is adequate for all operational cases.

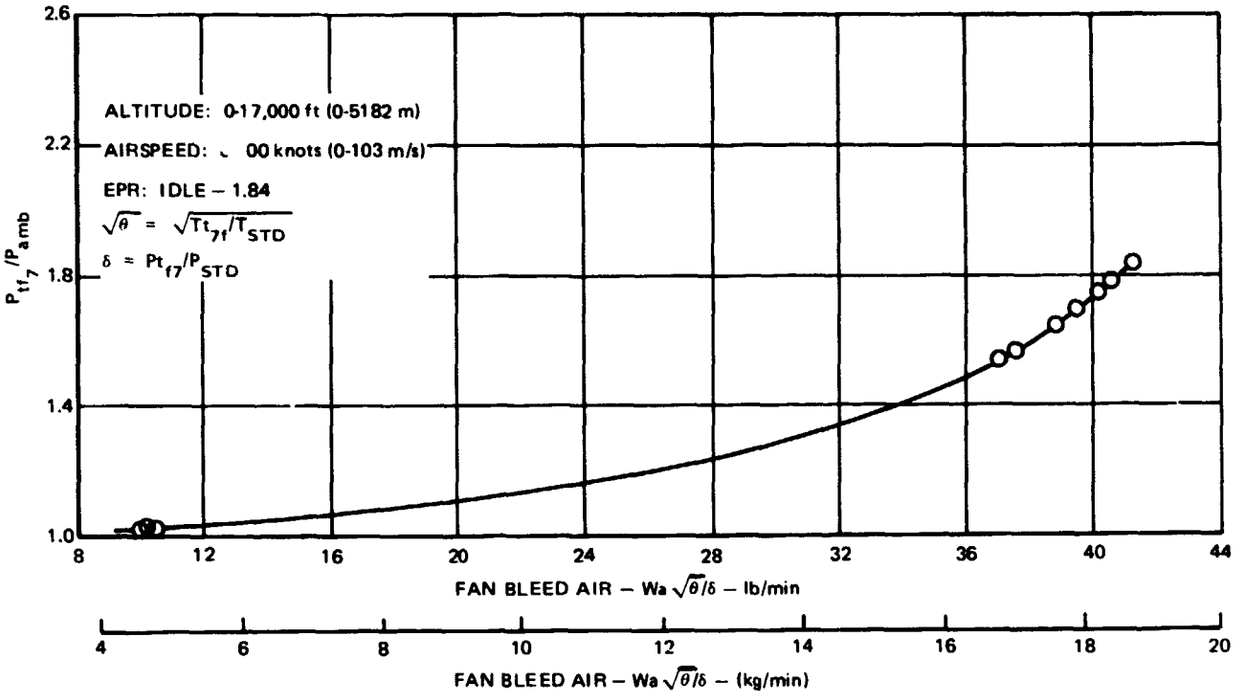

FIGURE 68. DC-9 REFAN WESTINGHOUSE 40-kva GENERATOR BLEED AIR AVAILABLE

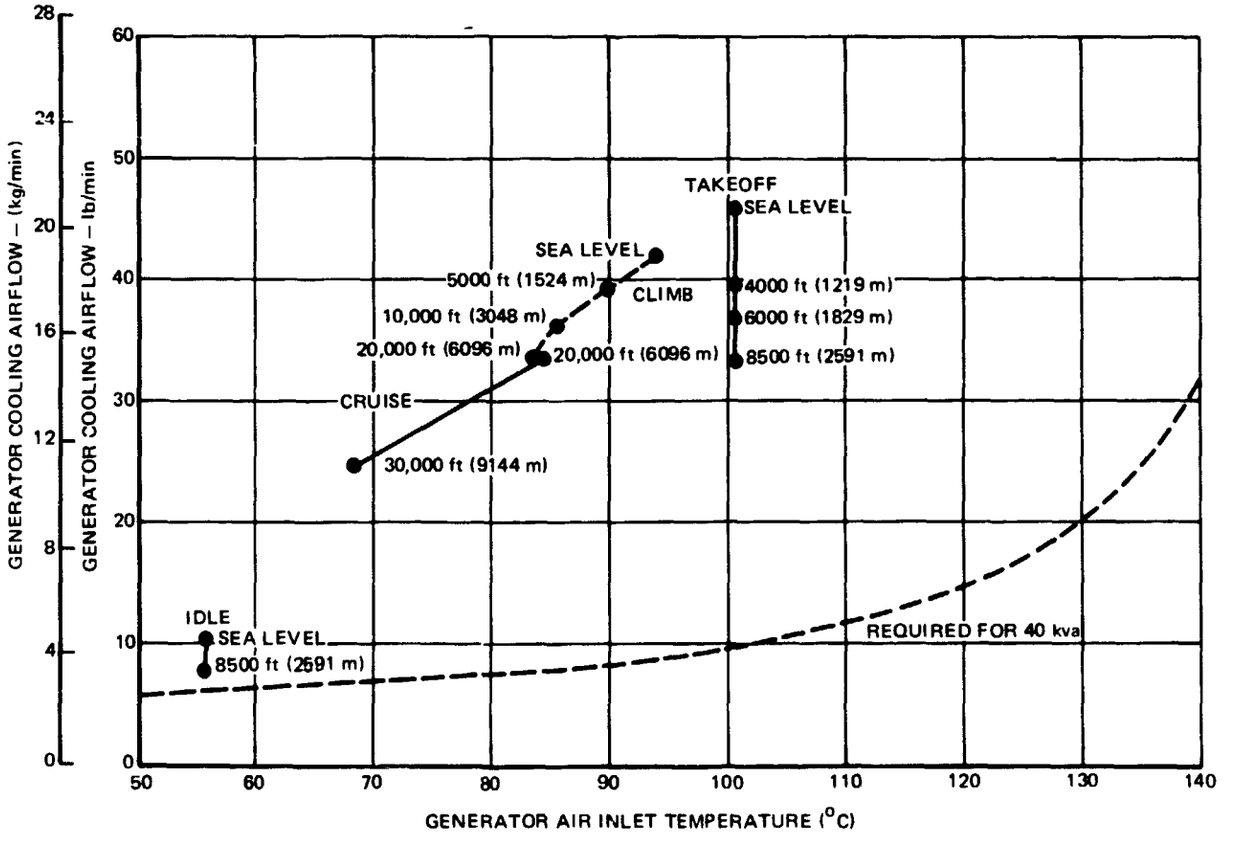

FIGURE 69. DC-9 REFAN GENERATOR AIRFLOW REQUIREMENTS. FAA CERTIFIED HOT DAY CONDITIONS

Engine Fire Detector System

The engine fire detector test was performed on the ground and in flight to determine if the engine fire detector system alarm trip setting loop margin is adequate (same as production) for the JT8D-109 engine installation on the DC-9 Refan airplane.

Data was obtained on the pylon (apron) loop and the engine loop. The engine loop resistance versus time for the ground and flight test is shown in figures 70 and 71. The pylon (apron) loop resistance values are shown in figure 72.

The pylon and engine detector elements are wired in parallel to the detector control unit, therefore the detector control unit is set to trip the fire alarm when the parallel equivalent resistance lowers to 400 ohms. Due to the distance separating the engine and pylon elements, the analytical procedure used was to allow the engine loop or the pylon loop to be heated individually until the parallel equivalent resistance of the system became 400 ohms.

An analysis was made to correct the test data to hot day conditions, 50°C (122°F) day for an altitude of sea level to 2 591 m (8,500 ft) and std. +35°C (63°F) above 2 591 m (8,500 ft); after which, the minimum trip warning margin was determined.

The production fire detector loop control unit trip setting of 400 ohms resulted in a minimum trip margin of 101°C (182°F). Trip margins are acceptable between 83-139°C (150-250°F).

The minimum trip warning setting on the Refan installation results in a 101°C (182°F) margin and will assure freedom from false alarms.

These results are comparable with data previously accepted by the FAA as data conforming to regulations.

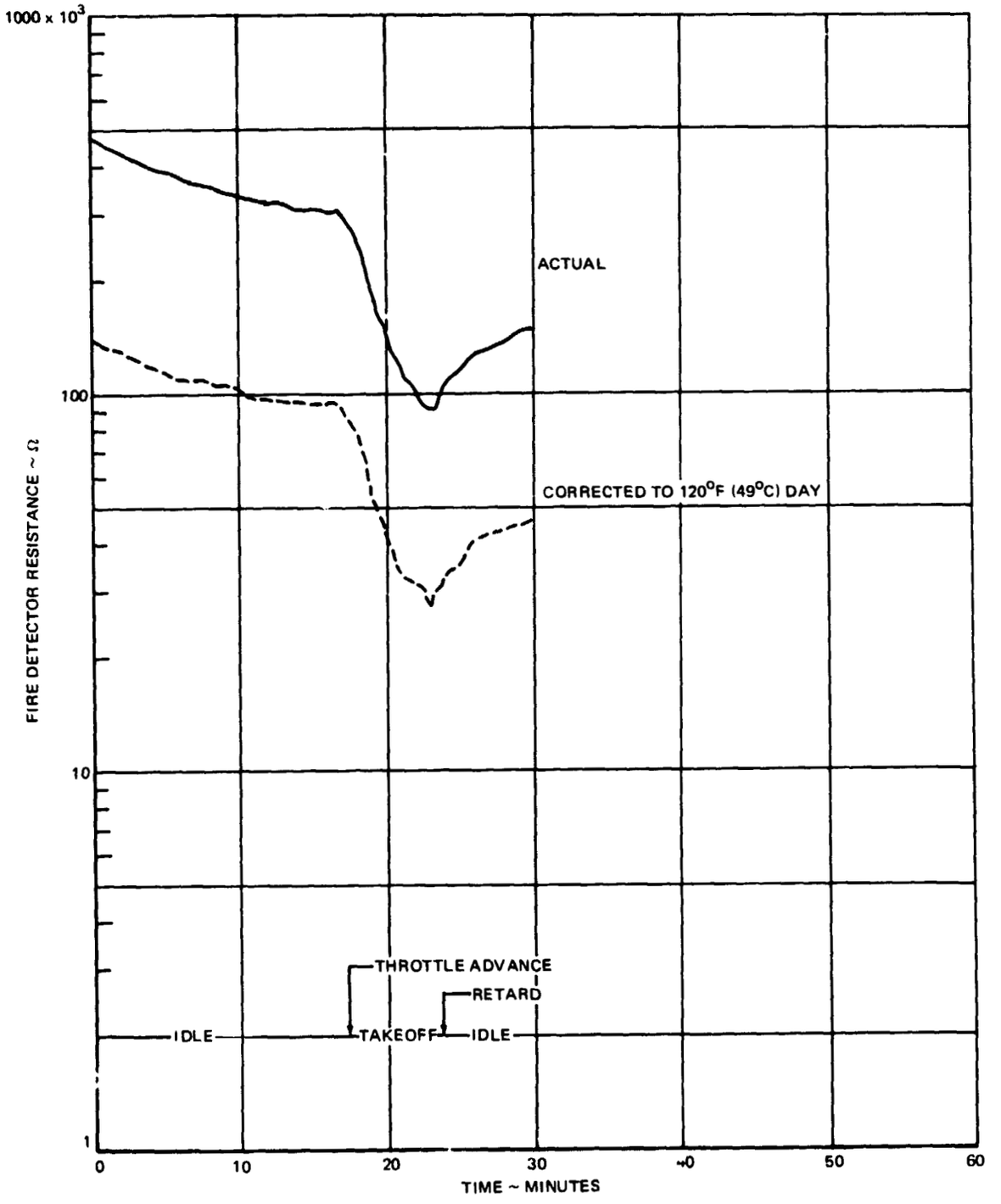

FIGURE 70. DC-9 REFAN FIRE DETECTOR LOOP RESISTANCE, ENGINE ELEMENT – GROUND STATIC

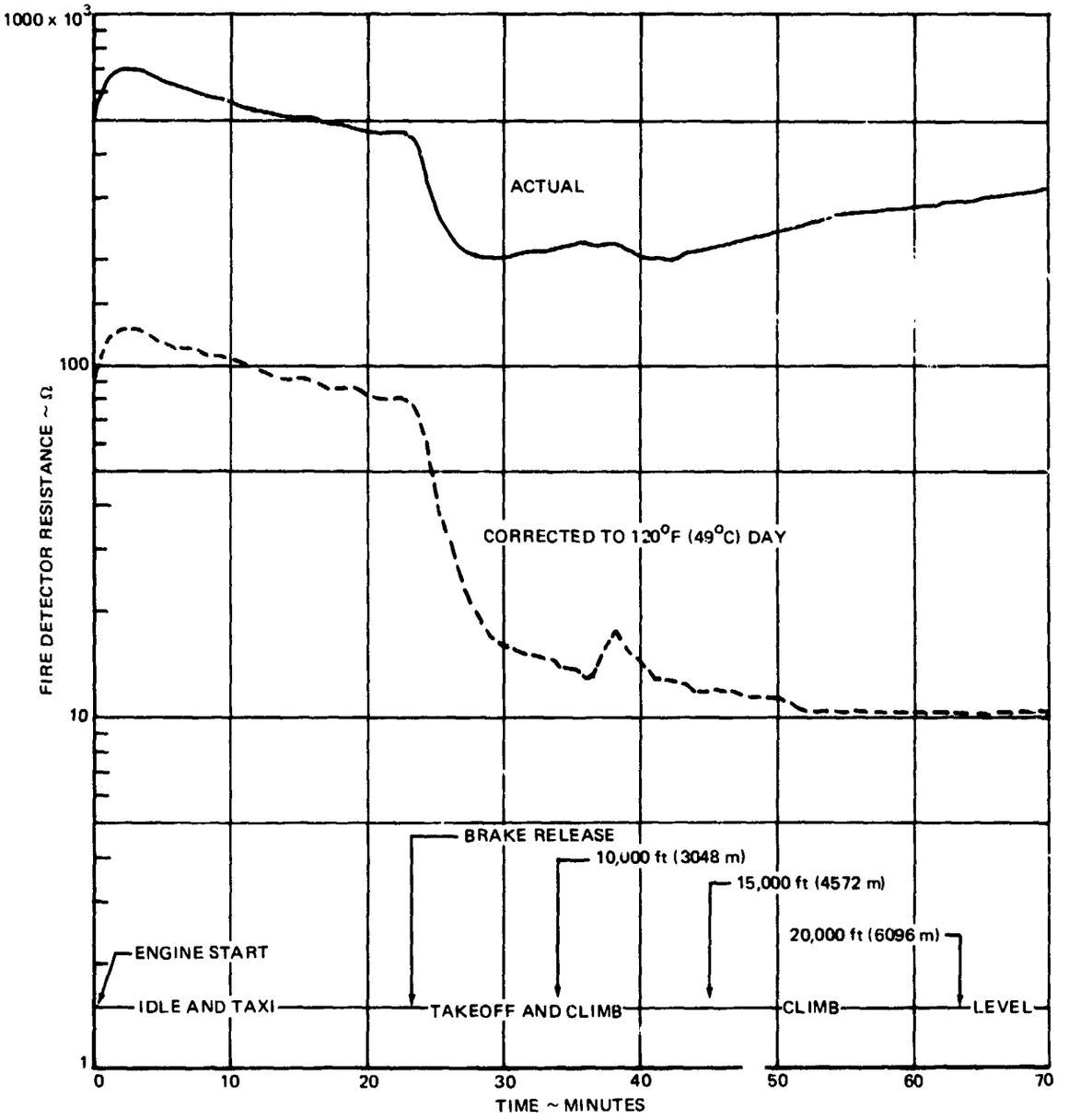

FIGURE 71. DC-9 REFAN FIRE DETECTOR LOOP RESISTANCE, ENGINE ELEMENT – TAKEOFF, CLIMB AND LEVEL FLIGHT

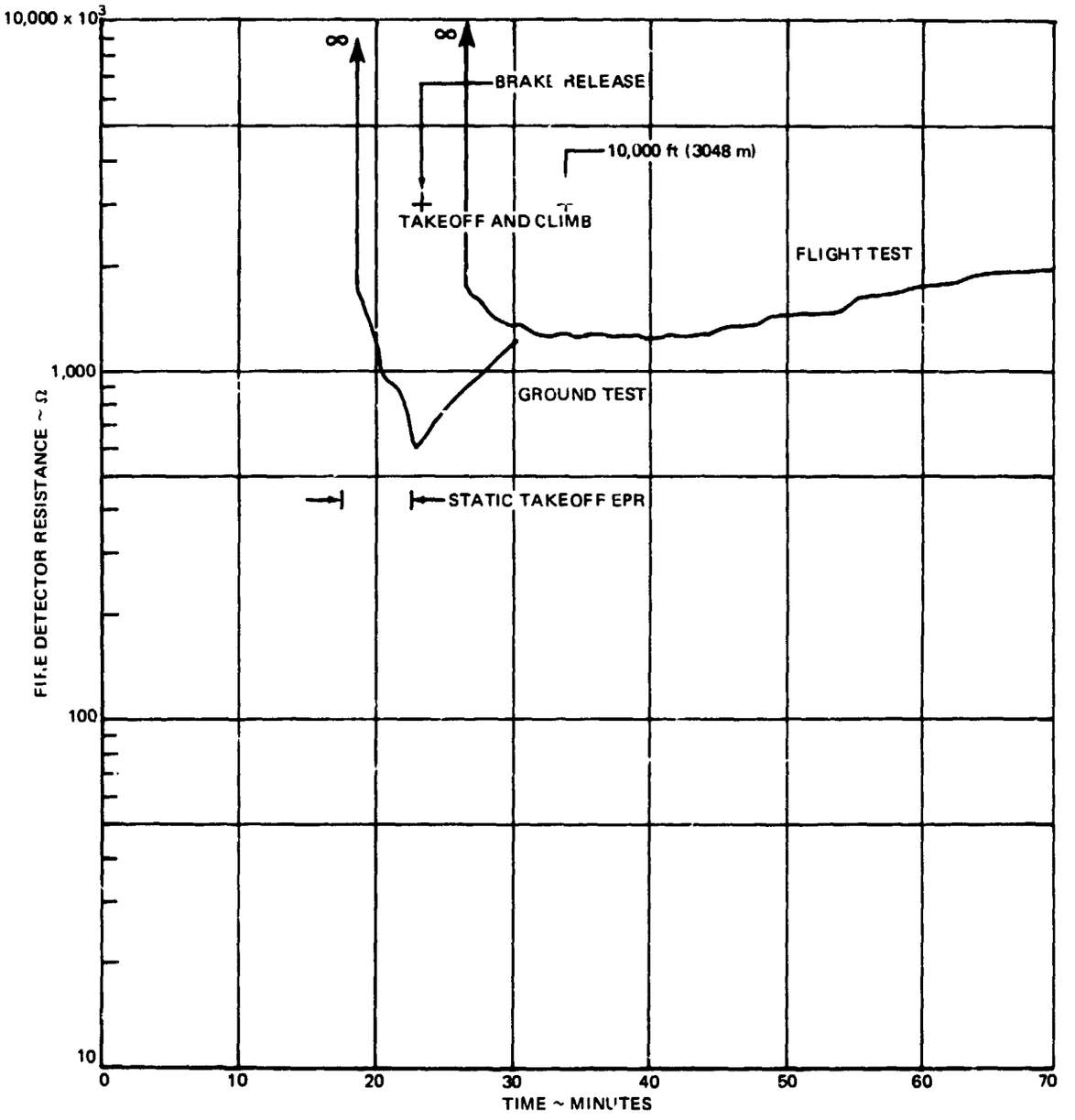

FIGURE 72. DC-9 REFAN FIRE DETECTOR LOOP RESISTANCE, PYLON APRON – GROUND STATIC AND FLIGHT

Engine Vibration Measurement

The engine vibration test was conducted to obtain installed JT8D-109 engine vibration measurements to verify that Engine Vibration Measurement (EVM) levels present are acceptable and to compare levels with the Pratt and Whitney Aircraft test stand results.

Engine vibration measurements were obtained throughout the normal flight envelope of the airplane and included the following flight conditions.

1) Takeoff and normal climb to 10 668 m (35,000 ft) with LH engine power scans at 3 048 m (10,000 ft), 6 096 m (20,000 ft), 9 144 m (30,000 ft) and 10 568 m (35,000 ft).

2) Aircraft stalls, aircraft slow down with MCT on the LH engine and operation at high angle of attack.

3) Cruise at 6 096 m (20,000 ft) and 9 144 m (30,000 ft) with a moderate accel/decel on the LH engine.

4) Normal descent with moderate LH power scans at 9 144 m (30,000 ft) 6 096 m (20,000 ft), 3 048 m (10,000 ft) and 1 524 m (5,000 ft) (with the RH engine at idle for scans).

5) Normal approach, landing and rollout with normal reverse thrust.

6) Ground operation at stabilized power settings of 1.12, 1.17, 1.215, 1.38, 1.56 and 1.72 EPR, and a power scan, idle to takeoff to idle.

The maximum safe operating vibration limits for the JT8D-109 engine are shown in table 17. The engine vibration acceptance limits are listed in table 18.

TABLE 17

*JT8D-109 Engine Maximum Safe Vibration (Single Amplitude) Limits

Location	Overall mil	Overall (mm)	Low Rotor Freq. mil	Low Rotor Freq. (mm)	High Rotor Freq. mil	High Rotor Freq. (mm)
Inlet Pickup	4.0	(0.102)	3.5	(0.089)	2.5	(0.064)
Rear Pickup	3.0	(0.076)	3.0	(0.076)	2.0	(0.051)

* Pratt and Whitney Report PWA 5114, 16 September 1974

TABLE 18

*JT8D-109 Engine Vibration (Single Amplitude) Acceptance Limits

Location	Overall mil	Overall (mm)	Low Rotor Freq. mil	Low Rotor Freq. (mm)	High Rotor Freq. mil	High Rotor Freq. (mm)
Inlet Pickup	-	-	1.5	(0.0381)	-	-
Rear Pickup	-	-	1.2	(0.030)	1.1	(0.028)

* Pratt and Whitney Report PWA-5114, 16 September 1974

Recorded EVM levels did not exceed .0254 mm (1.0 mil) during flight or ground test. A comparison of the Douglas ground test results to the Pratt and Whitney test stand results, table 19 revealed no significant difference between test stand values and installed readings.

The data for the acceleration, RMS and spectral analysis are presented in figures 73 through 92 for engine #1. These data were recorded during power scans at ground static and inflight at 1 524 m (5,000 ft), 152 m/s (295 knots) and plotted during the up-scan for the ground run and the down scan of the inflight power scan. Fan speed time histories for the ground and flight power scans are presented in figure 73 and 74.

Spectral (3-D) time history plots were produced and are presented in both 5-500 Hz and 5-2000 Hz ranges, in figures 75 through 78 and 79 through 82, respectively.

Acceleration spectra were plotted for both the 5-500 Hz and 5-2000 Hz ranges and reflect the rotor frequency components shown on the high speed ends of the spectral (3-D) time history plots, in figures 83 through 86 and 87 through 90 respectively.

The RMS acceleration versus fan speed data from the ground test power scan are shown in figures 91 and 92.

The RMS acceleration versus fan speed show no major peaks between idle and takeoff thrust, but the maximum vibration occurs at the highest speed. The installed engine displacement values are satisfactory for the airplane envelope and are comparable to test stand values.

The spectral time histories show the 5-500 Hz contains the contributing frequency components making up the displacement magnitude while the 5-2000 Hz range shows that much of the overall vibration acceleration lies above 500 Hz. Low pressure (fan) and high pressure rotor frequency components and their harmonics can be identified at the high speed end of the scans at approximately 123 Hz (86% N_1) and 192 Hz N_2 fundamental frequency.

TABLE 19

JT8D-109 ENGINE VIBRATION DISPLACEMENT MEASUREMENT

TEST CONDITION	P&WA TEST STAND*				DOUGLAS INSTALLED TEST			
	INLET		REAR		COMPRESSOR		TURBINE	
	mil	(mm)	mil	(mm)	mil	(mm)	mil	(mm)
ENGINE S/N 666995								
1.776 EPR	1.1	(0.028)	0.7	(0.018)	–	–	–	–
1.73	–	–	–	–	–	–	0.3-0.6	(0.008-0.015)
1.711	1.2	(0.030)	0.5	(0.013)	–	–	–	–
1.70	–	–	–	–	0.6-0.7**	(0.015-0.018)	–	–
1.68	–	–	–	–	0.2-0.4**	(0.005-0.010)	–	–
1.611	1.3	(0.033)	0.5	(0.013)	–	–	–	–
1.597	1.4	(0.036)	0.6	(0.015)	–	–	–	–
1.563	–	–	–	–	–	–	0.3-0.8	(0.008-0.020)
1.559	1.4	(0.036)	0.5	(0.013)	–	–	–	–
1.512	1.5	(0.038)	0.5	(0.013)	–	–	–	–
1.5	–	–	–	–	0.5-0.6**	(0.013-0.015)	–	–
1.467	1.5	(0.038)	0.4	(0.010)	–	–	–	–
1.423	1.4	(0.036)	0.7	(0.018)	–	–	–	–
1.386	1.5	(0.038)	0.3	(0.008)	–	–	–	–
1.384	–	–	–	–	–	–	0.4-0.7	(0.010-0.018)
1.315	0.5	(0.013)	0.3	(0.008)	–	–	–	–
1.253	0.8	(0.020)	0.4	(0.010)	–	–	–	–
1.215	–	–	–	–	–	–	0.2-0.5	(0.005-0.013)
1.192	0.9	(0.023)	0.9	(0.023)	–	–	–	–
1.18	–	–	–	–	0.2-0.4	(0.005-0.010)	–	–
1.17	–	–	–	–	–	–	0.5-0.7	(0.013-0.018)
1.124	–	–	–	–	–	–	0.3-0.6	(0.008-0.015)
1.12	–	–	–	–	0.1-0.3	(0.003-0.008)	–	–
1.068	0.2	(0.005)	0.3	(0.008)	–	–	–	–
SLOW ACCEL – IDLE TO TAKEOFF	1.3-1.5	(0.033-0.038)	0.3-0.8	(0.008-0.020)	–	–	0.2-1.0	(0.005-0.025)
SLOW DECEL – TAKEOFF TO IDLE	0.5-1.6	(0.013-0.041)	0.4-0.6	(0.010-0.015)	–	–	0.2-0.8	(0.005-0.020)
ACCEL – IDLE TO TAKEOFF	1.0	(0.025)	0.8	(0.020)	–	–	–	–
ENGINE S/N 666996								
1.88 EPR	–	–	–	–	–	–	0.2-0.5**	(0.005-0.013)
1.746	0.8	(0.020)	0.7	(0.018)	–	–	–	–
1.72	–	–	–	–	–	–	0.2-0.5**	(0.005-0.013)
1.700	0.8	(0.020)	0.7	(0.018)	–	–	–	–
1.68	–	–	–	–	–	–	0.2-0.4	(0.005-0.010)
1.640	0.8	(0.020)	0.7	(0.018)	–	–		
1.63	–	–	–	–	–	–	0.2-0.6**	(0.005-0.015)
1.628	0.5	(0.013)	0.5	(0.013)	–	–	–	–
1.62	–	–	–	–	–	–	0.3-0.7**	(0.008-0.018)
1.600	0.9	(0.023)	0.5	(0.013)	–	–	–	–
1.547	0.9	(0.023)	0.4	(0.010)	–	–	–	–
1.515	0.9	(0.023)	0.4	(0.010)	–	–	–	–
1.427	0.8	(0.020)	0.4	(0.010)	–	–	–	–
1.385	0.7	(0.018)	0.4	(0.010)	–	–	–	–
1.310	0.7	(0.018)	0.4	(0.010)	–	–	–	–
1.27	–	–	–	–	–	–	0.2-0.6**	(0.008-0.015)
1.246	0.8	(0.020)	0.4	(0.010)	–	–	–	–
1.190	0.8	(0.020)	0.8	(0.020)	–	–	0.1-0.5**	(0.003-0.013)
1.02	–	–	–	–	0.1**	(0.003)	–	–
ACCEL – IDLE TO TAKEOFF	0.8	(0.020)	0.6	(0.015)	–	–	0.2-0.7**	(0.008-0.018)
DECEL – TAKEOFF TO IDLE	0.0	(0.0)	0.5	(0.013)	–	–	0.2-0.5**	(0.008-0.013)
ACCEL – IDLE TO TAKEOFF	0.7	(0.018)	0.6	(0.015)			0.2-0.8**	(0.008-0.020)

*FROM THE LOG OF ENGINE ACCEPTANCE TEST DATA

**FROM INFLIGHT TEST, OTHER DAC INSTALLED TEST DATA FROM GROUND STATIC TESTS

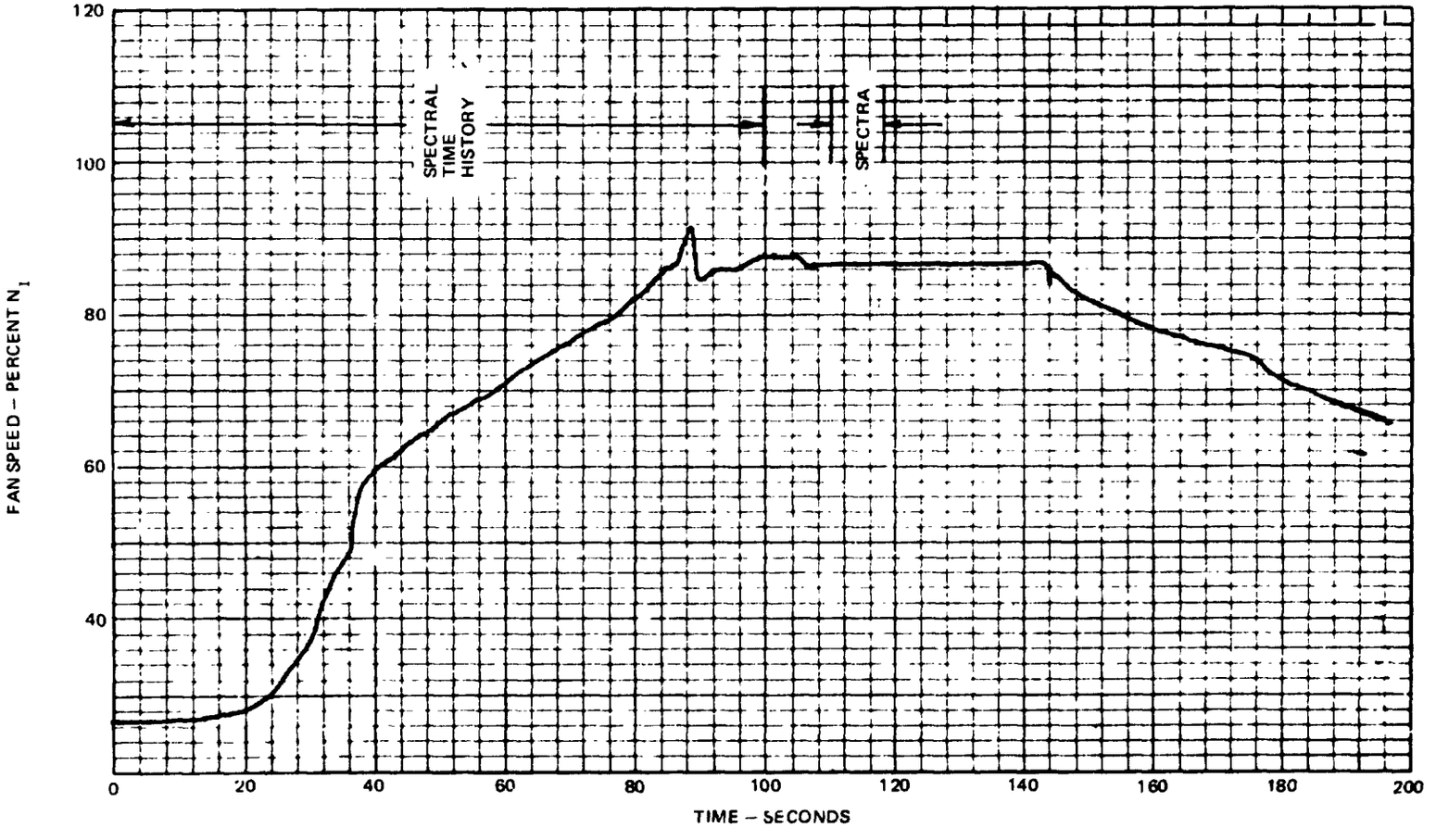

FIGURE 73. DC-9 REFAN, ENGINE NO. 1 FAN SPEED TIME HISTORY, POWER SCAN AT SEA LEVEL STATIC

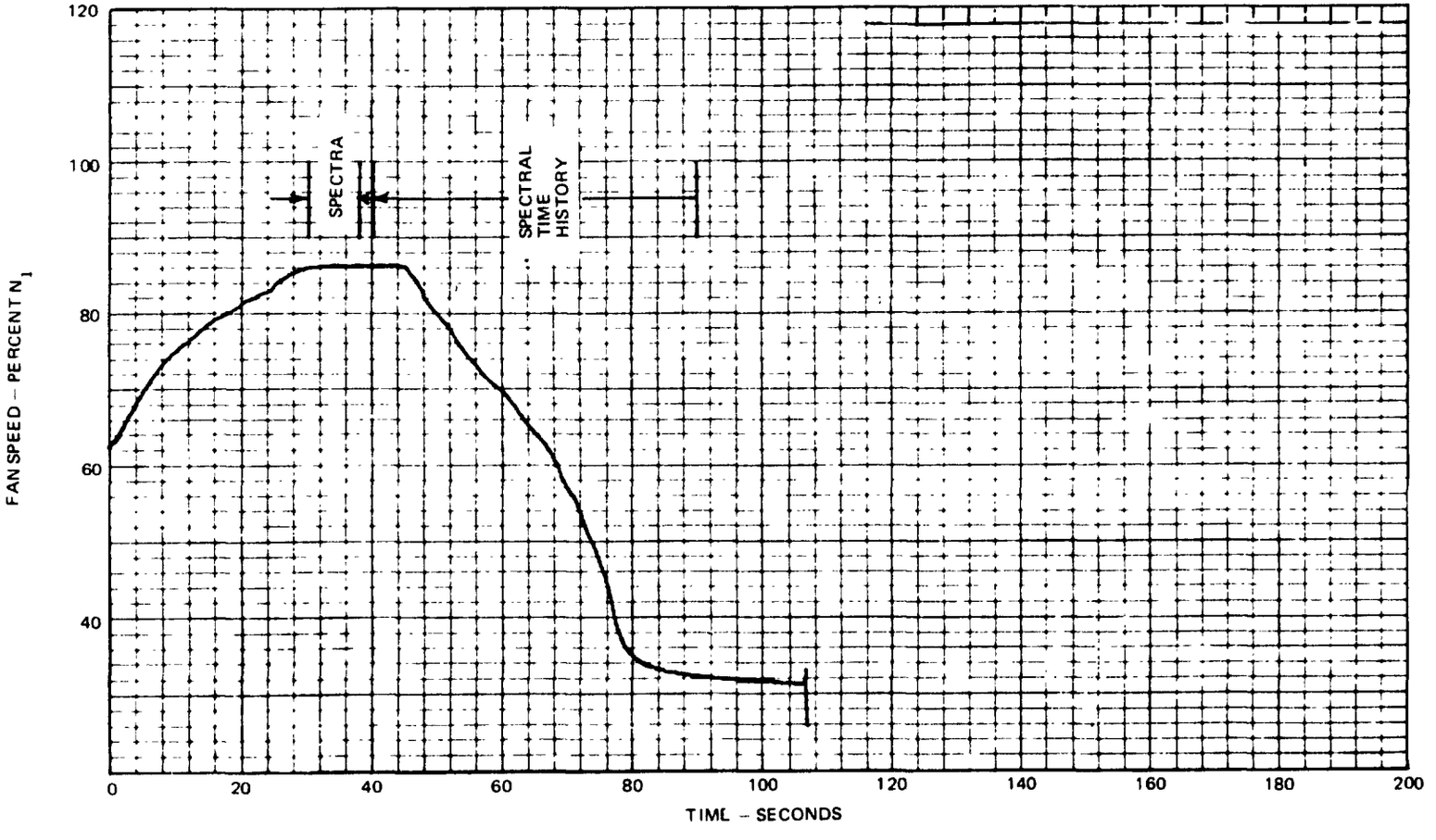

FIGURE 74. DC-9 REFAN, ENGINE NO. 1 FAN SPEED TIME HISTORY, POWER SCAN AT 5000 ft (1 524 m), 295 knots (152 m/s)

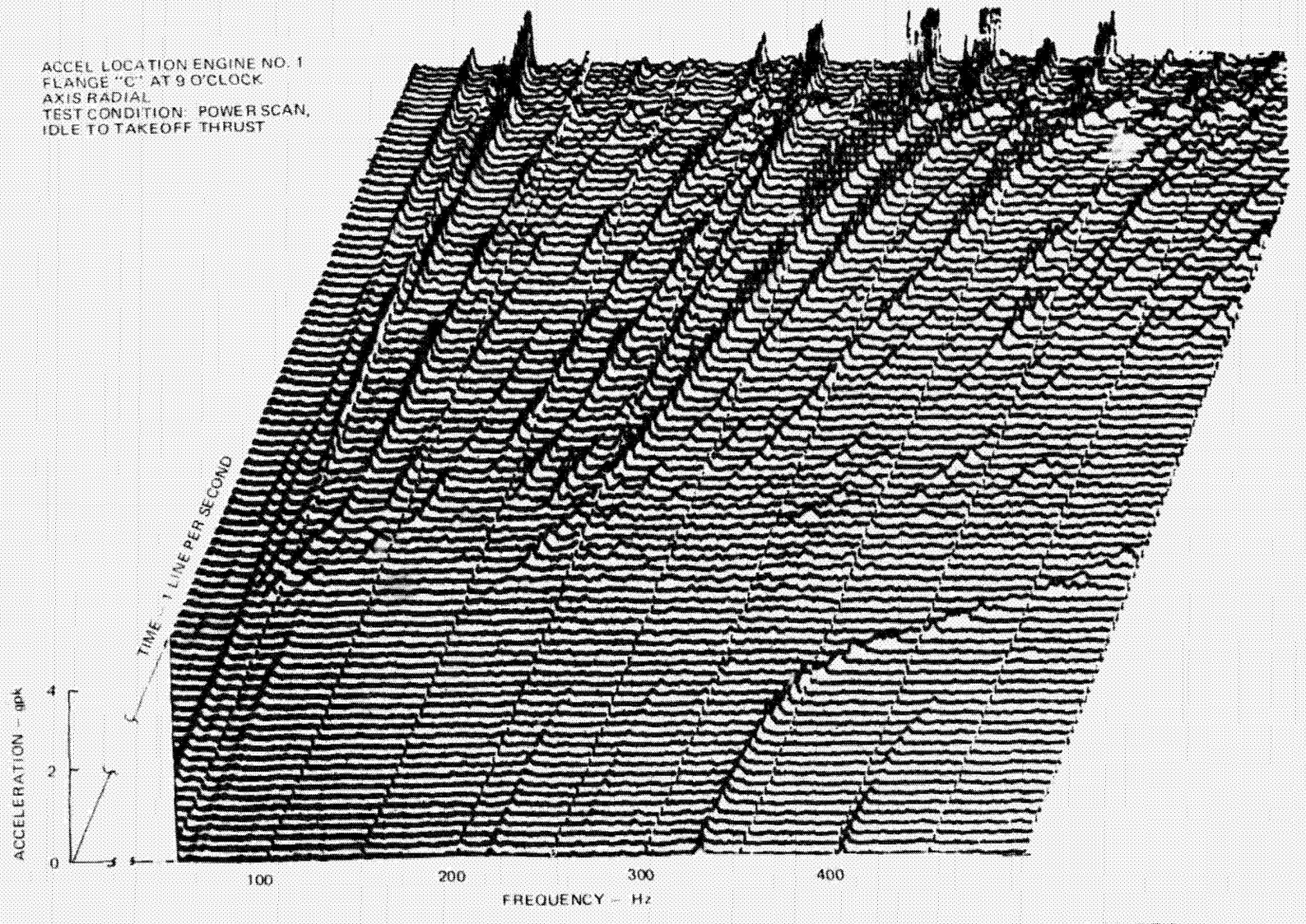

FIGURE 75. DC-9 REFAN COMPRESSOR ACCELERATION SPECTRUM, 3-D TIME HISTORY, 1.5-Hz BANDWIDTH – GROUND STATIC

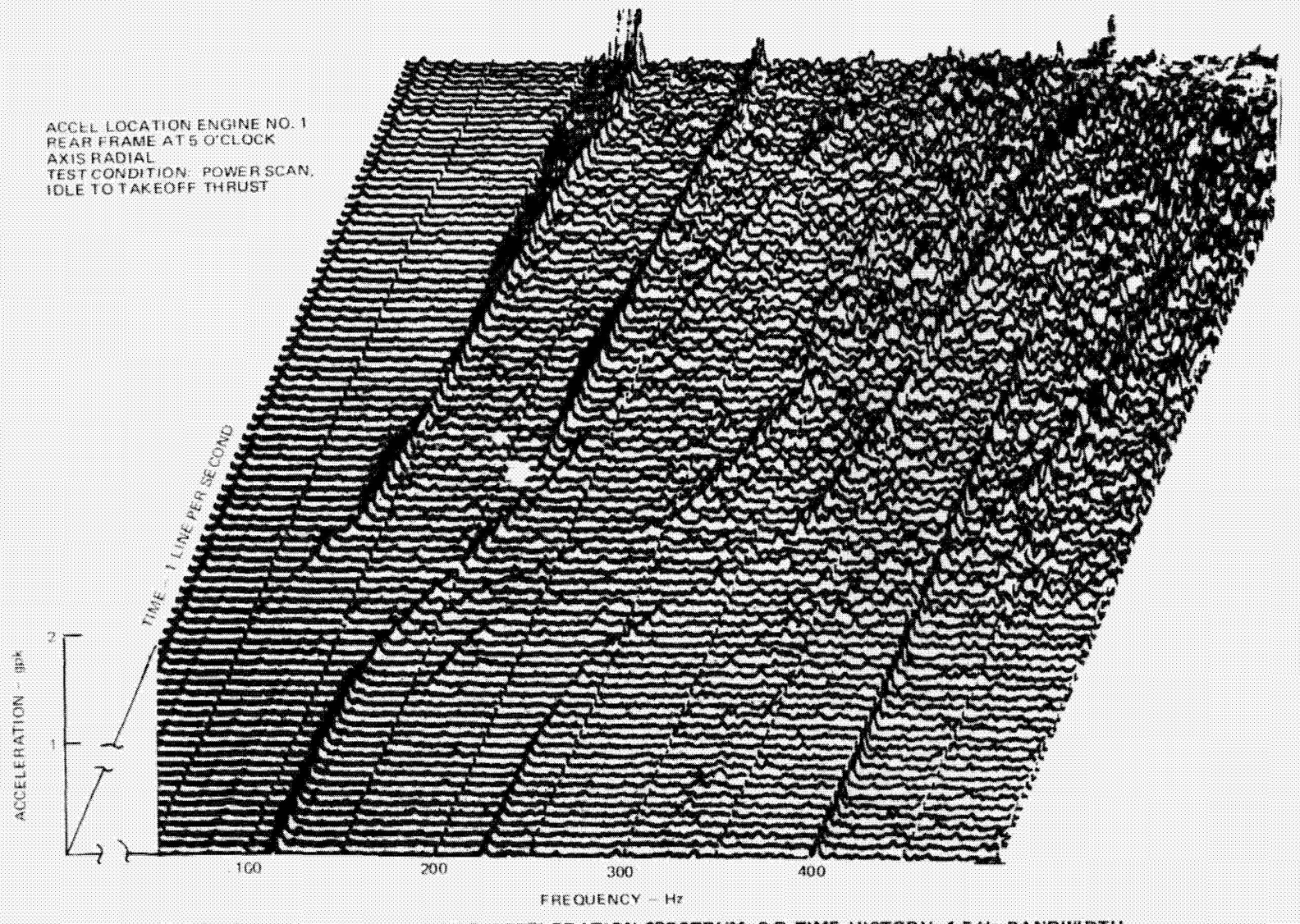

FIGURE 76. DC-9 REFAN TURBINE ACCELERATION SPECTRUM, 3-D TIME HISTORY, 1.5-Hz BANDWIDTH – GROUND STATIC

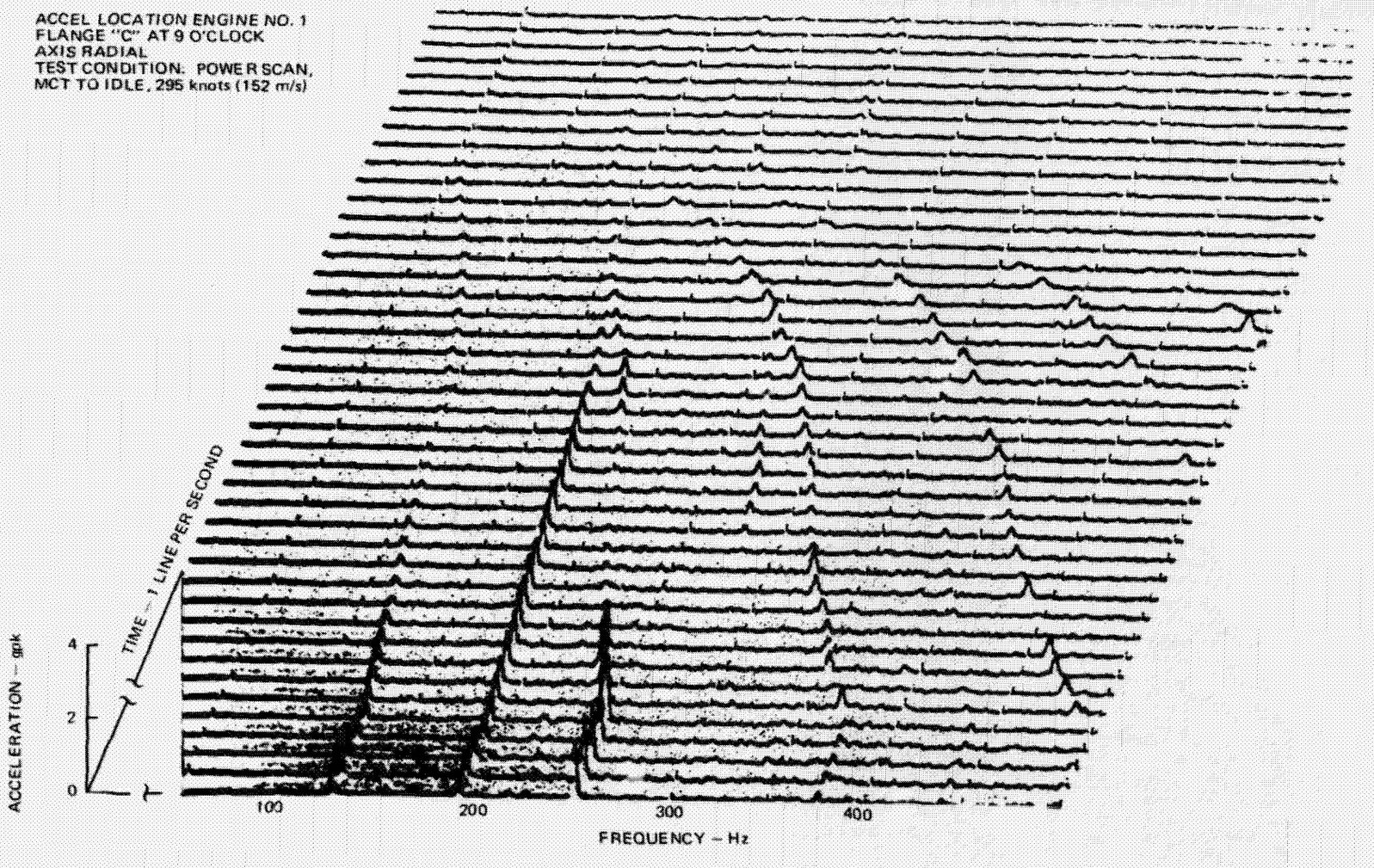

FIGURE 77. DC-9 REFAN COMPRESSOR ACCELERATION SPECTRUM, 3-D TIME HISTORY, 1.5-Hz BANDWIDTH – 5000 ft (1524 m)

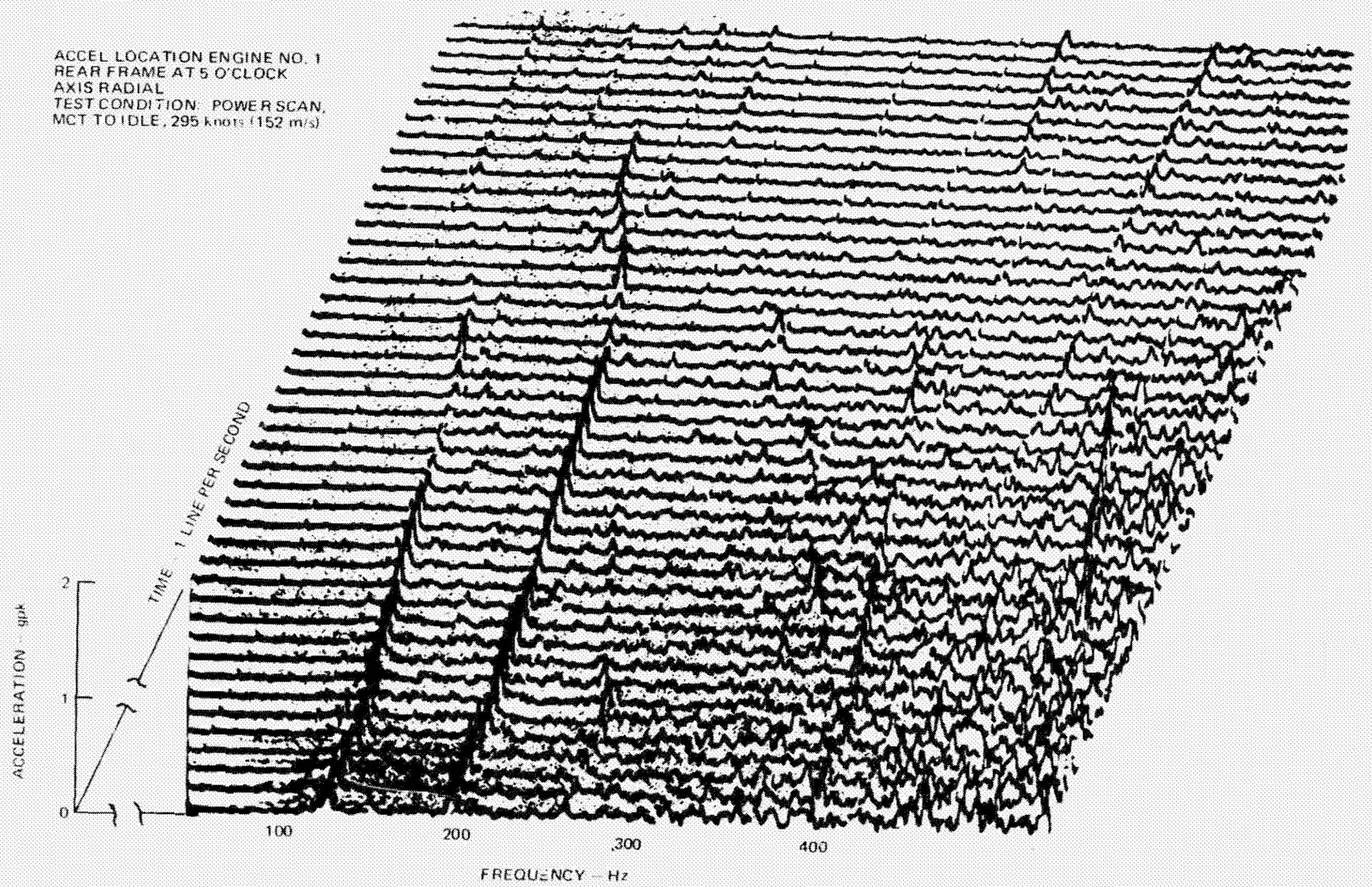

FIGURE 78. DC-9 REFAN TURBINE ACCELERATION SPECTRUM, 3-D TIME HISTORY, 1.5-Hz BANDWIDTH — 5000 ft (1524 m)

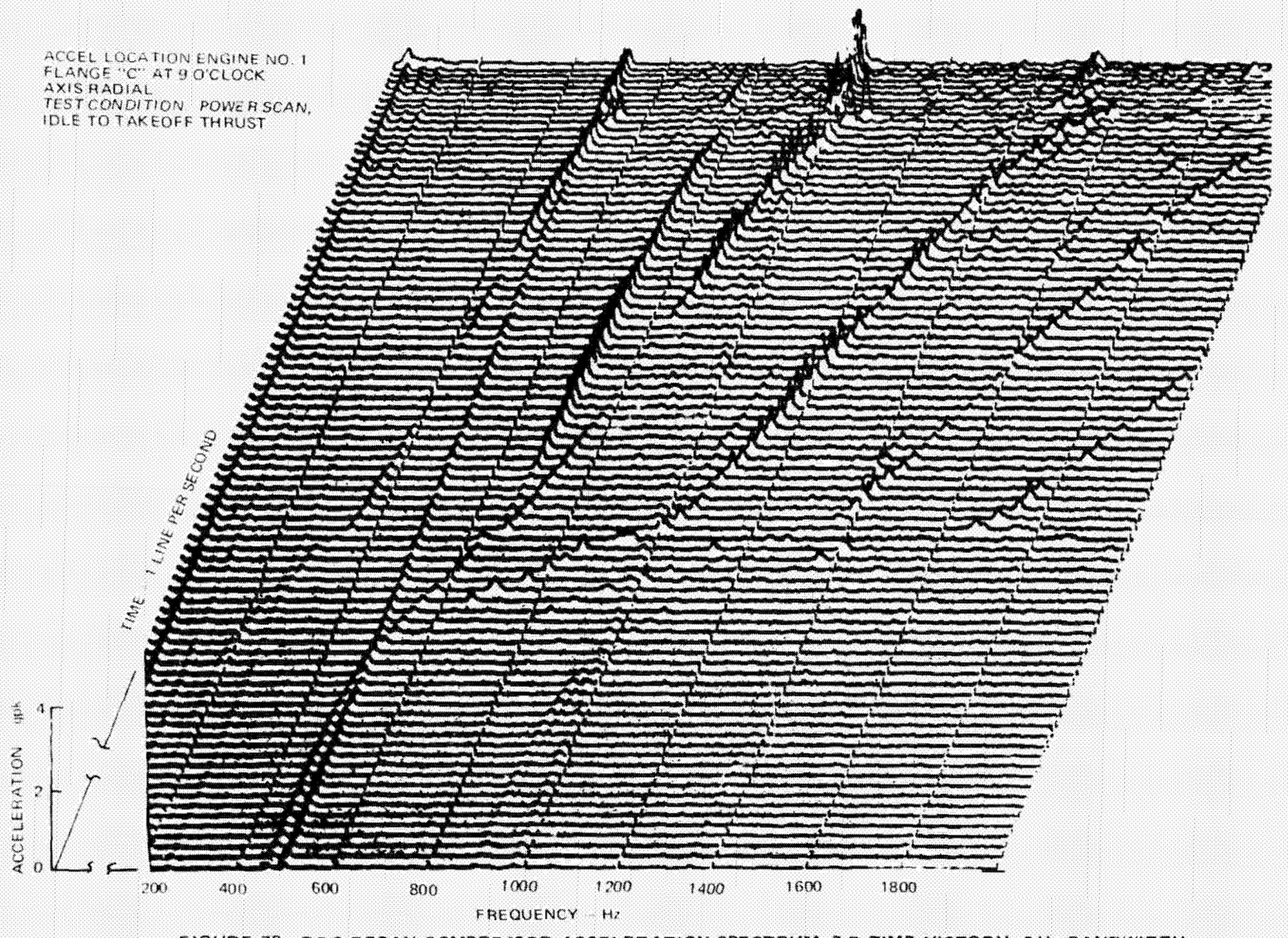

FIGURE 79. DC-9 REFAN COMPRESSOR ACCELERATION SPECTRUM, 3-D TIME HISTORY, 6-Hz BANDWIDTH – GROUND STATIC

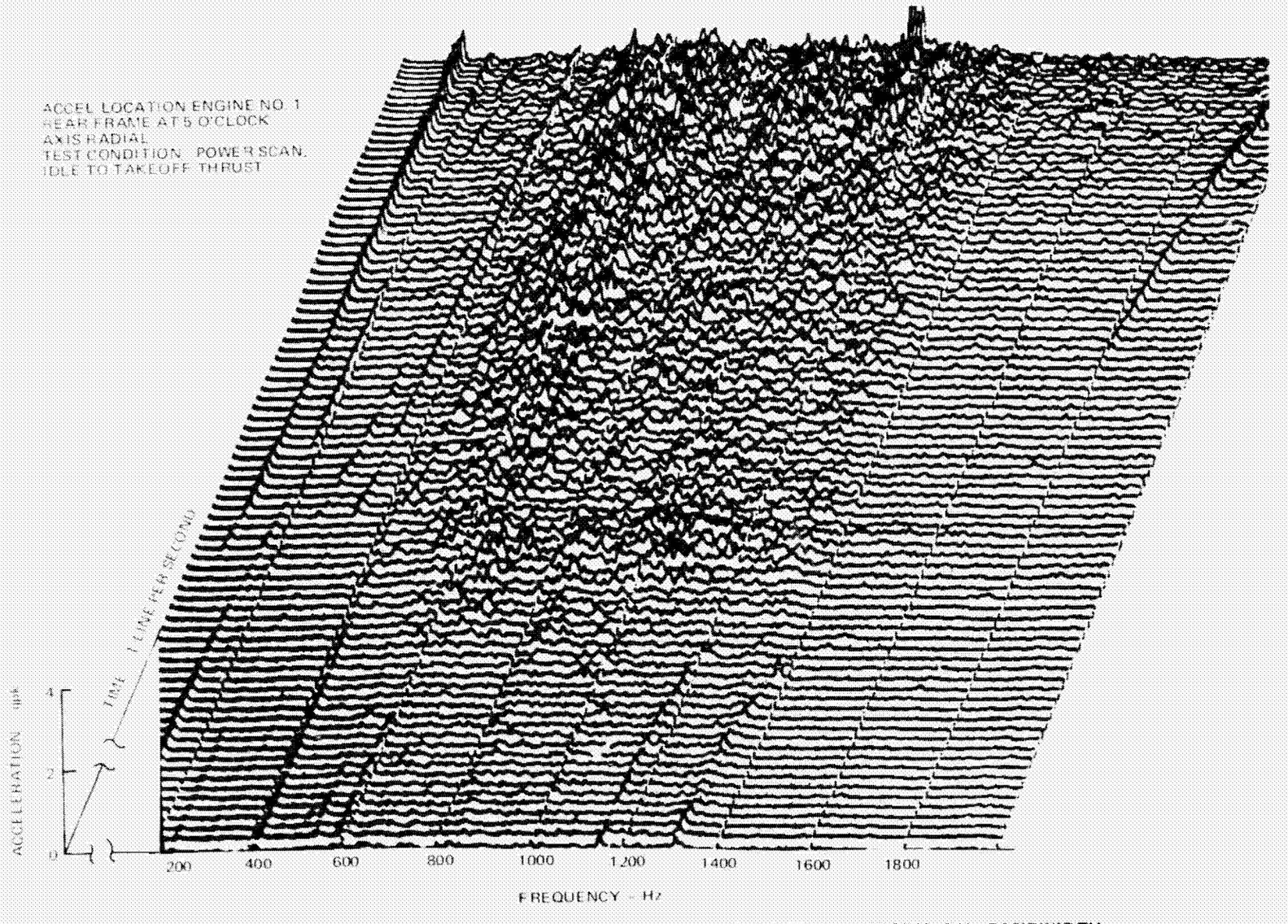

FIGURE 80. DC-9 REFAN TURBINE ACCELERATION SPECTRUM, 3-D TIME HISTORY, 6-Hz BANDWIDTH – GROUND STATIC

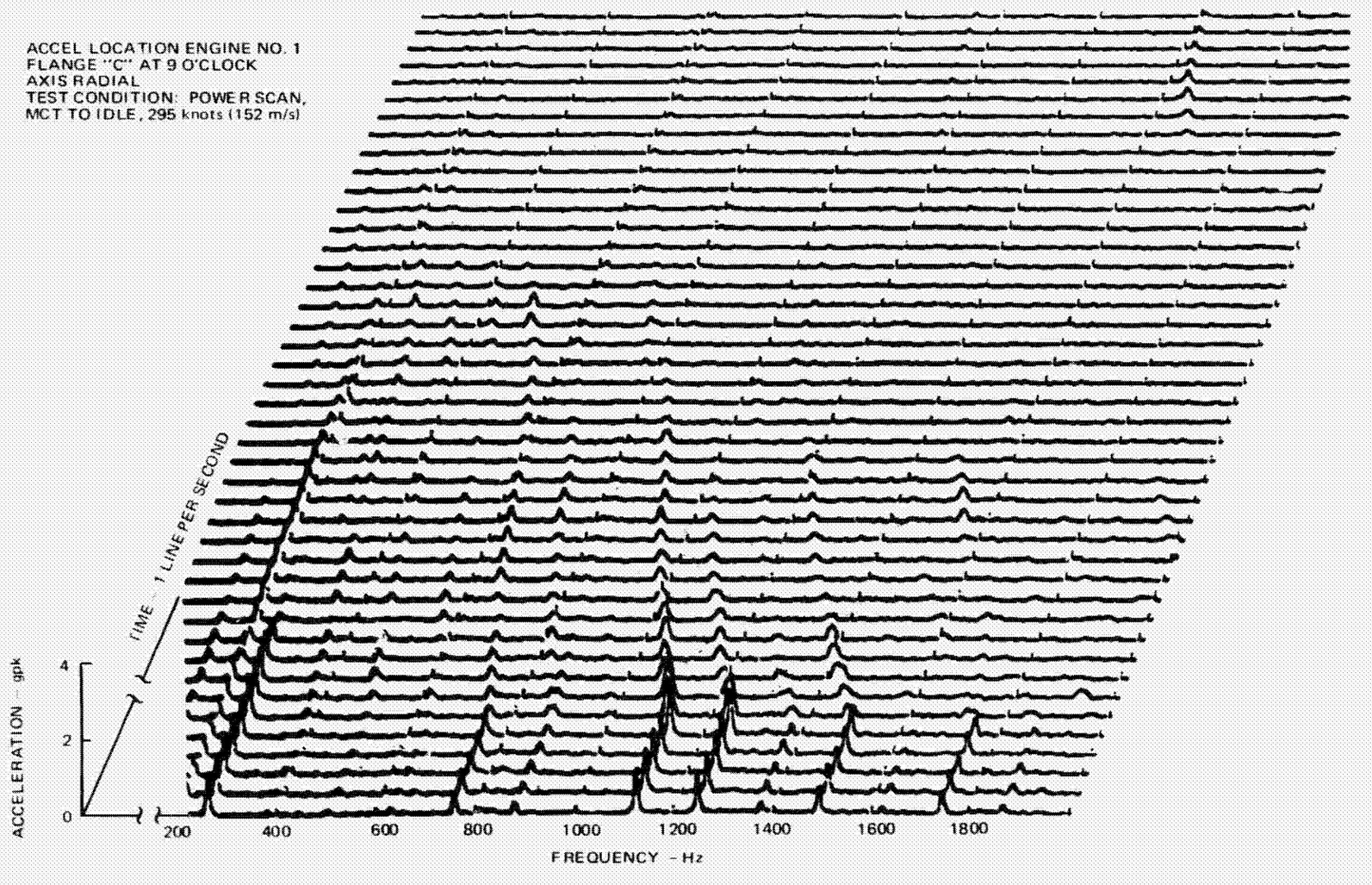

FIGURE 81. DC-9 REFAN COMPRESSOR ACCELERATION SPECTRUM, 3-D TIME HISTORY, 6-Hz BANDWIDTH – 5000 ft (1524 m)

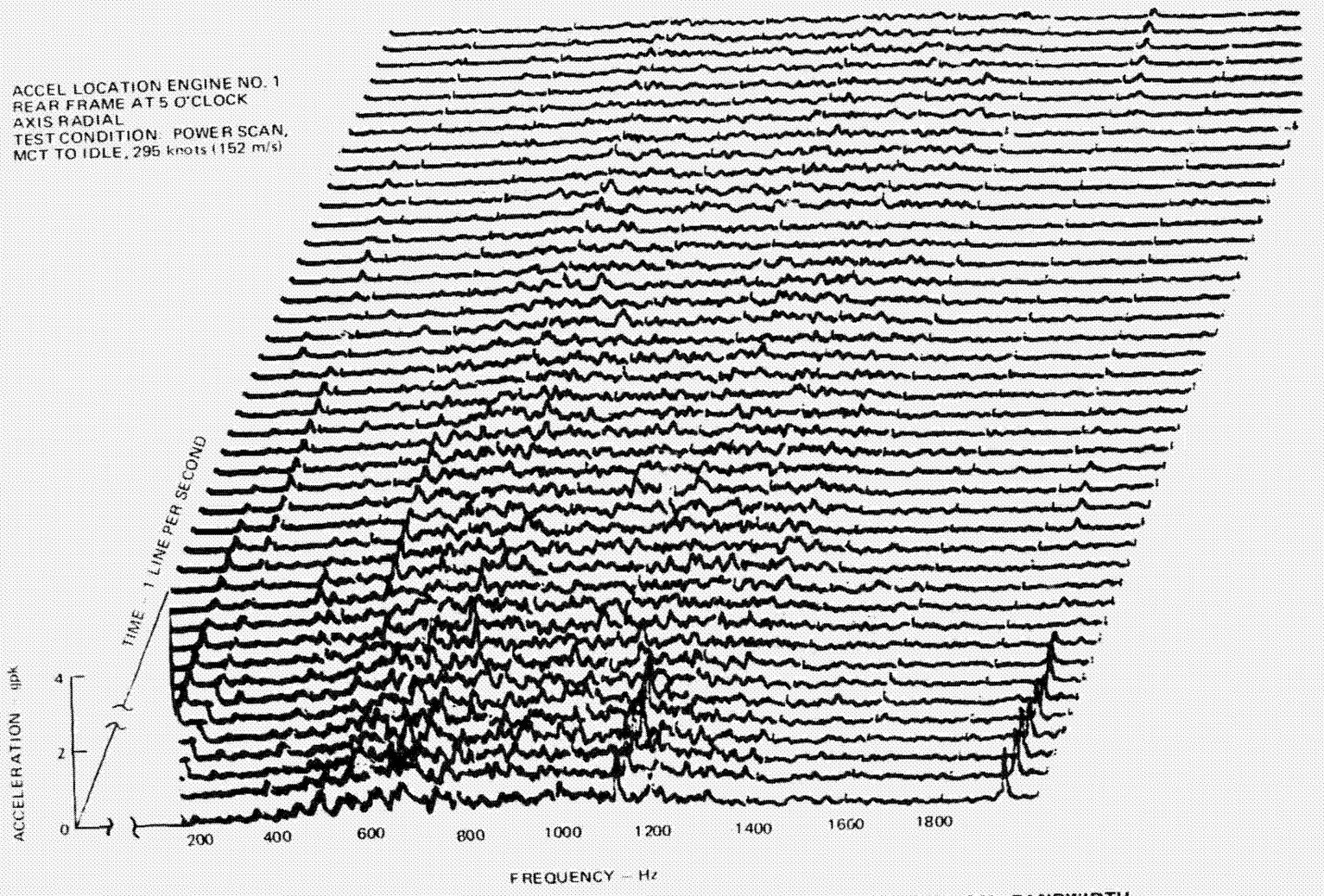

FIGURE 82. DC-9 REFAN TURBINE ACCELERATION SPECTRUM, 3-D TIME HISTORY, 6-Hz BANDWIDTH – 5000 ft (1524 m)

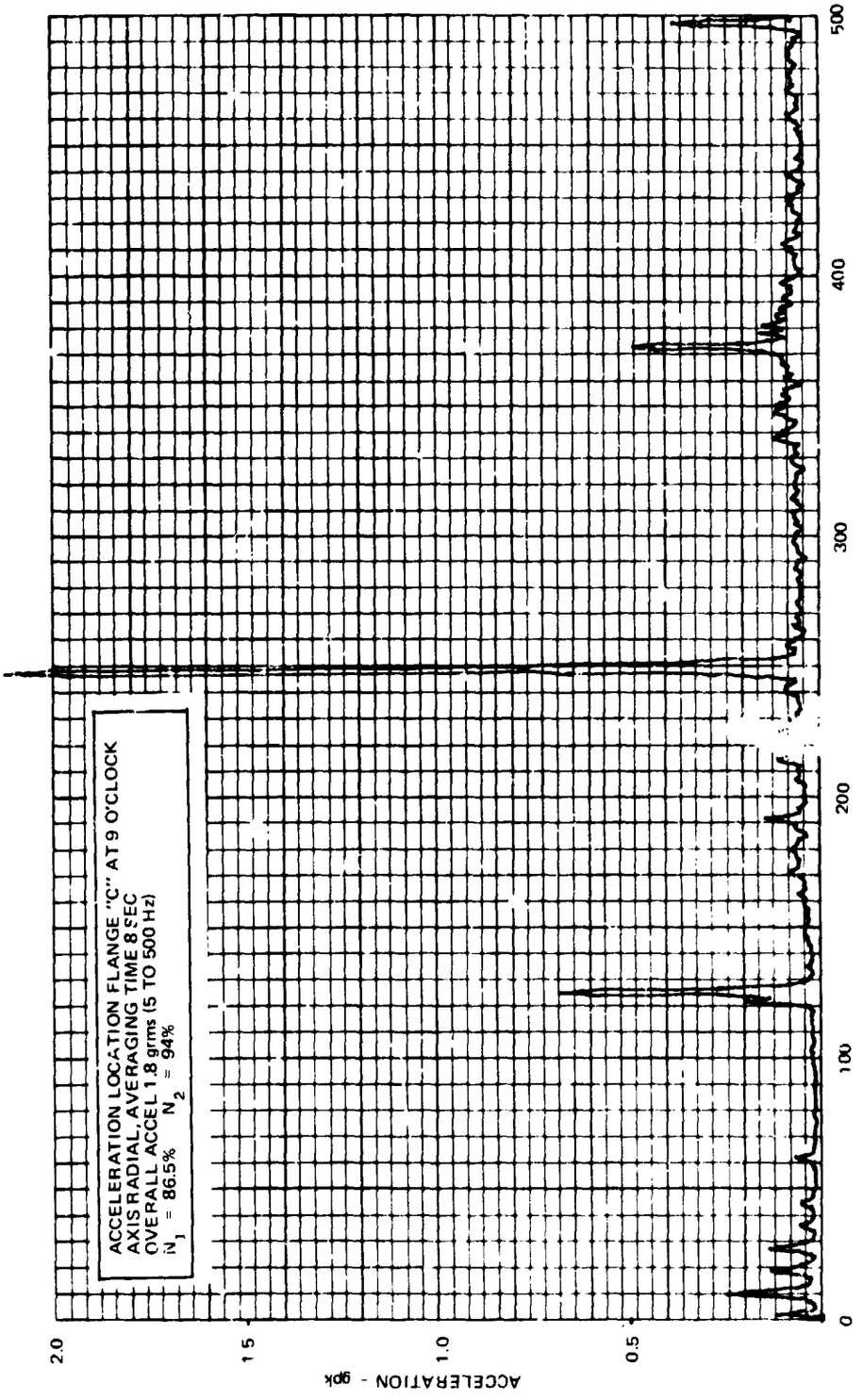

FIGURE 83. F'C-9 REFAN, ENGINE NO. 1 COMPRESSOR VIBRATION, 1.5-Hz BANDWIDTH – GROUND STATIC

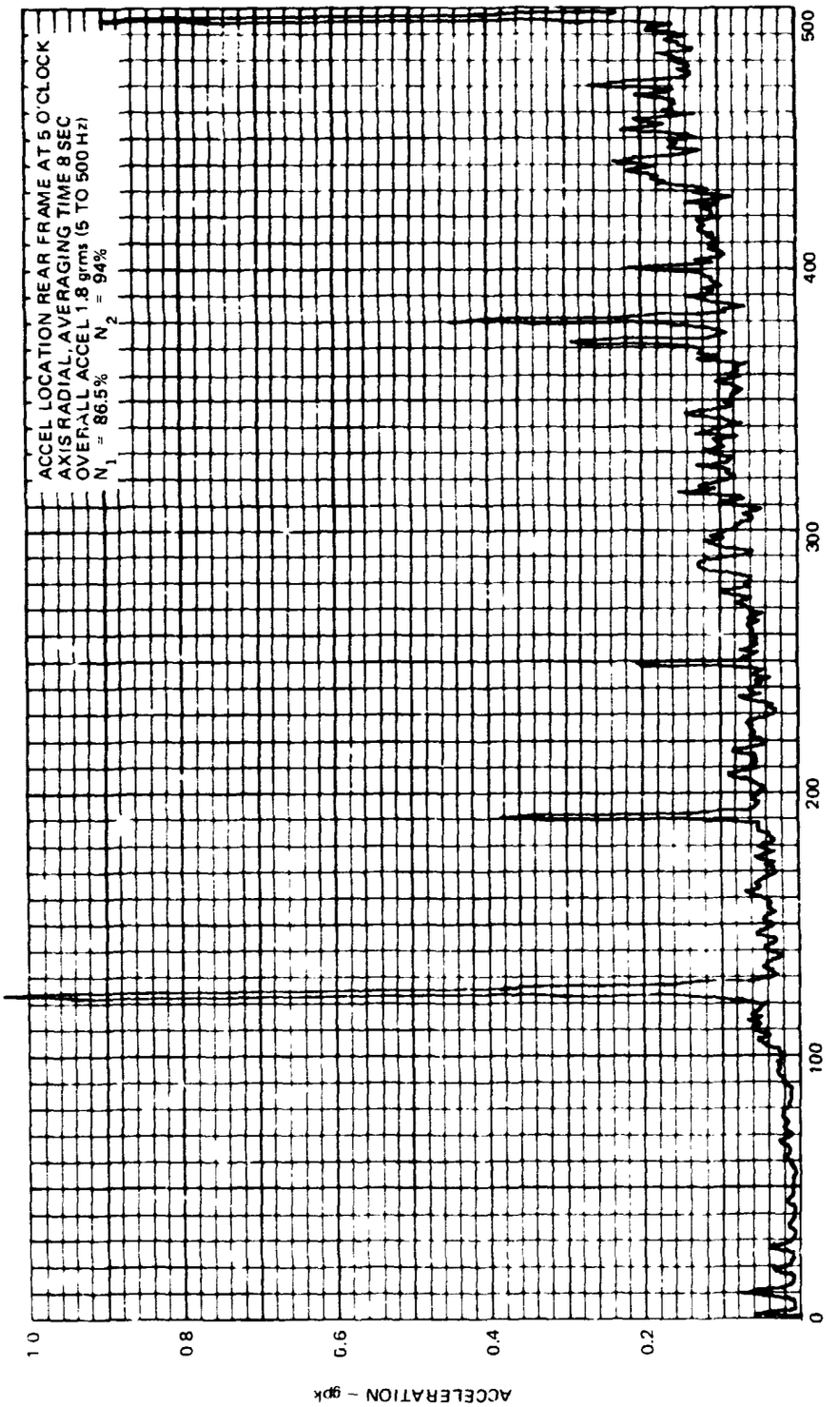

FIGURE 84. D. 9 REFAN, ENGINE NO. 1 TURBINE VIBRATION, 1.5-Hz BANDWIDTH – GROUND STATIC

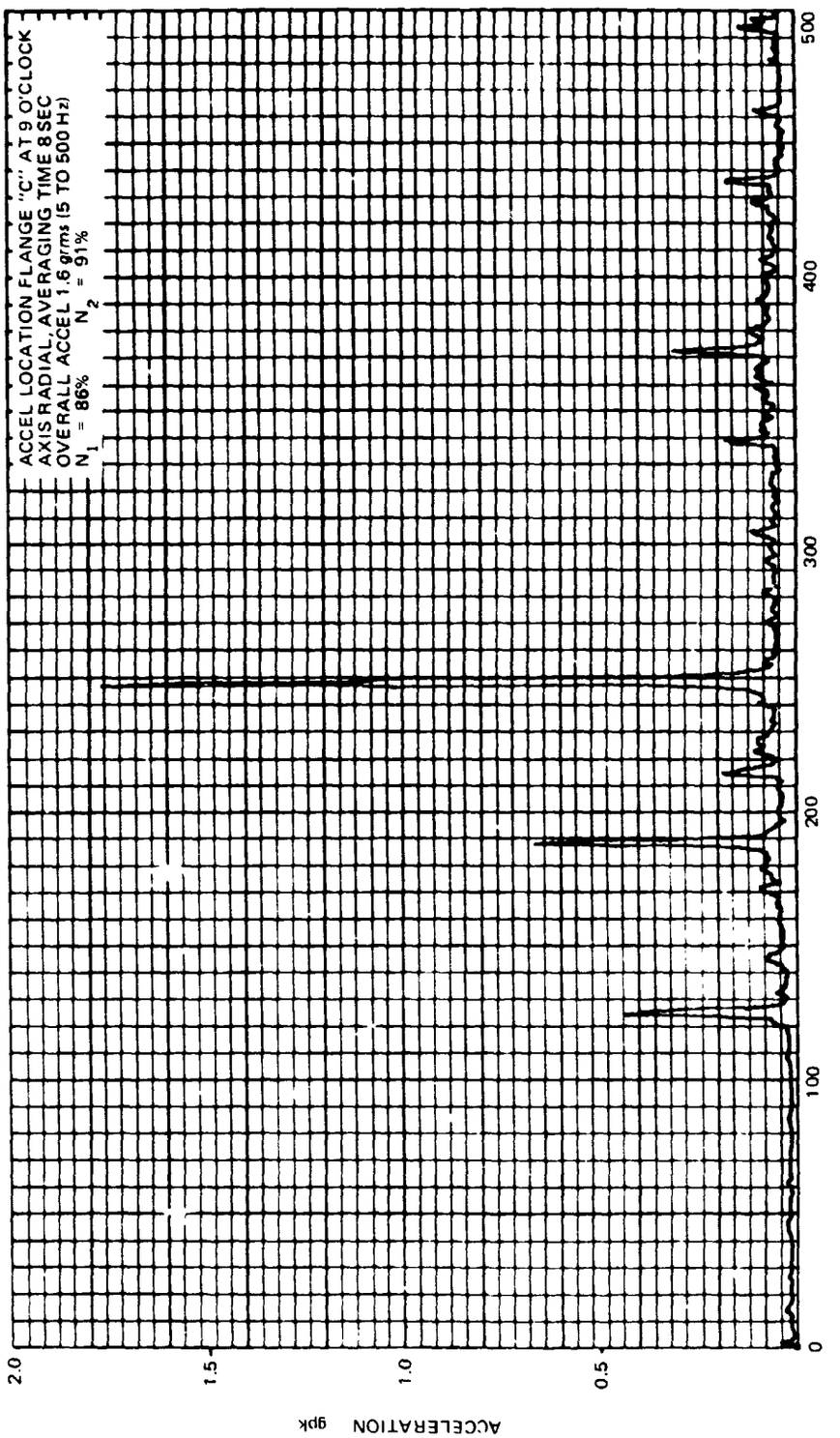

FIGURE 85. DC-9 REFAN, ENGINE NO. 1 COMPRESSOR VIBRATION, 1.5-Hz BANDWIDTH AT 295 knots (152 m/s), 5000 ft (1524 m)

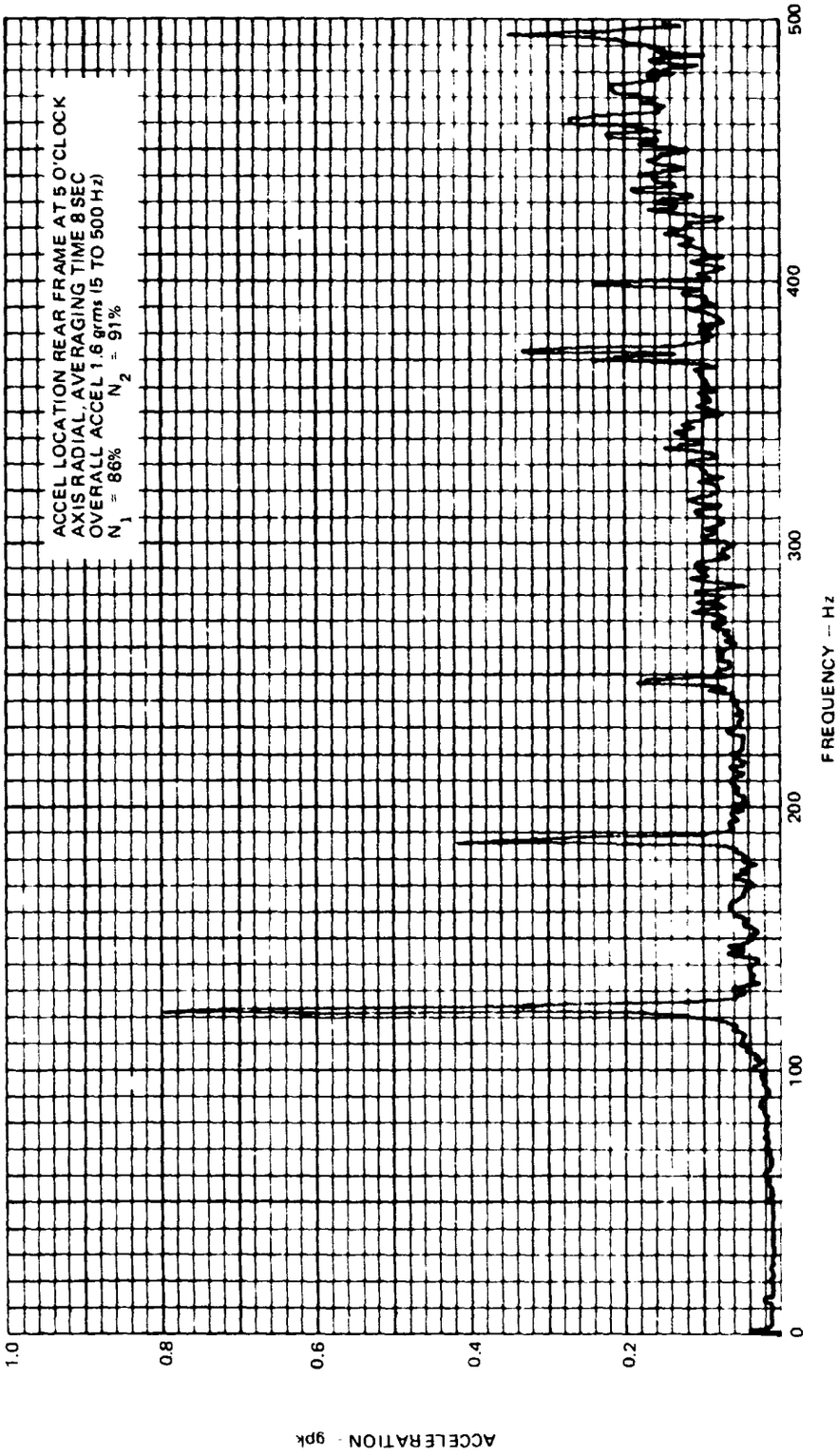

FIGURE 86. DC-9 REFAN, ENGINE NO. 1 TURBINE VIBRATION, 1.5-Hz BANDWIDTH AT 295 knots (152 m/s), 5000 ft (1524 m)

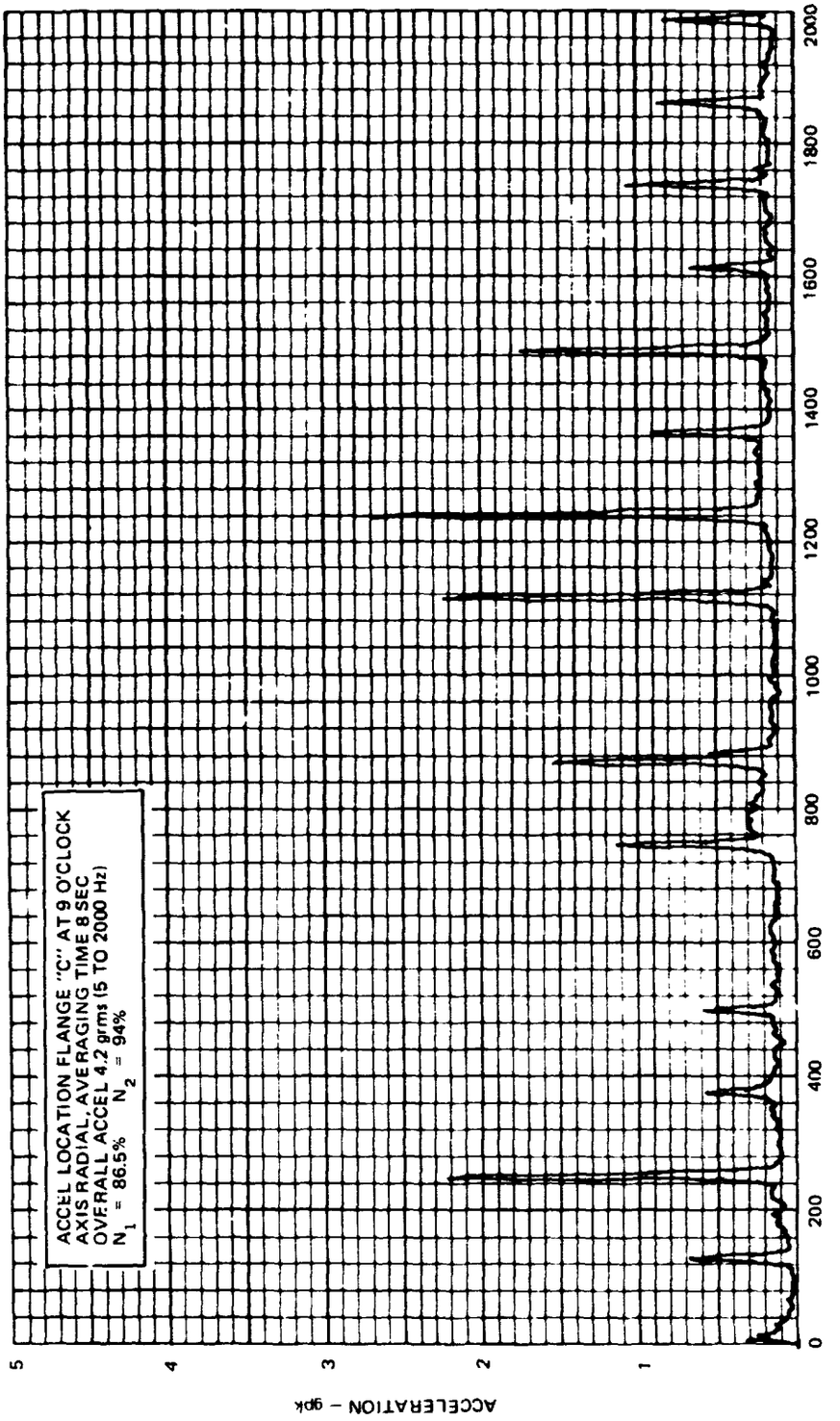

FIGURE 87. DC-9 REFAN, ENGINE NO. 1 COMPRESSOR VIBRATION, 6-Hz BANDWIDTH – GROUND STATIC

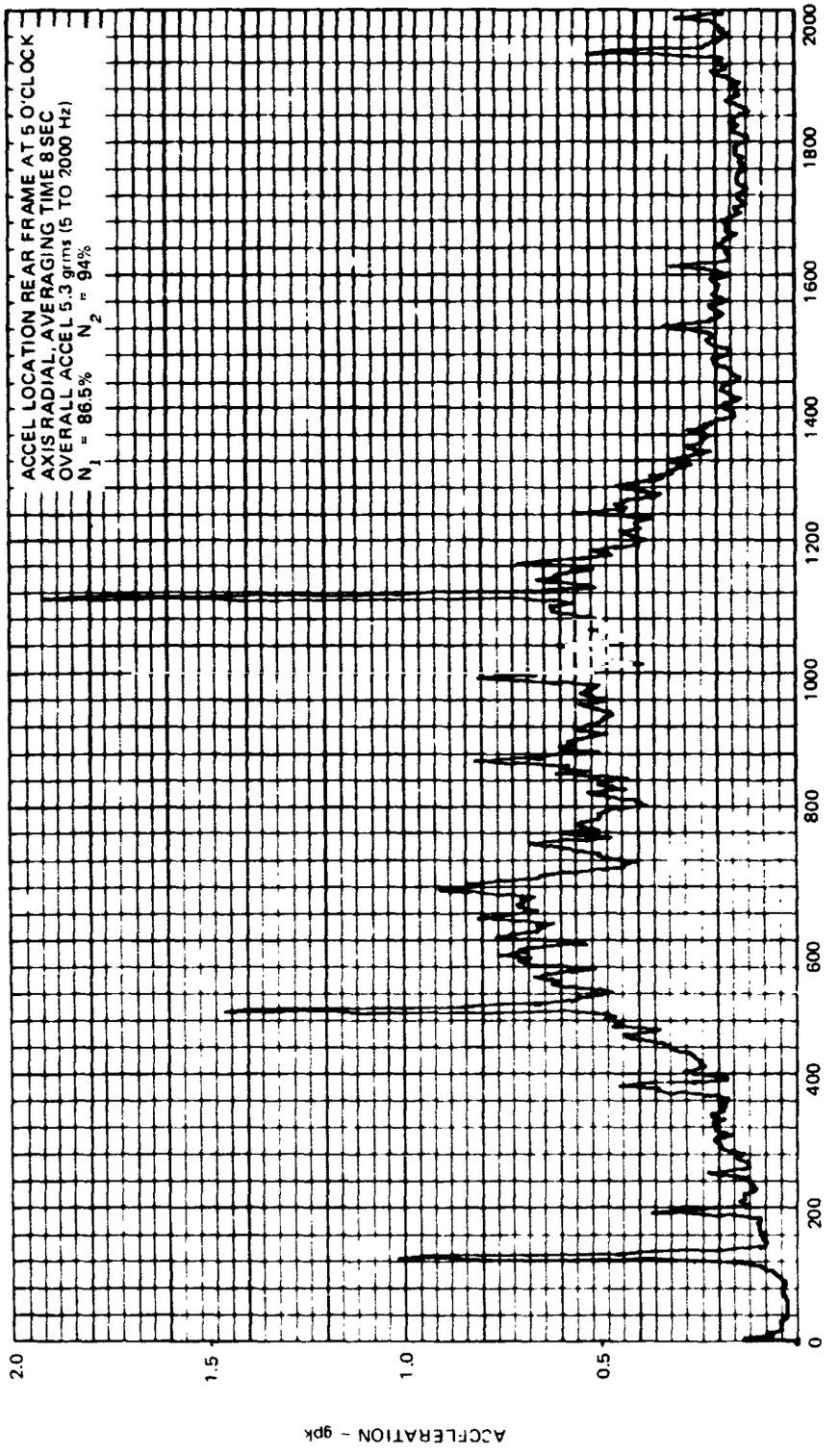

FIGURE 88. DC-9 REFAN, ENGINE NO. 1 TURBINE VIBRATION, 6-Hz BANDWIDTH – GROUND STATIC

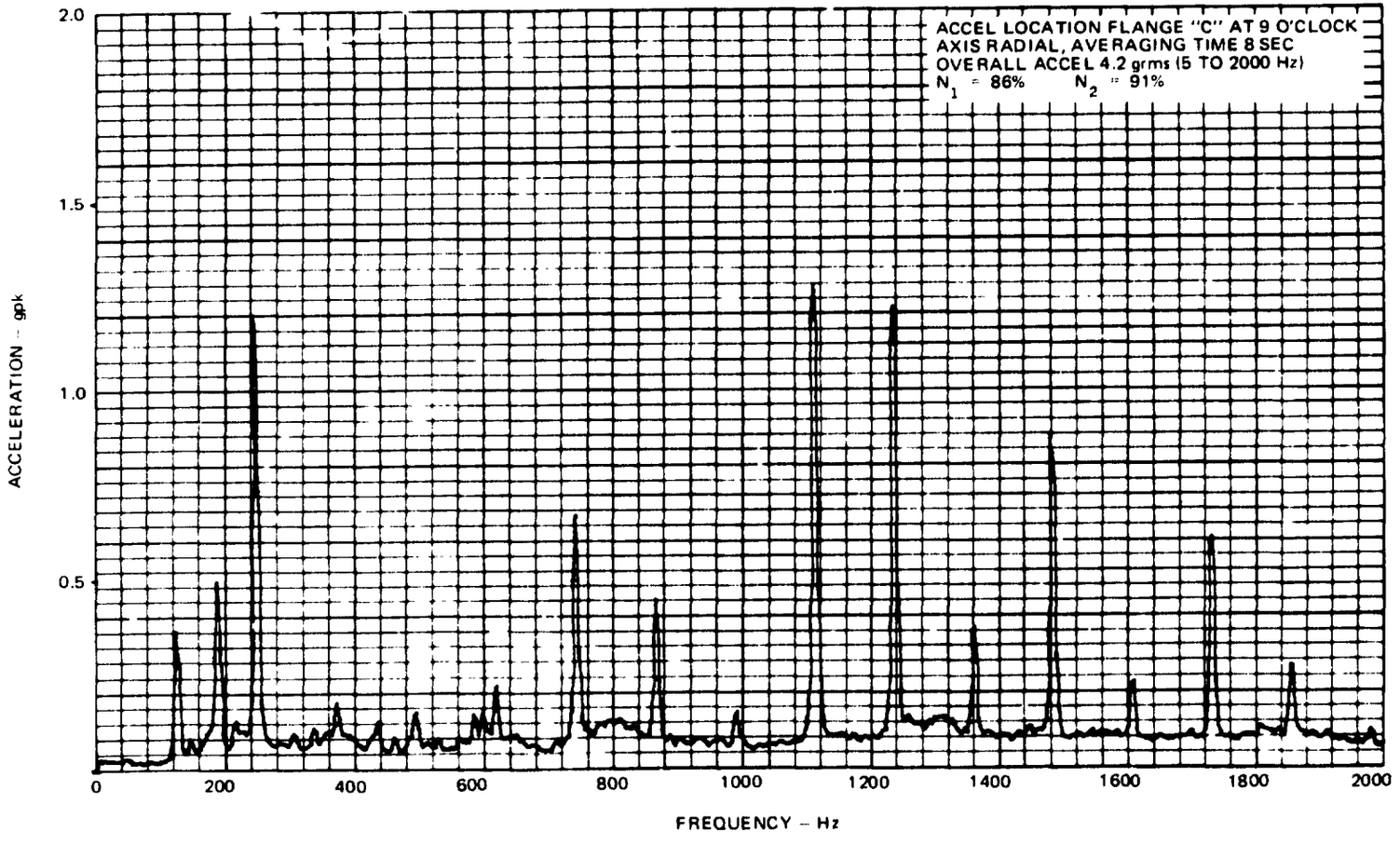

FIGURE 89. DC-9 REFAN, ENGINE NO. 1 COMPRESSOR VIBRATION, 6-Hz BANDWIDTH AT 295 knots (152 m/s), 5000 ft (1524 m)

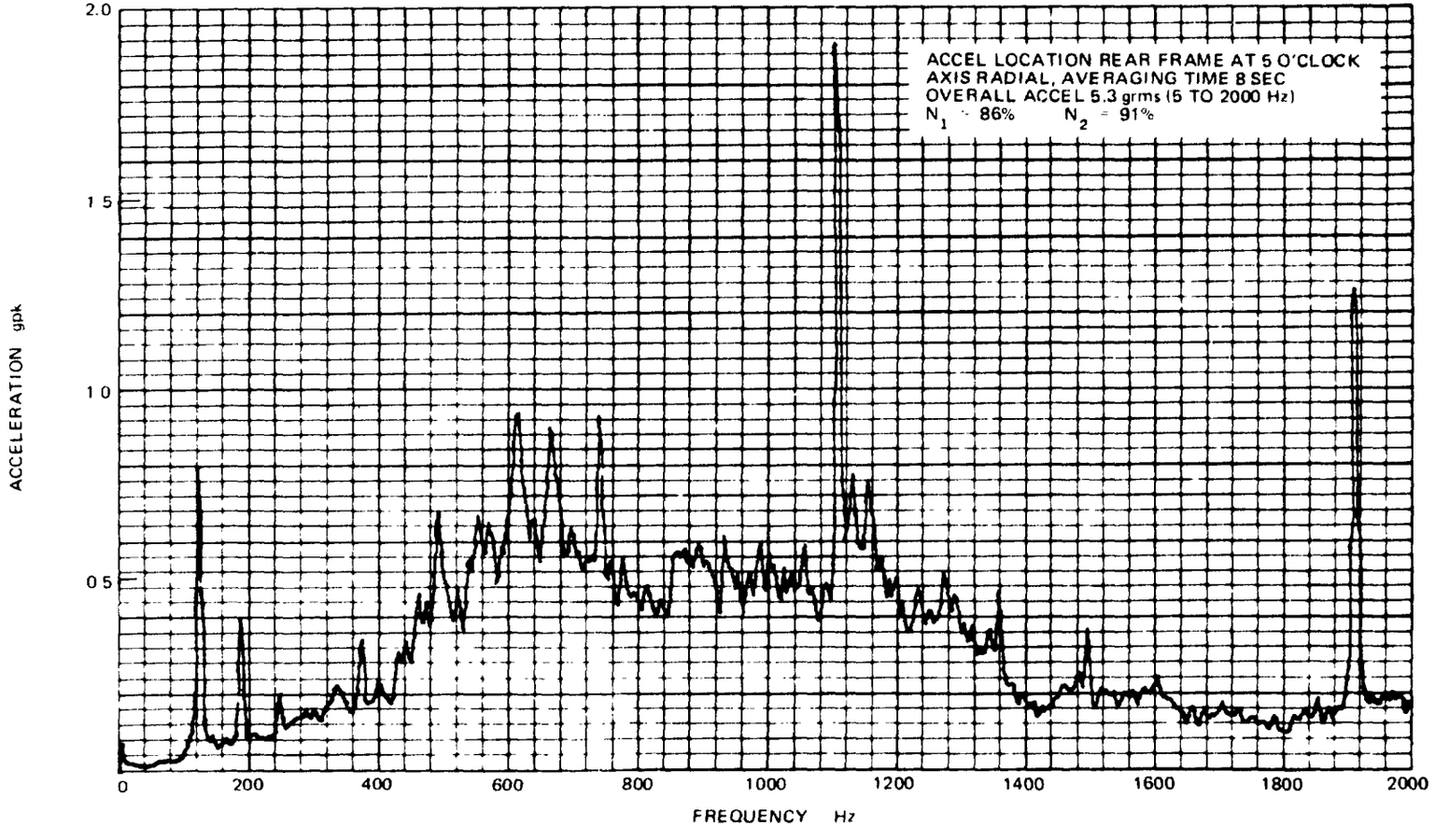

FIGURE 90. DC-9 REFAN, ENGINE NO. 1 TURBINE VIBRATION, 6-Hz BANDWIDTH AT 295 knots (152 m/s), 5000 ft (1524 m)

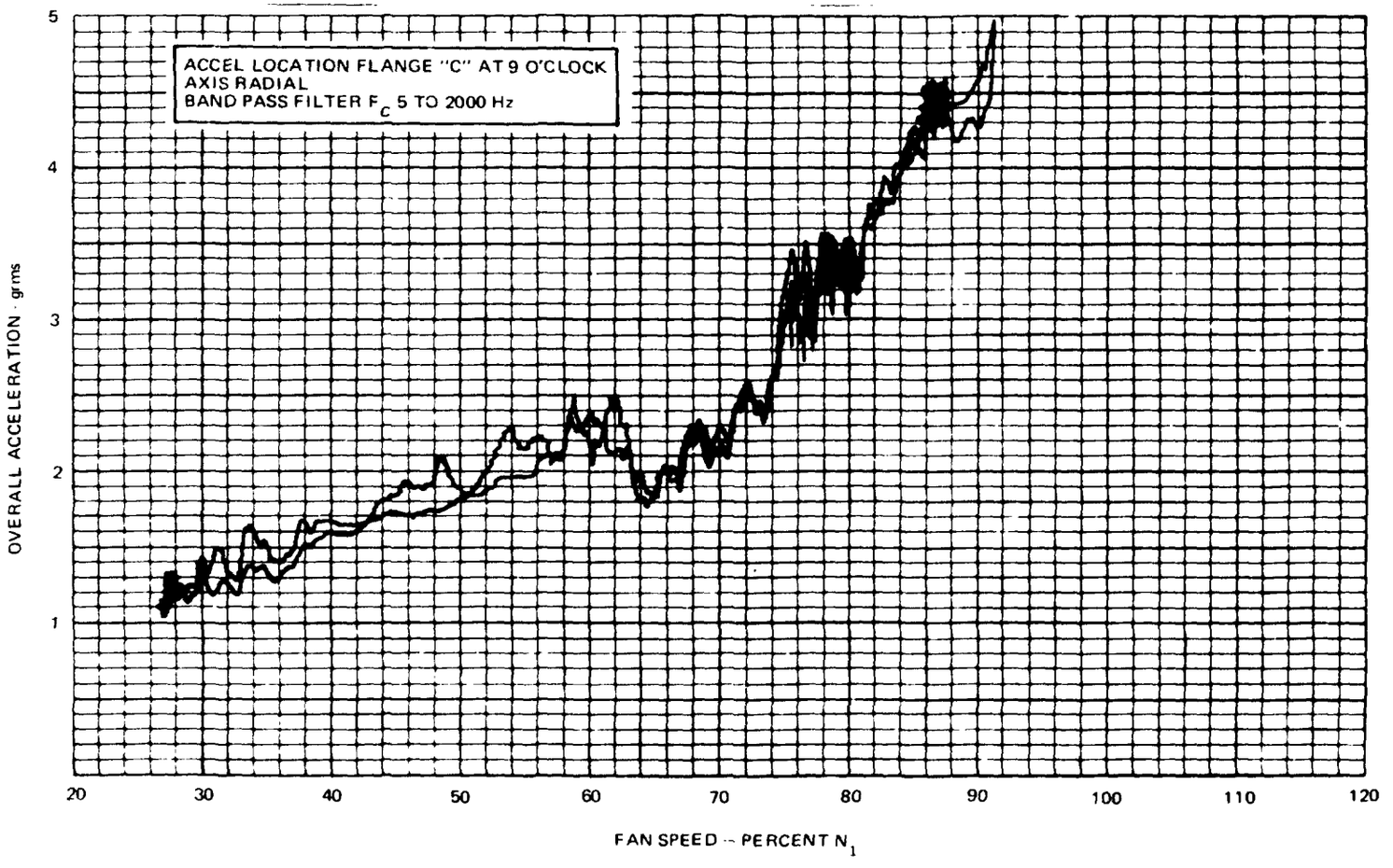

FIGURE 91. *DC-9 REFAN, ENGINE NO. 1* **COMPRESSOR VIBRATION OVERALL ACCELERATION, POWER SCAN, SEA LEVEL STATIC**

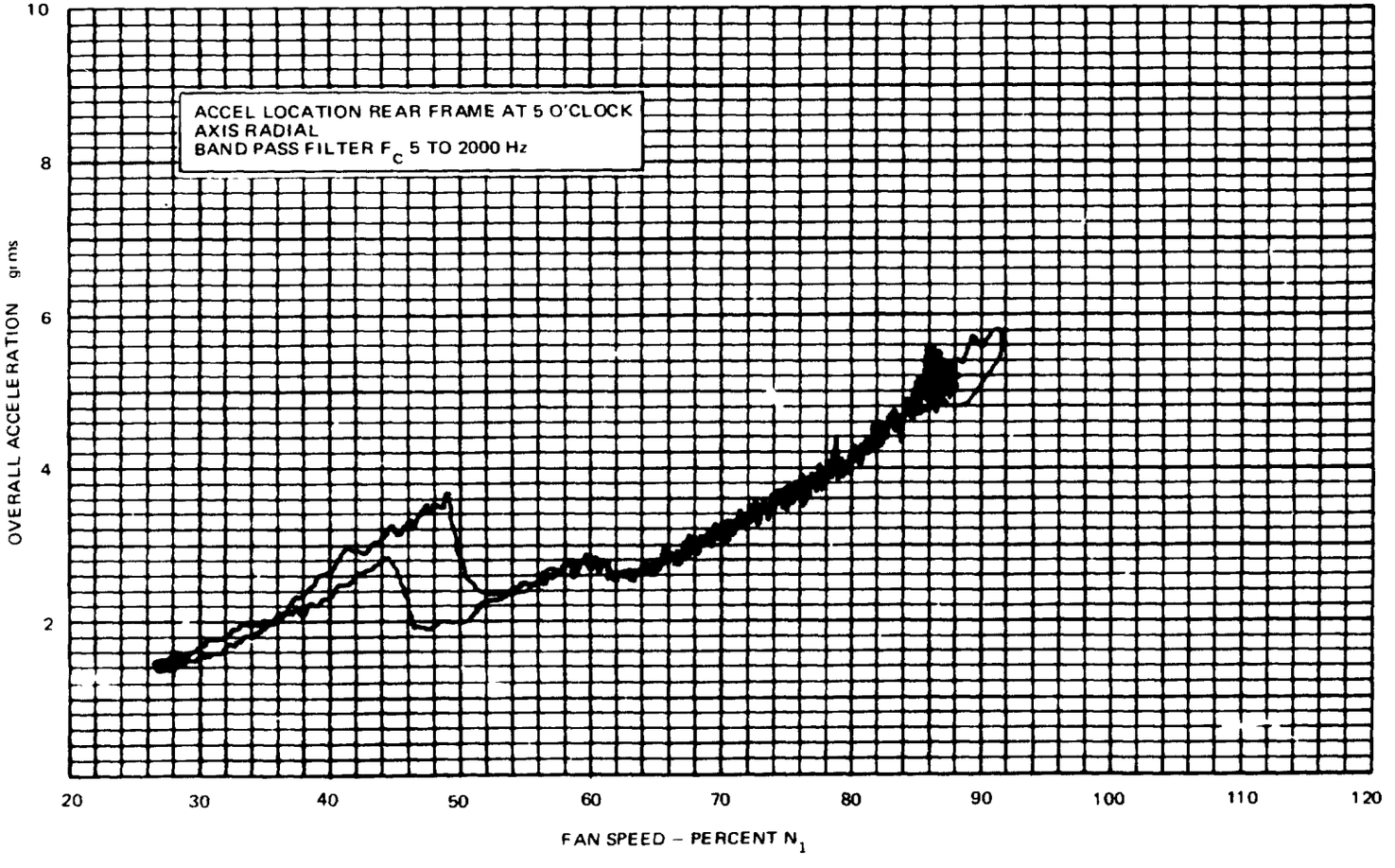

FIGURE 92 DC-9 REFAN, ENGINE NO. 1 TURBINE VIBRATION OVERALL ACCELERATION, POWER SCAN, SEA LEVEL STATIC

Thrust Reverser

Thrust reverser performance testing was conducted to evaluate the DC-9 Refan airplane deceleration capability, to determine the extent of thrust reverser reingestion, to monitor airplane control characteristics during normal and abnormal reverse thrust landings and survey the empennage skin temperatures in the area of the thrust reverser during reverse thrust operation.

The thrust reverser system configuration was the same as the current rotated production system except for the following changes.

1) Larger thrust reverser buckets

2) Increased hydraulic system component sizes and volumes

3) Fail safe latch incorporated on the upper and lower doors

4) Redesigned thrust reverser controls

5) Upper and lower bucket forward lips, 73.6 mm (2.90 in) tall

The airplane systems configuration for the reverse thrust landings were normal hydraulics, forward c.g. and flaps/slats 0.873 rad (50 deg)/Extend.

Thrust reverser thermocouples were installed as shown in figures 93 and 94. The empennage peak temperatures were monitored by temp-plates located as shown in figure 95.

Symmetrical reverse thrust decelerations were evaluated during high speed taxi tests and landings with varying amounts of reverse thrust from idle to takeoff. The airplane ground speed was obtained from laser tracking data and the airplane deceleration calculated and normalized to a standard airplane gross weight. The normalized deceleration for a reverse thrust target EPR of MCT (1.6) is presented in figure 96 versus equivalent airspeed.

Figure 97 shows the measured airplane deceleration normalized to 45 359 kg (100,000 lb) landing weight as a function of equivalent airspeed for nominal engine power settings from reverse idle (1.08) EPR to MCT (1.6).

The test procedure was to set EPR in reverse approximately 4 seconds after touchdown and hold this EPR to as low a speed as practical before engine instability or reingestion precluded further operation. For normal airline operation of production DC-9's, 1.6 EPR is set in reverse and cut back to 1.2 EPR is initiated at 30.87 m/s (60 knots). This procedure was established to prevent foreign object damage (FOD) due to kick up from the bottom reverser bucket jet efflux.

The Refanned engine LP compressor discharge pressure, P_{S3}, was monitored for evidence of engine instability during the tests; the JT8D-109 engine characteristics were normal for the thrust reverser operations with no evidence of instability or reingestion. The fact that the JT8D-109 engine

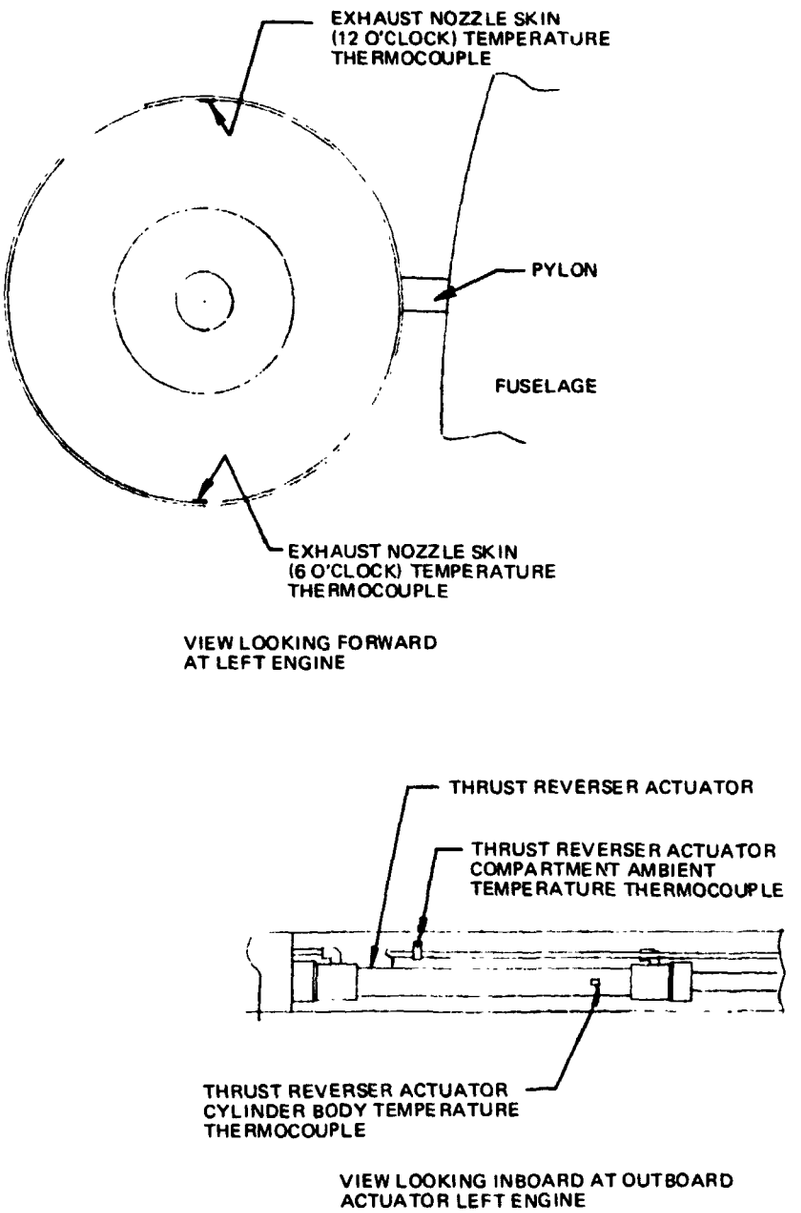

FIGURE 93. DC-9 REFAN THRUST REVERSER ACTUATOR AND EXHAUST NOZZLE THERMOCOUPLE LOCATIONS

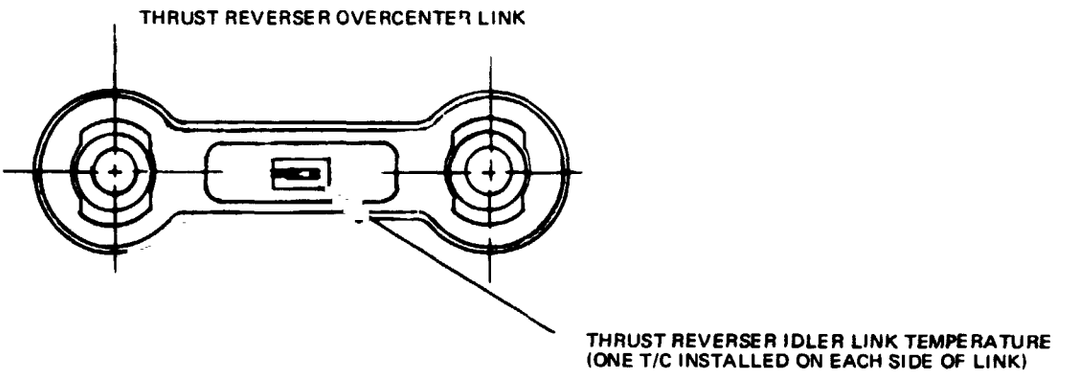

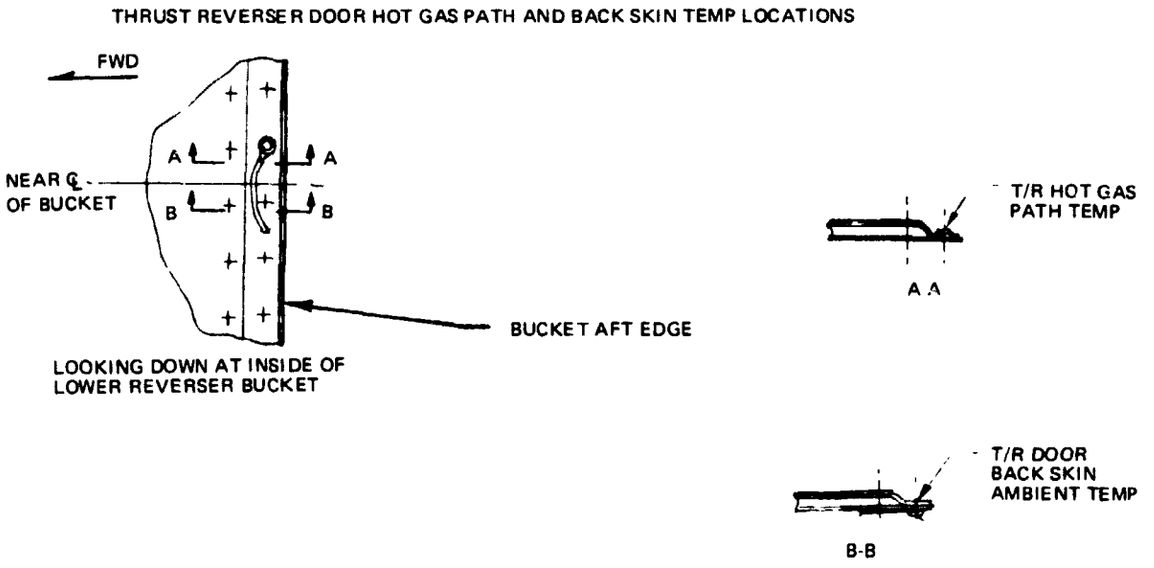

FIGURE 94. DC-9 REFAN THRUST REVERSER IDLER LINK AND DOOR THERMOCOUPLE LOCATIONS

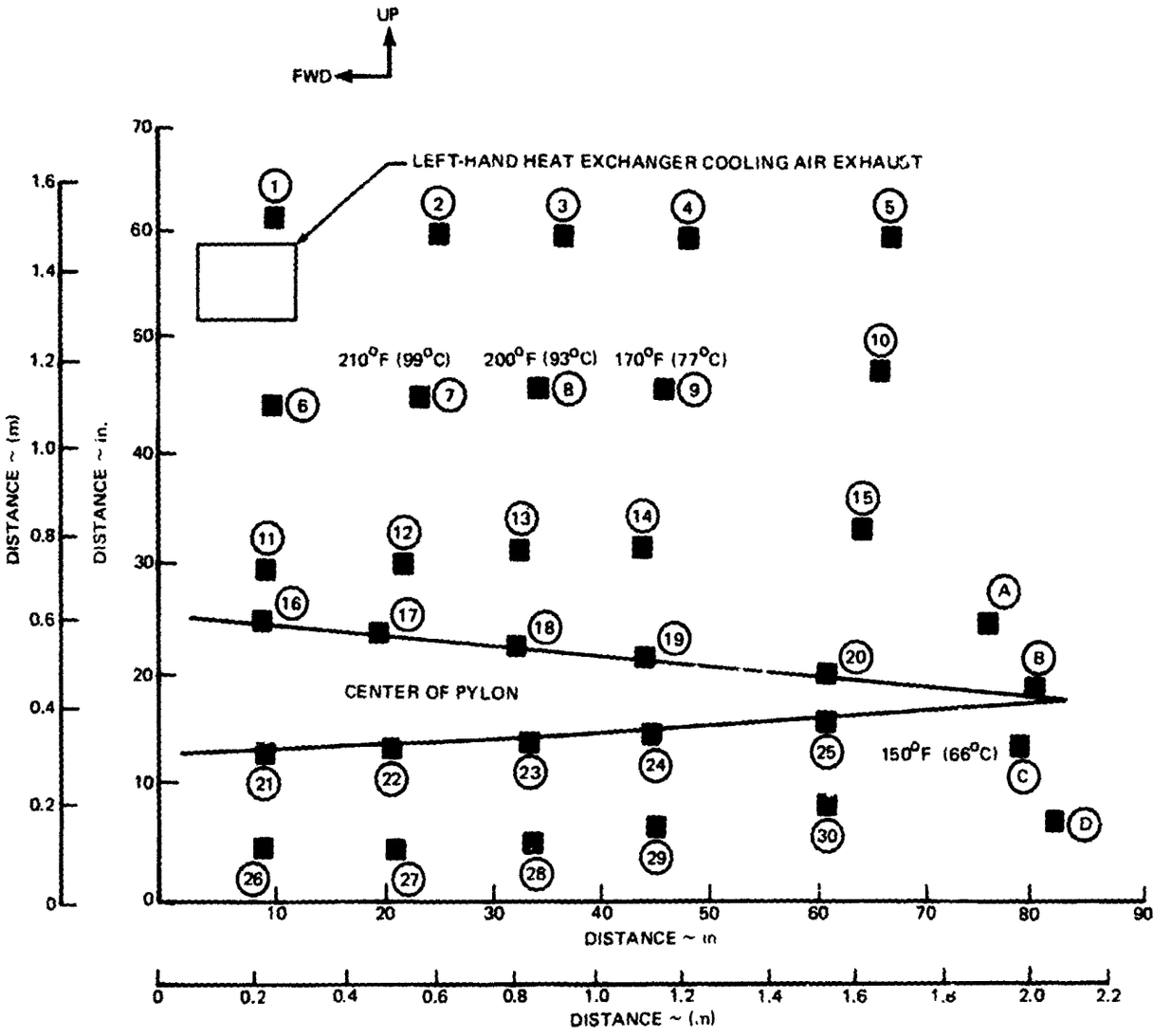

NOTES: 1. TEMPERATURES ARE LESS THAN 150°F (66°C) UNLESS NOTED
2. CIRCLED NUMBERS ARE APPROXIMATE LOCATIONS OF TEMP-PLATES

FIGURE 95. DC-9 REFAN ENGINE NACELLE AND FUSELAGE TEMP-PLATES AFTER REVERSE THRUST LANDING

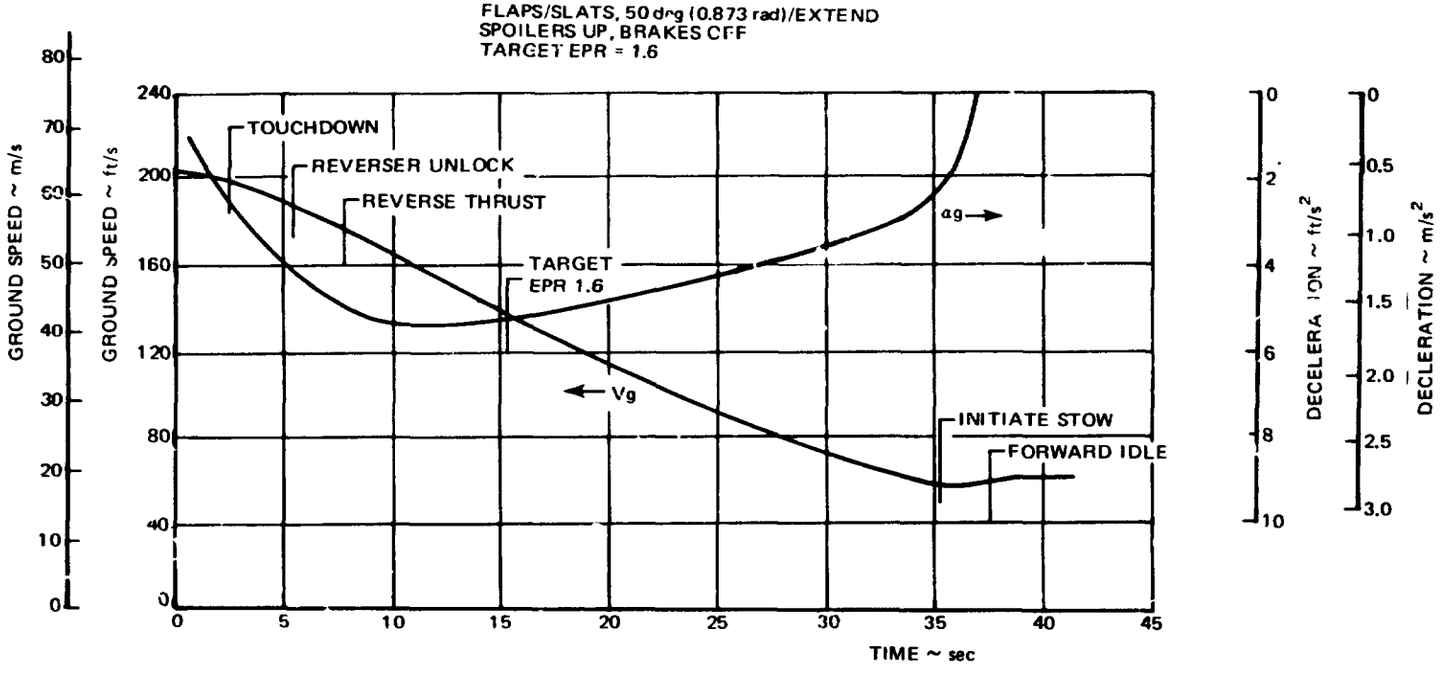

FIGURE 96. DC-9 RE-FAN THRUST REVERSER PERFORMANCE

SYM	GROSS WEIGHT lb (kg)	cg (% MAC)	T_{am} °F (°C)	EPR LH/RH
○	104,800 (47 536)	9.9	58 (14.5)	1.09/1.07
□	103,000 (47 720)	9.1	60 (15.5)	1.20/1.19
△	101,600 (46 085)	8.7	61 (16)	1.30/1.28
◇	99,800 (45 269)	8.1	62 (16.5)	1.42/1.43
⌂	98,200 (44 543)	7.7	62 (16.5)	1.47/1.48
◇	96,600 (43 817)	7.4	62 (16.5)	1.61/1.60

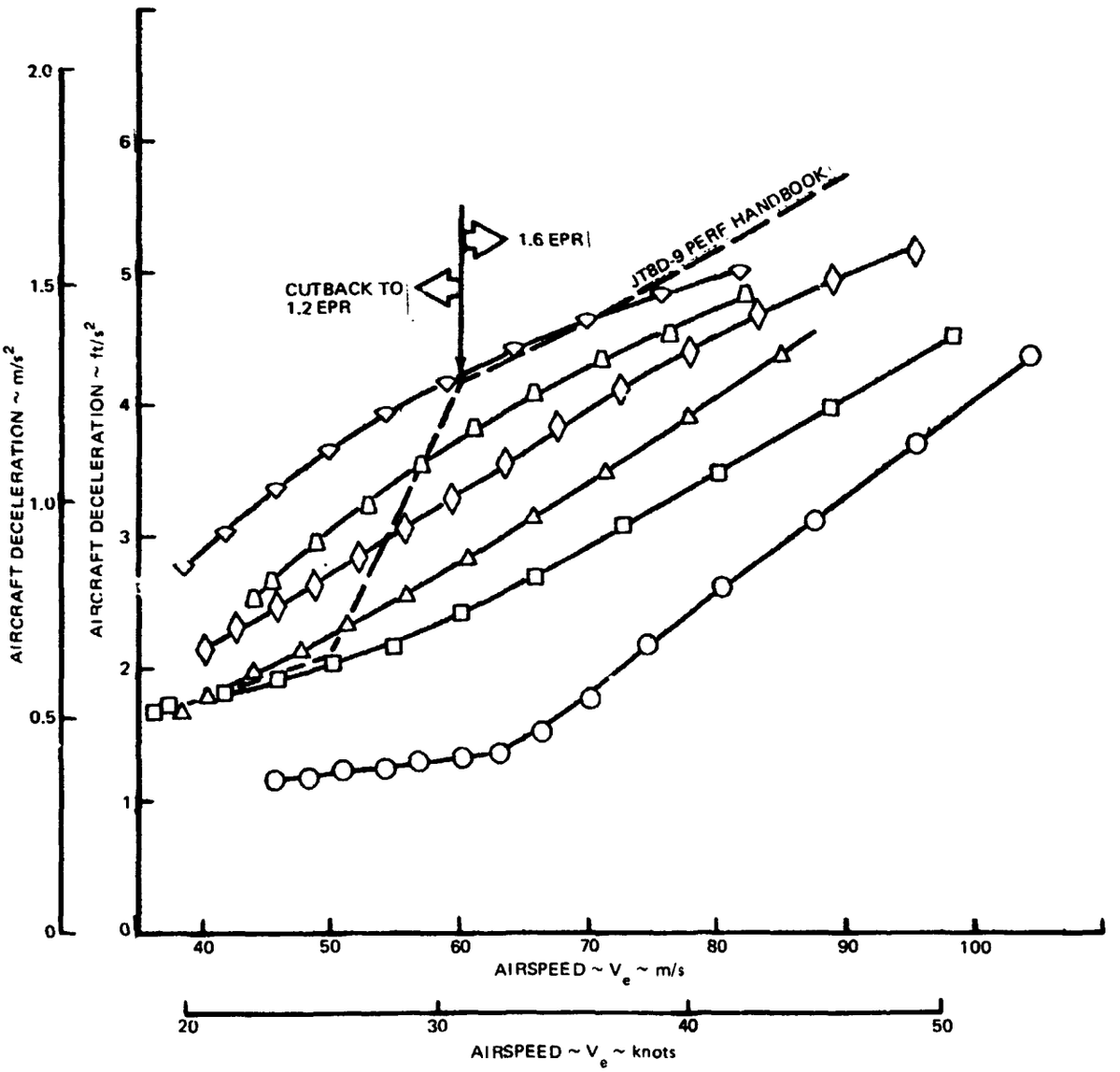

FIGURE 97. DC-9 REFAN THRUST REVERSER PERFORMANCE – W_S = 100,000 lb (45 359 kg) δ_{FLAPS} = 50 deg (0.873 rad) (LANDING), SPOILERS UP, BRAKES OFF – ZERO WIND

does not appear to experience instability down to speeds as low as 15.4 m/s (30 knots) suggests that the 31 m/s (60 knots) cutback speed of the production DC-9 fleet could be retained for the JT8D-109 engine installation.

The design of the JT8D-109 reverser was based on obtaining the same retarding force as the production DC-9-30/JT8D-9 (less reverser efficiency for the JT8D-109 due to its higher thrust rating). Figure 97 shows the performance handbook brakes-off deceleration capability of the DC-9-30 with JT8D-9 engines using the described operating procedure. To achieve the same deceleration capability an EPR = 1.6 is required with the JT8D-109 engine. This is a higher percentage of MCT thrust than for the JT8D-9 engine.

Empennage peak temperatures were recorded for normal thrust reverser landings and remained below the maximum allowable 121°C (250°F) for the aluminum skin. The instrumentation was located on the LH side of the airplane and was not affected by the APU exhaust. The fuselage skin in the pylon region is aluminum except for a titanium area surrounding the pylon and extending outward about .762 mm (3 in.). Unless noted, the temperature at the temp-plate locations was less than 66°C (150°F) (figure 95). The maximum temperature measured was 99°C (210°F) at temp-plate location No. 7 (aluminum skin).

The Refan reverser tests indicated that in order to achieve the same aircraft deceleration with the JT8D-109 engine reverse thrust as with the existing DC-9/JT8D handbook performance, an engine EPR of 1.6 is required. Normal reverse thrust operation was demonstrated at speeds below the operational cutback speed of 60 knots with acceptable engine operation; and the peak empennage temperatures remained below the maximum allowable 121°C (250°F) for the aluminum skin.

Ice Protection

Flight testing of the DC-9 Refan cowl ice protection system was conducted to obtain clear air cowl ice protection temperature and pressure data at stabilized and transient flight conditions and show that the system will provide safe flight in icing conditions.

The left engine cowl ice protection system was instrumented to provide measurements of cowl lip skin structure temperature and anti-icing air temperatures and pressures. The location of the cowl lip outer surface temperature instrumentation is shown in figure 98.

Data were recorded for transient flight conditions of takeoff, climb, descent, approach and landing. Data were also recorded at stabilized altitudes of about 9 144 m (30,000 ft) and 4 572 m (15,000 ft) at cruise airspeeds and about 1 524 m (5,000 ft) for a hold condition.

Evaluation of the flight test data as well as the cowl ice protection design analysis which preceded the flight test program employed the standard heat transfer analysis techniques used for ice protection system analysis. Comparisons of the measured and analytically derived surface temperatures show that the performance of the nose cowl anti-icing system will meet or exceed the performance level predicted by the analysis.

Plots of the anti-icing surface temperature profiles at various altitudes during climb, cruise, descent and approach are shown in figures 99, 100 and 101. The cowl lip outer surface thermocouple locations (figure 98) are also plotted on these figures.

The DC-9 Refan cowl lip geometry, the ice protection air supply system, and the ice protection heating requirements were based on the design configuration and heating requirements of the production DC-9 Series 30 cowl ice protection system which is certified by the FAA. The clear air flight evaluation of the Refan cowl ice protection system shows that the system provides ice protection performance which is equal to or in excess of predictions.

System design similarities with the FAA certified DC-9 system and the past demonstrated conservative nature of the analytical method show that the DC-9 Refan cowl ice protection system can be operated without restrictions and is suitable for unlimited dispatch into known icing conditions.

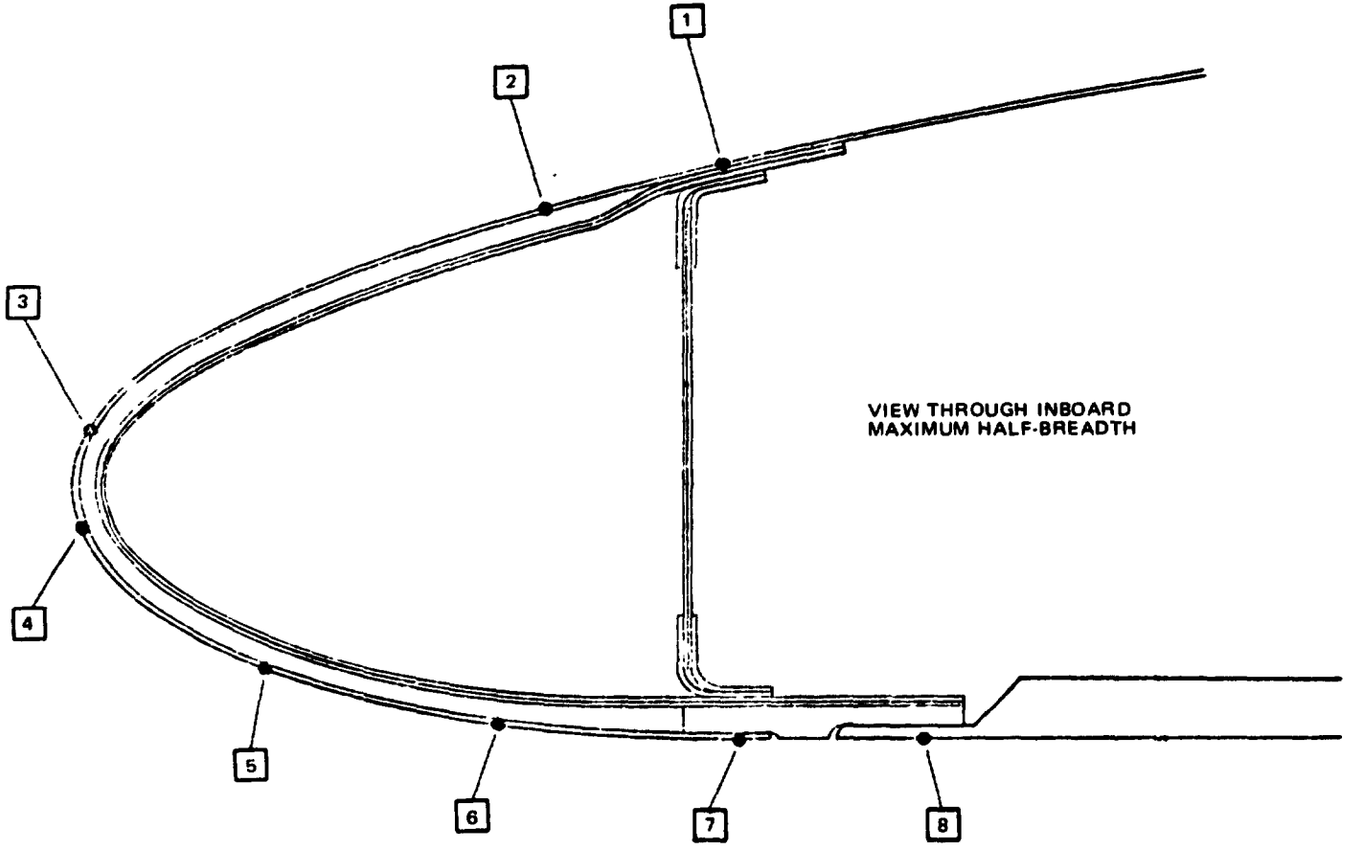

FIGURE 98. DC-9 REFAN COWL LIP OUTER SURFACE THERMOCOUPLE LOCATIONS

CONDITION	ALTITUDE ft	(m)	INDICATED AIRSPEED knots	(m/s)	RAT deg F	deg (C)
1	0	(0)	0	(0)	66	(19)
2	5,000	(1524)	252	(130)	59	(15)
3	10,000	(3048)	248	(128)	46	(8)
4	15,000	(4572)	317	(163)	47	(8)
5	25,000	(7620)	309	(159)	15	(−9)

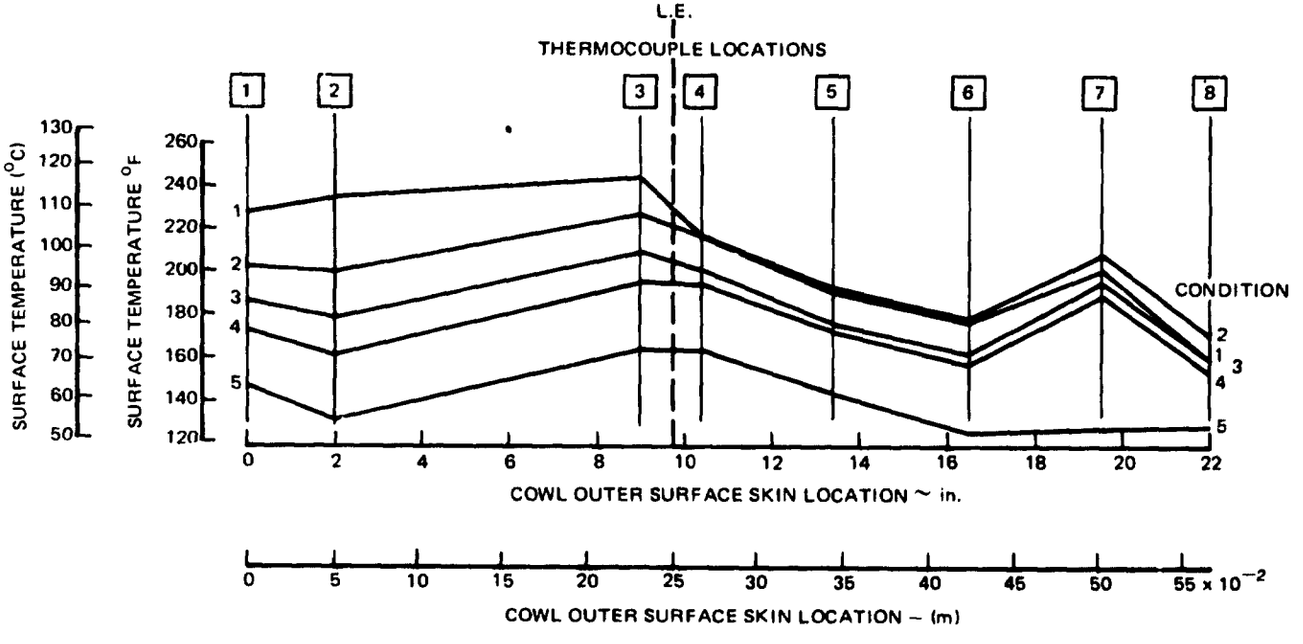

FIGURE 99. DC-9 REFAN COWL ANTI-ICING LIP OUTER SURFACE TEMPERATURE PROFILES DURING CLIMB.

CONDITION	ALTITUDE ft	(m)	INDICATED AIRSPEED knots	(m/s)	RAT deg F	deg (C)
1	5,500	(1676)	200	(103)	5.	(11)
2	15,000	(4572)	321	(165)	47	(8)
3	15,000	(4572)	255	(131)	36	(2)
4	30,000	(9144)	300	(154)	−6	(−21)

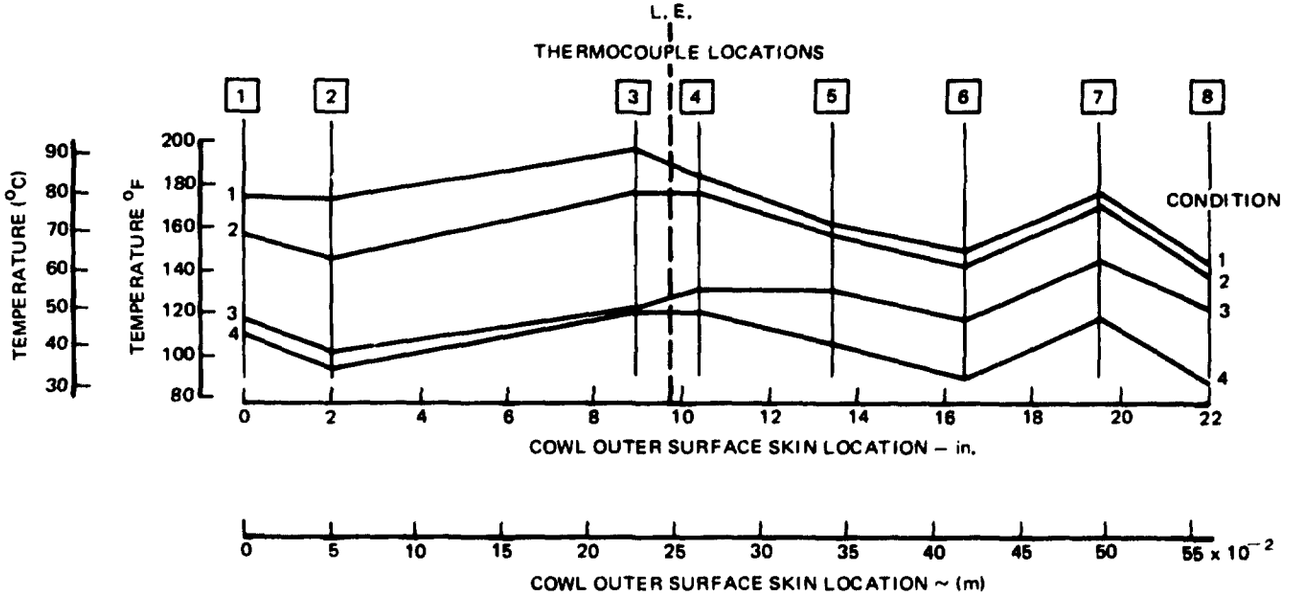

FIGURE 100. DC-9 REFAN COWL ANTI-ICING LIP OUTER SURFACE TEMPERATURE PROFILES DURING CRUISE

CONDITION	ALTITUDE ft	(m)	INDICATED AIRSPEED knots	(m/s)	RAT deg F	deg (C)
1	APPROACH		148	(76)	60	(16)
2	5,500	(1676)	260	(134)	55	(13)
3	15,000	(4572)	311	(160)	44	(7)

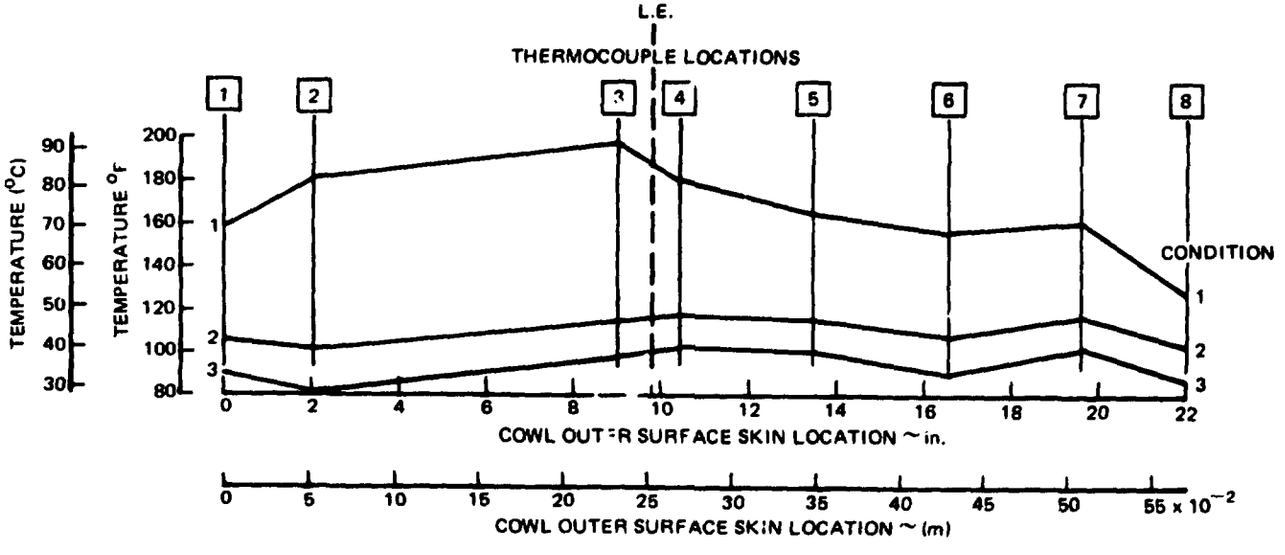

FIGURE 101. DC-9 REFAN COWL ANTI-ICING LIP OUTER SURFACE TEMPERATURE PROFILES DURING DESCENT AND APPROACH

Auxiliary Power Plant

This test was conducted to determine the effect of the redesigned APU exhaust deflector on the APU performance and starting characteristics (ground and inflight); and to evaluate the effectiveness of the deflector in preventing direct impingement of the APU exhaust on the larger and closer Refanned engine nacelle and thrust reverser surfaces during ground operation.

The APU is the same type production unit currently installed in production DC-9's. The APU exhaust was redesigned (louvered) and installed as shown in figures 102, 103, and 104.

Temp-plates were installed on the right hand nacelle and fuselage aluminum surfaces near the APU exhaust as shown in figures 105, 106 and 107. The temp-plates (used to measure APU exhaust impingement) were read and recorded at various surface winds for the ground starts and after each flight. The winds noted in table 20, were measured at the Yuma Control Tower approximately 2.41 km (1.5 mi.) from the Douglas facility.

Electric and windmill airstarts were conducted throughout the production DC-9 APU airstart envelope. Starting EGT and RPM limits were observed for ground and airstarts.

- Ground Starts

No unusual starting or operating characteristics were noted by flight development personnel.

- Inflight Starts

Electric and windmill airstarts with the modified exhaust were accomplished at the extremes of the certified airstart envelope for the production APU. This comparison is shown on figure 108 and the airstarts are tabulated in tat e 21. One unsuccessful electric start attempt occurred at 10 668 m (35,000 ft), 134 m/s (260 knots) after about 2-1/4 hours of cold soak (outside the APU airstart envelope), but a second attempt was successful.

Although there is some indication that windmill RPM's prior to starts are lower which might be expected from increased back pressure, the data indicate that the modified exhaust does not have a noticeably detrimental effect on airstarts. Start times and maximum EGT's are comparable to the production APU. Inflight performance was noted as being normal by flight development personnel.

- APU Exhaust Impingement

A summary of the results from the APU exhaust impingement tests are mapped on figures 106, 107 and 108 and tabulated in table 20. Considering the recorded surface temperatures and estimated APU exhaust temperatures 315°C-427°C (600°F to 800°F), it appears there was no direct impingement of the exhaust core flow on the JT8D-109 engine nacelle.

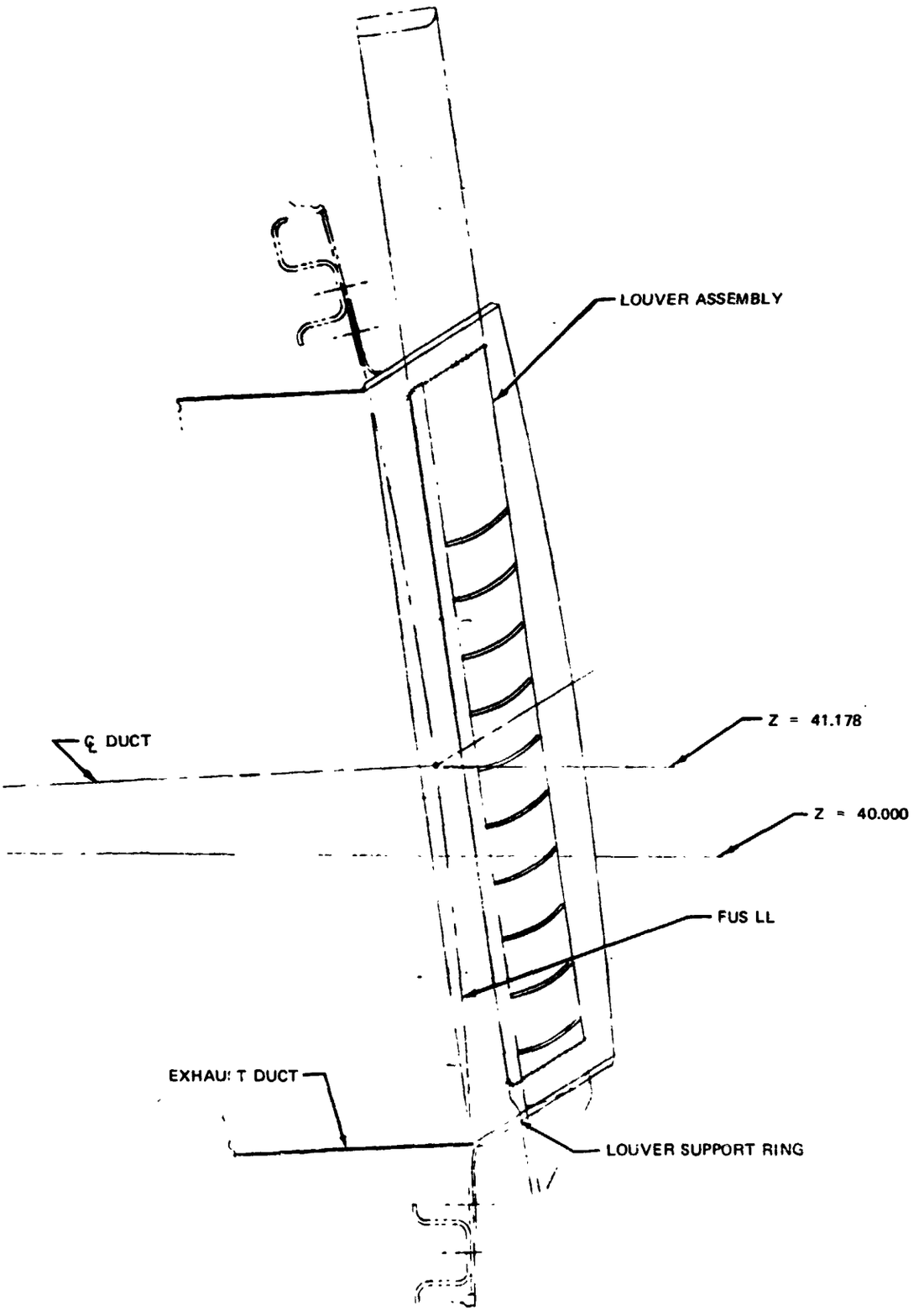

FIGURE 102. DC-9 REFAN – APU LOUVERED EXHAUST – VIEW LOOKING FORWARD, Y = 1069.00

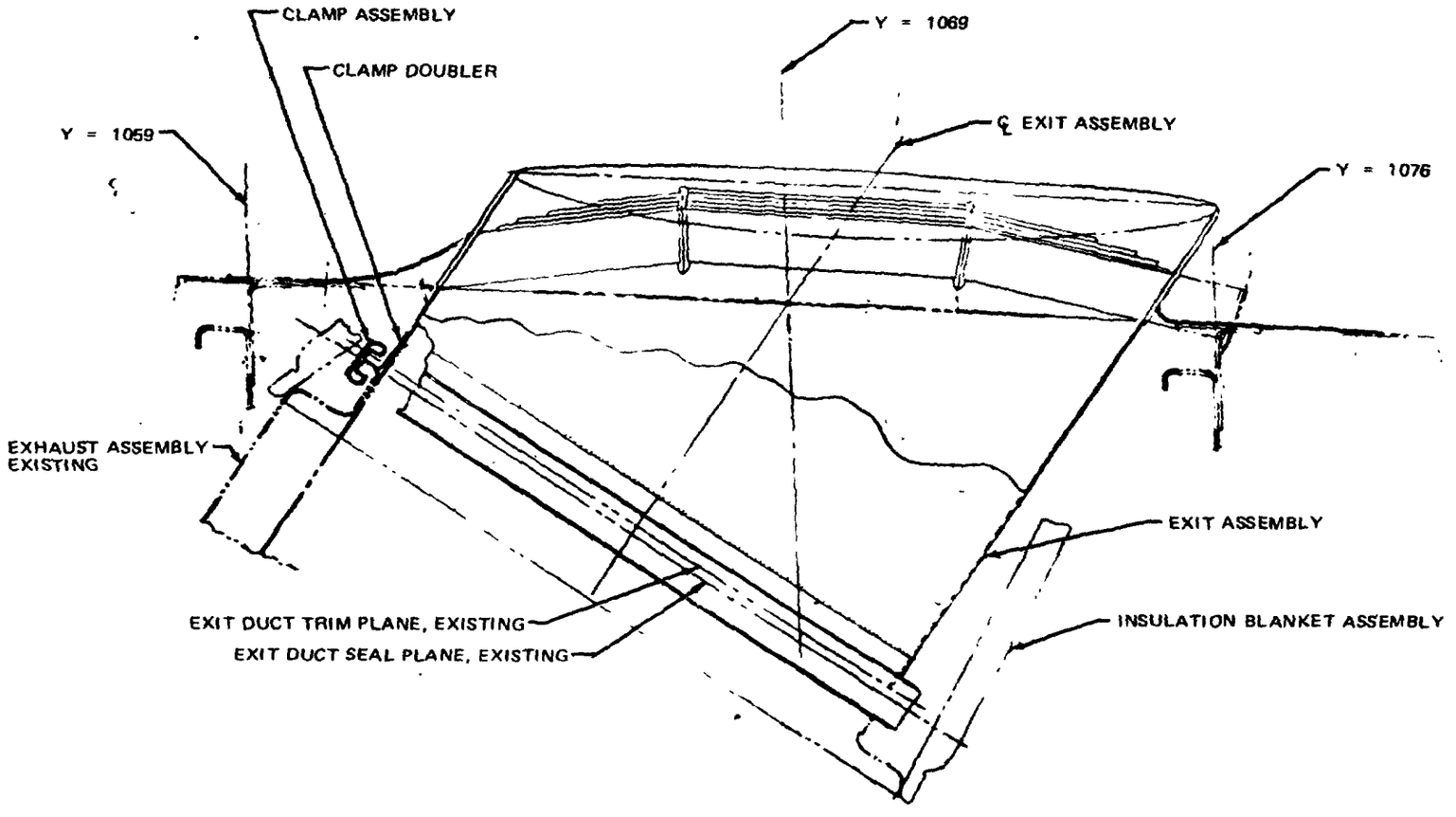

FIGURE 103. DC-9 REFAN – APU LOUVERED EXHAUST – PLAN VIEW

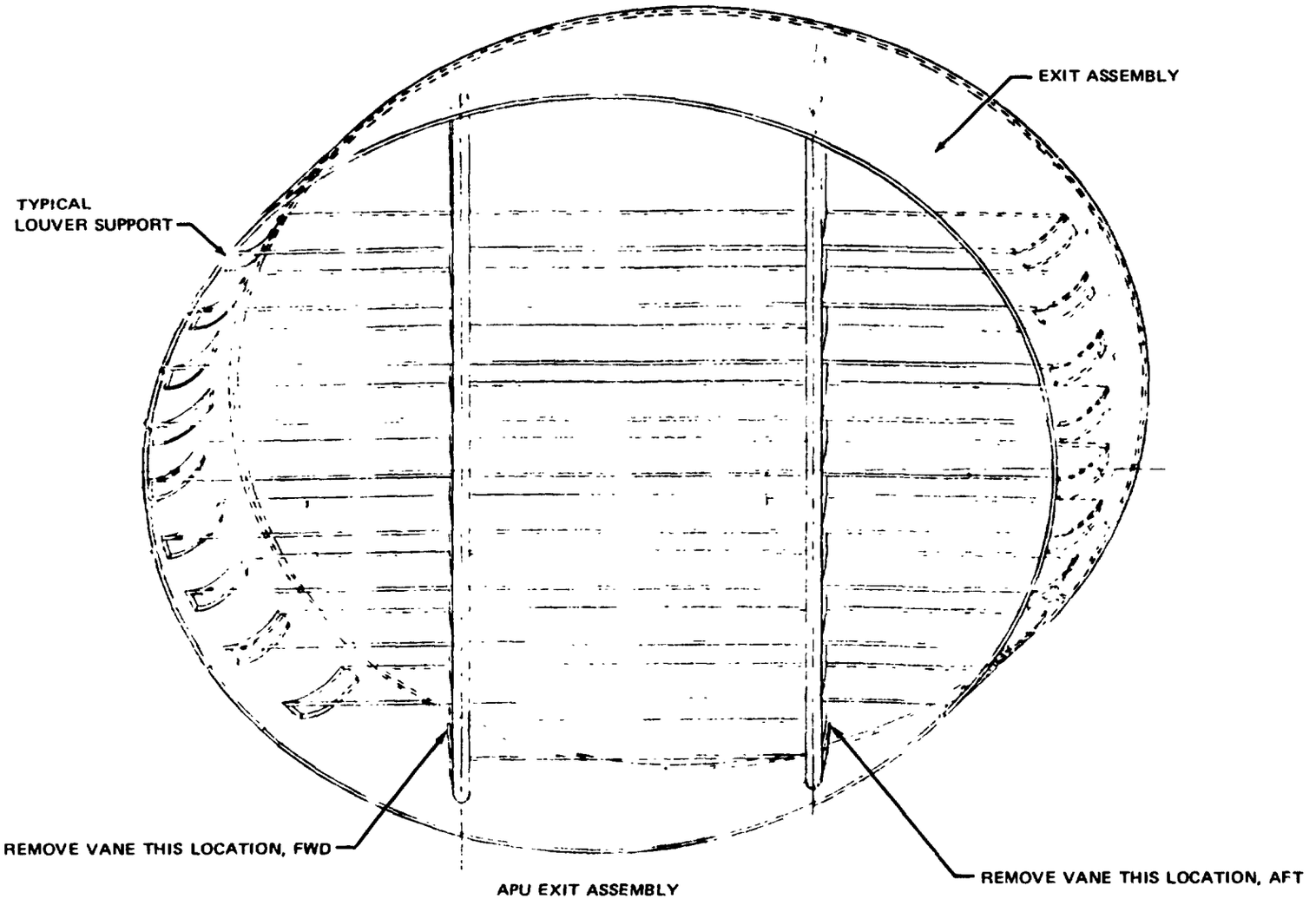

FIGURE 104. DC-9 REFAN – APU LOUVERED EXHAUST – VIEW LOOKING OUTBOARD

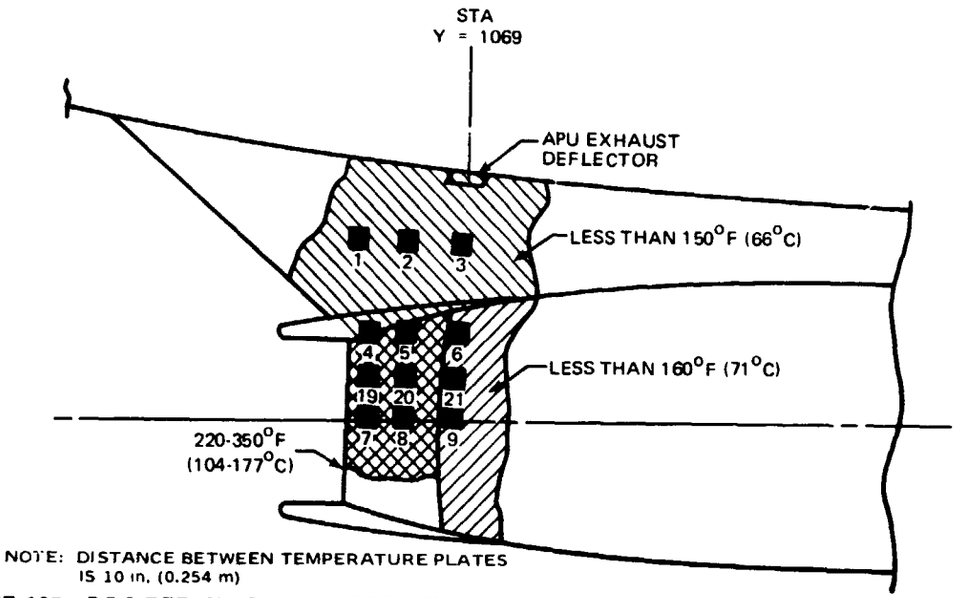

FIGURE 105. DC-9 REFAN APU LOUVERED EXHAUST EFFLUX PATTERN SUMMARY (NACELLE AND PYLON)

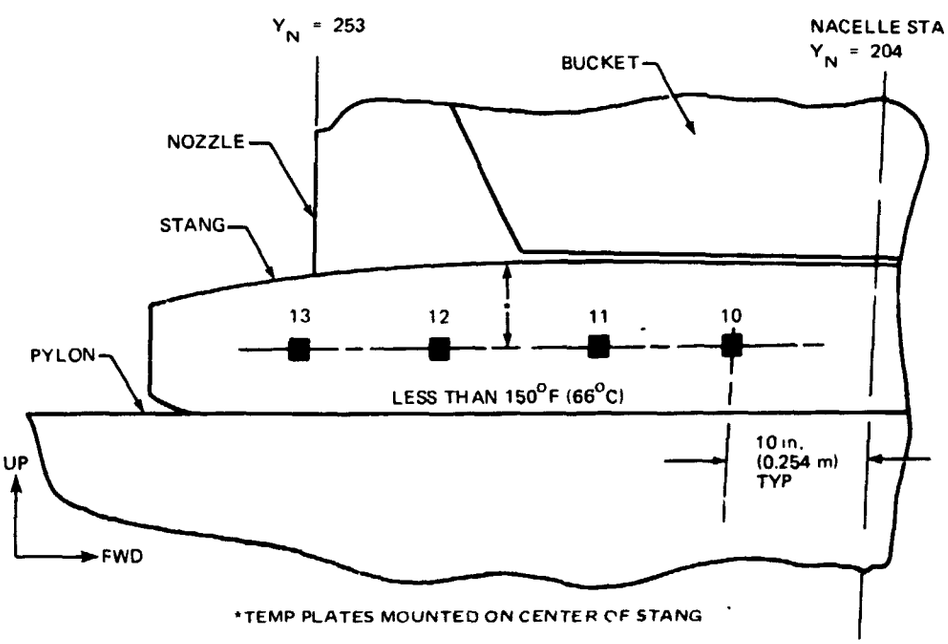

FIGURE 106. DC-9 REFAN APU LOUVERED EXHAUST EFFLUX PATTERN SUMMARY (STANG FAIRING)

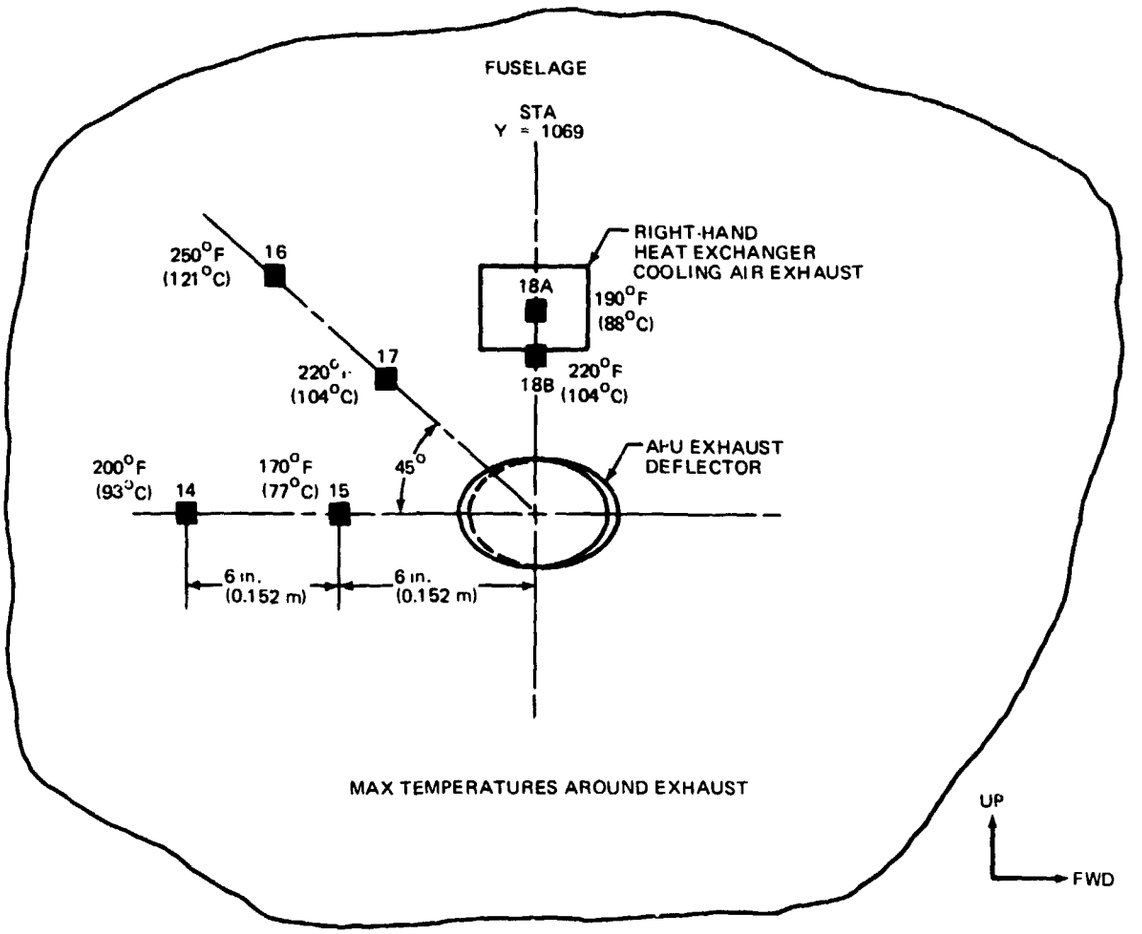

FIGURE 107. DC-9 REFAN APU LOUVERED EXHAUST EFFLUX PATTERN SUMMARY (FUSELAGE)

However, the top surface of the thrust reverser bucket was distinctly affected by its proximity to the exhaust efflux. The surface temperatures noted in figure 105 and table 20 appear similar to that of the production installation without the exhaust deflector.

None of the surface temperatures exceeded the established maximum allowable skin temperature of 177°C (350°F). The data indicates that under normal APU operating procedures and loading, the louvered exhaust helps direct the exhaust flow away from the larger and closer Refanned engine installation.

The redesigned APU exhaust deflector had no detrimental effect on ground starting or performance characteristics.

The airstart envelope was verified for this configuration with the exception of one unsuccessful start, which was outside the envelope.

Measured fuselage and nacelle skin temperatures resulting from APU exhaust impingement were acceptable for the non-load carrying aluminum skin locations.

TABLE 20

DC-9 REFAN APU EXHAUST IMPINGEMENT TEST
SUMMARY OF RECORDED SURFACE TEMPERATURES

FLIGHT NO.	6	7/8	9	10	11	12	14
WIND DIRECTION deg (rad)	030 (0.524)	–	350 (6.109)	50 (0.873)	40 (0.698)	140 (2.443)	NA
WIND VELOCITY knots(m/s)	5 (2.6)	0	12 (6.2)	5 (2.6)	4 (2.1)	10 (5.1)	NA
A/P HEADING deg (rad)	130 (2.269)	–	NA	NA	160 (2.793)	128 (2.234)	NA
APU CYCLES	1	2	1	1	1	1	1
REVERSER CYCLES	1	1	1	1	1	1	1
INFLIGHT START	–	–	–	–	–	–	2
TEMPTAB NO.	°F (°C)	°F (°C)	°F (°C)	°F (°C)	°F (°C)	°F (°C)	°F (°C)
1	•	•	•	•	•	•	•
2	•	•	•	•	•	•	•
3	•	•	•	•	•	•	•
4	210 (99)	350 (166)	220 (104)	220 (104)	220 (104)	220 (104)	220 (104)
5	220 (104)	220 (104)	220 (104)	220 (104)	220 (104)	220 (104)	220 (104)
6	•	•	•	•	•	150 (66)	150 (66)
7	300 (149)	300 (149)	300 (149)	300 (149)	300 (149)	300 (149)	300 (149)
8	220 (104)	220 (104)	200 (93)	220 (104)	220 (104)	220 (104)	220 (104)
9	•	•	•	•	•	•	•
10	•	•	•	•	•	•	•
11	•	•	•	•	•	•	•
12	•	•	•	•	•	•	•
13	•	•	•	•	•	•	•
14	160 (71)	160 (71)	160 (71)	160 (71)	180 (82)	200 (93)	200 (93)
15	150 (66)	150 (66)	150 (66)	150 (66)	160 (71)	170 (77)	170 (77)
16	•	•	•	•	250 (121)	250 (121)	250 (121)
17	180 (82)	180 (82)	180 (82)	180 (82)	220 (104)	220 (104)	220 (104)
18A	170 (77)	170 (77)	170 (77)	170 (77)	170 (77)	190 (88)	190 (88)
18B	180 (82)	180 (82)	180 (82)	180 (82)	220 (104)	220 (104)	220 (104)
19	250 (121)	350 (177)	220 (104)	220 (104)	220 (104)	250 (121)	250 (121)
20	300 (149)	300 (149)	300 (149)	300 (149)	300 (149)	300 (149)	300 (149)
21	160 (71)	160 (71)	160 (71)	160 (71)	160 (71)	160 (71)	160 (71)

*LESS THAN 150°F (66°C)

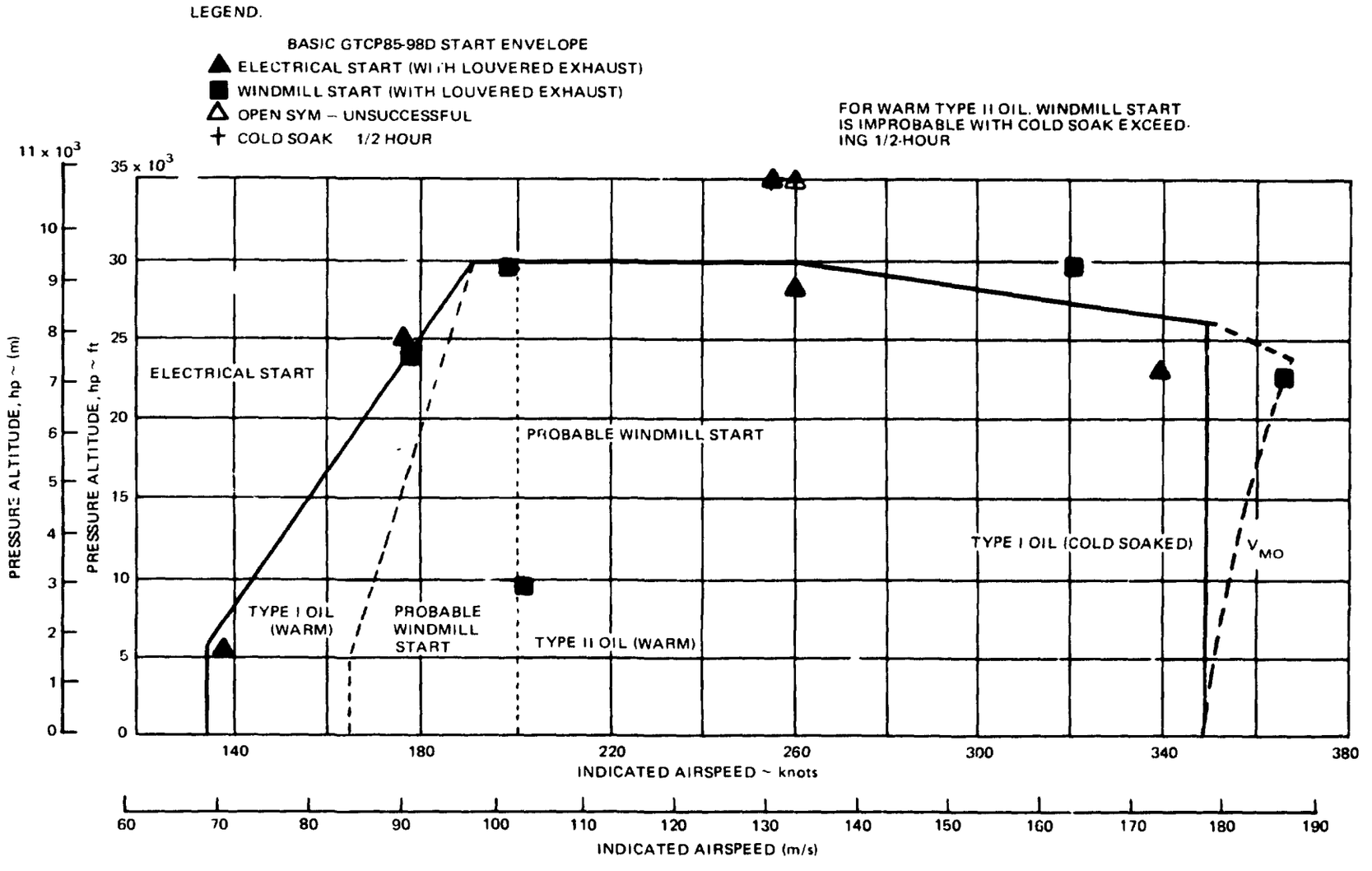

FIGURE 108. DC-9 REFAN APU AIR START ENVELOPE, AIRESEARCH MODEL GTCP85-98D (WITH LOUVERED EXHAUST)

TABLE 21

APU INFLIGHT STARTS – LOUVERED EXHAUST

FLT NO.	KIAS knots (m/s)	ALT ft (m)	MAX EGT °C	MAX RPM %	ELECTRIC/ WINDMILL	SUCCESSFUL/ UNSUCCESSFUL	COMMENTS
2	260 (134)	28,500 (8 687)	340	100.5	ELECTRIC	SUCCESSFUL	
3	175 (90)	25,000 (7 620)	380	100.0	ELECTRIC	SUCCESSFUL	
14	260 (134)	35,000 (10 668)	–	–	ELECTRIC	UNSUCCESSFUL	OUTSIDE ENVELOPE
14	255 (131)	35,000 (10 668)	–		ELECTRIC	SUCCESSFUL	
34	338 (174)	23,000 (7 010)	260	–	ELECTRIC	SUCCESSFUL	TO WARM OIL FOR W/M STARTS
34	366 (188)	23,000 (7 010)	420	101.5	WINDMILL	SUCCESSFUL	STABLE AT 8% W/M RPM PRIOR TO START
34	197 (101)	29,890 (9 110)	510	101.5	WINDMILL	SUCCESSFUL	STABLE AT 0.5% W/M RPM PRIOR TO START
34	321 (165)	29,600 (9 022)	385	101.5	WINDMILL	SUCCESSFUL	STABLE AT 1.8% RPM IN SLIGHT DESCENT
34	202 (104)	9,760 (2 975)	435	101.0	WINDMILL	SUCCESSFUL	0.8% RPM PRIOR TO START
34	138 (71)	5,400 (1 646)	360	100.9	ELECTRIC	SUCCESSFUL	

AIRPLANE STRUCTURAL INTEGRITY AND DYNAMICS

Structural and dynamic analyses were performed during Phase II of the Refan Program to substantiate three basic requirements: (1) The new nacelle and thrust reverser hardware and the modifications to the airplane structure were required to be flightworthy and certifiable to the Federal Aviation Regulations; (2) The DC-9 with JT8D-109 engine installed would meet or exceed required flutter speed margins; (3) The airplane in the Refan flight test configuration would qualify for an experimental flight test permit to be issued by the FAA.

In addition to the analyses performed in Phase II, ground tests were conducted prior to the flight test for verification of certain analytical predictions. These tests included an airplane ground vibration test (GVT), thrust reverser cycling to maximum reverse power, cabin pressurization and engine runup to takeoff power. Strain gauges and accelerometers were installed on primary structural components to monitor load levels, deflections and accelerations during the ground tests and subsequent flight tests.

The GVT results verified that the airplane normal modes of vibration were not significantly changed due to the Refan modifications. Likewise, the damping characteristics compared well with those of the basic production airplane.

Evaluation of the data from the ground and flight tests was accomplished to the extent that significant parameters were compared with analytical results. All pertinent data which were collected during the tests have been filed for future reference in the event a production program is initiated. The primary objective will be to use the test data to optimize the structural weight of the Refan hardware. Except for potential weight savings, the test results indicate that the structural configuration of the Refan hardware is satisfactory for use as a production retrofit of DC-9 airplane.

Structural and aerodynamic damping flight tests were conducted to substantiate the flutter integrity of the Refan airplane and to obtain frequency and damping response data to show correlation with analytical results. The test data shows that the DC-9-31 with JT8D-109 engines exhibit the same or slightly improved damping characteristics compared to the production airplane. Likewise, there were no instabilities or excessive vibration within the demonstrated flight envelope.

Structural Analysis

During Phase I of the Refan Program, preliminary structural analyses were performed to determine the structural feasibility of retrofitting DC-9 airplanes with refanned JT8D engines (ref. 1). In Phase II the structural modifications which were identified in Phase I were finalized and designed for incorporation into the flight demonstration airplane. Design criteria and structural analyses were documented during Phase II in sufficient detail to meet the program objectives. Maximum advantage was taken of the similarities between the structural arrangements of the Refan and production airplane configurations. Likewise, selection of materials and material heat treats for the Refan hardware was limited to those of proven quality and reliability. This policy was intended to minimize any risk associated with a potential high rate of production of retrofit kits for the DC-9 fleet.

Design criteria were established for the Refan modifications which meet or exceed the production certification basis. The DC-9 was certified to the requirements of CAR 4b dated December 31, 1953, amendments 4b-1 through 4b-15. To provide structural commonality of the retrofit hardware for all DC-9 airplane models, the JT8D-117 engine was selected as the basis for the structural analyses since it produced the most critical loadings. Details of the analysis engine weight, c.g. and forward and reverse thrust are given in table 22.

TABLE 22

DC-9 REFAN ENGINE WEIGHT AND THRUST FOR STRENGTH ANALYSIS

ANALYSIS WEIGHT AND c.b.	WEIGHT		Y (c.g.)	
	lb	(kg)	in	(m)
JT8D-17 (BASIC DEMOUNTABLE ENGINE PLUS NACELLE)	4,699	(2 133)	989	(25.12)
WEIGHT INCREMENT FOR REFAN	570	(259)	942	(23.93)
WEIGHT INCREMENT FOR ACOUSTICALLY TREATED NACELLE	655	(297)	1,000	(25.40)
JT8D-117 ENGINE AND NACELLE	5,924	(2 689)	990	(25.15)
5% FOR CONTINGENCIES	296	(134)	990	(25.15)
JT8D-117 ANALYSIS WEIGHT AND c.g.	6,220	(2 823)	990	(25.15)

ANALYSIS FORWARD AND REVERSE THRUST

JT8D-117 NET INSTALLED FORWARD THRUST F_T = 17,500 lb (77.84 kN)

REVERSE THRUST PER ENGINE.

$F_R = \xi F_T + D_{RAM} + D_{BASE} + P_{REV} dA_{FR} + D_{NAC}$

ξ = 0.4 (ASSUMED EFFICIENCY FOR DESIGN)

D_{RAM} = 4,470 lb (19.88 kN), RAM DRAG AT 175 KEAS (89.95 m/s)

D_{BASE} = 2,751 (12.24 kN), BASE DRAG AT 175 KEAS (89.95 m/s)

$P_{REV} dA_{FR}$ = −460 lb (−2.05 kN), INDUCED PRESSURE FORCE

D_{NAC} = 104 lb (462 N), NACELLE DRAG AT 175 KEAS (89.95 m/s)

F_R = 13,865 lb (61.67 kN)

New hardware required to accommodate the JT8D-109 engine included the engine nacelle, thrust reverser and pylon. In addition, structural modifications to the fuselage structure which supports the pylon and the lower centerline keel were required due to the increased loads of the JT8D-109 engine. Design details of the Refan hardware are presented in reference 3.

Pylon/Fuselage. - The pylon attachment to the fuselage transmits engine and nacelle inertia, thrust and aerodynamic loads. The structural configuration includes several redundant load paths. For this reason, an internal loads analysis employing a finite element model was performed to give load distributions for the strength analyses.

An existing DC-9 airplane finite element analysis model was modified to include the structural configuration and geometry of the Refan pylon. The model which includes the pylon, fuselage, vertical stabilizer and wing stubs is shown in figure 109.

The idealization details of the pylon/fuselage interface in the analysis model are shown in an enlargement of that area in figure 110. The model includes a simple representation of the engine since the engine mount system is also redundant. Engine bending and torsional stiffnesses were provided by Pratt and Whitney Aircraft. The loads were applied to the analysis model at the centerline of the engine as shown in figure 110. The external load conditions which were analyzed are given in table 23. To expedite the design, an envelope of arbitrary load conditions was selected for the internal loads analysis. Subsequently an investigation of airplane flight and landing conditions was made to verify that the arbitrary conditions were in fact representative of the actual critical loads. Table 23 gives the comparison of the arbitrary and airplane conditions.

Strain gauges were installed on the pylon for the ground and flight tests to monitor data for comparison with analytical predictions. A summary of analytical and strain gauge shear stresses for two loading conditions is given in table 24. Generally the results show good correlation, however, the lower surface of the pylon appears to have substantially reduced shear stresses based on the test data. The internal loads analysis conservatively assumed that the majority of the lower surface shear would be reacted in the forward section of the lower pylon since the aft section contains a series of access door cutouts. The framing around the access doors has shear carrying capability and as shown by the test results, relieves the forward section shear stresses.

A major design consideration regarding the pylon/fuselage interface was the amount of relative deflection which could be permitted between the pylon and the side of fuselage in the area of the fuselage pressure bulkhead. Figure 111 shows the analytical deflections for the static takeoff thrust load condition including the effects of fuselage pressurization and engine 1.0 g inertia. The pylon attachment to the fuselage between the frames at Y = 980 and Y = 1019 was designed as a flexible joint which transmits shear only to the fuselage skin. This arrangement was required to avoid lateral loading of the pressure bulkhead under engine loading conditions. As shown in figure 111, the resulting relative deflection between the pylon and fuselage as calculated by the internal loads analysis is approximately 2.8 mm (0.11 in). The flexible joint concept, to be practical and also exhibit adequate fatigue life, required

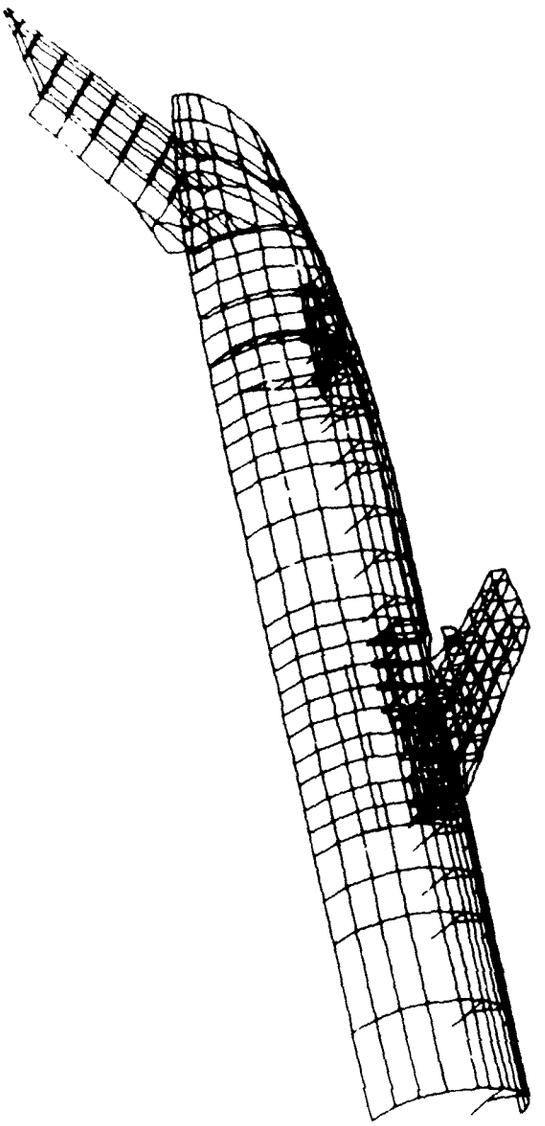

FIGURE 109. DC-9 REFAN FINITE ELEMENT ANALYSIS MODEL

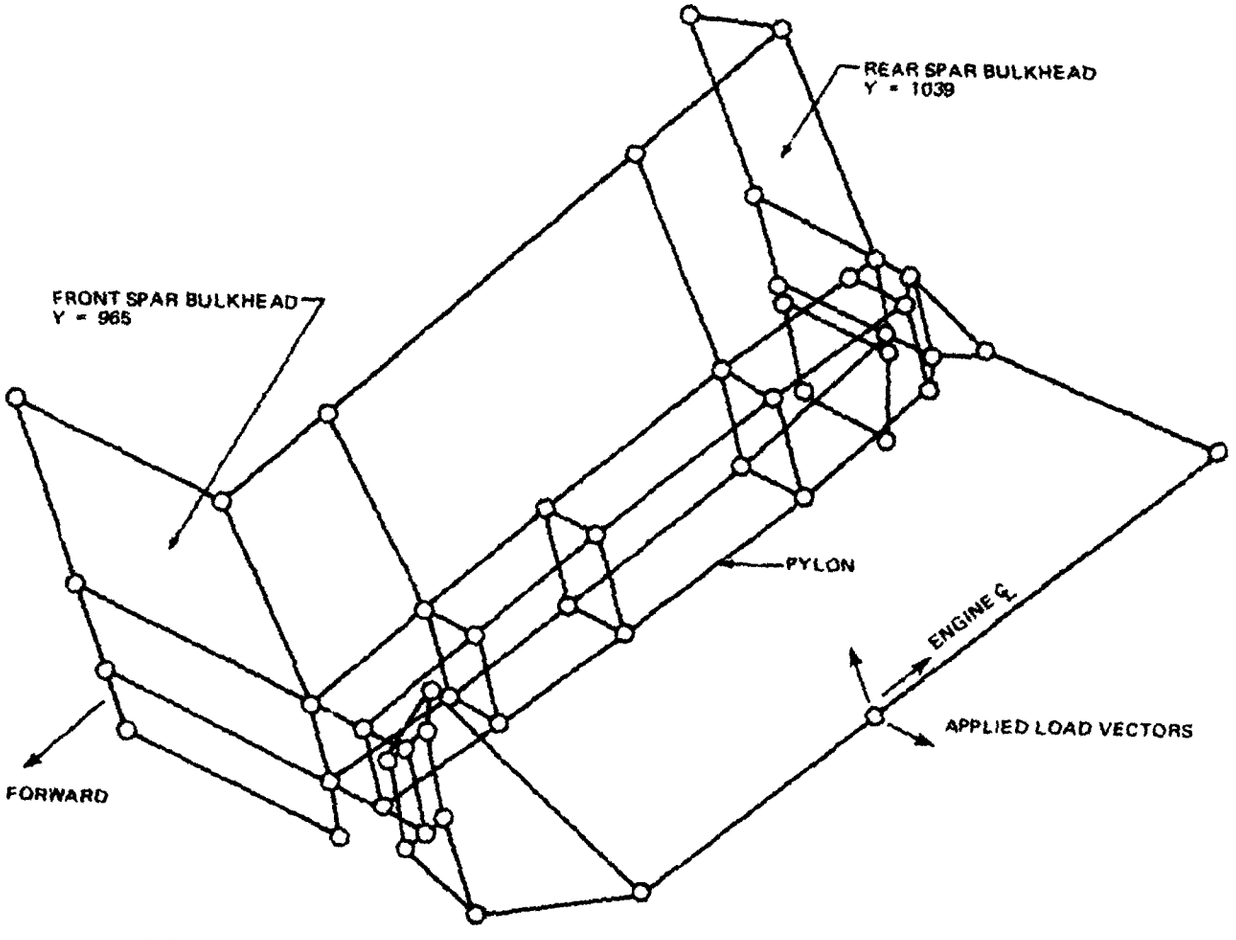

FIGURE 110. DC-9 REFAN ENGINE/PYLON FINITE ELEMENT ANALYSIS MODEL

TABLE 23

DC-9 REFAN ENGINE MOUNT/PYLON DESIGN CONDITIONS

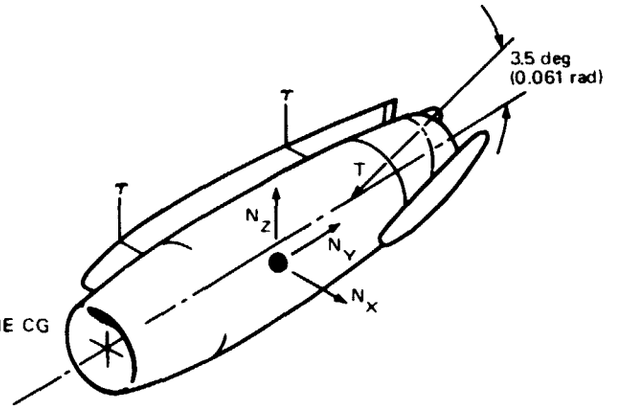

N_X, N_Y, N_Z – ACCELERATION LOAD FACTORS AT ENGINE CG

T – ENGINE THRUST

CONDITION DESCRIPTION	ARBITRARY CONDITIONS					AIRPLANE CONDITIONS				
				T					T	
	N_X	N_Y	N_Z	lb	(N)	N_X	N_Y	N_Z	lb	(N)
VERTICAL GUST	−0.66	–	5.33	17,500	(77 840)	–	−0.04	4.1	11,300	(50 262)
VERTICAL GUST	−0.66	–	−3.33	17,500	(77 840)	–	−0.04	−2.1	11,300	(50 262)
LATERAL GUST	−3.33	–	–	–	–	−0.88	−0.08	1.0	11,300	(50 262)
LATERAL GUST	3.33	–	–	–	–	0 88	−0.08	1.0	11,300	(50 262)
DYNAMIC LANDING	−1.0	–	4.0	−16,000	(−71 168)	–	0.24	3 9	−14,300	(−63 606)
DYNAMIC LANDING	1.0	–	4.0	−16,000	(−71 168)	–	0.8	3.29	−14,300	(−63 606)
DYNAMIC LANDING	−1 0	–	−2.0	−16,000	(−71 168)		0.24	−1.9	−14,300	(−63 606)
CRASH (ULTIMATE)	–	12.0	6.0	–	–	–	12 0	6.0	–	–

TABLE 24

DC-9 REFAN PYLON SHEAR STRESS

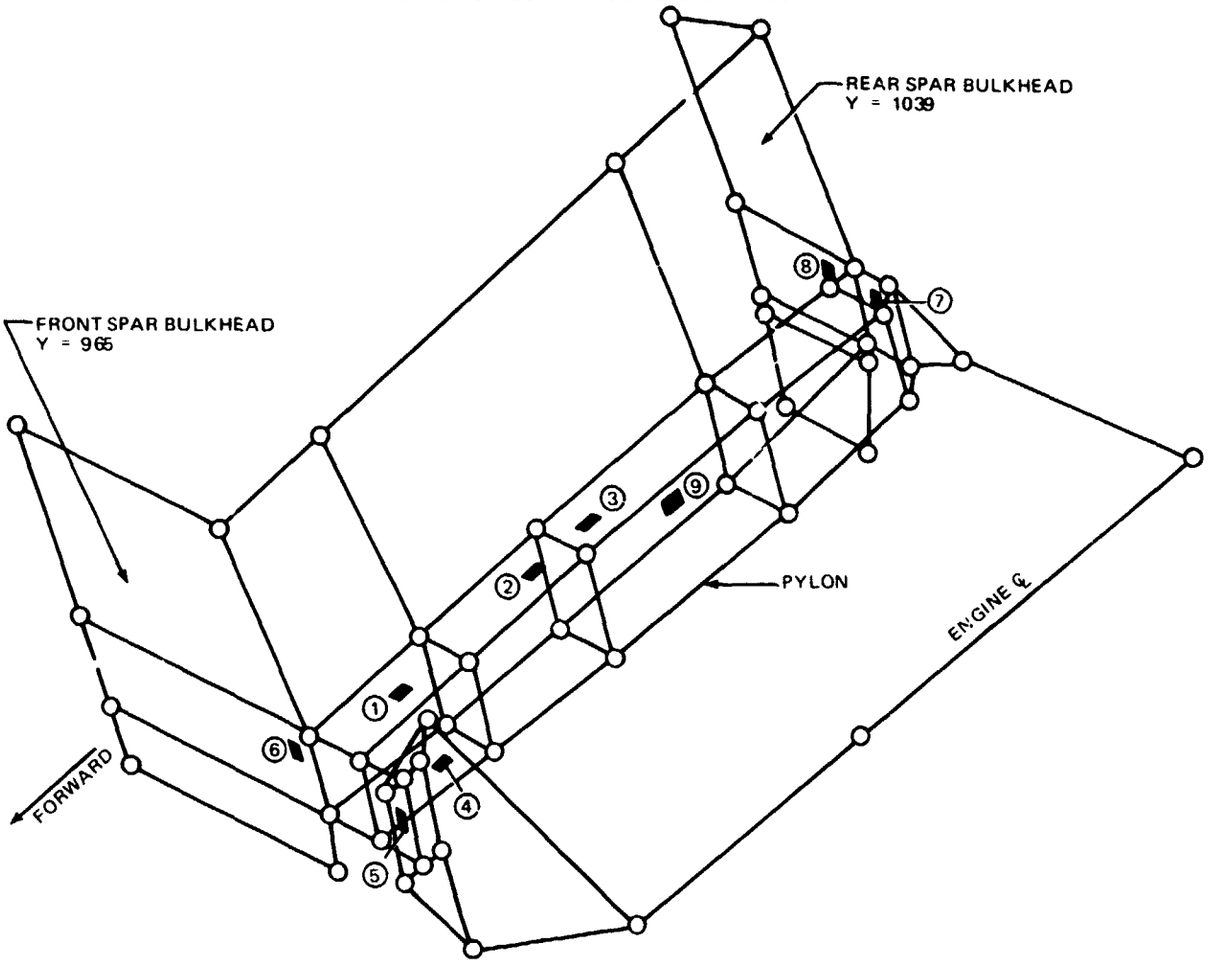

	CONDITION: ENGINE INSTALLATION WEIGHT = 4750 lb (2155 kg)				CONDITION: STATIC TAKEOFF THRUST NET THRUST, F_N = 16,266 lb (72 351 N)			
PYLON LOCATION (SEE DIAGRAM)	SHEAR STRESS				SHEAR STRESS			
	ANALYTICAL		TEST		ANALYTICAL		TEST	
	psi	(k Pa)	psi	(k Pa)	psi	(k Pa)	psi	(k Pa)
BOX UPPER SURFACE								
① Y = 973.5	1160	(7 998)	1070	(7 377)	4500	(31 026)	5220	(35 991)
② Y = 996	254	(1 75[illegible])	380	(2 620)	4650	(32 061)	5040	(34 750)
③ Y = 998.5	390	(2 689)	950	(6 550)	8060	(55 572)	6130	(42 265)
BOX LOWER SURFACE								
④ Y = 973.3	900	(6 205)	550	(3 792)	6280	(43 299)	2030	(13 996)
FRONT SPAR								
⑤ SHEAR FITTING	6440	(44 402)	6750	(46 540)	0	(0)	820	(5 654)
⑥ FUSELAGE FRAME	3690	(25 442)	4330	(29 854)	210	(1 448)	280	(1 931)
REAR SPAR								
⑦ SPAR WEB	2380	(16 410)	2450	(16 892)	1080	(7 446)	1550	(10 687)
⑧ FUSELAGE FRAME	970	(6 688)	1060	(7 308)	430	(2 965)	420	(2 896)
CLOSING RIB								
⑨ Y = 1009	1440	(9 928)	1070	(7 377)	3440	(23 718)		

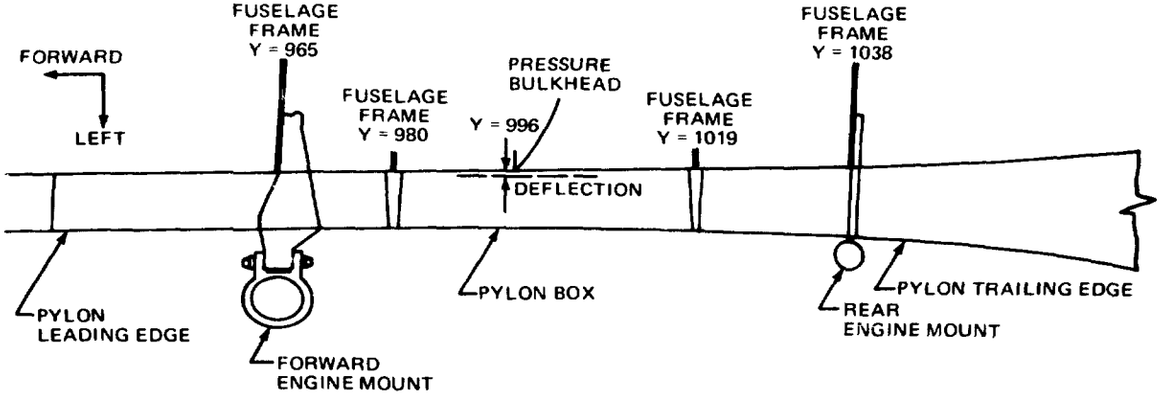

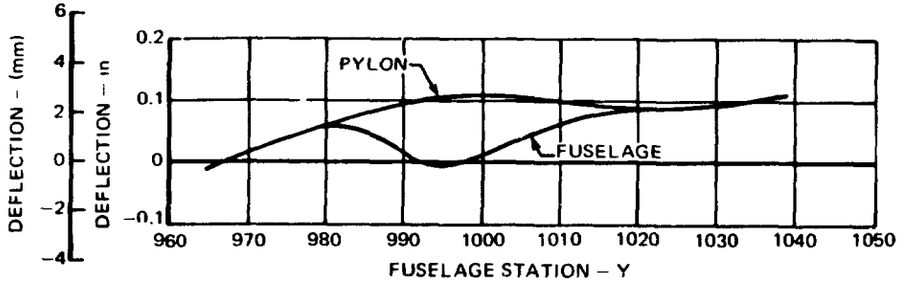

FIGURE 111. DC-9 REFAN FUSELAGE TO PYLON ANALYTICAL DEFLECTION STATIC TAKEOFF THRUST PLUS PRESSURIZED FUSELAGE

a relative deflection in the order of 1.5 mm (0.06 in). Previous experience with the fuselage shell analysis model indicated that for the magnitude of the analytical deflections, smaller test deflections could be expected. Therefore, instrumentation was placed at the flexible joint on the Refan airplane at Station Y = 996 to monitor the actual deflections during the test program. Figures 112, 113, and 114 show the test deflections for net thrust, engine inertia and cabin pressurization respectively. Utilizing these data table 25 gives total deflections based on the test results for the two critical fatigue conditions: (1) cruise thrust, 2.0 g engine inertia due to a vertical gust and cabin pressurization; (2) takeoff thrust and 1.0 g engine inertia. These results indicate that the flexible joint design based on a 1.5 mm (0.06 in) deflection criteria for fatigue, should be structurally adequate.

TABLE 25

DC-9 REFAN FUSELAGE TO PYLON DEFLECTIONS FOR FATIGUE

Fatigue Condition Description	Pylon to Fuselage Relative Deflection		Reference Figure No.
	in.	(mm)	
(1) 5000 lb (22 240 N) Cruise Thrust	0.0115	(0.292)	112
2.0 g Engine Inertia	0.0283	(0.719)	113
7.46 psi (51.43 kPa) Differential Cabin Pressure	0.0275	(0.698)	114
TOTAL	0.0673	(1.709)	
(2) 16000 lb (72 351 N) Takeoff	0.0368	(0.935)	112
1.0 g Engine Inertia	0.0141	(0.358)	113
TOTAL	0.0509	(1.293)	

The effect of the JT8D-109 engines on the aft fuselage critical vertical bending condition for flight is shown in figure 115. Although the heavier refanned engines produce an increase in the bending moments along the aft fuselage, the increased moments do not exceed the original production design bending moments. Revised production bending moments shown in figure 115 represent a subsequent refinement of the production DC-9 external loads analysis. Those refined analysis methods formed the basis for the calculation of Refan fuselage loads.

Fuselage loads for the critical DC-9 landing conditions with JT8D-109 engines installed exceeded the strength capability of the fuselage lower centerline keel in the area of the main landing gear wheel well. An add-on modification to the existing keel structure was designed to accommodate the higher loads. Figure 116 shows the effect the structural modifications had on the fuselage stress levels at Station Y = 737 which is a section through the wheel well area aft of the wing rear spar.

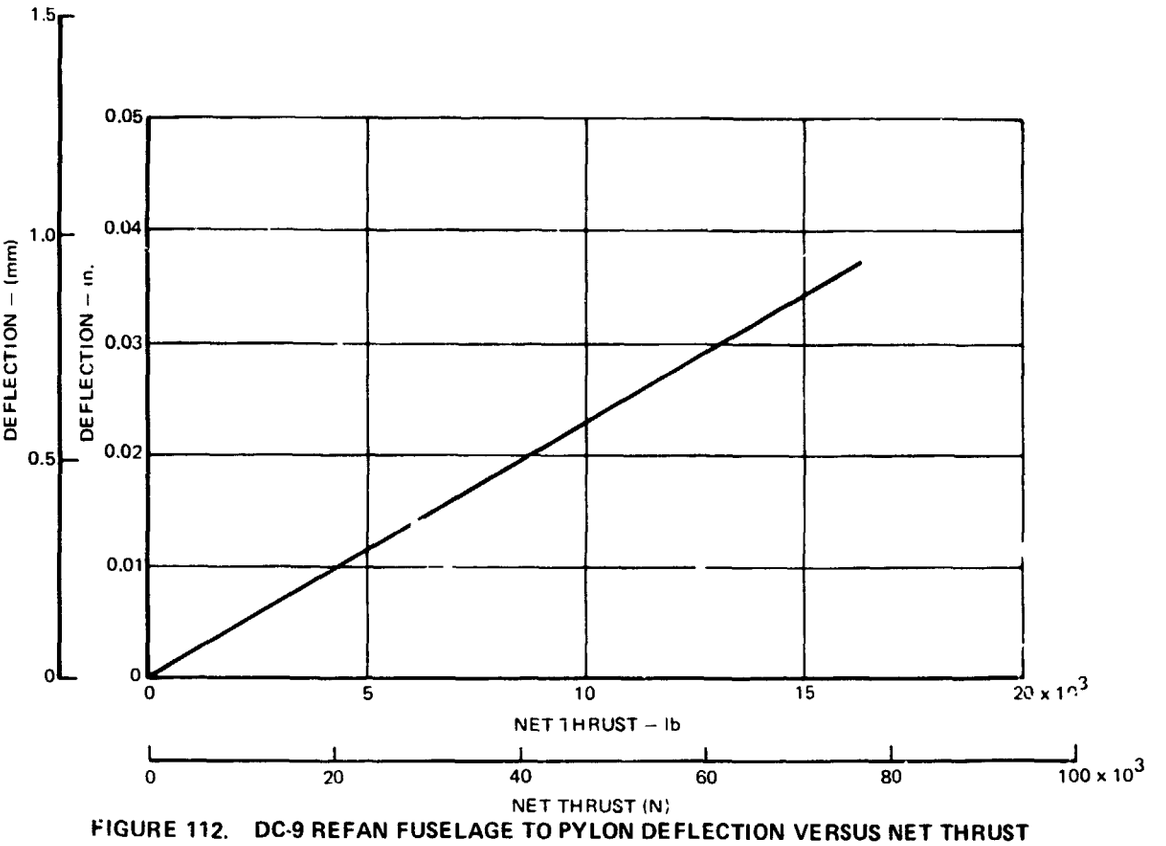

FIGURE 112. DC-9 REFAN FUSELAGE TO PYLON DEFLECTION VERSUS NET THRUST

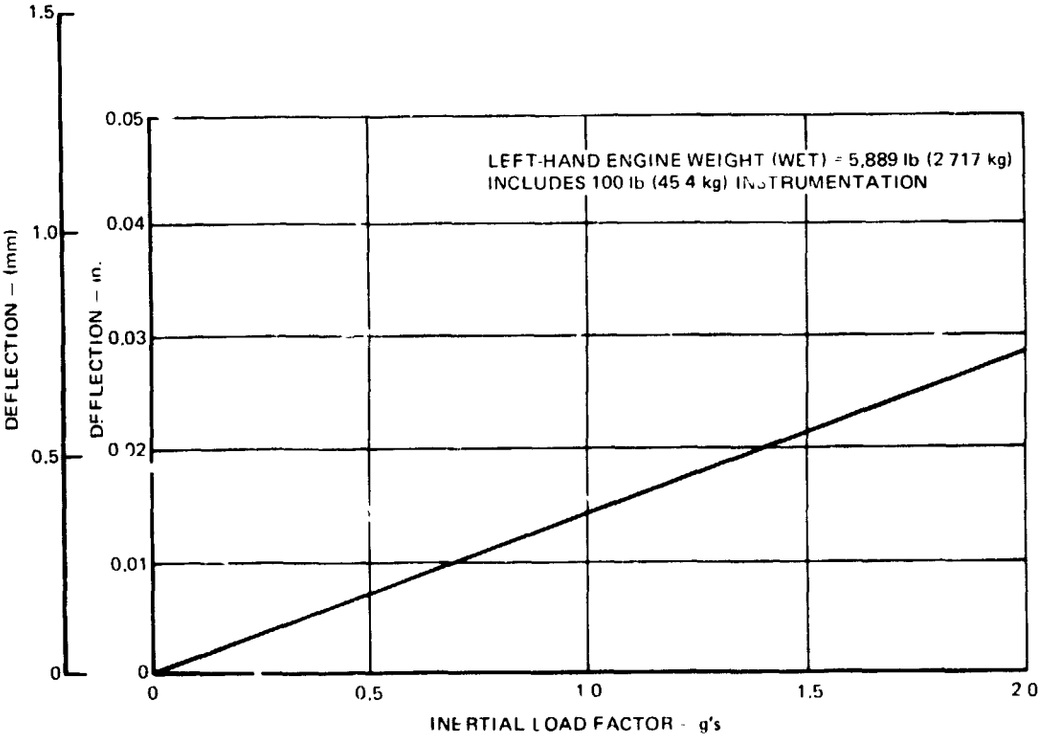

FIGURE 113. DC-9 REFAN FUSELAGE TO PYLON DEFLECTION VERSUS ENGINE INERTIA

FIGURE 114. DC-9 REFAN FUSELAGE TO PYLON DEFLECTION VERSUS CABIN PRESSURE

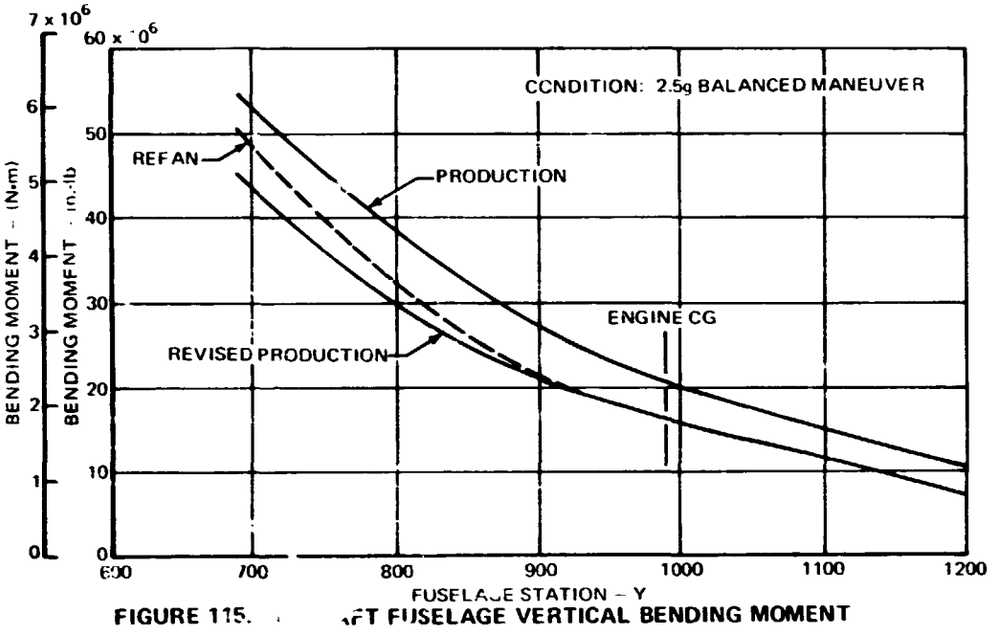

FIGURE 115. AFT FUSELAGE VERTICAL BENDING MOMENT

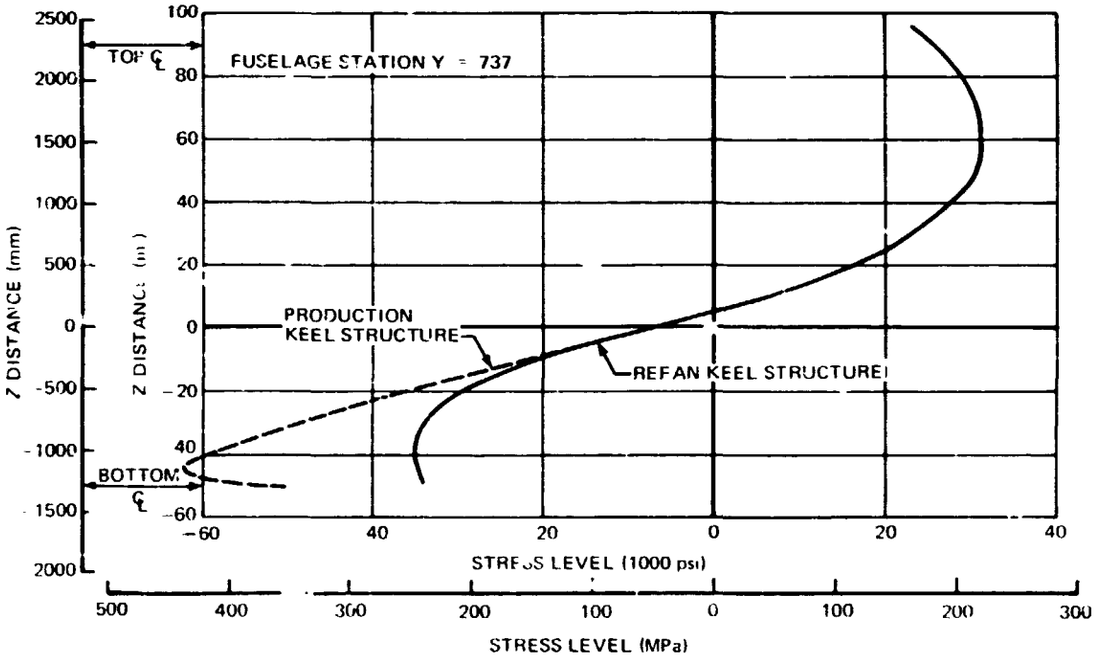

FIGURE 116. DC-9 FUSELAGE BENDING STRESS COMPARISON

Nacelle. - The nacelle components (nose cowl, inlet bullet, access doors, pylon apron and exhaust duct aerodynamic fairings) were designed to a loading envelope which included the following conditions:

1. Combined airplane pitching and dynamic pressure ($\pm$ q), yawing and dynamic pressure ($\pm$ q) and maximum dynamic pressure (q) for windmilling and maximum continuous thrust.

2. Maximum takeoff thrust at sea level.

3. Rejected takeoff at sea level.

4. High altitude corners of the flight envelope.

In addition, loads resulting from a pneumatic duct failure causing high nacelle internal pressures was considered. The access doors and their supporting structure were also designed to withstand a 33.4 m/sec (65 knots) ground gust while in the open position. Table 26 gives a summary of the loading conditions and the differential pressures for the access doors and the pylon apron. The loads imposed on the pylon apron by the access door for the ground gust condition and the pneumatic duct failure condition are shown in figure 117.

TABLE 26

DC-9 REFAN ACCESS DOORS AND PYLON APRON LOAD CONDITIONS

CONDITION DESCRIPTION	AIRPLANE VELOCITY (EQUIVALENT) knots (m/s)	DYNAMIC PRESSURE psf (kPa)	AIRPLANE ANGLE OF ATTACK deg (rad)	AIRPLANE YAW ANGLE deg (rad)	LIMIT DIFFERENTIAL PRESSURE psi (kPa)
MAXIMUM q	425 (218.6)	610 (29.2)	0	0	2.88 (19.86) BURST
MAXIMUM αq	273 (140.4)	252 (12.1)	14.9 (0.260)	0	3.93 (27.10) BURST
MAXIMUM $-\alpha q$	350 (180.0)	414 (19.8)	−4.6 (−0.080)	0	−1.33 (−9.17) COLLAPSE
MAXIMUM βq	240 (123.5)	195 (9.4)	4.7 (0.082)	17.0 (0.297)	1.50 (10.34) BURST
65 KNOT (33.4 m/s) GROUND GUST (DOORS OPEN)	–	–	–	–	0.18 (1.24)
PNEUMATIC DUCT FAILURE	–	–	–	–	6.25 BURST (ULTIMATE)

The load conditions which produce maximum loads on the nose cowl are given in table 27 in the form of total loadings summed at the engine forward flange. Also given for comparison are the Pratt and Whitney Aircraft allowable forward flange loads. The Refan nose cowl structural arrangement and materials are very similar, except for length, to the production DC-9 nose cowl. An important consideration in the strength analysis of the nose cowl was the effect of temperature and pressure imposed by the anti-icing system. Table 28 gives a comparison of temperatures and pressures for the nose cowl and inlet bullet for the critical anti-icing system design condition. The prototype JT8D-109 engines are actually less critical than the JT8D production engine, therefore those components affected by temperature and pressure, such as the leading edge "D" duct and the epoxy bonded acoustic sandwich in the inlet, were satisfactory by comparison.

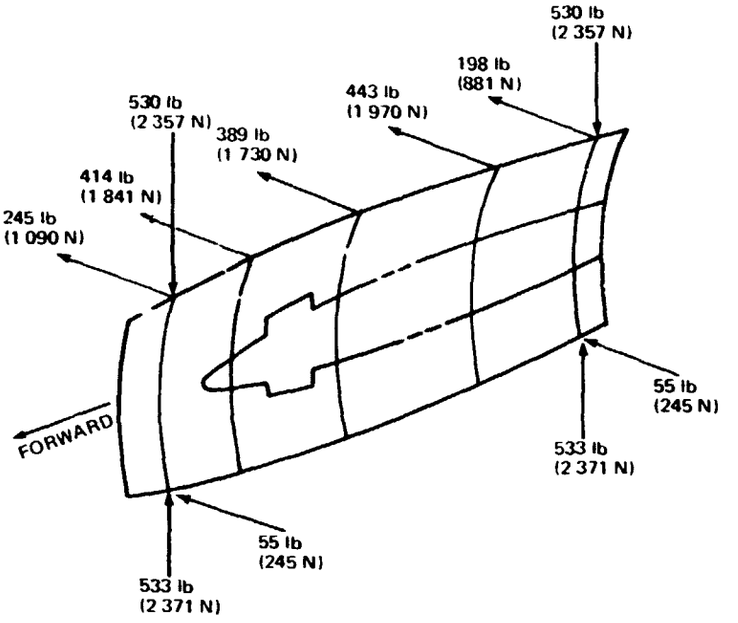

(a) 65 knot (3.34 m/s) LIMIT GROUND GUST WITH ACCESS DOORS OPEN

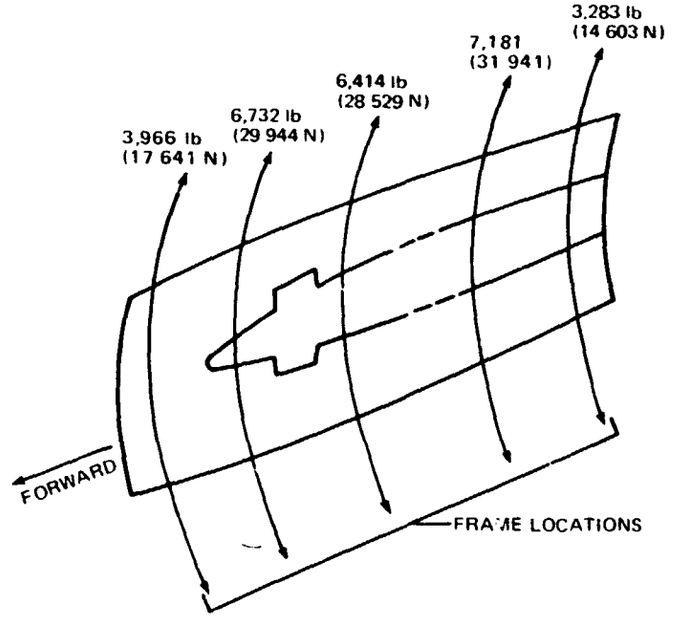

(b) 6.25 psi (43.1 kPa) ULTIMATE PNEUMATIC DUCT FAILURE WITH ACCESS DOORS CLOSED

FIGURE 117. DC-9 REFAN PYLON APRON LOADS

TABLE 27

DC-9 REFAN NOSE COWL ATTACHMENT LOADS

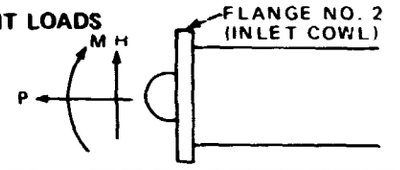

CONDITION DESCRIPTION	F lb (N)	M in lb (N m)	H lb (N)	ATTACH BOLT LOAD lb (N)
DAC APPLIED LOADS:				
MAXIMUM q (LIMIT)	6,887 (30 633)	40,165 (4 538)	−1,270 (−5 649)	418 (1 859)
MAXIMUM αq (LIMIT)	842 (3 745)	66,716 (7 538)	906 (4 030)	252 (1 121)
MAXIMUM −αq (LIMIT)	1,972 (8 771)	−104,133 (−11 765)	−3,595 (−15 991)	421 (1 873)
CRASH (ULTIMATE)	3,860 (17 169)	63,650 (7 191)	1,932 (8 594)	370 (1 646)
P&W ALLOWABLE LOADS:				
LIMIT	6,900 (30 691)	±233,000 (±26 329)	±9,800 (±43 590)	1,740 (7 740)
ULTIMATE	10,350 (46 037)	±349,500 (±394 935)	±14,700 (±65 386)	2,610 (11 609)

TABLE 28

DC-9 NOSE COWL AND BULLET DESIGN PRESSURES AND TEMPERATURES

Engine Model	Nose Cowl				Inlet Bullet	
	"D" Duct		Aft Compartment			
	P max psi (kPa)	T max °F (°C)	P max psi (kPa)	T max °F (°C)	P max psi (kPa)	T max °F (°C)
JT8D-9	18.2(125.5)	600(315.6)	15.2(104.8)	480(248.9)	22.1(152.4)	380(193.3)
JT8D-109	17.8(122.7)	590(310.0)	14.9(102.7)	480(248.9)	20.7(142.7)	344(173.3)
JT8D-117	18.0(124.1)	590(310.0)	15.0(103.4)	480(248.9)	21.0(144.8)	360(182.2)

Design Condition: Takeoff Power, Mach No. = 0.484, Ambient Air Temperature = -60°F (-51.1°C) to 120°F (48.9°C), Anti-icing System Operating

The exhaust duct of the refanned engine was designed to withstand loads imposed by the thrust reverser, internal pressures, thermal effects and maximum inertia load factors. Figures 118 and 119 show the critical exhaust duct internal pressure and temperature distributions, respectively, for the JT8D production and JT8D-109 prototype engines. The two load conditions which gave maximum loads on the exhaust duct are given in table 29. The loads are

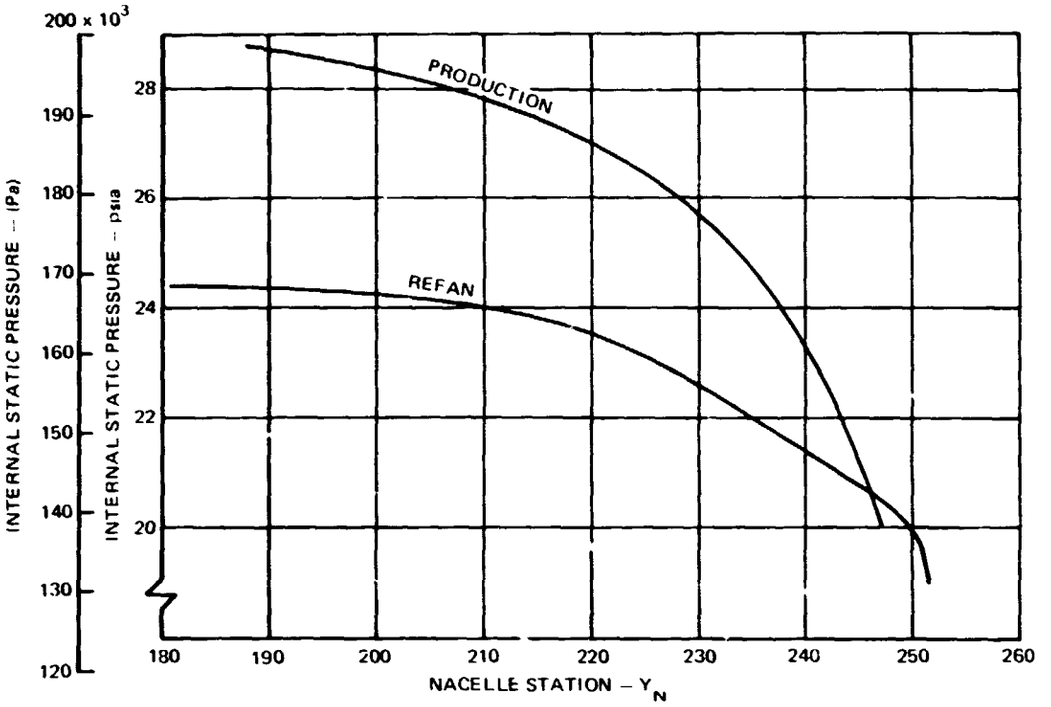

FIGURE 118. DC-9, JT8D EXHAUST DUCT PRESSURE DISTRIBUTION, MAX CONTINUOUS THRUST V_D AT SEA LEVEL STANDARD DAY

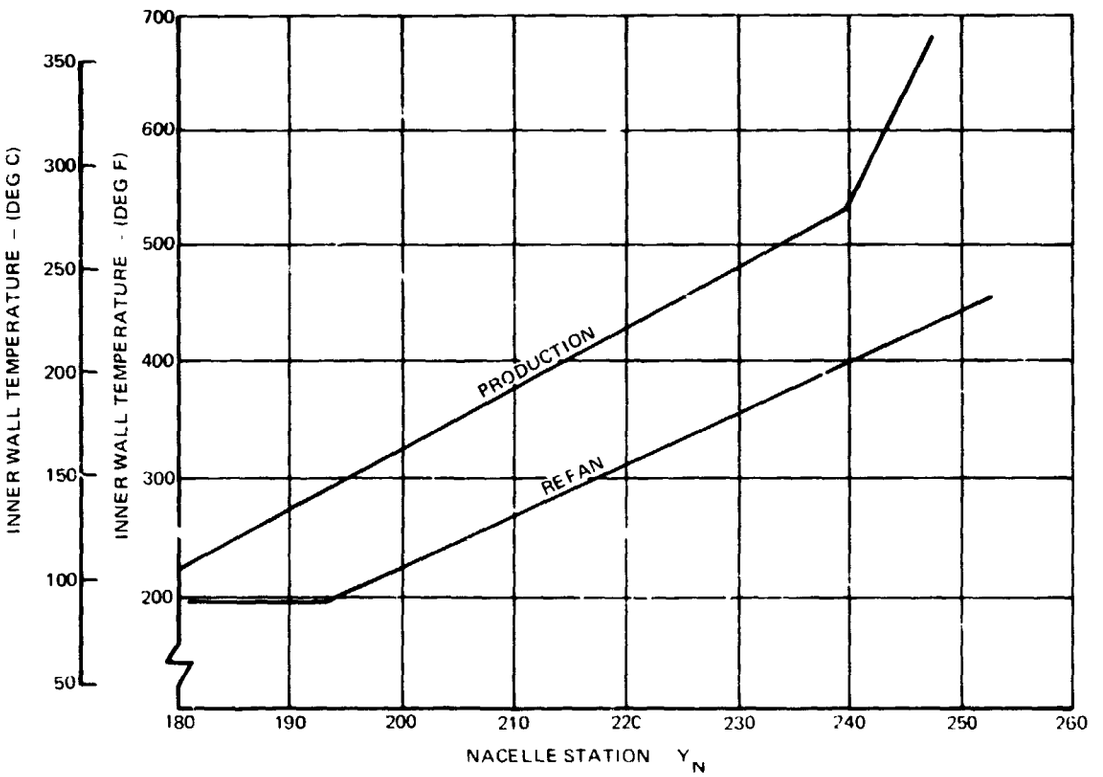

FIGURE 119. DC-9, JT8D EXHAUST DUCT TEMPERATURE DISTRIBUTION, MAX CONTINUOUS THRUST V_D AT SEA LEVEL STANDARD DAY

TABLE 29

DC-9 REFAN EXHAUST DUCT ATTACHMENT LOADS

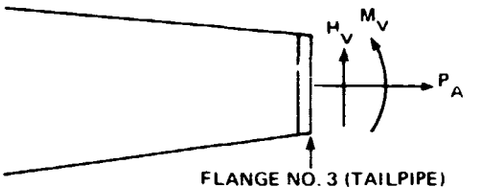

CONDITION DESCRIPTION	H_V lb (N)	M_V in-lb (N-m)	P_A lb (N)	ATTACH BOLT LOAD lb (N)
DAC APPLIED LOADS:				
REVERSE THRUST + MAXIMUM INERTIA (LIMIT)	2,870 (12 766)	−196,000 (−22 144)	19,400 (86 291)	700 (3 114)
CRASH (ULTIMATE)	3,260 (14 500)	−202,475 (−22 876)	12,000 (53 376)	110 (489)
P&WA ALLOWABLE LOADS:				
LIMIT	±4,900 (±21 795)	±301,000 (±34 007)	45,700 (203 274)	1,740 (7 740)
ULTIMATE	±7,350 (±32 693)	±451,500 (±51 010)	68,550 (304 910)	2,610 (11 609)

summed at the tailpipe mounting flange of the engine. The first condition combines maximum reverse thrust and exhaust system inertia in extra loads corresponding to 3.9 g's during landing. The crash condition is a combination of 12 g's forward and 6 g's down. Table 29 also gives the Pratt and Whitney Aircraft tailpipe mounting flange allowable loads.

Thrust reverser. - The thrust reverser for the JT8D-109 engine is similar in concept to the production thrust reverser. Basically, two doors are support by a system of linkages and driven by two hydraulic actuators. The structural design criteria for the thrust reverser include the following:

1. The thrust reverser doors and linkage shall have the strength to withstand the loads imposed from the stowed to the fully deployed position due to an airplane velocity of 92.6 m/sec (180 knots) and maximum takeoff power.

2. The actuator cylinder and linkage shall have the strength to withstand the snubbing loads imposed during rejected takeoff at 92.6 m/sec (180 knots) under engine power, and considering the effects of the time for actual operation.

3. The actuator cylinder shall have operational stowing capability at an airplane velocity of 87.4 m/sec (170 knots) with the engine at idle power.

4. The thrust reverser doors and linkage shall be designed to remain stowed, independent of the latch mechanism, through V_D (airplane dive speed) with maximum continuous thrust, in the absence of actuation to deploy.

5. The thrust reverser latch mechanism shall withstand failsafe loads consisting of aerodynamic forces on the doors at V_C (airplane cruise speed) with maximum continuous thrust combined with actuator hydraulic opening forces due to 20 684 kPa (3,000 psi) maximum accumulator pressure.

The thrust reverser door force versus actuator stroke is shown in figure 120 as a function of one, two and three second engine spooldown time from maximum takeoff thrust. The rejected takeoff loads used for design of the Refan thrust reverser and actuators were conservatively based on the one second spooldown condition. The anticipated normal deploy time was 2.0 to 2.5 seconds.

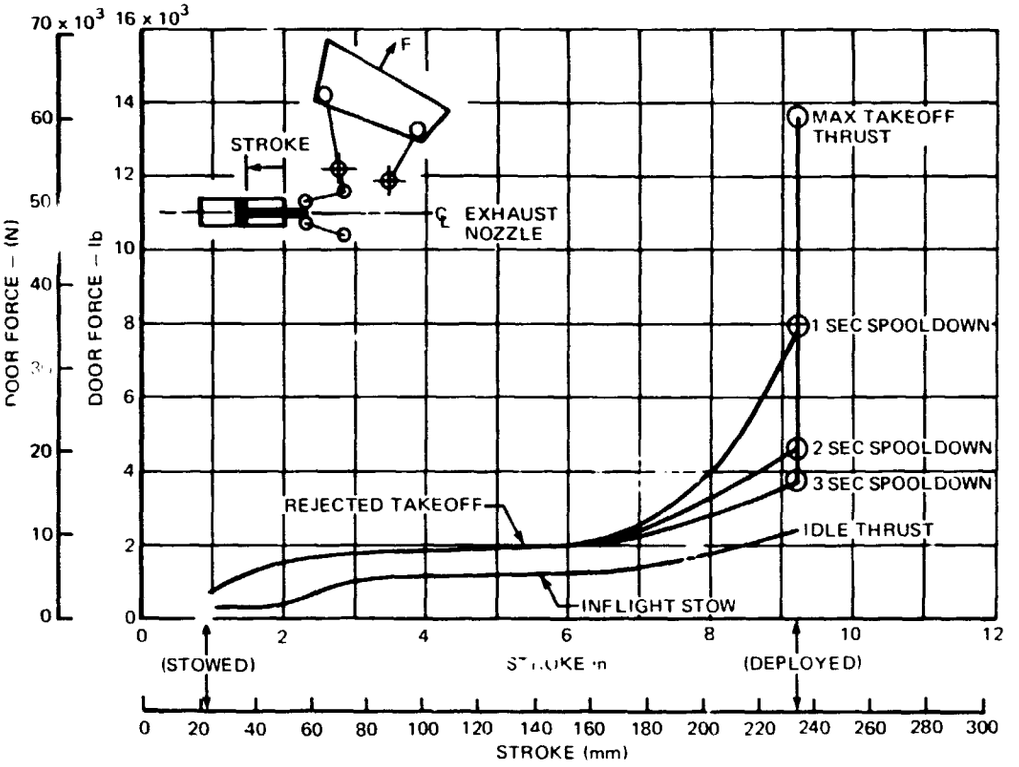

FIGURE 120. DC-9 REFAN THRUST REVERSER DOOR LOADS VERSUS ACTUATOR STROKE

Thrust reverser mechanism loads for the rejected takeoff design condition are given in table 30. The loads are given as a function of the driver arm deployment angle measured from its stowed position. Loads for a typical operational condition are given in table 31. The engine was assumed to be at idle power when the thrust reverser was deployed and the airplane velocity was 56.6 m/sec (110 knots). These are characteristics of normal DC-9 landing condition. These predicted loads will be used for comparison with test results.

Predicted actuator loads versus actuator stroke are shown in figure 121 for the two critical design conditions (rejected takeoff and inflight stow) and the normal landing condition.

TABLE 30

DC-9 REFAN THRUST REVERSER LOADS, REJECTED TAKEOFF

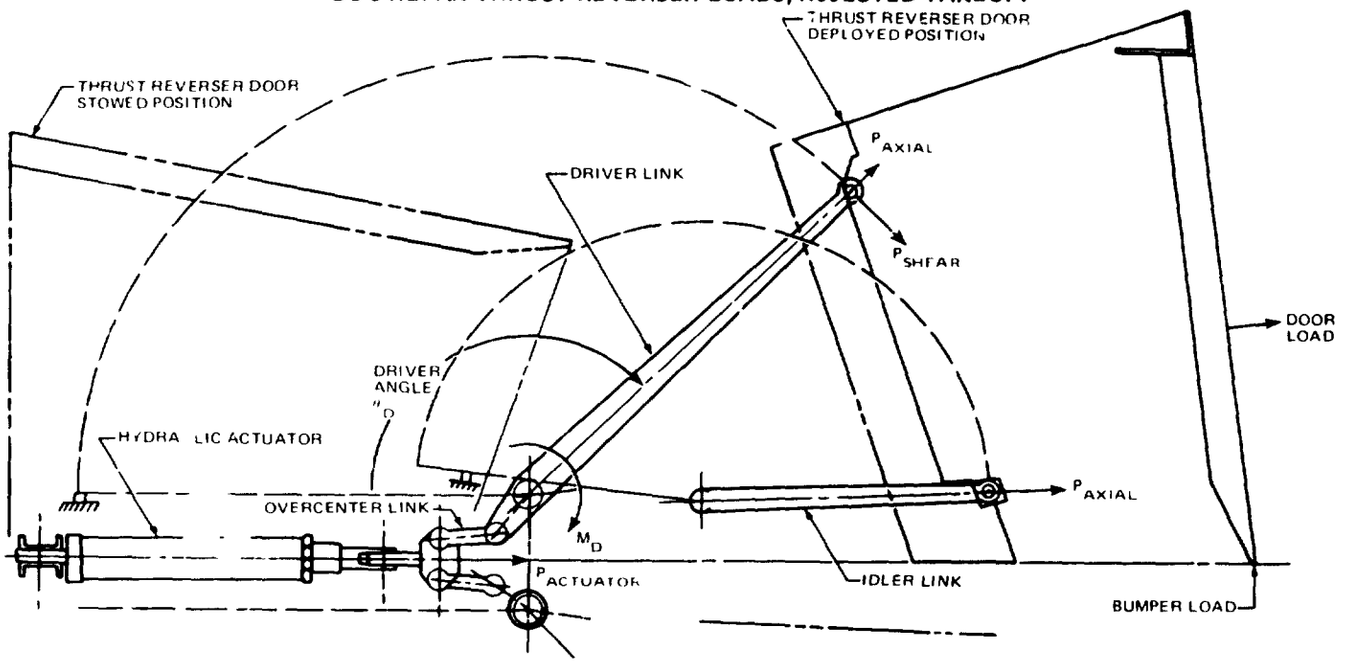

THRUST REVERSER LOAD DIAGRAM

DRIVER LINK ANGLE θ_D		DOOR LOAD		DRIVER LINK LOADS						IDLER LINK		OVER-CENTER LINK		ACTUATOR LOAD		BUMPER LOAD	
				M_D		P_{AXIAL}		P_{SHEAR}		P_{AXIAL}		P_{AXIAL}		$P_{ACTUATOR}$			
deg	(rad)	lb	(N)	in lb	(Nm)	lb	(N)	lb	(N)	lb	(N)	lb	(N)	lb	(N)	lb	(N)
TRANSIENT																	
0	(0)	650	(2 891)	8,562	(967)	- 274	(- 1 219)	292	(- 1 299)	203	(903)	2,659	(11 827)	1,323	(- 5 885)		
15 5	(0 271)	1 650	(7 339)	22,949	(2 593)	484	(2 153)	784	(3 487)	407	(1 810)	8,255	(36 718)	11,675	(51 930)		
35 5	(0 616)	1 800	(8 006)	25,058	(2 831)	136	(605)	856	(3 807)	256	(1 139)	-9,350	(-41 589)	17,269	(76 813)		
55 5	(0 969)	1,900	(8 451)	24,816	(2 803)	140	(623)	848	(3 772)	198	(881)	-8,768	(39 000)	17,414	(77 457)		
75 5	(1 318)	2,000	(8 896)	23,167	(2 617)	371	(1 650)	791	(3 518)	174	(774)	7,401	(-32 920)	14,770	(65 697)		
95 5	(1 667)	2 300	(10 230)	21 526	(2 432)	519	(2 309)	735	(3 269)	282	(1 254)	6,257	(- 27 831)	12,388	(- 55 102)		
125 5	2 190)	5 700	(25 354)	31,049	(3 508)	1250	(5 560)	1060	(4 715)	1213	(5 395)	9,825	(43 702)	19,638	(87 350.		
136 21	2 377)	7 800	(34 694)	32 418	(3 663)	1300	(8 006)	1100	(4 893)	1815	(8 073)	12,373	(55 035)	24,530	(109 109)		
FULLY DEPLOYED																	
136 21	2 377)	13 627	(60 613)	6,560	(741)	3211	(14 283)	112	(498)	5043	(22 431)	2,503	(11 133)	5,000	(22 240)	2101	(9345)

TABLE 31

DC-9 REFAN THRUST REVERSER LOADS, NORMAL LANDING

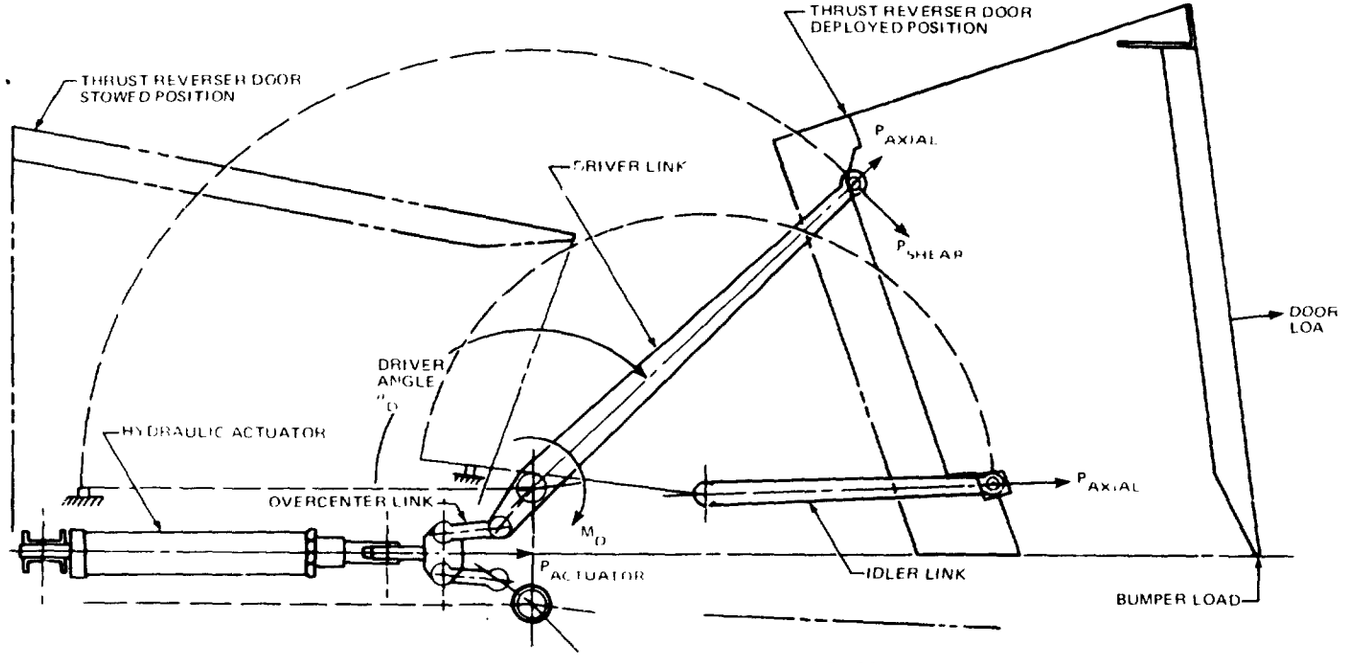

THRUST REVERSER LOAD DIAGRAM

DRIVER LINK ANGLE D		DOOR LOAD		DRIVER LINK LOADS						IDLER LINK		OVER-CENTER LINK		ACTUATOR LOAD		BUMPER LOAD	
				M_D		P_{AXIAL}		P_{SHEAR}		P_{AXIAL}		P_{AXIAL}		$P_{ACTUATOR}$			
deg	(rad)	lb	(N)	in lb	(Nm)	lb	(N)	lb	(N)	lb	(N)	lb	(N)	lb	(N)	lb	(N)
TRANSIENT																	
0	(0)	150	(667)	1976	(223)	63	(280)	67	(298)	47	(209)	614	(2 731)	305	(1 357)		
15.5	(0.271)	300	(1 334)	4173	(471)	88	(391)	142	(632)	74	(329)	1501	(6 676)	2123	(9 443)		
35.5	(0.619)	430	(1 913)	5986	(676)	32	(142)	204	(907)	61	(271)	2234	(9 937)	4125	(18 348)		
55.5	(0.969)	490	(2 180)	6400	(723)	36	(160)	219	(974)	51	(227)	2261	(10 057)	4491	(19 976)		
75.5	(1.318)	510	(2 268)	5908	(667)	95	(423)	202	(898)	44	(196)	1887	(8 393)	3766	(16 751)		
95	(1.658)	590	(2 624)	5522	(624)	133	(592)	189	(841)	72	(320)	1605	(7 139)	3178	(14 136)		
125.5	(2.190)	980	(4 359)	5 338	(603)	215	(956)	182	(810)	209	(930)	1689	(7 513)	3376	(15 016)		
140.21	(2.447)	1 167	(5 190)	4850	(548)	269	(1 197)	165	(734)	272	(1 210)	1851	(8 233)	3695	(16 436)		
FULLY DEPLOYED																	
140.21	(2.447)	10 735	(47 749)	6560	(741)	2532	(11 262)	112	(498)	3990	(17 748)	2503	(11 133)	5000	(22 240)	1693	(7 530)

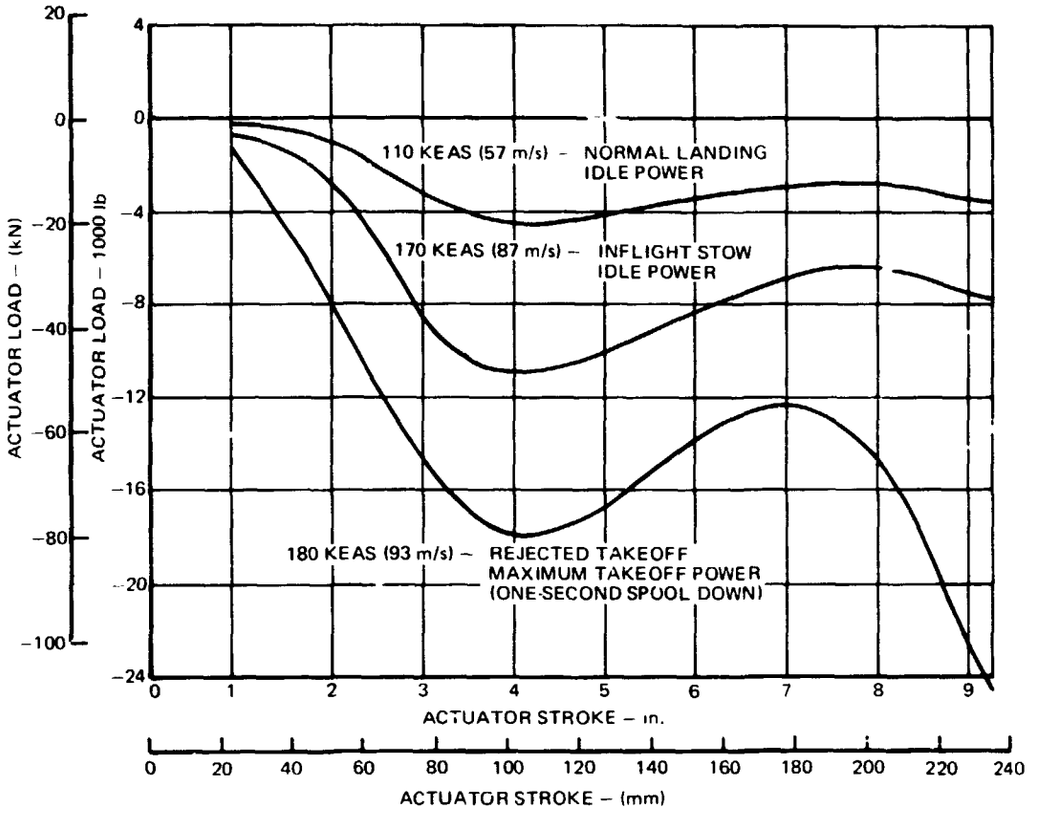

FIGURE 121. DC-9 REFAN THRUST REVERSER ACTUATOR LOAD VERSUS STROKE

In addition to the loads imposed on the linkage during thrust reverser operation, preloading of the linkage in the stowed position was necessary to meet the requirement that the doors remain closed at the airplane dive speed. A summary of the predicted critical linkage loads is given in table 32 and includes the rejected takeoff (one second spooldown), latch failsafe (system attempting to deploy inflight with maximum hydraulic pressure) and stowed (preloaded) design conditions.

TABLE 32

DC-9 REFAN SUMMARY OF CRITICAL THRUST REVERSER LINKAGE LOADS

LINK	CONDITION DESCRIPTION	DRIVER LINK ANGLE θ_D deg (rad)	BENDING MOMENT in-lb (N.m)	AXIAL LOAD lb (N)	SHEAR LOAD lb (N)
IDLER	LATCH FAILSAFE	1.9 (0.033)	–	6,970 (31 003)	–
	REJECTED TAKEOFF	136.21 (2.377)	–	5,043 (22 431)	
	STOWED (PRELOAD)	0	2,795 (316)	2,935 (13 055)	641 (2 851)
OVER CENTER	LATCH FAILSAFE	1.9 (0.033)		6,400 (28 467)	
	STOWED (PRELOAD)	0	–	14,822 (65 931)	
DRIVER	LATCH FAILSAFE	1.9 (0.033)	21,000 (2 [illegible]	6,516 (28 983)	717 (3 189)
	REJECTED TAKEOFF	136.21 (2.377)	6,560 (742)	3,211 (14 283)	112 (498)
	STOWED (PRELOAD)	0	-47,728 (5 392)	-3,049 (13 562)	1,630 (7 251)

The idler, overcenter and driver links were load calibrated prior to the ground and flight testing. Test data recorded for the thrust reverser in the stowed position and fully deployed during a normal landing are shown in table 33 with comparable analytical predictions. No structural modifications would appear likely for a production reverser based on the close agreement of these loads.

TABLE 33

DC-9 REFAN THRUST REVERSER LINKAGE LOADS (ANALYTICAL vs TEST)

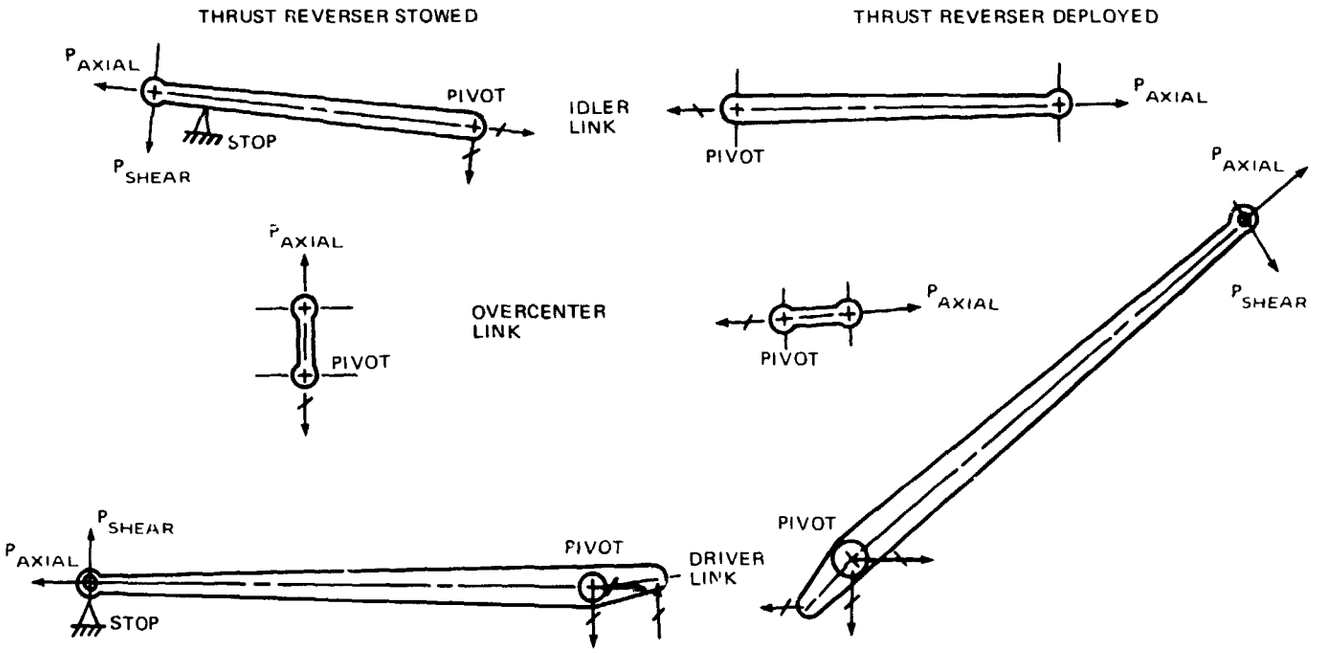

THRUST REVERSER COMPONENT LOAD DIAGRAMS

LINK	THRUST REVERSER STOWED				THRUST REVERSER DEPLOYED			
	ANALYTICAL		TEST		ANALYTICAL		TEST	
	P_{AXIAL} lb (N)	P_{SHEAR} lb (N)	P_{AXIAL} lb (N)	P_{SHEAR} lb (N)	P_{AXIAL} lb (N)	P_{SHEAR} lb (N)	P_{AXIAL} lb (N)	P_{SHEAR} lb (N)
IDLER	2,935 (13 055)	836 (3 719)	2,900 (12 900)	700 (3 114)	3,990 (17 748)		4,000 (17 793)	
OVER-CENTER	−14,822 (− 65 931)		14,010 (− 62 319)		2,503 (11 133)		2,300 (10 231)	
DRIVER	− 3,049 (−13 563)	1,630 (7 251)	−2,870 (12 766)	1,670 (7 428)	2,532 (11 262)	112 (498)	2,142 (9 528)	125 (556)

Each hydraulic actuator clevis was calibrated for axial load to provide comparison load versus stroke test data. Figure 122 shows test data for left side hydraulic actuator for several test conditions and the predicted load versus stroke for normal landing. Also included in figure 122 is the load versus stroke calculated from differential hydraulic pressure data recorded for the actuator. The comparison of results indicates that considerably reduced loads occur toward the end of the stroke for the test conditions. These results suggest that potential exists for reducing the weight of a production actuator cylinder configuration.

Variation of actuator load and overcenter link load as a function of actuator stroke, with deployment times indicated, are shown in figures 123 and 124, respectively. The data shown are for the normal landing condition. Performance of the thrust reverser with respect to deployment characteristics was within the system design objectives.

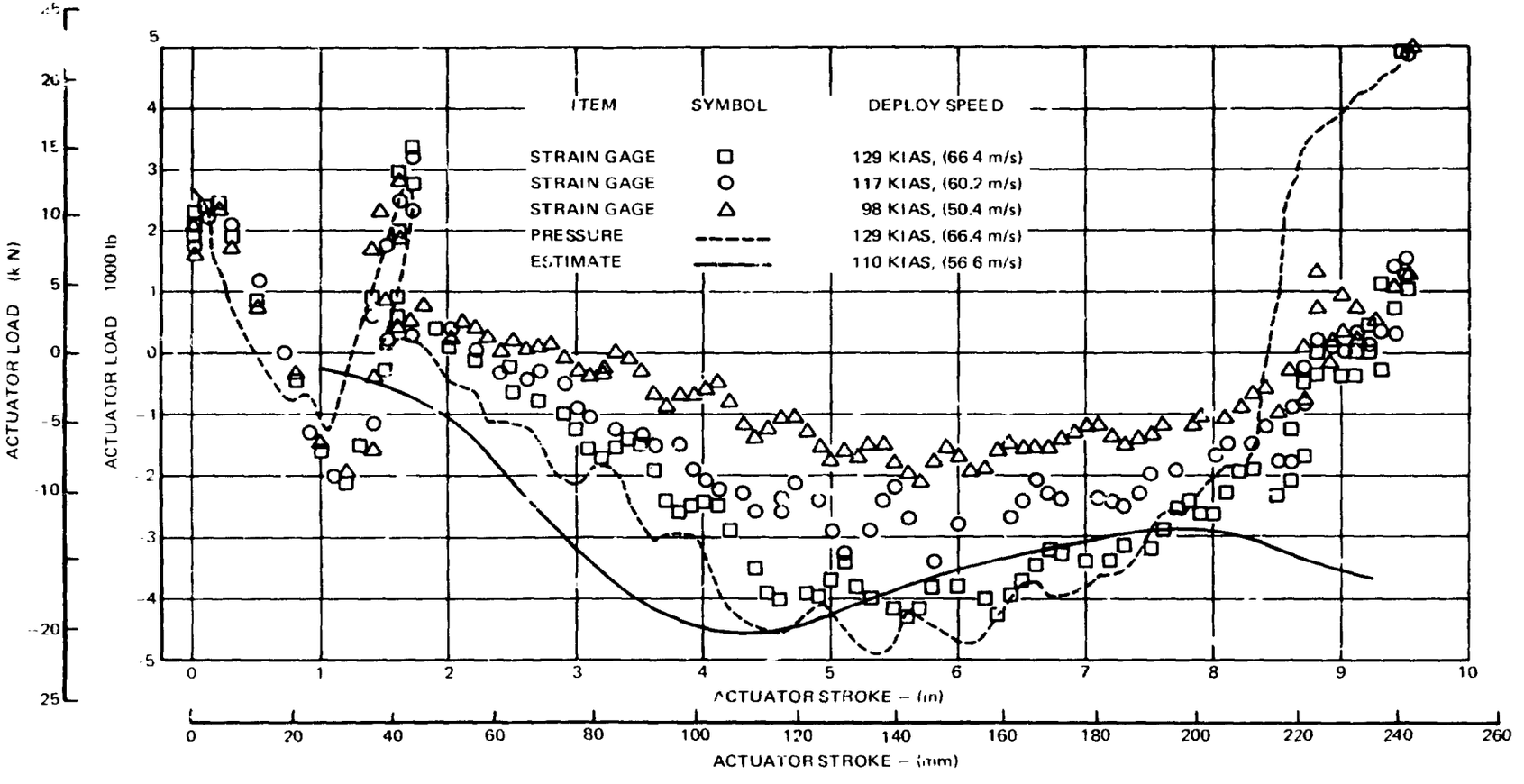

FIGURE 122. DC-9 REFAN THRUST REVERSER ACTUATOR LOAD VERSUS STROKE

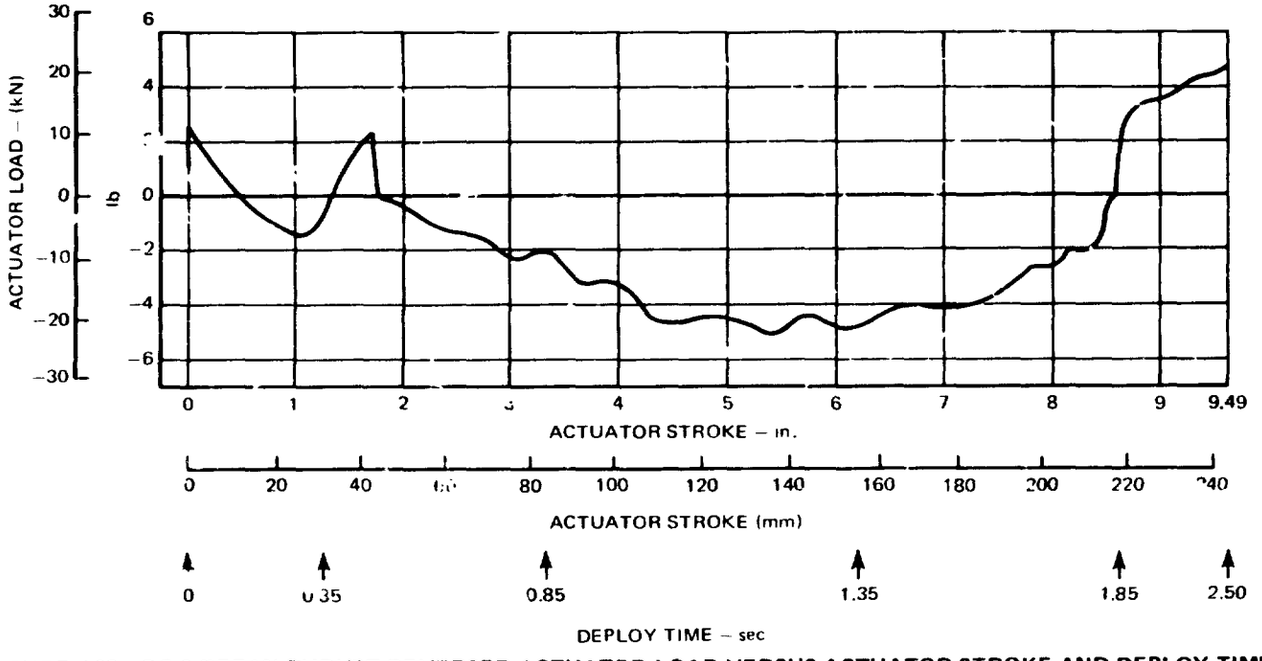

FIGURE 123. DC-9 REFAN THRUST REVERSER ACTUATOR LOAD VERSUS ACTUATOR STROKE AND DEPLOY TIME

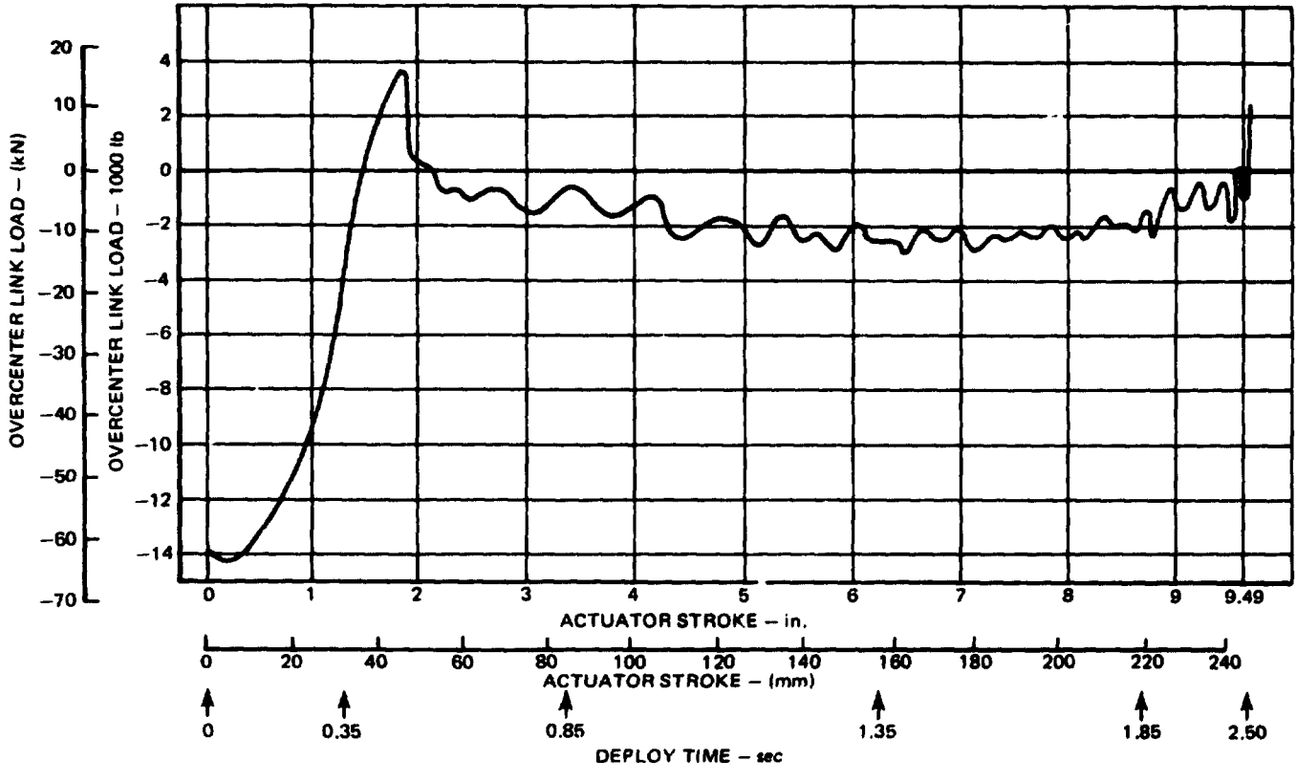

FIGURE 124. DC-9 REFAN THRUST REVERSER OVERCENTER LINK LOAD VERSUS ACTUATOR STROKE AND DEPLOY TIME

Flutter Analyses

Flutter analyses of the DC-9 Refan were performed and compared to analytical results for the production DC-9 airplane. The DC-9 is required by the Federal Aviation Regulations to be free from flutter and divergence at speeds up to 1.2 V_D (design dive speed). The design dive speed profile is shown in figure 125. The critical flutter mode for all versions of the production DC-9 is the antisymmetric T-tail flutter mode. This mode is comprised of coupling between the rigid body modes, fin first bending and fin first torsion. Only the antisymmetric cases are shown as the symmetric analyses resulted in significantly higher flutter speeds.

All flutter analyses were performed using a Douglas developed computer program. The method used is the standard "required damping vs velocity method". Antisymmetric analyses were performed with the Refan engine and the basic engine using orthogonal modes. Control surface rotation modes (8 Hz rudder and aileron and elevator free) were also included in the analyses.

Previous DC-9 flutter analyses were performed using unsteady aerodynamic coefficients based on a modified aerodynamic strip theory. However, the analyses performed for the Refan program used unsteady aerodynamic influence coefficients (AIC's) based on the Doublet Lattice Method. The Doublet Lattice Method is a recent development in unsteady lifting surface theory. The AIC's computed with this method demonstrate good correlation with experimental data and NASA Kernel Function Method calculations. The AIC's used in the flutter analysis were computed for 0.87 Mach Number, which is the critical Mach Number for DC-9 flutter.

The increased JT8D-109 engine weight and shortened pylon do not significantly change the modes that couple to produce the T-tail flutter mode. Hence, the critical flutter speeds and frequencies are not significantly changed from those of the DC-9 production airplane.

The 3.0 Hz T-tail flutter mode exhibits a shallow damped flutter crossing resulting in significant variation in flutter speed with modal structural damping. Therefore, the flutter speeds were conservatively taken at the g = 0 crossing.

A comparison of flutter results is also shown in figure 125. The Refan configuration resulted in slightly higher flutter speeds at all altitudes compared to the production DC-9 configuration. The flutter margin is well in excess of the 1.2 V_D requirement for FAA certification under CAR 4b, paragraph 4b.308.

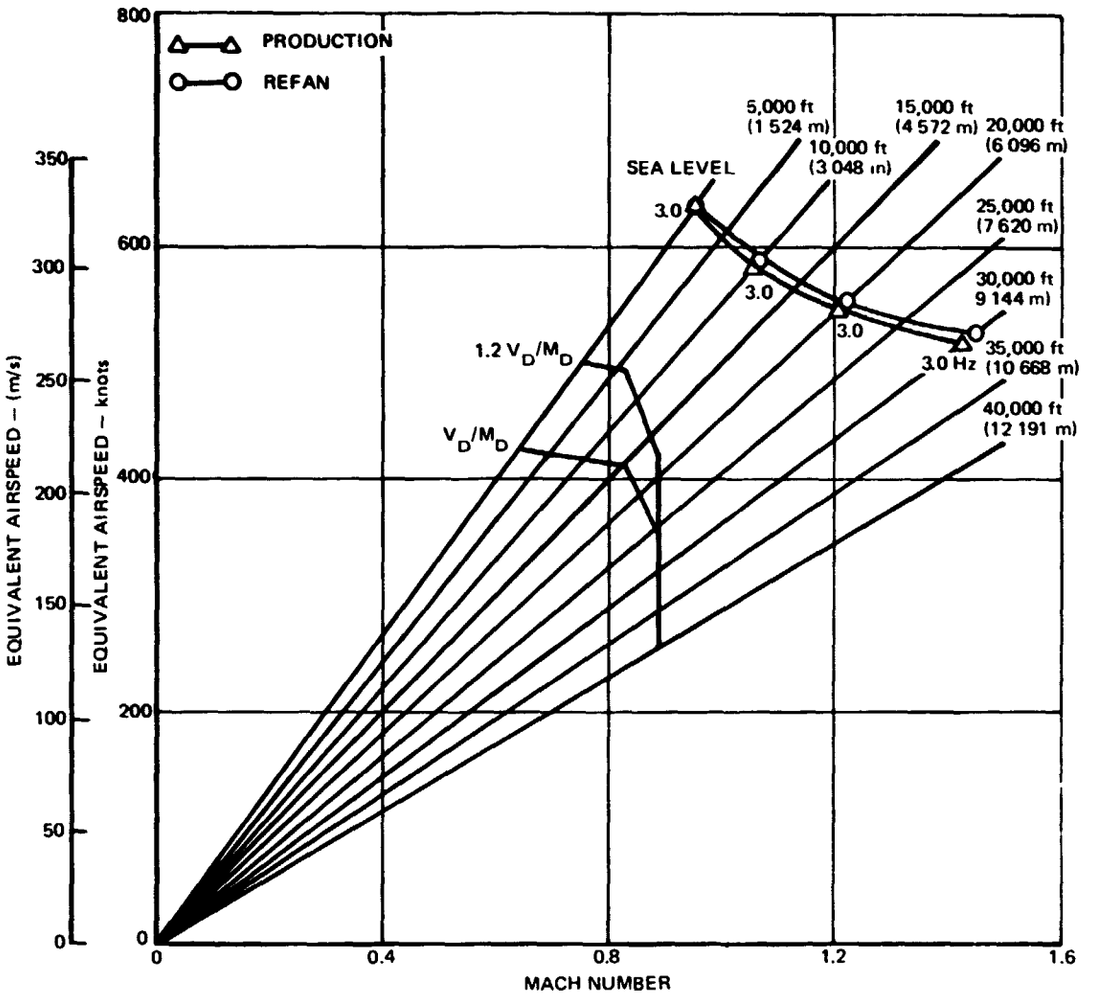

FIGURE 125. DC-9 REFAN ANTISYMMETRIC FLUTTER BOUNDARY

Ground Vibration Test Modes and Frequencies

Ground vibration tests were conducted on the DC-9 Refan airplane, to evaluate the effects of the pylon, fuselage, nacelle and engine stiffness and weight changes on the normal modes of vibration. The normal modes were used to validate the basic structural stiffness and mass properties and to evaluate flutter and structural dynamic characteristics.

The test objectives were: (1) to determine the frequency response characteristics of the airplane between 2 and 20 Hz; and (2) to measure the significant low frequency symmetric and antisymmetric modes of vibration together with the associated frequency and structural damping.

The GVT was performed in a manner similar to those conducted on previous DC-9 airplanes. Vibration data were obtained for the zero fuel configuration. The airplane was structurally complete, however, ballasting was necessary to simulate the passenger, interior and cargo distributions. The total airplane test weight was 34 714 kg (76,531 lb) with the center of gravity located at 35.2 percent M.A.C. The airplane was supported on the main landing gear inboard tires inflated to 1 172 kPa (170 psi) and a soft bungee suspension system at the nose landing gear.

Airplane modes of vibration were excited by applying periodic forces with electromagnetic shakers and varying the frequency until resonance was attained. At resonance, modal amplitudes, frequency and structural damping were measured.

Prior to measuring modal vibration amplitudes, frequency response plots were taken using x-y plotters. These response plots were used as a guide for fine tuning the mode to the desired resonant conditions. Upon completion of each modal survey, a direct-write recorder was used to measure the still-air damping following sudden removal of the excitation force.

The antisymmetric and symmetric structural modes of vibration measured on the Refan airplane are presented in tables 34 and 35 along with those obtained earlier on a production DC-9. The comparison shows that the weight and structural modifications to the Refan airplane caused minor changes to the modal frequencies. The modal damping also did not vary significantly from values measured for the production DC-9.

TABLE 34

RESONANT FREQUENCY COMPARISON

CONFIGURATION:	ZERO FUEL		
ANTISYMMETRIC MODES	SHIP NO.	48	741
	MODEL	-31	-31
	GROSS WEIGHT	76,531 lb (34 714 kg)	76,938 lb (34 899 kg)
	c.g. (% MAC)	35.2	34.9
MODAL DESCRIPTION		MODAL FREQUENCY HZ	MODAL FREQUENCY HZ
FIN BENDING		2.56	2.576
FIN TORSION		3.11	3.15
HORIZONTAL STABILIZER YAW		4.02	3.98
FUSELAGE BENDING		--	5.95
WING FIRST BENDING		6.80	6.86

TABLE 35

RESONANT FREQUENCY COMPARISON

CONFIGURATION:	ZERO FUEL		
SYMMETRIC MODES	SHIP NO.	48	741
	MODEL	-31	-31
	GROSS WEIGHT	76,531 lb (34 714 kg)	76,938 lb (34 899 kg)
	c.g.(% MAC)	35.2	34.9
MODAL DESCRIPTION		MODAL FREQUENCY HZ	MODAL FREQUENCY HZ
WING FIRST BENDING		3.41	3.405
FIN PITCHING IN PHASE WITH FUSELAGE		4.25	4.34
HORIZONTAL STABILIZER FIRST BENDING AND PYLON BENDING		6.01	6.29
FUSELAGE BENDING		7.08	7.18

Structural and Aerodynamic Damping

Flight tests were conducted to obtain structural frequency response data to demonstrate that the Refan airplane is free from flutter and/or excessive vibration within an arbitrary flight envelope defined as approximately half way between the V_{MO}/M_{MO} (cruise) and V_D/M_D (dive) speeds.

Previous tests on the DC-9-31 airplane indicated that critical empennage flutter modes were not sensitive to fuel loading, therefore, the Refan tests were conducted over a range of 100 percent to 52 percent fuel. The airplane was ballasted to an aft center of gravity. The minimum zero fuel weight was 32 207 kg (71, 004 lb), and the gross weights varied between 40 597 kg (89,500 lb) and 37 195 kg (82,000 lb) within center of gravity limits ranging from 32.8 percent to 33.5 percent M.A.C.

The method of testing consisted of exciting the structure with pilot induced control surface pulses. Tests on production DC-9 airplanes have shown that control surface inputs adequately excite the important modes. Control surface inputs were made for level flight, pushovers, pull ups and rudder power on and off conditions.

Instrumentation consisted of acceleration and control surface position tranducers. The outputs of these tranducers were recorded on airborne oscillographs. Selected outputs were telemetered to a ground station for monitoring. Structural response was monitored in real-time to assess the airplane damping characteristics as the speed envelope was expanded. This was accomplished by monitoring such characteristics as amplitude, damping and frequency of the various responses.

The real-time data display utilized two strip charts and two cathode ray tube displays during the flights. Modal frequency and damping were plotted against airspeed to indicate trends as the airplane speed was increased.

Aerodynamic damping characteristics were evaluated with pilot induced control surface pulses about 3 axes (aileron, rudder and elevator) at calibrated speeds of 134 m/s (300 knots) to 172 m/s (384 knots) at 5 182 m (17,000 ft) altitude and up to Mach = 0.87 at 7 163 m (23,500 ft) altitude.

The critical antisymmetric T-tail empennage mode responded at 3.0 Hz. The damping in this mode was predominant on fin lateral acceleration. In general, the damping in this mode exceeded 4 percent critical damping (8 percent structural damping) up to highest speeds tested with no rapid change in damping.

For the flight conditions tested, the DC-9-31 Refan airplane displayed similar or slightly improved damping characteristics as compared to the production DC-9-31 airplane. Structural damping was in excess of 8 percent for the speeds tested with no rapid deterioration in damping. Turning the rudder hydraulic power off had no detectable effect on structural damping.

RETROFIT AND ECONOMIC ANALYSIS

The economics, performance, and noise impact of retrofitting DC-9 airplanes with JT8D-100 series engines are based on analyses of the nacelle, thrust reverser, and fuselage design described in reference 3. The analysis was performed specifically on the DC-9-30 Refan airplane with JT8D-109 engines installed; however, it is applicable to all DC-9 airplanes with hardwall nacelles powered by existing JT8D engines.

The market for DC-9 Refan retrofit airplanes was estimated at between 525 and 550 aircraft depending, in part, upon the date of noise abatement rule making. During the early 1980's approximately 800 DC-9's are anticipated to be in service worldwide. The retrofit market amounts to approximately two-thirds of the total aircraft delivered. Of the 500 aircraft it was estimated that two-thirds would be retrofitted by domestic airlines.

The estimated unit cost of the retrofit program is 1.338 million in mid-1975 dollars. While this estimate has increased substantially from the 1972 levels the increase was almost solely due to price inflation and the lower aerospace industry operating levels currently being experienced. The total price in millions of 1975 dollars, including 4 percent NASA royalty is as follows:

Non Recurring	.088
Engine Kit	.629
Nacelle Kit	.400
Airframe Kit	.056
Installation	.165
TOTAL Price	1.338

Retrofitting the DC-9 airplane with the JT8D-109 engine modification could be accomplished in about 16-1/2 days after some experience has been accumulated. Five major tasks would be required:

Task Description	Elapsed Time - Days
Airline Preparation and Delivery to Modification Center	1
Acceptance Inspection	1
Airplane Rework	11 1/2
Test and Acceptance	2 1/2
Return to Customer	1/2
TOTAL	16 1/2

The entire domestic and foreign retrofit program could be accomplished by early 1983 based upon assumed retrofit program ATP in mid-1976, figure 126.

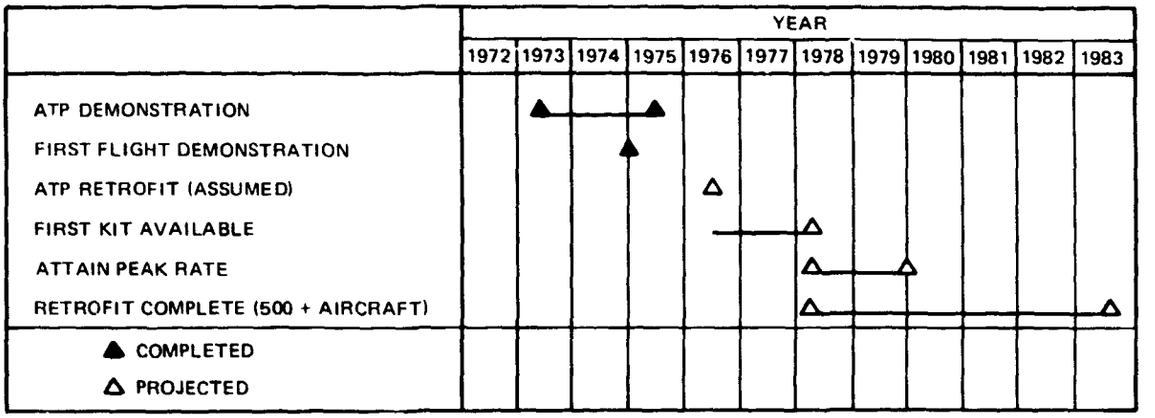

FIGURE 126. DC-9 REFAN RETROFIT SCHEDULE SUMMARY

Direct operating costs are presented for the DC-9-30, JT8D-9 and the JT8D-109 configurations for the typical mission 4 572 kg (15,000 lb) payload case, using both high speed cruise and long range cruise at 10 668 m (35,000 ft) cruise altitude. The modified ATA methodology is presented in table 36. At 740 km (400 n.mi.) the cost difference is .09 cents per seat mile, 2.04 vs 1.95 cents per seat mile in 1975 dollars, figure 127. This difference amounts to about $34 per trip in total direct cost. However, only a fraction of the $34, $6.67, can be traced to an increase in cash operating costs. This smaller amount is due to higher maintenance costs associated with the Refan configuration. The fuel burned and consequently, the costs are almost identical for equivalent conditions as shown in tables 7, 8, 9, and 10.

Although the JT8D-109 Refan engine has slightly better fuel specifics, the gain is offset by the increased weight of the airplane and actual fuel costs are nearly a toss up. At longer stage lengths the Refan airplane would burn slightly more fuel. The total $6.67 cash cost differential for typical missions would increase cash operating costs by about $18,000 per airplane per year or about $6,700,000 for the estimated domestic fleet of 375 DC-9 Refan airplanes.

An initial investment of slightly over $600 million would be required to retrofit the domestic fleet. At the end of 8 years the total cost of Refan retrofit and other introduction costs would amount to a total of $660 million plus interest.

The noise generated by a single flight for a given set of flight conditions can be described by a representative set of noise contours. Figures 128 and 129 present the 90 and 95 EPNdB, effective perceived noise level, noise contours for a production DC-9 powered with the JT8D-9 and the DC-9 Refan airplane for a typical mission. Similar contours for other conditions are presented in reference 4.

Noise contour area comparisons provide a way to compare the relative noise of alternative configurations under parallel conditions. Another measure can be obtained from the noise level differences at the FAR Part 36 measurement points. These differences, derived from flyover noise test data obtained during the DC-9 Refan flight demonstration program, are tabulated in table 37.

TABLE 36

1967 ATA AND REFAN INTERNATIONAL DOC FORMULAS

	1967 ATA	ATA (1975 COEFFICIENT)
CREW PAY ($/BLK-HR)		
2 MAN JET (SUBSONIC)	$0.05\ (TOGW/1000) + 100.00$	$21.58\ [V_{cr}\ (TOGW/10^3)]^{0.3} + 51.76$
FUEL ($/GAL)	0.11	0.30
NONREVENUE FACTOR ON FUEL	1.02	INCLUDED IN FUEL PRICE
AIRFRAME MAINTENANCE CYCLE		
MATERIAL ($/CYC)	$6.24\ (Ca/10^6)$	
DIRECT LABOR (MH/CYC)	$0.05\ (Wa/1000) + 6 \cdot \frac{630}{(Wa/1000) + 120}$	
AIRFRAME MAINTENANCE HOURLY		
MATERIAL ($/FH)	$3.08\ (Ca/10^6)$	
DIRECT LABOR (MH/FH)	$0.59\left[0.05\ (Wa/1000) + 6 \cdot \left(\frac{630}{(Wa/1000) + 120}\right)\right]$	DOUGLAS EXPERIENCE
ENGINE MAINTENANCE – CYCLE		
MATERIAL ($/CYC)	$20.0\ (Ce/10^6)\ Ne$	
DIRECT LABOR	$[0.6 + 0.027\ (T/10^3)]\ Ne$	
ENGINE MAINTENANCE – HOURLY		
MATERIAL ($/FH)	$25.0\ (Ce/10^6)\ Ne$	
DIRECT LABOR (MH/FH)	$[0.6 + 027\ (T/10^3)]\ Ne$	
BURDEN MH/DIRECT LABOR MH	1.8	
MAINTENANCE LABOR RATE ($/MH)	4.00	
INSURANCE (PERCENT PRICE/YR)	2.0	1.0
INVESTMENT SPARES RATIO (PERCENT)		
AIRFRAME	10	6
ENGINE	40	30
DEPRECIATION SCHEDULE (YEARS/PERCENT RESIDUAL)	12/0	14/10
UTILIZATION (HR/YEAR)	FORMULA: $U = \frac{4500}{1 + 1/(T_b + 0.30)} + 500$	FORMULA: $U = \frac{4500}{1 + 1/(T_b + 0.30)} + 500$

DEFINITION OF TERMS AND UNITS

TOGW	MAXIMUM TAKEOFF GROSS WEIGHT (LB)	Wa	AIRFRAME WEIGHT (LB)
Vcr	CRUISE SPEED (MPH)	M	MACH NUMBER
Ca	AIRFRAME PRICE ($)	FH	FLIGHT HOURS
Ce	ENGINE PRICE ($)	MH	MAN HOURS
Ne	NUMBER OF ENGINES	CYC	CYCLE
T	SEA LEVEL STATIC THRUST (LB)	T_b	BLOCK TIME (HR)

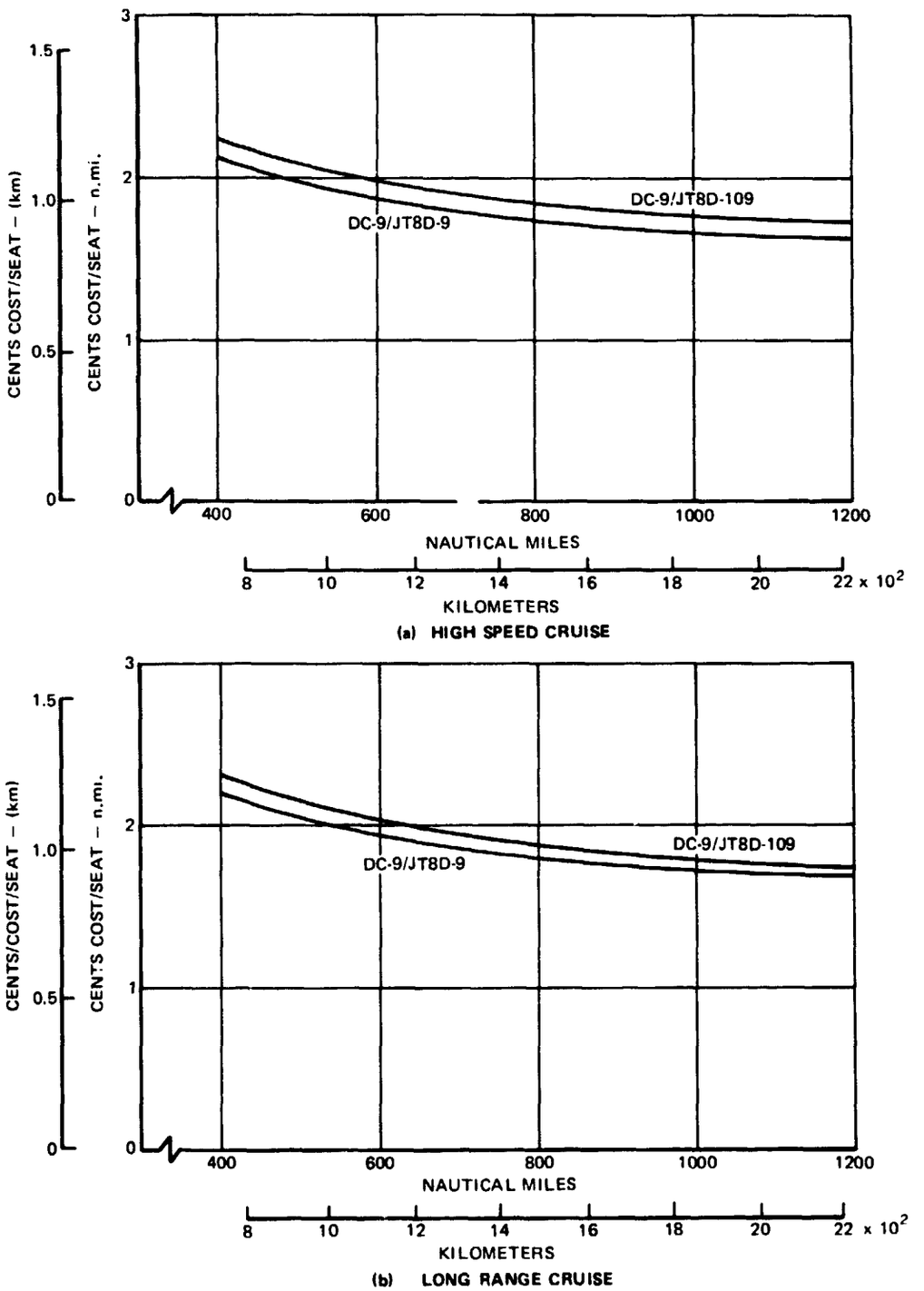

FIGURE 127. DIRECT OPERATING COST VERSUS STAGE LENGTH – CENTS PER SEAT MILE FOR A TYPICAL MISSION, 15,000 lb (4 572 kg) PAYLOAD – 1975 ATA – MODIFIED

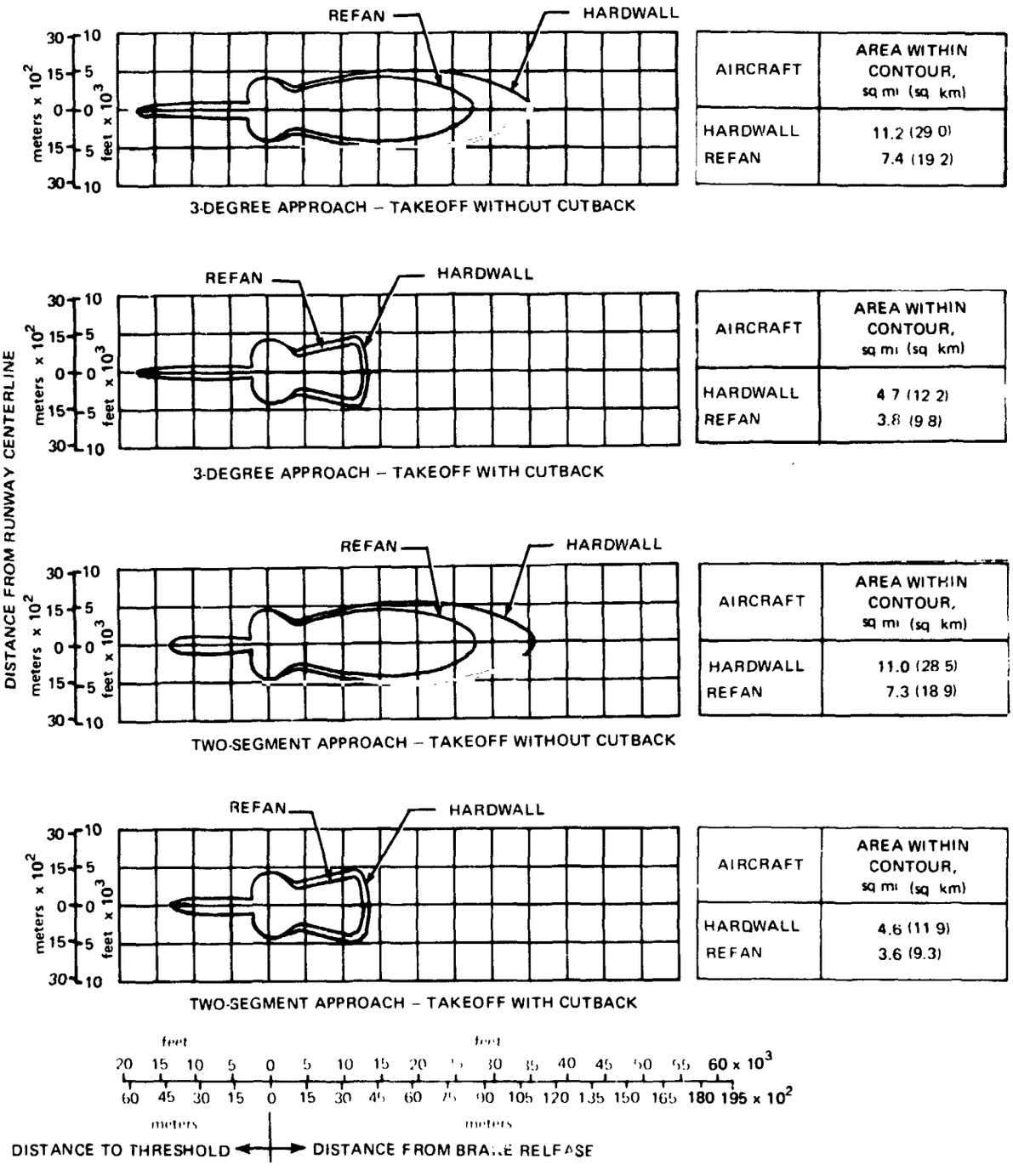

AIRCRAFT	AREA WITHIN CONTOUR, sq mi (sq km)
HARDWALL	11.2 (29 0)
REFAN	7.4 (19 2)

AIRCRAFT	AREA WITHIN CONTOUR, sq mi (sq km)
HARDWALL	4 7 (12 2)
REFAN	3.8 (9 8)

AIRCRAFT	AREA WITHIN CONTOUR, sq mi (sq km)
HARDWALL	11.0 (28 5)
REFAN	7.3 (18 9)

AIRCRAFT	AREA WITHIN CONTOUR, sq mi (sq km)
HARDWALL	4.6 (11 9)
REFAN	3.6 (9.3)

FIGURE 128. 90-EPNdB NOISE CONTOURS FOR HARDWALL AND REFAN DC-9-30 AIRCRAFT FOR TYPICAL MISSION OPERATION

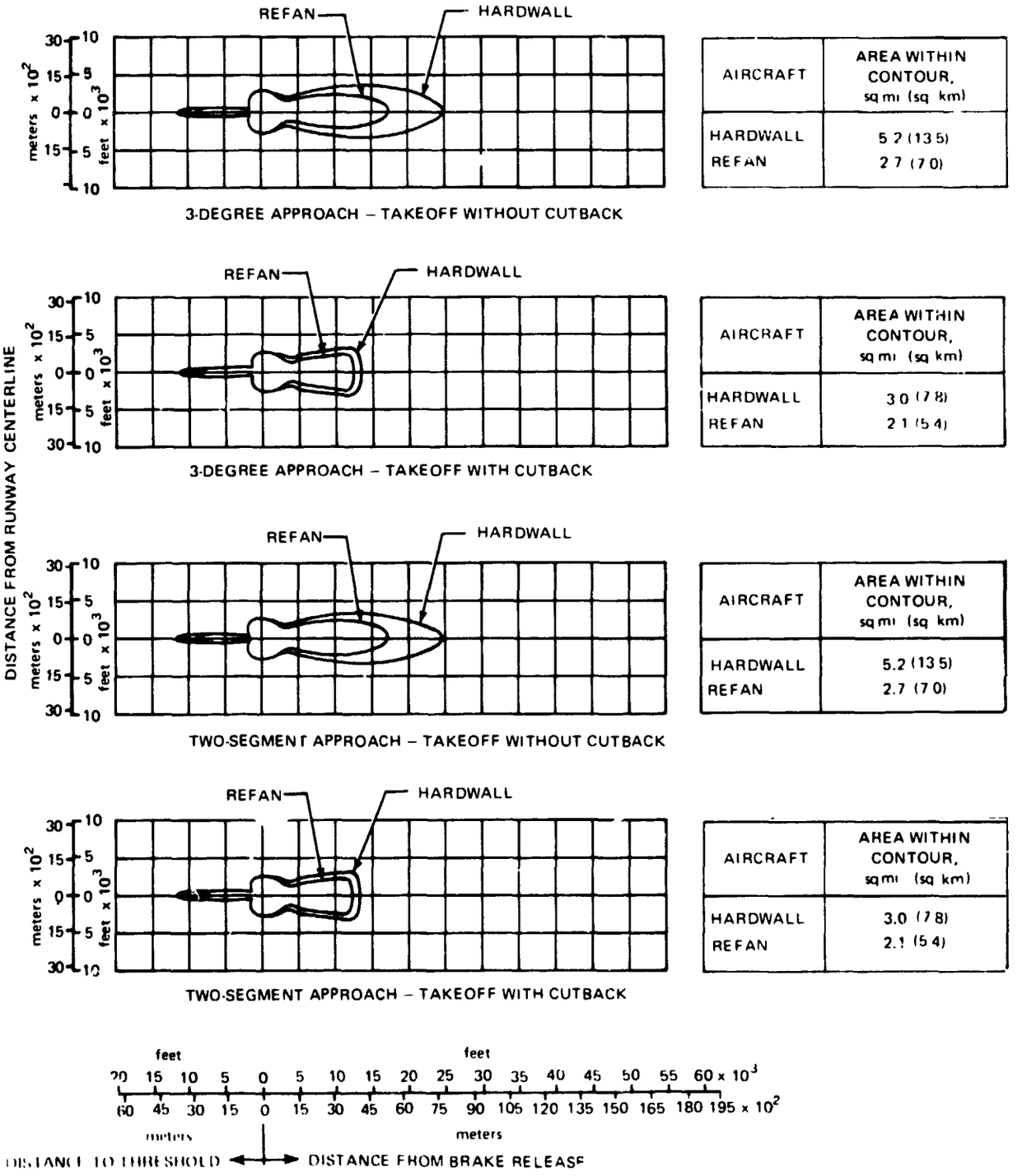

AIRCRAFT	AREA WITHIN CONTOUR, sq mi (sq km)
HARDWALL	5.2 (13.5)
REFAN	2.7 (7.0)

AIRCRAFT	AREA WITHIN CONTOUR, sq mi (sq km)
HARDWALL	3.0 (7.8)
REFAN	2.1 (5.4)

AIRCRAFT	AREA WITHIN CONTOUR, sq mi (sq km)
HARDWALL	5.2 (13.5)
REFAN	2.7 (7.0)

AIRCRAFT	AREA WITHIN CONTOUR, sq mi (sq km)
HARDWALL	3.0 (7.8)
REFAN	2.1 (5.4)

FIGURE 129. 95-EPNdB NOISE CONTOUR FOR HARDWALL AND REFAN DC-9-30 AIRCRAFT FOR TYPICAL MISSION OPERATION

TABLE 37

NOISE LEVEL DIFFERENCES AT THE FAR PART 36 MEASUREMENT POINTS

Condition	Refan~ EPNdB	Refan vs Hardwall ~ΔEPNdB
Takeoff with Cutback	87	10
Sideline	95	5
Approach	97	9

SUMMARY OF RESULTS AND CONCLUSIONS

The purpose of the Refan Program was to determine the technical and economic feasibility of reducing airport community noise produced by JT8D powered airplanes through modifications of existing engines and nacelles. This report presents an evaluation of analytical, ground and flight test data obtained from studies and tests conducted during the DC-9 Refan Program.

The JT8D-109 engine, a derivative of the basic Pratt and Whitney JT8D-9 turbofan engine, was selected for installation in the DC-9 Refan flight demonstration airplane. The sea level static, standard day bare engine takeoff thrust for the production JT8D-109 is 73 840 N (16,600 lb).

The bare engine performance of the production JT8D-109 engine relative to the JT8D-9 shows that for sea level static, standard day the takeoff thrust is 14.5 percent higher, the cruise TSFC at 9 144 m (30,000 ft), M = 0.80 and 19 571 N (4,400 lb) thrust is 1.5 percent lower, and the maximum cruise thrust available at the same Mach number and altitude is 4 percent higher.

The installation of the JT8D-109 engine results in an operational weight increase of 1 041 kg (2,294 lb) and an aft operational empty weight (OEW) center of gravity shift of 6 to 7 percent M.A.C. The weight increase is split about equally between the airframe and the engine. Retrofit kit weights will be approximately 91 kg (200 lb) less than the flight test weights because of weight reduction items that were identified during hardware design and DC-9 Refan flight test data analysis.

A comparison of the DC-9-32 FAA takeoff field length as a function of gross weight for the JT8D-109 and JT8D-9 production engine installations show that at sea level standard day conditions the additional thrust of the JT8D-109 results in 2 040 kg (4,500 lb) additional takeoff gross weight capability for a given field length.

The DC-9-32 payload range characteristics with the JT8D-109 engine installed relative to the JT8D-9 indicate the range changes for long range cruise at 10 668 m (35,000 ft) and payloads illustrating takeoff-gross-weight and fuel capacity limited cases are -352 km (-190 n.mi.) and -54 km (-29 n.mi.) respectively. Also, the range changes for 0.78 Mach number cruise at 9 144 m (30,000 ft) and payloads same as above are -326 km (-176 n.mi.) and -50 km (-27 n.mi.) respectively.

Although the JT8D-109 Refan engine has slightly better specific fuel consumption characteristics, this gain is offset by the increased weight of the engine, nacelle, and airframe modification hardware, and for typical stage lengths the actual fuel costs are about the same. At longer stage lengths the Refan airplane would burn slightly more fuel.

The stability and control characteristics of the DC-9 Refan airplane were evaluated to determine the affect of the installation of the larger diameter JT8D-109 engine and nacelle, the reduced span pylon, and weight increases, and to verify airplane airworthiness.

The Refan airplane demonstrated stall, static longitudinal stability, longitudinal control, longitudinal trim, air and ground minimum control speeds, and directional control characteristics similar to the DC-9-30 production airplane and did comply with production airplane airworthiness requirements.

The DC-9 Refan airplane and installed JT8D-109 engine performance was evaluated with respect to the production (DC-9-30/JT8D-9) airplane to determine the affect of the airplane, engine and nacelle modifications.

Test flights were conducted to establish the performance levels of the airplane and engine during takeoff, climb, cruise and landing. Engine performance was evaluated during suction fuel feeding, windmill and ground engine starts, snap throttle retards, jam accelerations, airplane stall, high sideslip angles and abused takeoffs. Airplane/engine subsystem performance and the auxiliary power plant (APU) performance and starting characteristics (ground and flight) were also evaluated.

Refan takeoff acceleration performance when compared with DC-9 Series 30 production airplane data corrected for the difference in thrust showed good agreement.

The climb performance of the DC-9 Refan airplane relative to the JT8D-9 powered DC-9-30 production airplane shows an 8 percent improvement in second segment and approach limiting weights and a 5 percent improvement in enroute limiting weight.

The cruise performance testing of the DC-9 Refan airplane, with the two prototype JT8D-109 engines installed, showed the range factor from 5 to 7 percent lower than an equivalent JT8D-9 powered DC-9-30 production airplane. While approximately 2 percent of this increment was due to the drag increase of the larger nacelle, the balance was due to the higher engine SFC of the prototype JT8D-109 engines.

During the JT8D-109 engine performance tests no signs of engine instability were noted by the pilots while the maximum climb thrust maneuver utilizing fuel suction feed was being conducted. Engine ground starting characteristics were satisfactory with little or no change from other JT8D versions. The low speed inflight starting envelope was also verified to be satisfactory. Overall, the engine operations were excellent with no major problems encountered and engine performance very close to predicted levels.

The airplane/engine subsystem performance tests showed that the JT8D-109 engine nacelle compartment ventilation and component cooling requirements were satisfied for ground and inflight conditions. The JT8D-109 engine generator and CSD cooling systems were demonstrated satisfactorily for the critical (100% load) ground idle condition and for all inflight conditions.

During the thrust reverser performance evaluation normal reverse thrust operation was demonstrated at speeds below the operational cutback speed of 30.87 m/s (60 knots) with acceptable engine operation; and the peak empennage temperatures remained below the maximum allowable 121°C (250°F) for the aluminum skin.

The Refan cowl ice protection system flight evaluation shows that the system provides ice protection performance which is equal to or in excess of predictions. System design similarities with the certified production DC-9 system and the conservative nature of the analytical method indicate that the DC-9 Refan cowl ice protection system can be operated without restrictions.

The auxiliary power plant (APU) tests showed no unusual starting or operating characteristics during ground starts; and electric and windmill airstarts with the modified exhaust were accomplished at the extremes of the production APU certified airstart envelope.

Structural and dynamic analyses, ground and flight tests were performed on the DC-9 Refan airplane to substantiate three basic program requirements:

1) The nacelle, thrust reverser hardware, and the airplane structural modifications are to be flightworthy and certifiable.

2) The Refan airplane will meet flutter speed margins.

3) The Refan airplane will qualify for an experimental flight test permit.

Evaluation of the results from the ground and flight tests revealed that the structural configuration of the Refan hardware is satisfactory for use in production and/or retrofit kits for the DC-9 airplane.

The Refan airplane ground vibration test (GVT) results verified that the airplane normal modes of vibration are not significantly changed; also, the damping characteristics compared well with those of the DC-9 production airplane.

Structural and aerodynamic damping flight test data shows that the Refan airplane exhibited the same or slightly improved damping characteristics relative to the production DC-9-30 and there were no instabilities or excessive vibration within the demonstrated flight envelope.

The retrofit and economic analysis indicates that the estimated unit cost of the retrofit program is 1.338 million in mid-1975 dollars with about an equal split in cost between airframe and engine. This estimate has increased substantially from the 1972 levels and is almost solely the result of price inflation and the current lower aerospace industry operating levels.

REFERENCES

1. Anon., "DC-9/JT8D Refan Phase I Final Report", Douglas Aircraft Company, NASA CR-121252, 1973.

2. Anon., "DC-9 Flight Demonstration Program with Refanned JT8D Engines", Volume I, Summary, Douglas Aircraft Company, NASA CR-134857, 1975.

3. Anon., "DC-9 Flight Demonstration Program with Refanned JT8D Engines", Volume II, Design and Construction, Douglas Aircraft Company, NASA CR-134858, 1975.

4. Anon., "DC-9 Flight Demonstration Program with Refanned JT8D Engines", Volume IV, Flyover Noise, Douglas Aircraft Company, NASA CR-134860, 1975.

SYMBOLS

a	Acceleration
ADDS	Airborne Digital Data System
a_g	Ground Deceleration
AGL	Above Ground Level
ALT	Altitude
AND	Airplane Nose Down
ANU	Airplane Nose Up
APU	Auxiliary Power Unit
a_s	Acceleration Corrected to Standard Conditions
ATA	Air Transport Association
BPR	By-Pass Ratio
BRGW	Brake Release Gross Weight
D	Drag
dB	Decibels
D_{BASE}	Base Drag
D_{NAC}	Nacelle Drag
D.P. or P	Differential Pressure
D_{RAM}	Ram Drag
DOC	Direct Operating Cost
EAS	Equivalent Airspeed
EPNL	Effective Perceived Noise Level
EGT	Exhaust Gas Temperature
EPR	Engine Pressure Ratio
EXT	Slats extended
FAR	Federal Aviation Regulations

FDC	Flight Data Center
Fe	Elevator Column Force
F_N	Uninstalled Net Thrust
F_{NC}	Installed Net Thrust
F_{NT}	Total Airplane Net Thrust
FPR	Fan Pressure Ratio
Fwd	Forward
g	Acceleration of gravity
G.W.	Gross Weight
h_p	Pressure Altitude
h_{pm}	Observed Pressure Altitude Corrected for Instrument Error
h_{pr}	Observed Pressure Altitude
HUB	Blade Hub
Hz	Hertz
IAS	Indicated Airspeed
IGV	Inlet Guide Vanes
i_h	Horizontal Stabilizer Angle
Inflt	In Flight
K or Kt	Knot
KCAS	Knots Calibrated Airspeed
KEAS	Knots Equivalent Airspeed
KIAS	Knots Indicated Airspeed
L	Nozzle Length
L.E.	Leading Edge
LH	Left Hand
L/H	Nozzle length-to-height ratio
LPT	Low Pressure Turbine

M	Flight Mach Number
M.A.C.	Mean Aerodynamic Chord
MALT	Mobile Automatic Laser Tracker
MART	Mobile Atmospheric Recording Tower
MAX	Maximum
MCL	Maximum Climb Thrust
MCT	Maximum Continuous Thrust
M_D	Design Mach Number
MEW	Manufacturer's Empty Weight
M_{FC}	Maximum Mach Number for Stability Characteristics
MIN	Minimum
M_L	Local Mach Number
MLW	Maximum Design Landing Weight
Mm	Observed Mach Number Corrected for Instrument Error
MMH	Maintenance Man Hour
M_{MO}	Maximum Operating Mach Number
M_o	Freestream Mach Number
M_{REL}	Blade Row Relative Inlet Mach Number
MTC	Mach Trim Compensator
MTOGW	Maximum Takeoff Gross Weight
MTW	Maximum Design Taxi Weight
N_1	Engine Low Pressure Compressor Rotor Speed
N_2	Engine High Pressure Compressor Rotor Speed
NEF	Noise Exposure Forecast
OAT	Outside Air Temperature
OEW	Operational Empty Weight
ovrd	Override

P_{amb}	Freestream Ambient Pressure
P_L	Local Static Pressure
PNdB	Units of PNL in Decibels
PNL	Perceived Noise Level
PNLT	Tone Corrected Perceived Noise Level
PNLTM	Maximum Tone Corrected Perceived Noise Level
P_o	Freestream Static Pressure
PRBC	Pressure Ratio Bleed Control
psi	Pounds Per Square Inch
psid	Pounds Per Square Inch Differential
P_{to}	Freestream Total Pressure
P_{t2}	Engine Compressor Inlet Total Pressure
P_{t7}	Engine Turbine Discharge Total Pressure
P_{tf7}	Engine Fan Discharge Total Pressure
$P_{T_{10}*}$	Nozzle Total Mixed Discharge Pressure
q	Dynamic Pressure
qc	Impact Pressure Corresponding to V_c
qcm	Impact Pressure Corresponding to V_m
Ref	Reference
RAT	Ram Air Temperature
RH	Right Hand
RPM	Revolutions Per Minute
SAT	Static Air Temperature
Sec	Seconds
SFC	Specific Fuel Consumption
SL	Sea Level
SLS	Sea Level Static

SPL	Sound Pressure Level
T	Temperature
TAT	Total Air Temperature
T_{am}	Ambient Temperature
TEU	Trailing Edge Up
TED	Trailing Edge Down
TFLF	Thrust for Level Flight
TSFC	Thrust Specific Fuel Consumption
TO	Takeoff
TMT	Treatment
TSFC	Thrust Specific Fuel Consumption
T_{tf7}	Engine Fan Discharge Total Temperature
TYP	Typical
V	Speed, knots
V_C	Calibrated Airspeed
V_D	Design Airspeed
V_e	Equivalent Airspeed
V_{ew}	Equivalent Airspeed Corrected to Standard Weight
V_{FC}	Maximum Airspeed for Stability Characteristics
V_{FE}	Maximum Airspeed for Flap Extension
V_g	Airplane Ground Speed
V_{LE}	Maximum Airspeed for Landing Gear Extension
V_{LO}	Airspeed at Lift-off
V_M	Observed Airspeed Corrected for Instrument Error
V_{mw}	V_m Corrected to Standard Weight
V_{mca}	Air Minimum Control Speed
V_{mcg}	Ground Minimum Control Speed

V_{MO}	Maximum Operating Airspeed
V_R	Airspeed for Rotation
$V_{R_{Max}}$	Maximum Airppeed for Rotation
V_s	Stall Speed
V_{SE}	Maximum Airspeed for Slat Extension
V_1	Critical Engine Failure Speed
$V_{1_{ew}}$	Equivalent Airspeed and Corrected to Standard Weight
V_2	Takeoff Safety Speed
W	Airplane Gross Weight
W_R	Airplane Gross Weight Ratio
W_s	Airplane Standard Gross Weight
W/M	Windmill
X	Aircraft Inboard-Outboard Station
Y	Aircraft Fore-Aft Station
Z	Aircraft Vertical Station

GREEK LETTERS

α	Angle-of-Attack
β	Angle-of-Sideslip
δ	Relative Absolute Pressure
δ_T	Relative Absolute Total Pressure
γ	Flight Path Angle
γ_z	Climb Gradient
θ	Relative Absolute Static Temperature
θ_T	Relative Absolute Total Temperature
ϕ	Airplane Attitude in Roll
σ	Relative Density
δ_e	Elevator Deflection - Positive Trailing Edge Down
δ_F	Flap Deflection